CHAPTER 3

Results and discussion

3.1 Thermodynamic studies of piroxicam

3.1.1. Intrinsic solubility of piroxicam

The determination of intrinsic solubility was determined concomitantly to the phase solubility study. The intrinsic solubilities were obtained at the absence of CDs. Table 1 showed the solubility of piroxicam in distilled water at various temperatures. Structurally, piroxicam is an amphoteric drug containing two ionizable moieties, the enolic and 2-pyridyl group, which exerts the pKa value of 1.8 and 5.1(5.46) respectively (Tsai et. al., 1993). The pH of the medium has pronounced effect on its ionization, which consequently affects the solubility. In aqueous solution of pH 0.9-7.0 the drug exists as zwitterions of very low solubility. In alkaline solution (pH> 7.0) the anionic species is predominant and the solubility increases significantly. The U-shaped solubility-pH profile, demonstrating the increasing solubility at both lower and higher pH values has been shown (Luger et. al., 1996). However, the value obtained at 25°C was comparable to that previously reported; that was 12 mcg/ml at pH 5.0 (Yazdanian, et.al., 2004). The slightly higher value obtained was due to the higher pH value of distilled water (mean pH value 6.74 ±0.14). Obviously, the solubility of piroxicam was prominently temperature-dependent shown by the high value of the linear regression coefficient in Figure 7. Accordingly, these solubility values were used to calculate the stability constant of the piroxicam-CDs inclusion complexes instead of the Y-intercept values obtained from the individual phase solubility

diagram. From the slope of straight line of the solubility plot, the heat of solution of the drug was 16.18 kJ/mol.

Table 4 Intrinsic solubility of piroxicam in distilled water at various temperatures

Temperature,°C	Solubility, So	
	(mcg/ml)	mM
25	13.98	0.042
30	16.10	0.049
37	18.49	0.056
45	21.20	0.064

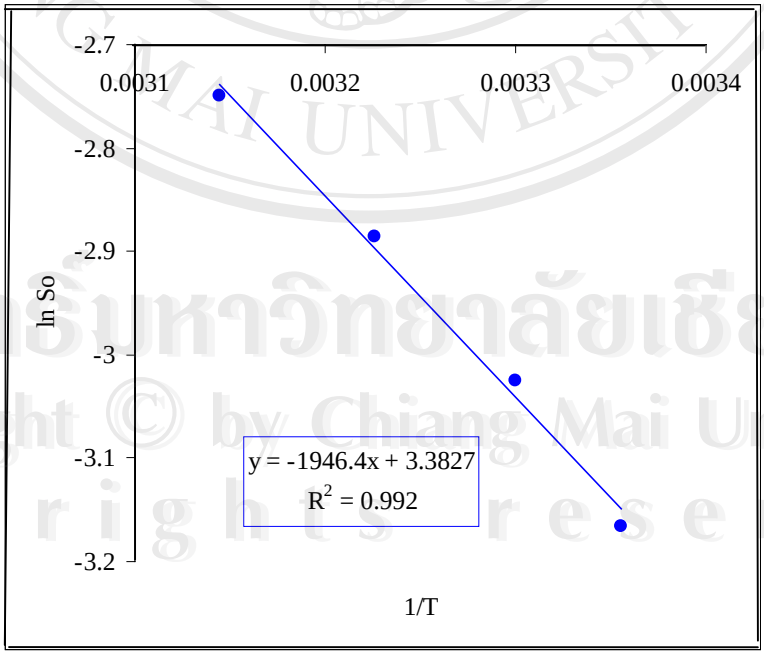

Figure 7 Solubility plot of piroxicam in distilled water at various temperature

3.1.2 Phase solubility diagrams of piroxicam-CD inclusion complexes

The phase solubility diagrams at 25° C, 30° C, 37° C and 45° C of piroxicam-BCD, piroxicam-GCD, piroxicam-HPBCD and piroxicam-MeBCD inclusion complexes were shown in Figure 8-11 respectively. The correspondent linear regression equation accompanying by the linear regression coefficient, r^2 values and the stability constants of the complexes were summarized in Table 5-8. The higher r^2 values (higher than 0.9) indicated the good linear correlation between the increased drug solubility and the increasing CD concentrations According to Higuchi and Connors (Higuchi and Connors, 1965).These solubility diagrams are characterized as the A_L-type. The slope values which were less than one suggested the 1:1 complex formation. The stability constant of the complex, K value is therefore calculated from the slope of the straight line and the intrinsic solubility (So) of the drug, as described in the following relationship:

$$K_{1:1} = \text{Slope}/\text{So}*(1-\text{slope}) \quad (1)$$

Generally, A_L-type phase solubility diagram signifies the linear relationship between the drug solubility and the CD concentration This relationship is observed at low CD concentration, at higher CD concentration, the linearity sometimes deviates due to two main factors, firstly, the limited intrinsic solubility of the CD, for example BCD, which usually giving the Bs-type. Secondly, due to the formation of higher order complex with increased or decreased solubility. In the latter case, the Ap- or A_N- type phase solubility diagram might be observed.

From the phase solubility diagrams shown in Figure 8-11, it is noted that the solubility of the drug increases not only with the CD concentration but, also more or less with the increasing temperature.

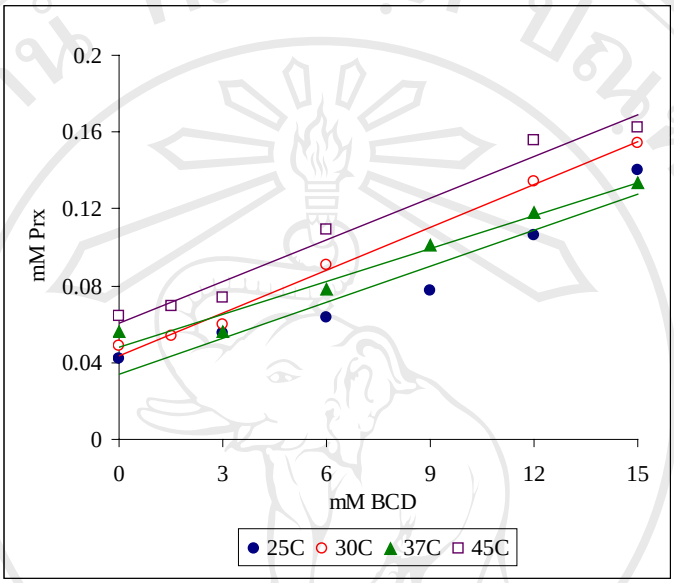

Figure 8 Phase solubility diagrams of piroxicam--BCD complexes in distilled water

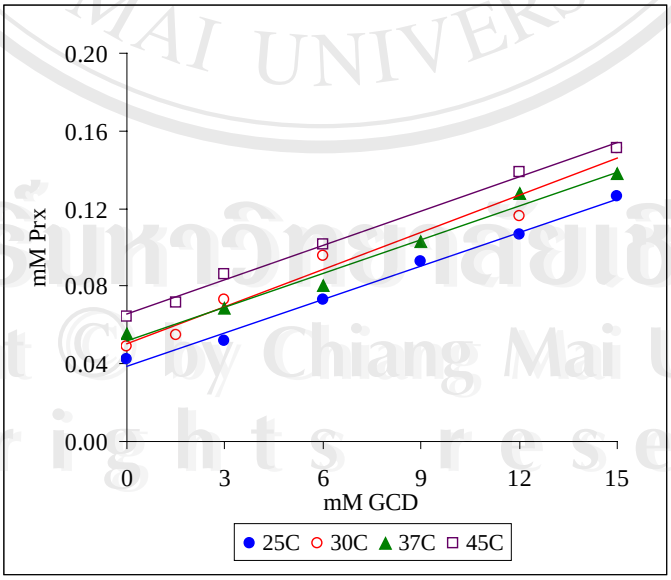

Figure 9 Phase solubility diagrams of piroxicam-GCD complexes in distilled water

Table 5 Stability constants of piroxicam-BCD complexes in distilled water obtained from phase solubility diagrams

T, °C	Equation(r^{2*})	K, M^{-1}	K, M^{-1} (Mean±SD)
25	y = 0.0063x+ 0.0314 (0.9058)	150.2	149.4±6.0
	y = 0.0065x + 0.0345 (0.9513)	155.0	
	y = 0.006x + 0.0355 (0.9095)	143.0	
30	y = 0.0075x + 0.0455 (0.9985)	155.5	154.1±2.4
	y = 0.0073x + 0.0443 (0.9854)	151.3	
	y = 0.0075x + 0.0415 (0.9804)	155.5	
37	y = 0.0056x + 0.0497 (0.9504)	100.9	102.7±1.8
	y = 0.0057x + 0.0491 (0.9815)	102.7	
	y = 0.0058x + 0.0452 (0.9442)	104.6	
45	y = 0.0073x + 0.0621 (0.9723)	114.9	113.8±3.3
	y = 0.0074x + 0.060 (0.9750)	116.5	
	y = 0.0070x + 0.0592 (0.9746)	110.1	

r^{2*} Linear regression coefficient of phase solubility diagram

The phase solubility diagrams of each series were shown in Appendix A

Table 6 Stability constants of piroxicam-GCD complexes in distilled water obtained from phase solubility diagrams

T, °C	Equation(r^{2*})	K, M^{-1}	K, M^{-1} (Mean±SD)
25	y = 0.0058x+ 0.0371 (0.9903)	138.2	136.6±2.8
	y = 0.0058x + 0.0384 (0.9931)	138.2	
	y = 0.0056x + 0.0413 (0.9910)	133.4	
30	y = 0.0063x + 0.0484 (0.9588)	130.4	132.5±2.1
	y = 0.0065x + 0.0498 (0.9707)	134.6	
	y = 0.0064x + 0.0519 (0.9753)	132.5	
37	y = 0.0057x + 0.0524 (0.9642)	102.7	104.6±1.8
	y = 0.0059x + 0.0504 (0.9873)	106.4	
	y = 0.0058x + 0.0525 (0.9876)	104.6	
45	y = 0.0056x + 0.0657 (0.9912)	88.0	93.3±4.8
	y = 0.0060x + 0.0648 (0.9865)	94.3	
	y = 0.0062x + 0.0656 (0.9937)	97.5	

r^{2*} linear regression coefficient of phase solubility diagram

The phase solubility diagrams of each series were shown in Appendix A

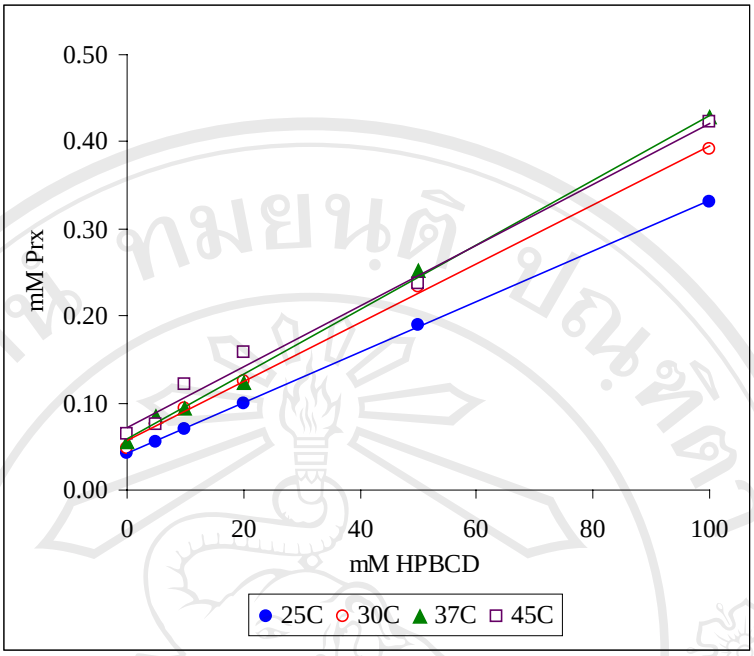

Figure 10 Phase solubility diagrams of piroxicam-HPBCD complexes at various temperatures

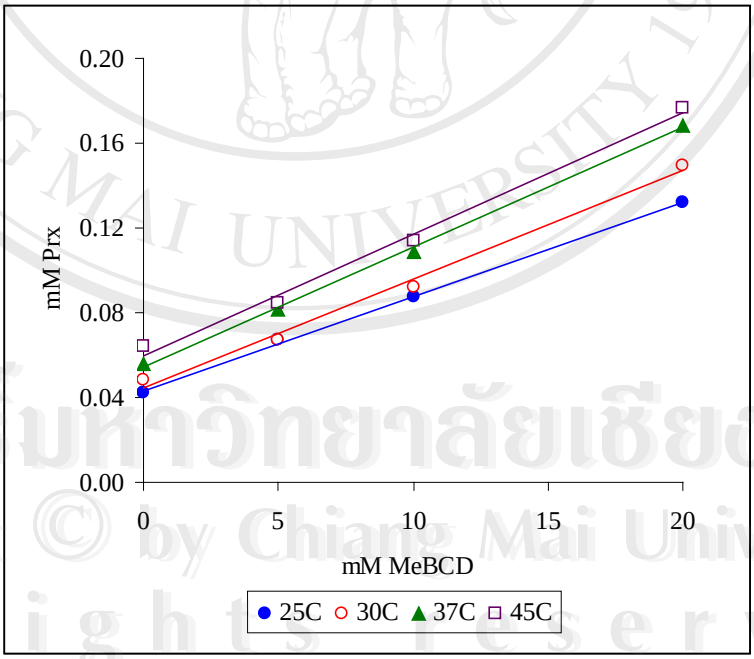

Figure 11 Phase solubility diagrams of piroxicam-MeBCD complexes at various temperatures

Table 7 Stability constants of piroxicam-HPBCD complexes in distilled water obtained from phase solubility diagrams

T, °C	Equation(r^{2*})	K, M^{-1}	K, M^{-1} (Mean±SD)
25	y = 0.0029x+ 0.0379 (0.9995)	68.9	68.9±0.0
	y = 0.0029x + 0.0415 (0.9998)	68.9	
	y = 0.0029x + 0.0454 (0.9998)	68.9	
30	y = 0.0034x + 0.0537 (0.9987)	70.2	70.2±0.0
	y = 0.0034x + 0.0570 (0.9983)	70.2	
	y = 0.0034x + 0.0593 (0.9979)	70.2	
37	y = 0.0037x + 0.0579 (0.9991)	66.6	67.2±1.0
	y = 0.0038x + 0.0568 (0.9980)	68.4	
	y = 0.0037x + 0.0601 (0.9959)	66.6	
45	y = 0.0034x + 0.0723 (0.9922)	53.3	54.4±0.9
	y = 0.0035x + 0.0716 (0.9899)	54.9	
	y = 0.0035x + 0.0730 (0.9890)	54.9	

r^{2*} Linear regression coefficient of phase solubility diagram

The phase solubility diagrams of each series were shown in Appendix A

Table 8 Stability constants of piroxicam-MeBCD complexes in distilled water obtained from phase solubility diagrams

T, °C	Equation(r^{2*})	K, M^{-1}	K, M^{-1} (Mean±SD)
25	y = 0.0045x+ 0.0422 (0.9999)	107.1	105.5±1.4
	y = 0.0044x + 0.0436 (0.9967)	104.7	
	y = 0.0044x + 0.0444 (0.9993)	104.7	
30	y = 0.0052x + 0.0427 (0.9946)	107.6	105.5±2.1
	y = 0.0051x + 0.0442 (0.9931)	105.5	
	y = 0.005x + 0.0468 (0.9874)	103.4	
37	y = 0.0055x + 0.0556 (0.9945)	99.1	102.1±2.8
	y = 0.0058x + 0.0531 (0.9999)	104.6	
	y = 0.0057x + 0.0539 (0.9979)	102.7	
45	y = 0.0057x + 0.0597 (0.9711)	89.6	89.6±1.6
	y = 0.0058x + 0.0584 (0.9989)	91.1	
	y = 0.0056x + 0.061 (0.9984)	88.0	

r^{2*} Linear regression coefficient of phase solubility diagram
The phase solubility diagrams of each series were shown in Appendix A

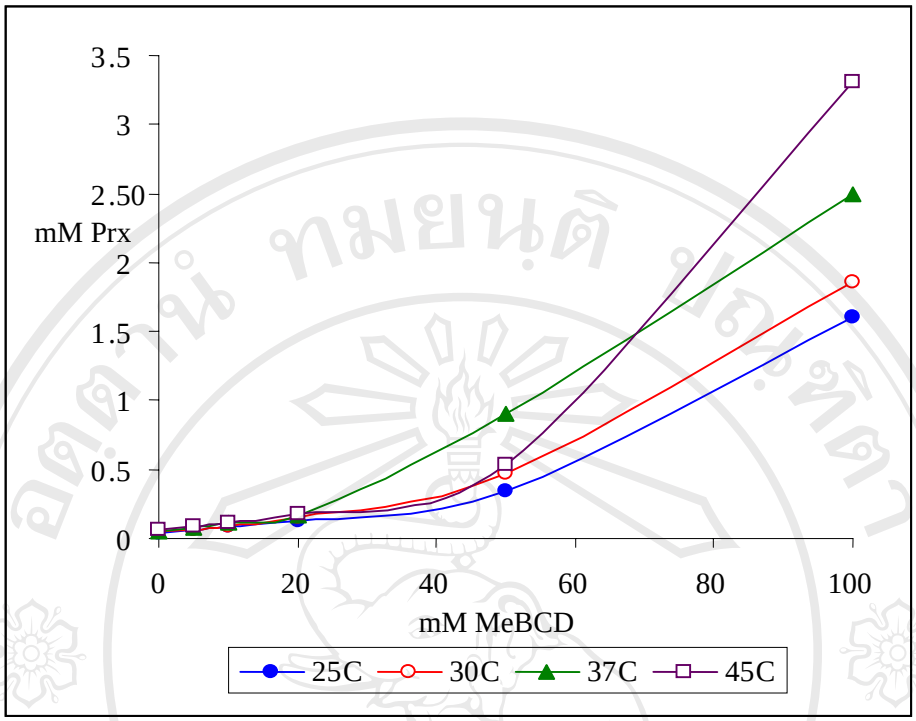

Figure 12 Phase solubility diagrams of piroxicam-MeBCD at high MeBCD concentrations at various temperatures

Figure 12 showed the phase solubility of piroxicam-MeBCD complex which was A_P-type. The approximately linear increase of the solubility can be observed only at low concentrations (up to 20 mM) of MeBCD. At higher concentrations of CDs the solubility curve deviates from linearity. This phenomenon does not depend on the temperature. The A_P-type solubility diagram implies the formation of higher order complexes with respect to the CD concentration. At equilibrium, the 1:1 and the higher order complexes exist simultaneously. The K values of Prx-MeBCD complexes were calculated from the initial linear part of the plot using the simple equation (1).

The mean K values of piroxicam-CD inclusion complexes from Table 5-8 were compared graphically in Figure 13. This bar chart demonstrates the effect of the CD

types and temperature on the K values. The quantitative statistical comparison was shown in Table 9.

The highest K value (154.1 M^{-1}) is obtained from the piroxicam-BCD inclusion complex indicating the highest complexation ability of BCD with piroxicam compared to the other investigated CDs.

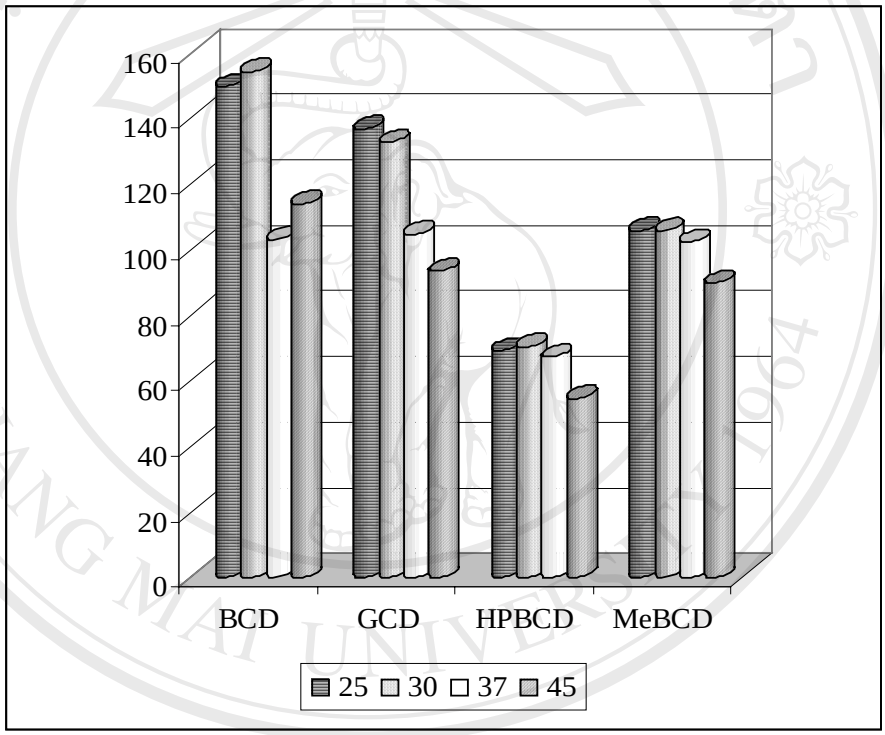

Figure 13 Stability constants, K of piroxicam-CD inclusion complexes at various temperatures

Table 9 Statistical comparison of the stability constants (K) of piroxicam-CDs complexes at various temperatures

CDs	T,°C	K, M^{-1}	Effect of temperature*	Effect of CD type*
BCD	25	149.4	$K_{25} \sim K_{30} > K_{37} > K_{45}$	**25°C,** $K_{BCD} > K_{GCD} > K_{MeBCD} > K_{HPBCD}$
	30	154.1		
	37	102.7		
	45	113.8		
GCD	25	136.6	$K_{25} \sim K_{30} > K_{37} > K_{45}$	**30°C,** $K_{BCD} > K_{GCD} > K_{MeBCD} > K_{HPBCD}$
	30	132.5		
	37	104.6		
	45	93.3		
HPBCD	25	68.9	$K_{25} \sim K_{30} > K_{37} > K_{45}$	**37°C,** $K_{BCD} \sim K_{GCD} \sim K_{MeBCD} > K_{HPBCD}$
	30	70.2		
	37	67.2		
	45	54.4		
MeBCD	25	105.5	$K_{25} \sim K_{30} \sim K_{37} > K_{45}$	**45°C,** $K_{BCD} > K_{GCD} \sim K_{MeBCD} > K_{HPBCD}$
	30	105.5		
	37	102.1		
	45	89.6		

* One-way ANOVA Post hoc range tests.
Significant and non-significant difference (~) at $p < 0.05$

Table 9 shows the statistical comparison of the K values which is affected by two factors, the CD type and the temperature. Based on the experimental design, these two factors simultaneously affect the K values of the complexes. Thus, the following

multiple linear regression (MLR) model was developed to verify the significance of these factors.

MLR model: K = -0.545CDtype* - 0.404Temperature*

$R^2 = 0.460$, *p<0.001

It is evident that both factors, the CD types and temperature significantly affect the piroxicam-CDs complex formation (p<0.001). The K values of the complexes show the tendency of decreasing when the CD types are changed from BCD, GCD, HPBCD and MeBCD respectively. Similarly, the K values show decreasing tendency with increasing temperature.

Based on the Post Hoc range test using LSD method, it was shown that, for all CD types, the K values are not significantly different upon temperature change especially from 25°C to 30°C. This finding can be easily detected in the Figure 7. The relatively temperature-independent phenomenon of the K values affects the further thermodynamic parameters calculation. By considering the effect of CD types, it is clear that the naturally CDs, BCD and GCD formed more stable complexes than the other two modified CDs.

By comparing the stability constant obtained from BCD to that of GCD, the parent CD with a larger cavity. The K value of piroxicam-GCD was somewhat lower. This might be due to the improper cavity size of GCD for a favorable fit of the drug molecule.

Generally, substitution at the CD rim by any constituent group leads to more or less the steric hindrance for the entering of the drug molecule. In the case of the piroxicam-HPBCD inclusion complex, the K values are lower compared to those of

piroxicam-BCD inclusion complexes. This is attributed by the effect of the steric hindrance caused by the bulky hydroxypropyl groups. This finding is in agreement with a previous report (Shoamin et.al., 2003) which reasoned the same findings based on the proposed complex conformations obtained by NMR studies.

Due to the temperature dependent nature of the stability constants, the thermodynamic parameters of the complex formation can be calculated by Van't Hoff plot shown in Figure 14 and the following relationships. The calculated values were summarized in Table 10

The enthalpy change, ΔH can be obtained from the slope of the Van't Hoff plots,

$$\Delta \ln K = -\Delta H/R * \Delta(1/T) \quad (2)$$

The free energy change, ΔG is calculated from

$$\Delta G = -RT \ln K \quad (3)$$

The entropy change, ΔS is obtained from the following equation

$$\Delta G = \Delta H - T\Delta S \quad (4)$$

3.1.3 Thermodynamic parameters of piroxicam-CD inclusion complexes

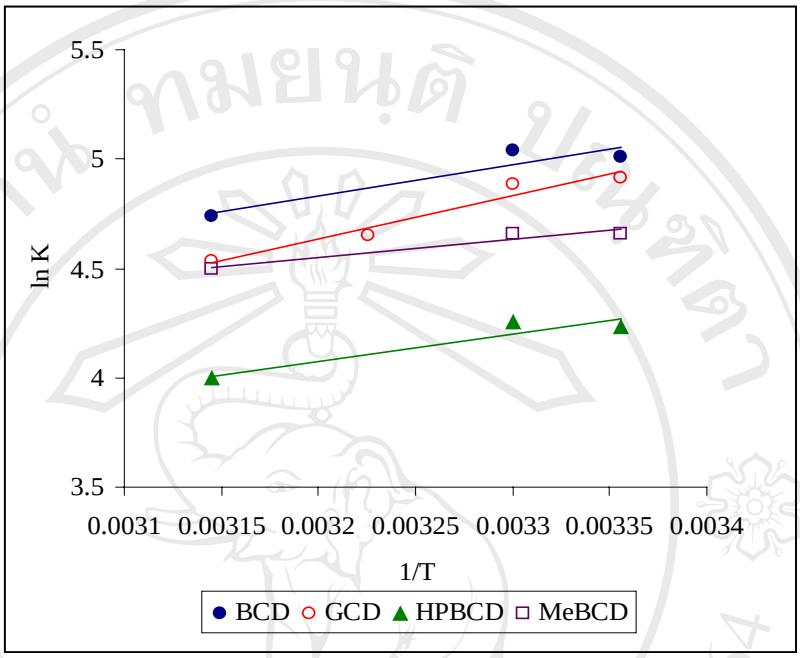

Figure 14 Van't Hoff plot of piroxicam-CDs inclusion complexes

As the thermodynamic parameters were essentially derived from the Van't Hoff plot, the quality of the plot thus influences the reliability of the parameters calculated. From Table 10, the relatively high linear regression coefficients of the Van't Hoff plot are shown which is indicating the reliability of the thermodynamic parameters obtained.

Table 10 Thermodynamic parameters of piroxicam-CDs complexes

CDs	ΔH, kJ/mol	ΔG, kJ/mol	ΔS, J/mol/K	Van't Hoff Equation	r^{2*}
BCD	-11.9	-12.5	2.1	y = 1431.7x + 0.2491	0.8838
GCD	-16.4	-12.1	-13.9	y = 1970.3x - 1.6694	0.9521
HPBCD	-10.3	-10.6	1.0	y = 1237.1x + 0.1186	0.9008
MeBCD	-6.9	-11.7	15.6	y = 836x + 1.873	0.9370

r^{2*} Linear regression coefficient of Van't Hoff plot

All piroxicam-CDs complexes exhibit negative values of free energy change, ΔG and enthalpy change, ΔH. The negative value of ΔG substantiates that the piroxicam-CDs inclusion complex formation is essentially a spontaneous exothermic process.

The negative ΔH value also indicates that the complex formation is driven by the enthalpy change. There are two postulations involving the negative value of enthalpy change upon guest-CD complex formation. Firstly, the large negative enthalpy change evokes from van der Waals interaction between the guest and CDs. This enthalpy is compensated by the reduction of the motional freedom of the guest molecules in the complex formation. Secondly, the large negative enthalpy change is also contributed by the replacement of the enthalpy-rich water molecules from the CD cavity upon the inclusion of the drug molecule. Nevertheless, the large negative ΔH value obtained from the drug and BCD complex evidences the stronger binding strength of the

complex. This is in consistent with the highest K values of piroxicam-BCD shown. Likewise, the lowest K values of piroxicam-HPBCD complex indicating the low stability of the complex is supported by the smallest ΔH value.

The positive entropy change is evidenced for a naturally occurred-exothermic process. Moreover, the release of the cavity-bound water molecules from CD cavity also provides a positive entropy change, resulted by the increase in the motional freedom of the water molecules by either translation or three-dimensional rotation. As a result, for guest-CD complexation, the positive entropy change would be commonly observed. Contrarily, in many cases, the entropy change is negative due to the enthalpy-entropy compensation phenomenon. This phenomenon occurs when the change in entropy is compensated by the smaller free energy change. From the results, only piroxicam-GCD complexes show enthalpy-entropy compensation phenomenon due to the large free energy change upon complexation.

3.1.4 Effect of pH on piroxicam –CD complex formation

The effect of pH on piroxicam-CDs complex formation was evaluated at 3 different pH values at 2.5, 5.5 and 7.4 respectively. The pH values were selected in order to obtain different ionic status of the drug. The different pH values incidentally resemble the pH of non-fasted gastrointestinal tract and the physiological fluid. The experiment has been conducted at 37° C for the purpose of an *in vivo* simulation

The solubility of piroxicam in natural CDs and modified CDs at different pH values were listed in Table 11-12. The relevant phase solubility diagrams were illustrated in Figure 15-18 for BCD, GCD HPBCD and MeBCD respectively.

Table 11 Solubility of piroxicam in BCD and GCD solutions of varying pH values at 37° C

CD	mM	Prx (mM)		
		pH 2.5	pH 5.5	pH 7.4
BCD	0	0.042	0.056	1.578
	3	0.059	0.056	1.823
	6	0.074	0.079	2.075
	9	0.104	0.101	2.323
	12	0.128	0.118	2.664
	15	0.155	0.134	2.877
GCD	0	0.042	0.056	1.578
	3	0.059	0.068	1.595
	6	0.069	0.079	1.787
	9	0.091	0.103	2.040
	12	0.106	0.127	2.245
	15	0.132	0.138	2.253

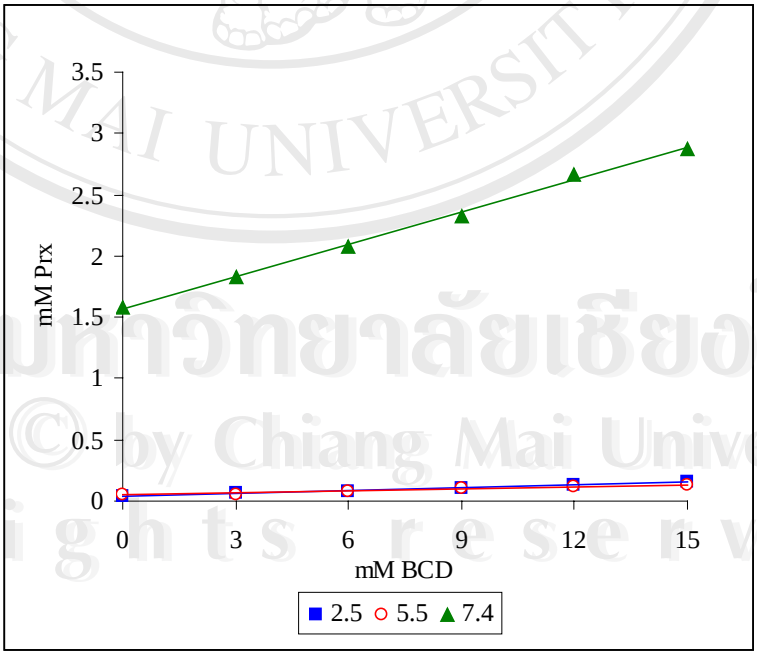

Figure 15 Phase solubility diagrams of piroxicam-BCD inclusion complex in solutions of varying pH values at 37° C

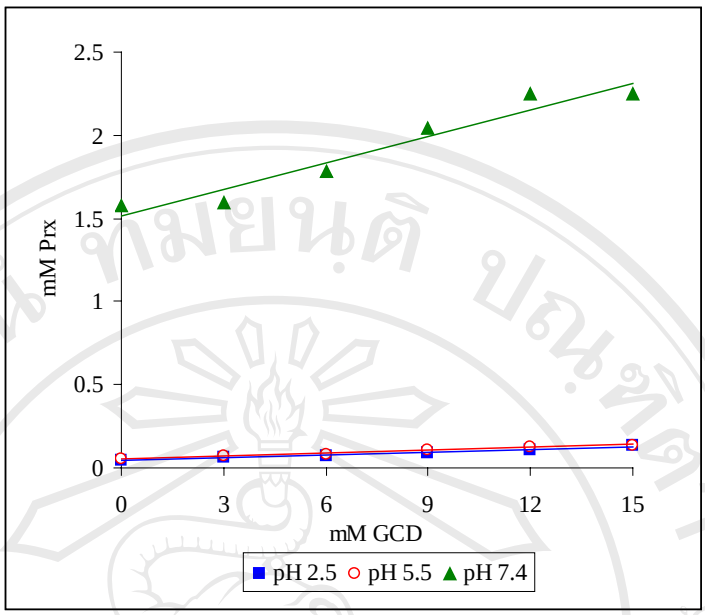

Figure 16 Phase solubility diagrams of piroxicam-GCD inclusion complex in solutions of varying pH values at 37° C

Table 12 Solubility of piroxicam in HPBCD and MeBCD solutions of varying pH values at 37° C

CD	mM	Prx (mM)		
		pH 2.5	pH 5.5	pH 7.4
HPBCD	0	0.045	0.056	1.578
	5	0.073	0.084	1.912
	10	0.099	0.094	2.486
	20	0.142	0.124	3.355
	50	0.265	0.252	5.555
	100	0.519	0.429	8.412
MeBCD	0	0.045	0.056	1.578
	5	0.074	0.082	1.866
	10	0.120	0.109	2.369
	20	0.194	0.169	3.206
	50	0.616	0.902	5.872
	100	3.012	2.494	9.794

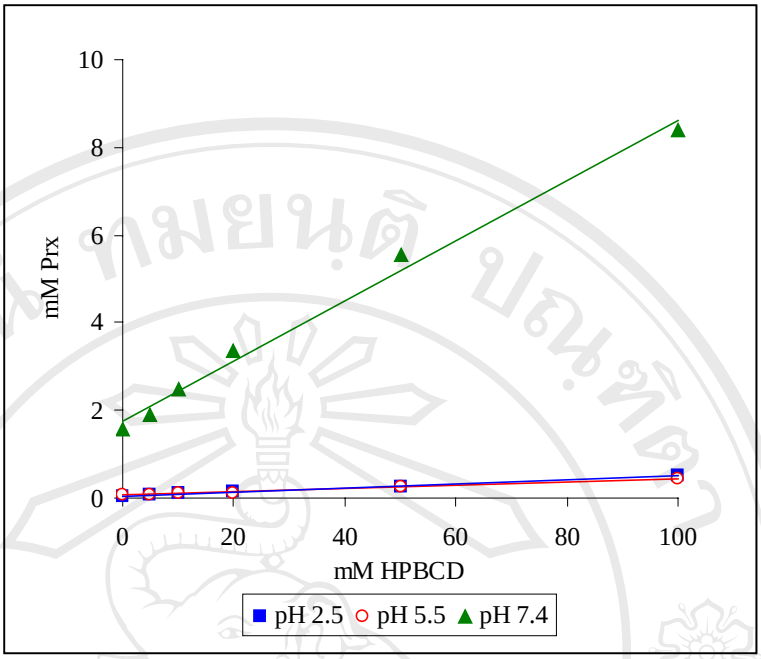

Figure 17 Phase solubility diagrams of piroxicam-HPBCD complex in solutions of varying pH values at 37° C

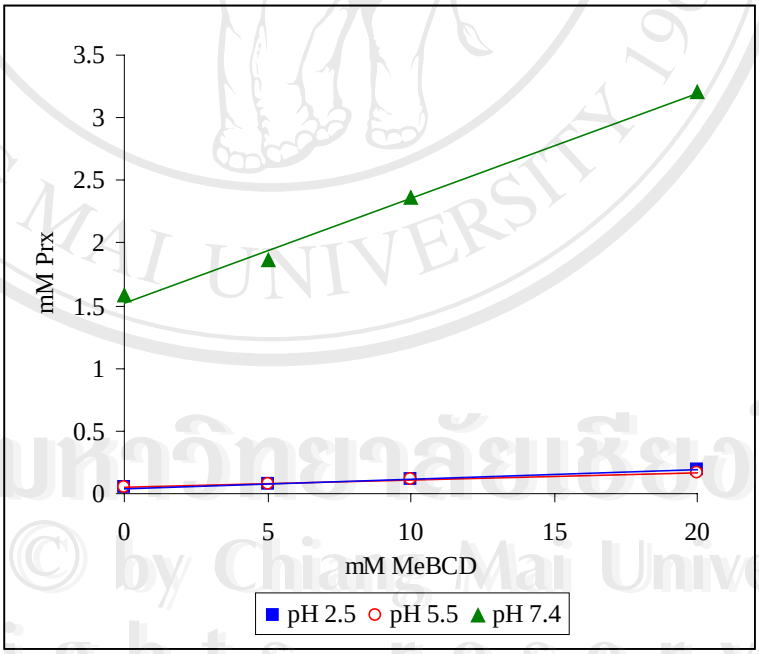

Figure 18 Phase solubility diagrams of piroxicam-MeBCD complex in solutions of varying pH values at 37°C

The phase solubility diagrams shown in Figure 9-12 are A_L-type irrespective of the CD types and pH values. The stability constant of the complex in each case was

thus calculated using the slope and the intrinsic solubility of the drug as previously described.

The effect of the pH on the solubility of the drug is clearly demonstrated for all CD types. The y-intercept and the slope of the solubility curves at pH 7.4 changed dramatically from those at pH 2.5 and 5.5. While the intrinsic solubility of the drug at pH 2.5 and 5.5 was not noticeably different, the solubility at pH 7.4 was nearly 30-fold higher. As the ionization of the drug plays important role on its solubility, in order to get more understanding on these findings, the extent of ionization at any particular pH value is then taken into consideration.

The pKa values of piroxicam reported in literatures are quite diverse; depending on the method of determination and the solvent system used. The pKa1 and pKa2 for the protonation of the enolic group and deprotonation of the 2-pyridyl group of piroxicam were 1.86 and 6.3 (Wiseman, et. al.,1976), 1.86 and 5.46 (Bernhard and Zimmermann, 1984), 1.90 and 5.26 (Tsai, et. al, 1993) and 1.80 and 5.1 respectively.

According to the experimental design, the pH value of 5.5 was chosen in order to mimic the pKa2 value of the drug, around this pH value, the ionization hardly takes place, resulting in the minimal solubility. The pH values of 2.5 and 7.4 were intentionally selected to obtain the condition of high and low pH values. These two values are approximately 2 pH units lower and higher than the pKa2, the increase in the drug solubility due to higher extent of ionization is generally anticipated. Accordingly, it is not unexpected to obtain the high solubility at pH 7.4 and the low solubility at pH 5.5. However, as a dibasic compound, piroxicam exhibits two distinct pKa values, the low solubility would be attained at the pH value around another pKa value. This fact explains a comparable solubility at pH 2.5 and that at pH 5.5.

This explanation could be supported by the recently published paper (Rozou, et.al., 2004) demonstrating the effect of pH on the molecular conformations of piroxicam. In acidic solution of pH less than 0.9, the drug exists as the protonated form whereas at the pH value between 0.9-7.0, the drug is in zwitterionic but, at different ratios. The anionic form predominantly occurs in the solution of pH higher than 7.0.

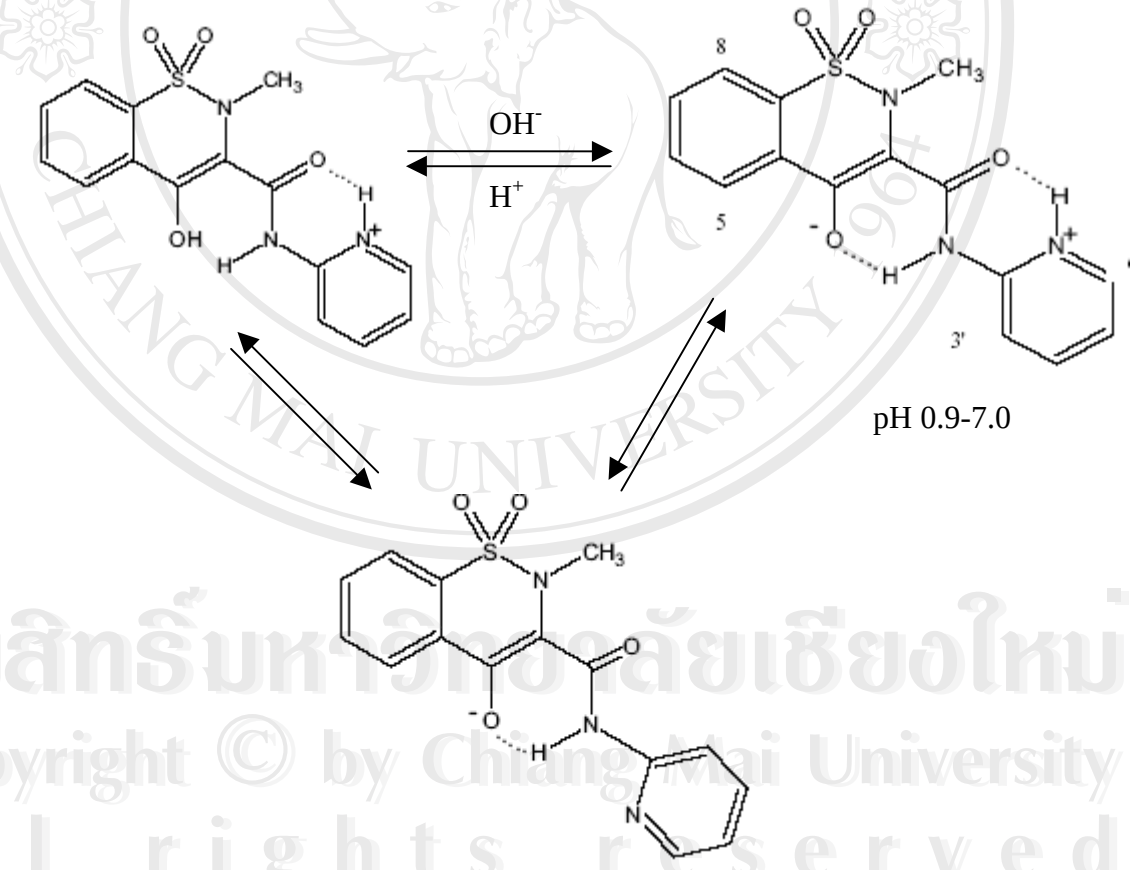

Table 13 summarized the regression equations of the solubility diagrams according with the linear regression coefficients, r^2 and the K values. The relationship

between the pH and the K values of all CD types is illustrated in Figure 19. The high r^2 value indicates the reliability of the K values obtained. It was found that the K values of the complexes irrespectively to the CD types decrease with increasing pH values. The significant effect of pH on the complex formation is demonstrated by the following MLR model.

$$K = -0.897pH^* - 0.127CDtype$$

$$R^2 = 0.820 \quad p<0.001$$

According to the MLR model, the negative regression coefficient substantiated the reduction of K values with the increasing pH. At any specific pH, the K values obtained from different CD types are not significantly different. The higher K values at low pH reveals that, the unionized drug forms more stable complexes with CDs than these ionized form.

It is more of interest that, at low pH, when higher K values were obtained, the total solubility of the drug is very low. And vice versa, at higher pH, the K value decreases but the solubility increases significantly. These findings notify that ionization plays more important role than complexation on the drug solubility enhancement.

Table 13 Stability constants of piroxicam-CDs complexes in solutions of varying pH values values at 37°C

CDs	pH	Equation	r^{2*}	K, M^{-1}
BCD	2.5	y = 0.0075x + 0.038	0.9820	167.2
	5.5	y = 0.0057x + 0.048	0.9578	102.7
	7.4	y = 0.0882x + 1.5615	0.9971	61.3
GCD	2.5	y = 0.0057x + 0.0408	0.9803	126.8
	5.5	y = 0.0064x + 0.050	0.9797	104.6
	7.4	y = 0.0531x + 1.5178	0.9432	35.5
HPBCD	2.5	y = 0.0047x + 0.0471	0.9981	104.5
	5.5	y = 0.0037x + 0.0582	0.9978	67.2
	7.4	y = 0.0686x + 1.7682	0.9914	46.7
MeBCD	2.5	y = 0.0076x + 0.042	0.9962	168.4
	5.5	y = 0.0057x + 0.0542	0.9987	102.1
	7.4	y = 0.037x + 1.6264	0.9657	24.4

r^{2*} Linear regression coefficient of phase solubility diagram.
x is molar concentration of CD, y is molar concentration of piroxicam

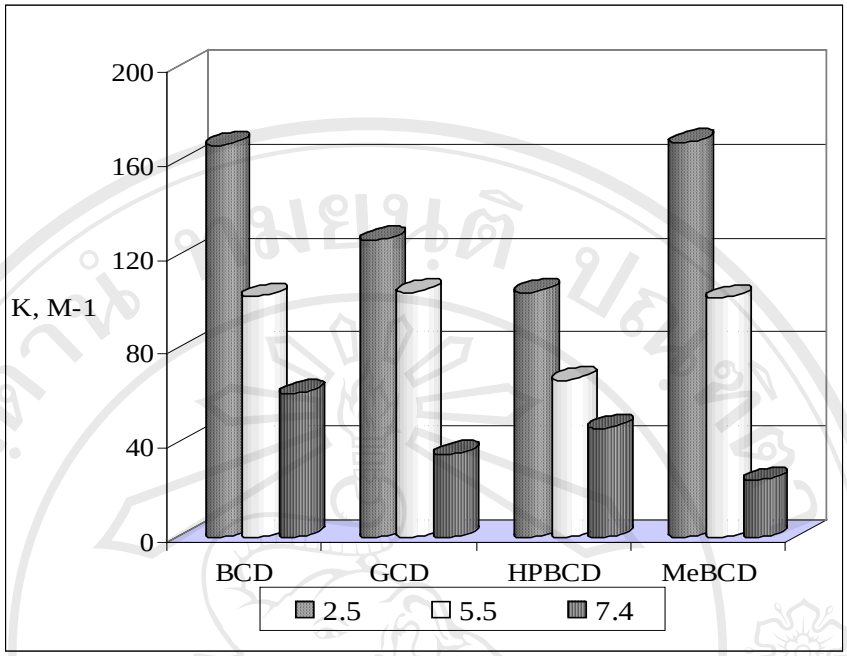

Figure 19 Stability constants, K of piroxicam-CD complexes, pH values: 2.5, 5.5 and 7.4

Table 14 shows the comparison of the K values of the piroxicam-CDs complexes in solution of different pH values. There is no doubt for the significant decrease in K values by increasing pH values for all CD types.

According to the MLR model, when both factors were considered simultaneously, it was shown that the complexation was not affected by the CD types. In other words, different CD types exhibit comparable K values at the same pH conditions. Nevertheless, when the comparison was made within any specific pH value, the significant difference of the K value obtained from different CDs was noticeable. For instance, at pH 7.4, the K values of piroxicam-BCD complex was substantially higher than the complexes formed by the other CDs. But, the significant difference of these K values was not clearly evidenced at lower pH values.

Based on the stability of the complexes, BCD is shown as the most satisfactory complex forming agent for piroxicam thorough a wide pH range. Whilst MeBCD

seems unfavorable especially for the preparations required maintaining at physiological pH.

Table 14 Comparison of the stability constants of piroxicam-CDs inclusion complexes in solutions of varying pH values at 37°C

CDs	pH	K, M^{-1}	Effect of pH*	Effect of CD type*
BCD	2.5	167.18	All CDs,	pH 2.5,
	5.5	102.74	$K_{pH\ 2.5} > K_{pH\ 5.5} > K_{pH\ 7.4}$	$K_{BCD} \sim K_{MeBCD} > K_{GCD} > K_{HPBCD}$
	7.4	61.31		
GCD	2.5	126.83		pH 5.5,
	5.5	104.55		$K_{BCD} \sim K_{MeBCD} \sim K_{GCD} > K_{HPBCD}$
	7.4	35.54		
HPBCD	2.5	104.47		pH 7.4,
	5.5	67.17		$K_{BCD} > K_{HPBCD} > K_{GCD} > K_{MeBCD}$
	7.4	46.68		
MeBCD	2.5	168.43		
	5.5	102.13		
	7.4	24.35		

* One-way ANOVA Post hoc range tests.
Significant and non-significant difference (~) at $p < 0.05$

3.2 Thermodynamic studies of meloxicam

3.2.1 Intrinsic solubility of meloxicam

Meloxicam is a weak acidic drug with a structure closely related to piroxicam. Similarly, ionization and solubility are drastically affected by pH. The effect of pH on the ionization and solubility of meloxicam was extensively investigated (Luger, et. al., 1996). In solution, four different ionic species of meloxicam are generally existing dependent on pH of the medium. In non-polar solvent, an enol form is present. Meloxicam zwitterion is observed in aqueous solutions of pH 7 or below. At very low pH, the cationic form can exist and an anionic species is predominant at pH 7.4 or higher. The ionic status as well as solubility, however, relates to the drug's pKa values. Different pKa values have been reported depending to the method of determination. From solubility-pH profile, the values of 4.35 and 1.29 were reported whereas the values of 4.18 and 1.09 were determined by UV spectral shift method (Tsai, et. al., 1993). Nevertheless, they were in comparable range. The solubility of meloxicam in water is lower compare to piroxicam. It is also more lipophilic than piroxicam throughout the whole pH range. The lowest solubility of meloxicam is observed at pH 2-3 where the drug solubility is less sensitive to pH change. A slightly increase in solubility is noted with decreasing pH value. But, on the opposite side, the solubility increase markedly by increasing pH. In pH range of 5-10, the solubility is the most sensitive to pH change

The pH values chosen in this study, 3.0 and 6.0, represent the pH values where the solubility is not affected by small changes of pH and fully affected respectively.

Due to the high sensitivity of the solubility to pH change, the pH of the solution was strictly controlled within the range of ± 0.01.

The intrinsic solubility of meloxicam in solutions pH 3.0 and pH 6.0 at different temperatures are summarized in Table 15. The values obtained at 25°C at pH 3.0 and 6.0 are in agreement with the values from the literature.

From the literature, the solubility of meloxicam in phosphate buffer solutions pH 2.99 and 5.99 after equilibrated for 20 minutes at 23°C were 0.001 and 0.077 mM respectively. Thus, the discrepancy between these values may arise from the differences in temperature and the equilibration time.

Table 15 Intrinsic solubility of meloxicam in solution pH 3.0 and 6.0 at various temperatures

Temperature,°C	Solubility, So			
	pH 3.0		pH 6.0	
	mcg/ml	mM	mcg/ml	mM
25	0.471	0.002	22.419	0.064
30	0.590	0.002	32.961	0.094
37	0.769	0.002	54.256	0.154
45	1.219	0.003	99.341	0.283

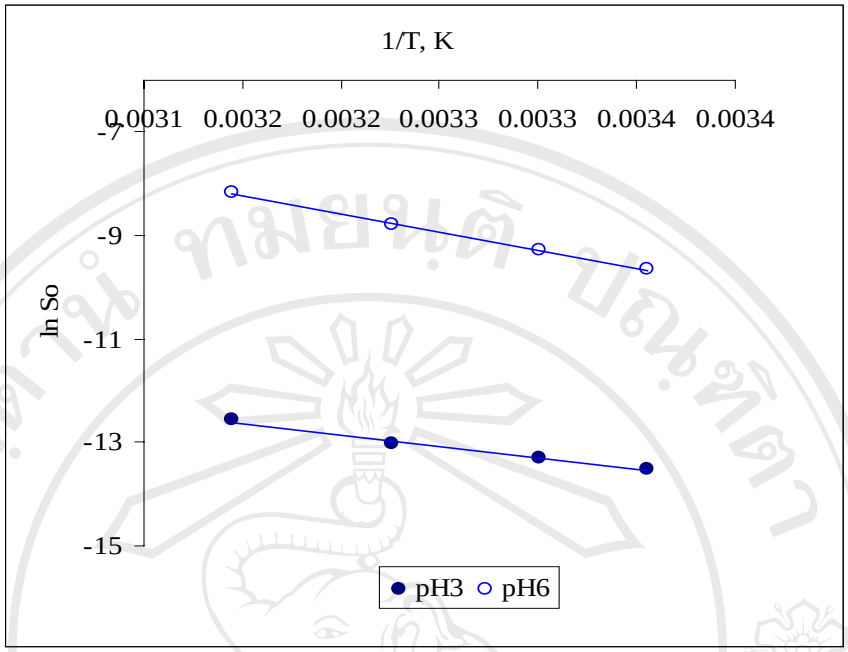

Figure 20 Solubility plot of meloxicam in solutions pH 3.and 6.0 at various temperatures

Figure 20 demonstrates the temperature-dependent solubility of meloxicam at pH 3.0 and 6.0 by Van't Hoff plot. From the slope of the plots, the heat of solution can be calculated. The regression equations, the regression coefficients and the heat of solution at particular pH value are shown in Table 16.

The results show that the heat of solution at pH 6.0 was 1.6 times lower than that of pH 3.0. This indicates that the dissolution process occurs readily at higher pH due to the higher degree of ionization.

The results also demonstrate that the solubility at pH 6.0 is more susceptible to temperature change than that at pH 3.0.

This finding implies that pH plays more important role than temperature on the solubility. At pH 3.0, the ratio of ionized to unionized drug is considerably smaller than that existing at higher pH. Even the amount of unionized species can be increased by increasing temperature; the apparent solubility was not appreciably

increased due to the limited degree of ionization. Oppositely, at pH 6.0, where the ionization can take place at higher extent, an increasing temperature leads to an increased amount of the unionized drug, in fact, it should be at the same extent to that exhibited at pH 3.0 but, the unionized drug occurs at higher pH can further subject to higher degree of ionization thus, resulting in the marked increase in the total solubility.

Table 16 Heat of solution, ΔH(So) of meloxicam in solutions pH 3.0 and 6.0

pH values	Van't Hoff equation	r^{2*}	ΔH(So), kJ/mol
3.0	y = -4433.7x + 1.33	0.9883	-36.9
6.0	y = -7022.8x + 13.90	0.9994	-58.4

3.2.2 Phase solubility diagrams of meloxicam-CD inclusion complexes in solution pH 3.0

Thermodynamic studies of meloxicam-CDs complexes were performed in solution pH 3.0 and pH 6.0 at 25° C, 30° C 37° C and 45° C. The CDs included in the study were BCD, GCD, HPBCD and HPGCD. The phase solubility diagrams at different temperatures of meloxicam-BCD, meloxicam-GCD, meloxicam-HPBCD and meloxicam-HPGCD in solution pH 3.0 are given in Figure 21-24 respectively. The corresponding regression equations obtained from the phase solubility curves, the regression coefficients and the stability constants were summarized in Table 17-20.

All phase solubility curves were characterized by A_L-type. (Higuchi and Connors, 1965). The linear relationship best fit between the drug concentrations and CD concentrations was substantiated by the high value of regression coefficient which was closed to one. This linear relationship accompanying by the slope values of less than one suggesting that a 1:1 stoichiometric ratio complex was formed. The phase solubility diagrams displayed temperature-dependent nature. The slope of the solubility curves at higher temperature was greater than that obtained at lower temperatures.

The stability constant in each case was calculated from the corresponding slope and the intrinsic solubility of the drug experimentally obtained. These values were compared graphically and statistically in Figure 25 and Table 21. The results will be discussed further.

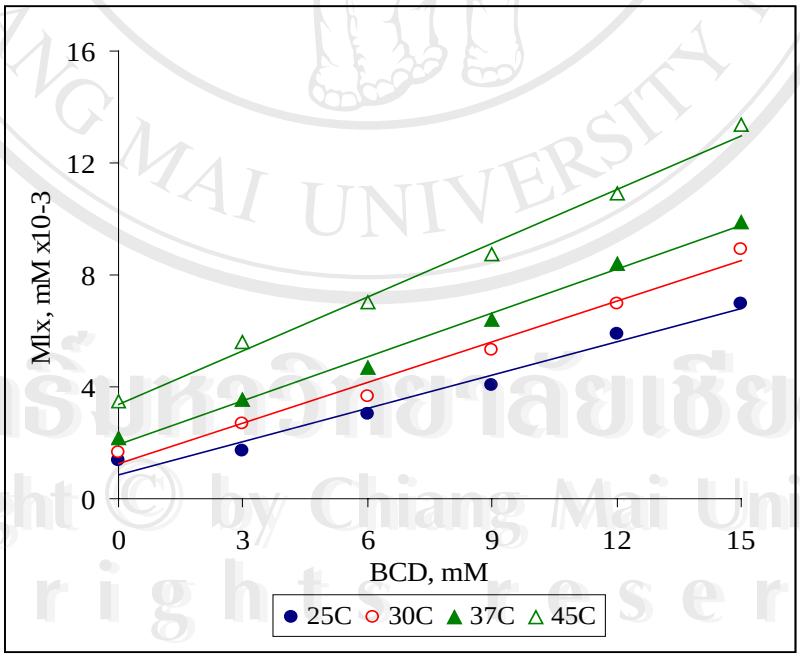

Figure 21 Phase solubility diagrams of meloxicam-BCD complexes in solution pH 3.0 at various temperatures

Table 17 Stability constants of meloxicam-BCD complexes in solution pH 3.0 obtained from phase solubility diagrams

T, °C	Equation(r^{2*})	K, M^{-1}	K, M^{-1} (Mean±SD)
25	y = 0.3889x + 0.9092 (0.9813)	290.3	295.4±6.5
	y = 0.3927x + 0.8646 (0.9762)	293.2	
	y = 0.4056x + 0.8234 (0.9685)	302.8	
30	y = 0.4820x + 1.2416 (0.9840)	286.7	287.7±1.1
	y = 0.4835x + 1.2529 (0.9839)	287.7	
	y = 0.4857x + 1.2418 (0.9792)	288.9	
37	y = 0.5064x + 1.9985 (0.9854)	231.4	237.8±10.0
	y = 0.5094x + 2.0593 (0.9934)	232.7	
	y = 0.5456x + 1.8273 (0.9931)	249.3	
45	y = 0.6496x + 3.3878 (0.9929)	187.3	184.4±2.8
	y = 0.6392x + 3.3758 (0.9930)	184.3	
	y = 0.63x + 3.3936 (0.9929)	181.7	

r^{2*} Linear regression coefficient of phase solubility diagrams
The phase solubility diagrams of each series are shown in Appendix B

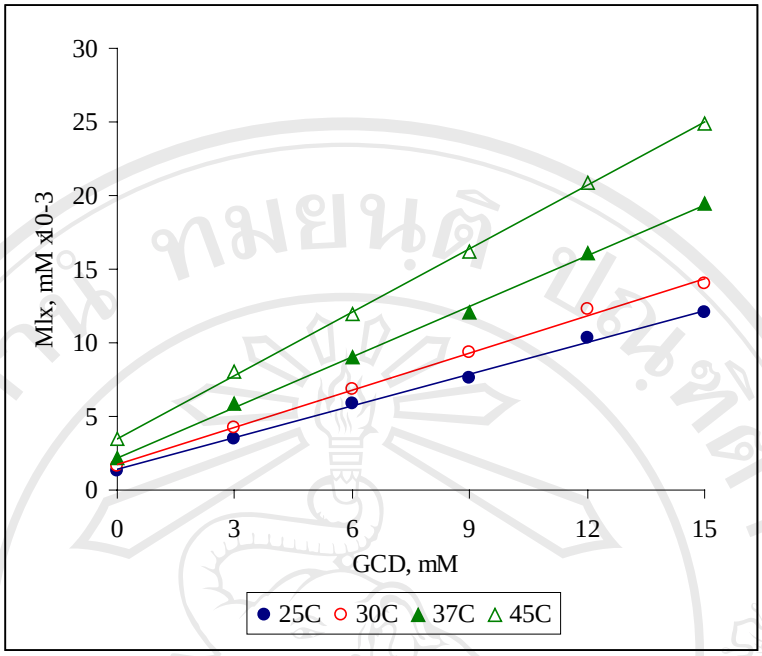

Figure 22 Phase solubility diagrams of meloxicam-GCD complexes in solution pH 3.0 at various temperatures

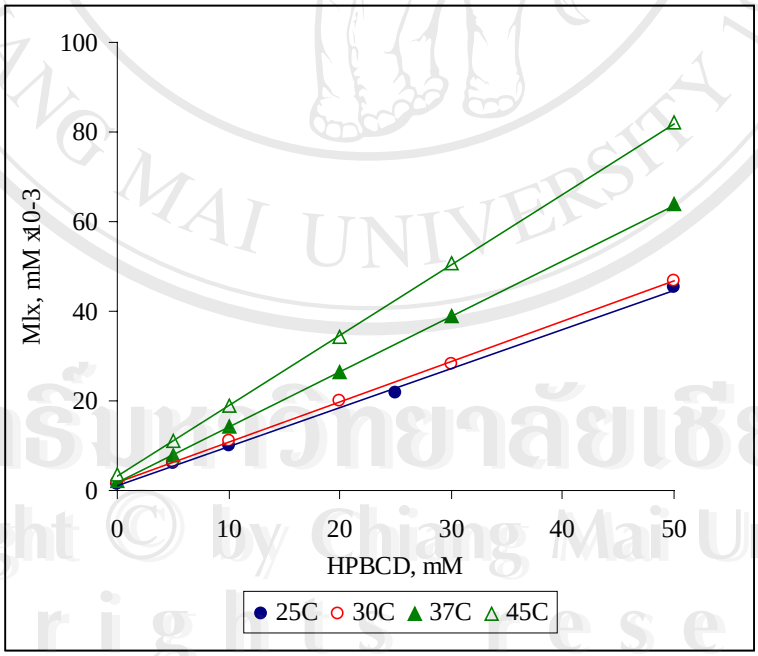

Figure 23 Phase solubility diagrams of meloxicam-HPBCD complexes in solution pH 3.0 at various temperatures

Table 18 Stability constants of meloxicam-GCD complexes in solution pH 3.0 obtained from phase solubility diagrams

T, °C	Equation(r^{2*})	K, M^{-1}	K, M^{-1} (Mean±SD)
25	y = 0.7229x + 1.4073 (0.9961)	539.9	540.2±0.4
	y = 0.7241x + 1.3605 (0.9978)	540.7	
	= 0.7226x + 1.3227 (0.9973)	539.9	
30	y = 0.8207x + 1.9198 (0.9929)	488.3	499.3±10.0
	y = 0.8429x + 1.7833 (0.9980)	501.6	
	y = 0.8536x + 1.5916 (0.9984)	507.9	
37	y = 1.1305x + 2.1305 (0.9977)	516.8	516.4±0.6
	y = 1.1284x + 2.1923 (0.9990)	515.6	
	y = 1.1303x + 2.1945 (0.9984)	516.7	
45	y = 1.4316x + 3.5697 (0.9996)	413.2	412.5±0.6
	y = 1.4283x + 3.5234 (0.9996)	412.2	
	y = 1.4279x + 3.4344 (0.9995)	412.1	

r^{2*} Linear regression coefficient of phase solubility diagram

The phase solubility diagrams of each series are shown in Appendix B

Table 19 Stability constants of meloxicam-HPBCD complexes in solution pH 3.0 obtained from phase solubility diagrams

T, °C	Equation(r^{2*})	K, M^{-1}	K, M^{-1} (Mean±SD)
25	y = 0.8842x + 0.6178 (0.9989)	660.4	652.5±8.0
	y = 0.8738x + 1.1196 (0.9981)	652.7	
	y = 0.8629x + 1.6377 (0.9960)	644.5	
30	y = 0.8955x + 1.8657 (0.9997)	532.9	531.5±1.3
	y = 0.8914x + 1.9567 (0.9997)	530.4	
	y = 0.8925x + 2.0613 (0.9995)	531.1	
37	y = 1.2028x + 2.2511 (0.9998)	549.9	564.7±15.9
	y = 1.2309x + 2.0052 (0.9999)	562.7	
	y = 1.272x + 1.5857 (0.9995)	581.6	
45	y = 1.5702x + 3.0865 (0.9999)	453.2	454.9±2.8
	y = 1.571x + 3.2363 (1.00)	453.4	
	y = 1.587x + 3.1656 (0.9998)	458.1	

r^{2*} coefficient of linear regression line of phase solubility diagram
The phase solubility diagrams of each series were shown in Appendix B

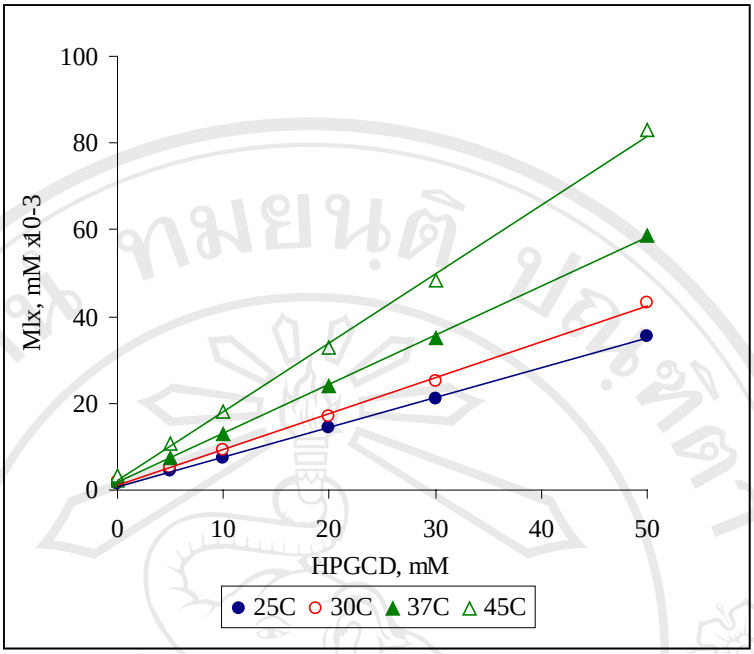

Figure 24 Phase solubility diagrams of meloxicam-HPGCD complexes in solution pH 3.0 at various temperatures

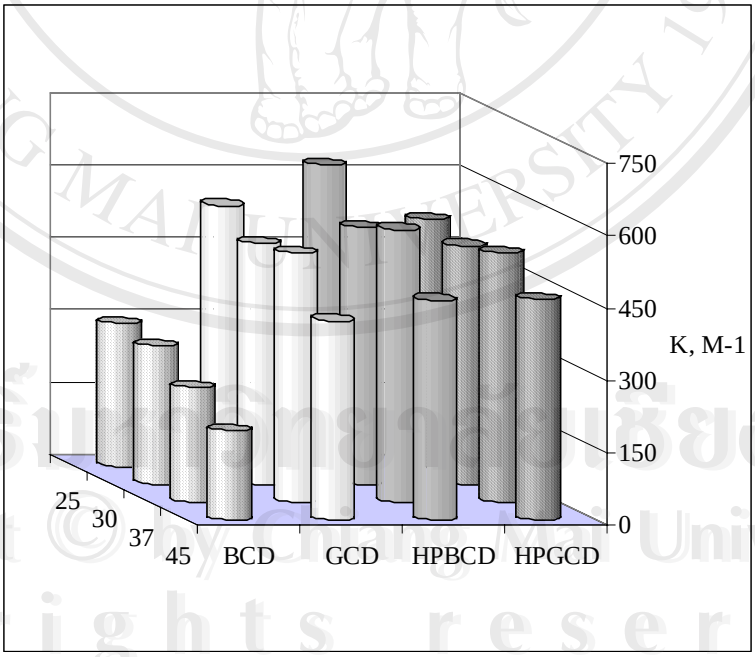

Figure 25 Comparison of the stability constants of meloxicam-CD complexes in solution pH 3.0 at different temperatures

Table 20 Stability constants of meloxicam-HPGCD complexes in solution pH 3.0 obtained from phase solubility diagrams

T, °C	Equation(r^{2*})	K, M^{-1}	K, M^{-1} (Mean±SD)
25	y = 0.6817x + 0.9249 (0.9988)	509.1	511.4±2.1
	y = 0.6857x + 0.8615 (0.9993)	512.1	
	y = 0.6871x + 0.7849 (0.9978)	513.1	
30	y = 0.814x + 1.2451 (0.9993)	484.3	493.6±10.1
	y = 0.8271x + 1.0459 (0.9989)	492.1	
	y = 0.8477x + 0.5965 (0.9977)	504.4	
37	y = 1.1265x + 1.5715 (0.9991)	514.9	517.1±2.0
	y = 1.132x + 1.6872 (0.9995)	517.5	
	y = 1.1349x + 1.7863 (0.9997)	518.8	
45	y = 1.5927x + 2.2977 (0.9979)	459.7	457.7±2.9
	y = 1.5902x + 2.3481 (0.9984)	459.0	
	y = 1.5742x + 2.5237 (0.9988)	454.4	

r^{2*} coefficient of linear regression line of phase solubility diagram
The phase solubility diagrams of each series are shown in Appendix B

Table 21 Comparison of the stability constants (K) of meloxicam-CDs complexes in solution pH 3.0 at various temperatures

CDs	T,°C	K, M^{-1}	Effect of temperature*	Effect of CD type*
BCD	25	295.4	$K_{25} \sim K_{30} > K_{37} > K_{45}$	**25°C,**
	30	287.7		$K_{HPBCD} > K_{GCD} > K_{HPGCD} > K_{BCD}$
	37	237.8		
	45	184.4		
GCD	25	540.2	$K_{25} > K_{37} > K_{30} > K_{45}$	**30°C,**
	30	499.3		$K_{HPBCD} > K_{GCD} \sim K_{HPGCD} > K_{BCD}$
	37	516.4		
	45	412.5		
HPBCD	25	652.5	$K_{25} > K_{37} > K_{30} > K_{45}$	**37°C,**
	30	531.5		$K_{HPBCD} > K_{HPGCD} \sim K_{GCD} > K_{BCD}$
	37	564.7		
	45	454.90		
HPGCD	25	511.4	$K_{25} \sim K_{37} > K_{30} > K_{45}$	**45°C,**
	30	493.6		$K_{HPBCD} \sim K_{HPGCD} > K_{GCD} > K_{BCD}$
	37	517.1		
	45	457.7		

* One-way ANOVA Post hoc range tests.
Significant and non-significant difference (~) at $p < 0.05$

The comparison of the stability constants values illustrated in Table 21 and Figure 25 shows that the K values of the complexes prepared from all CD types were essentially temperature-dependent. The values decrease with increasing temperature.

As shown in Figure 25, the K values of the drug and the three CDs namely GCD, HPBCD and HPGCD at 30°C and 37°C are significantly different ($p<0.05$).

The CD types also have high impact on the complex formation. Independent on temperatures, the K value of meloxicam-HPBCD complexes is significantly higher than the others implying that the unionized drug preferably forms more stable complexes with HPBCD rather than the other CDs. The meloxicam-BCD complex shows the lowest K value compared to the others. However, this finding was in contrary to that obtained from piroxicam-CDs complex. In that case, the most stable complex was obtained with BCD irrespective to pH conditions.

3.2.3 Phase solubility diagrams of meloxicam-CD inclusion complexes in solution pH 6.0

The thermodynamic studies of meloxicam-CDs in solution pH 6.0 at varying temperatures were also performed. The phase solubility diagrams of the complexes formed between the drug and BCD, GCD, HPBCD and HPGCD at different temperatures are shown in Figure 26-29 respectively. The corresponding regression equations of the phase solubility diagrams, the regression coefficients and the stability constants calculated are summarized in Table 22-25.

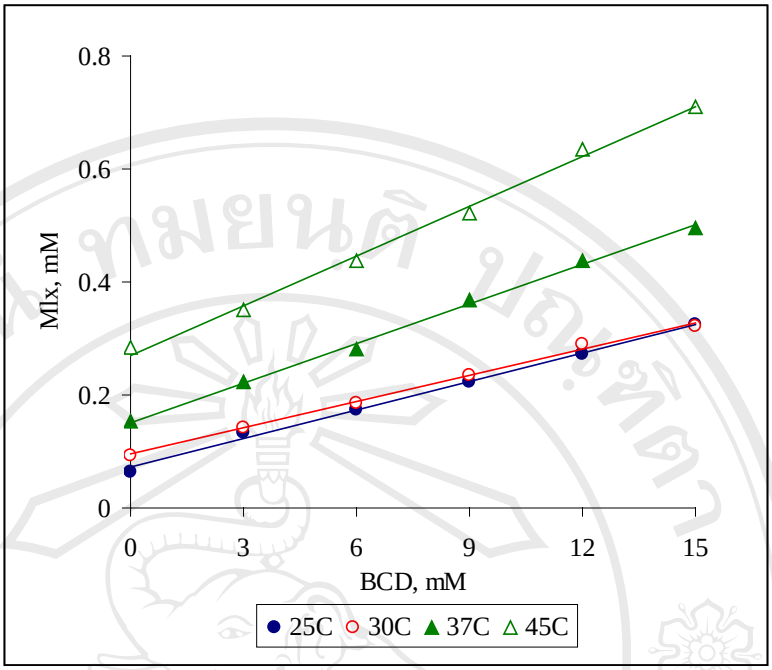

Figure 26 Phase solubility diagrams of meloxicam-BCD complexes in solution pH 6.0 at various temperatures

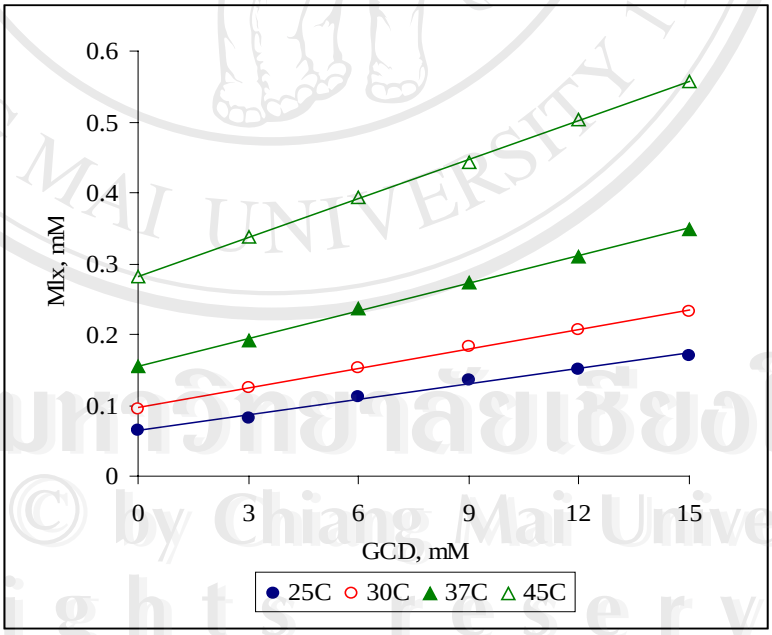

Figure 27 Phase solubility diagrams of meloxicam-GCD complexes in solution pH 6.0 at various temperatures

Table 22 Stability constants of meloxicam-BCD complexes in solution pH 6.0 obtained from phase solubility diagrams

T, °C	Equation(r^{2*})	K, M^{-1}	K, M^{-1} (Mean±SD)
25	y = 0.0167x + 0.0733 (0.9970)	266.2	269.4±4.3
	y = 0.0168x + 0.0727 (0.9964)	267.8	
	y = 0.0172x + 0.0697 (0.9940)	274.3	
30	y = 0.0154x + 0.0954 (0.9972)	166.8	167.8±2.9
	y = 0.0158x + 0.0913 (0.9968)	171.2	
	y = 0.0153x + 0.0969 (0.9969)	165.6	
37	y = 0.0237x + 0.1463 (0.9970)	157.2	154.1±2.7
	y = 0.023x + 0.1548 (0.9963)	152.5	
	y = 0.023x + 0.1547 (0.9965)	152.5	
45	y = 0.029x + 0.2716 (0.9955)	105.6	106.5±1.9
	y = 0.0289x + 0.2736 (0.9940)	105.3	
	y = 0.0298x + 0.2657 (0.9973)	108.6	

r^{2*} linear regression coefficient of phase solubility diagram

The phase solubility diagrams of each series are shown in Appendix B

Table 23 Stability constants of meloxicam-GCD complexes in solution pH 6.0 obtained from phase solubility diagrams

T, °C	Equation(r^{2*})	K, M^{-1}	K, M^{-1} (Mean±SD)
25	y = 0.0075+ 0.0632 (0.9869)	118.4	114.2±4.0
	y = 0.0072x + 0.065 (0.9998)	113.7	
	y = 0.007x + 0.0643 (0.9847)	110.5	
30	y = 0.0096x + 0.0918 (0.9966)	103.3	98.6±4.1
	y = 0.0090x + 0.0978 (0.9983)	96.8	
	y = 0.0089x + 0.0996 (0.9979)	95.7	
37	y = 0.0133x + 0.1495 (0.9951)	87.3	85.3±2.4
	y = 0.0126x + 0.1579 (0.9980)	82.6	
	y = 0.0131x + 0.1565 (0.9963)	85.9	
45	y = 0.0184x + 0.2818 (0.9989)	66.3	65.9±1.3
	y = 0.0179x + 0.2876 (0.9992)	64.5	
	y = 0.0186x + 0.2786 (0.9964)	67.0	

r^{2*} Linear regression coefficient of phase solubility diagram
The phase solubility diagrams of each series are shown in Appendix B

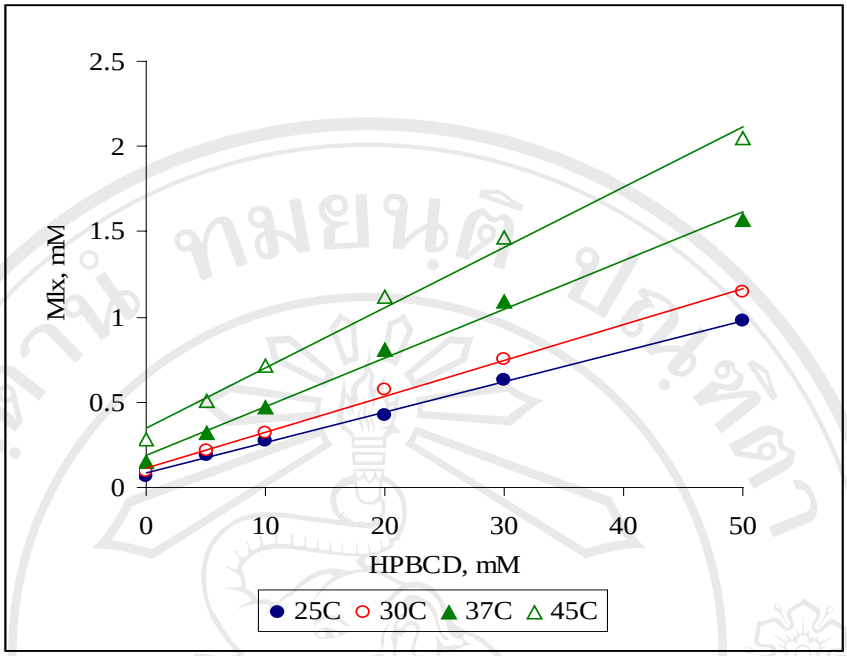

Figure 28 Phase solubility diagrams of meloxicam-HPBCD Complexes in solution pH 6.0 at various temperatures

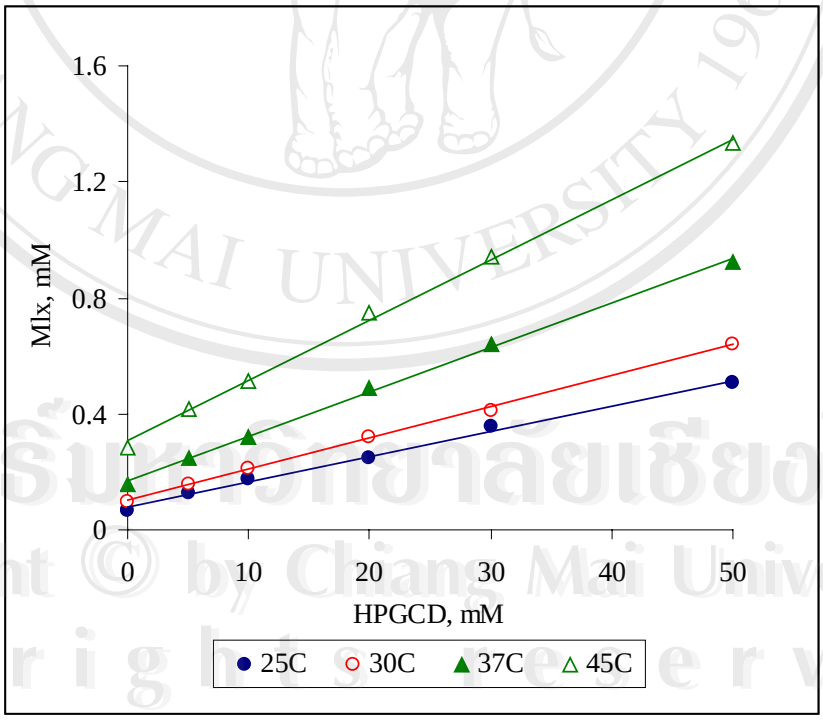

Figure 29 Phase solubility diagrams of meloxicam-HPGCD complexes in solution pH 6.0 at various temperatures

Table 24 Stability constants of meloxicam-HPBCD complexes in solution pH 6.0 obtained from phase solubility diagrams

T, °C	Equation(r^{2*})	K, M^{-1}	K, M^{-1} (Mean±SD)
25	y = 0.0169x+ 0.0886 (0.9961)	269.4	286.8±15.8
	y = 0.0182x + 0.0793 (0.9982)	290.6	
	y = 0.0188x + 0.0757 (0.9985)	300.3	
30	y = 0.0209x + 0.1154 (0.9926)	227.6	228.7±1.1
	y = 0.021x + 0.1158 (0.9968)	228.7	
	y = 0.0211x + 0.1128 (0.9991)	229.8	
37	y = 0.0282x + 0.1861 (0.9929)	187.9	190.9±3.5
	y = 0.0285x + 0.1909 (0.9942)	190.0	
	y = 0.0292x + 0.1863 (0.9961)	194.8	
45	y = 0.0355x + 0.3428 (0.9924)	130.2	129.4±0.7
	y = 0.0352x + 0.351 (0.9922)	129.1	
	y = 0.0352x + 0.3503 (0.9907)	129.1	

r^{2*} linear regression coefficient of phase solubility diagram
The phase solubility diagrams of each series are shown in Appendix B

Table 25 Stability constants of meloxicam-HPGCD complexes in solution pH 6.0 obtained from phase solubility diagrams

T, °C	Equation(r^{2*})	K, M^{-1}	K, M^{-1} (Mean±SD)
25	y = 0.0088x+ 0.0769 (0.9961)	139.2	138.1±0.9
	y = 0.0087x + 0.0784 (0.9954)	137.6	
	y = 0.0087x + 0.0788 (0.9932)	137.6	
30	y = 0.0108x + 0.097 (0.9989)	116.4	116.0±0.6
	y = 0.0107x + 0.1004 (0.9988)	115.3	
	y = 0.0108x + 0.1028 (0.9978)	116.5	
37	y = 0.0153x + 0.1628 (0.9976)	100.6	101.3±1.2
	y = 0.0153x + 0.1705 (0.9986)	100.6	
	y = 0.0156x + 0.1693 (0.9989)	102.6	
45	y = 0.0207x + 0.3081 (0.9974)	74.8	75.4±1.1
	y = 0.0212x + 0.3014 (0.9974)	76.6	
	y = 0.0207x + 0.3084 (0.9982)	74.8	

r^{2*} Linear regression coefficient of phase solubility diagram
The phase solubility diagrams of each series are shown in Appendix B

The complex formation of meloxicam-CDs in solution pH 6.0 is temperature-dependent. Moreover, the K values of the complexation decrease with increasing temperature.

Table 26 shows the statistically significant difference ($p<0.05$) of the K values obtained from different CDs. Considering the effect of CD types, BCD and its derivatives form more stable complex with meloxicam than the other two GCD types at all temperatures, whereas the K values obtained form HPBCD and BCD are not significantly different. This finding is also illustrated in Figure 30.

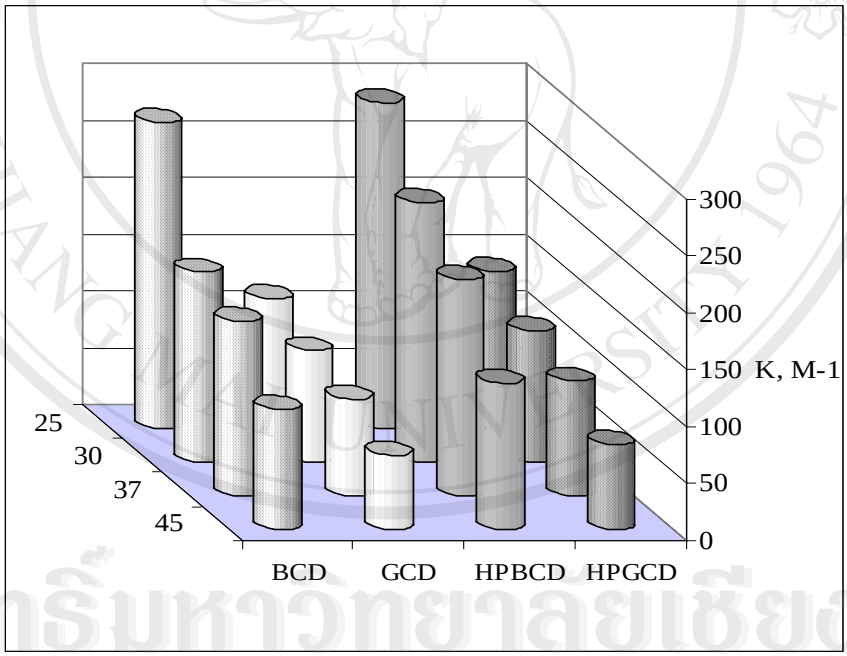

Figure 30 Stability constants, K of meloxicam-CD complexes in pH 6.0 at different temperatures

Table 26 Comparison of the stability constants of meloxicam-CDs in solution pH 6.0 at various temperatures

CDs	T,°C	K, M^{-1}	Effect of temperature*	Effect of CD type*
BCD	25	269.4		
	30	167.8	$K_{25} > K_{30} > K_{37} > K_{45}$	
	37	154.0		
	45	106.5		
GCD	25	114.2		
	30	98.6	$K_{25} > K_{30} > K_{37} > K_{45}$	
	37	85.3		
	45	65.9		**All temperatures,**
HPBCD	25	286.8		$K_{HPBCD} \sim K_{BCD} > K_{HPGCD} \sim K_{GCD}$
	30	228.7	$K_{25} > K_{30} > K_{37} > K_{45}$	
	37	190.9		
	45	129.4		
HPGCD	25	138.1		
	30	116.0	$K_{25} > K_{30} > K_{37} > K_{45}$	
	37	101.3		
	45	75.4		

* One-way ANOVA Post hoc range tests.
Significant and non-significant difference (~) at $p < 0.05$

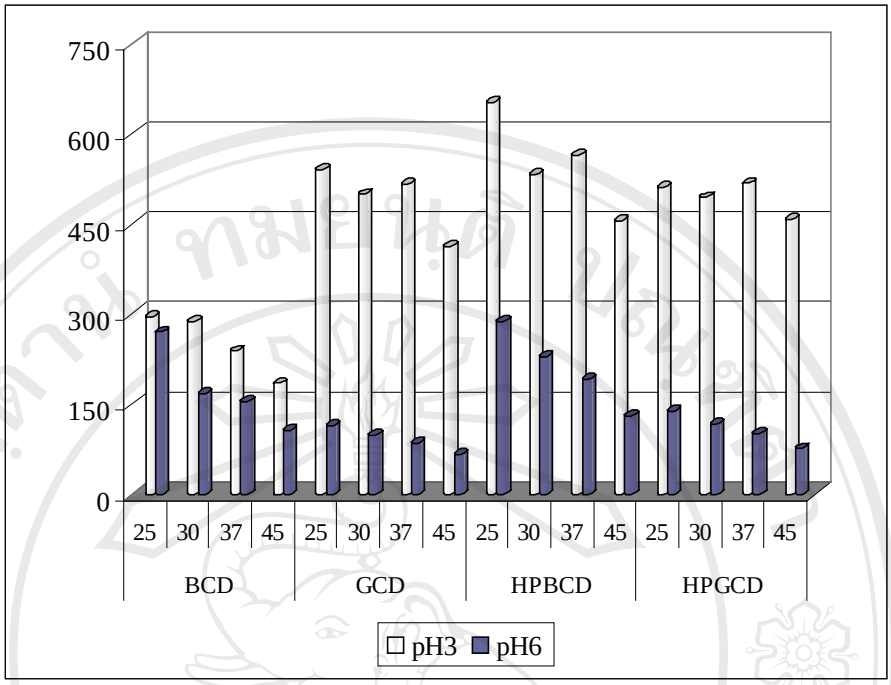

Figure 31 Temperature- , pH- and CD type-dependence of the stability constants of meloxicam-CD complexes in pH 3.0 and 6.0 at various temperatures

Figure 31 displays graphical comparison of the K values of all complexes as a function of temperature and pH. For a certain CD type and at a specific temperature, the K values at pH 3.00 were substantially higher than those at pH 6.00. This finding affords the fact that the CD cavity behaves like organic medium providing a non-polar environment for any guest molecule to accommodate. The inclusion complex between the unionized drug and various CDs was thus favorably occurred than the ionized drug. Furthermore, when the temperature and pH value were considered simultaneously, the CDs can be simply categorized into two groups according to the impact of those factors. The first group containing BCD, whose K values show high susceptibility to temperature change, but low susceptibility to pH changes. Contrarily, the second group including GCD, HPBCD and HPGCD is characterized by low sensitivity of their K values to temperature changes especially at pH 3.0 but, high

sensitive to pH changes at all temperatures. For instance, the K values of meloxicam-GCD complex observed at pH 6.0 are more than 5-fold substantially higher than the values obtained at pH 3.0. Although the temperature-dependent nature of the K values is significantly evident, the dependency was somewhat low. It turns out that the second CD group interacts strongly with unionized meloxicam while the complex formation occurs less when the drug is charged. This finding might be attributed by interaction existing between charged-drug and the substituted hydroxypropyl groups which impaired the inclusion complex formation. In contrast, the complex formation between the drug and BCD was somewhat unaffected by pH change. Based on the pH tolerance, BCD shows advantage over the other CDs for wide pH range applications. However, when a consideration is made on the magnitude of K values, it should be suggested that HPBCD is a proper CD for meloxicam-CD inclusion complex instead of BCD. The degree of temperature dependency of all complexes was further demonstrated by the MLR model and the Van't Hoff plots.

As the temperature, pH value and the CD type influence the complex formation, the following multiple linear regression model was developed in order to verify the relative significance of these factors.

$$K = -0.833pH^* + 0.218CDtype^* - 0.217T^*$$

$$R^2 = 0.782, \quad ^*p < 0.001$$

It was confirmed that all factors have significant impact on the stability of the complex. The pH value of the solution is the most important factor, due to the highest regression coefficient value, followed by the CD type and temperature. The effect of temperature and CD types is comparable but in reverse direction. The negative value

of the coefficients implies that the K values decrease with increasing in pH and temperature. The increasing tendency of the K values is that of BCD, GCD, HPBCD and HPGCD, respectively.

3.2.4 Thermodynamic parameters of meloxicam-CD inclusion complexes

According to the temperature-dependent nature of the complex formation, the thermodynamic parameters of the process were calculated from association constants of the complex using the Van't Hoff plot as follows:

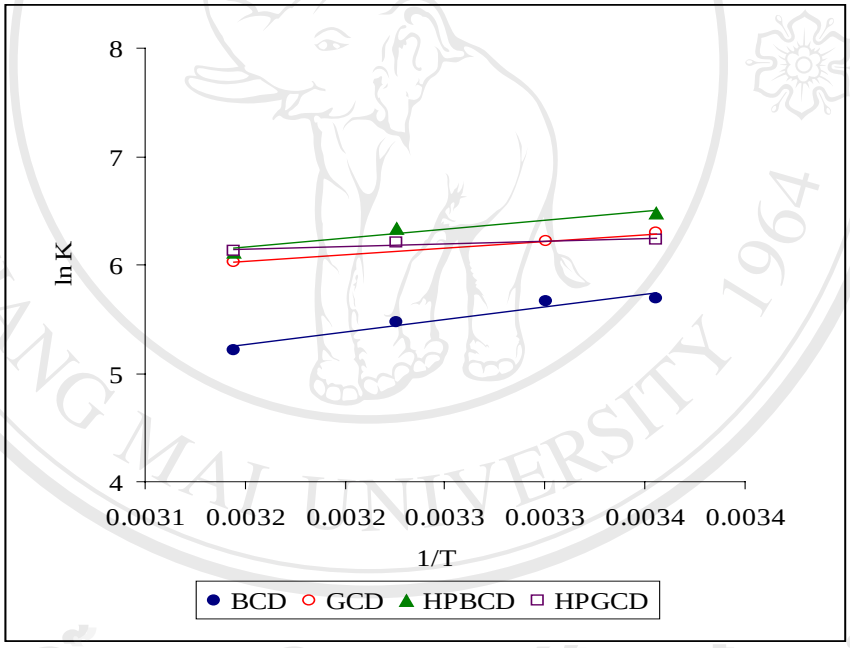

Figure 32 Van't Hoff plot of meloxicam-CDs complexes at pH 3.0

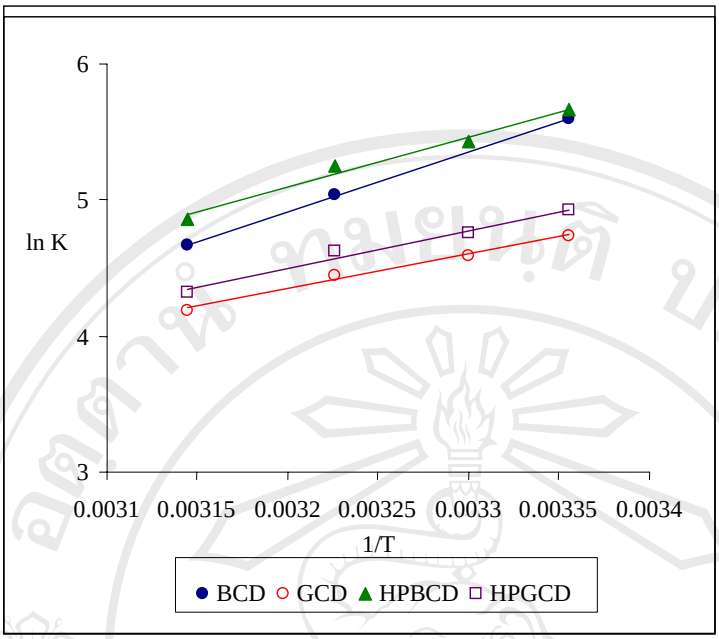

Figure 33 Van't Hoff plot of meloxicam-CD complexes at pH 6.0

Figure 32 and Figure 33 show the Van't Hoff plots of the meloxicam-CDs complexes in solution at pH 3.0 and at pH 6.0 respectively. These plots demonstrate the linearly decrease of the stability of the complexes in function of temperature. At higher temperature, the dissociation of the complexes occurs easily, thus it decreases the stability of the complexes. It is due to the fact that the molecular motion becomes greater with the rise of temperature. Hence, higher temperature was unfavorable for the formation of inclusion complex.

The best linear fit of the plots is assured by the high value of linear coefficients shown in Table 27. The relative slope of each line signifies the degree of temperature-dependency of the complex formation. In Figure 32, the relative higher slope was denoted. This is in agreement with the previous suggestion that at pH 3.0, the meloxicam-BCD complex is more susceptible to temperature changes than the others.

From the slope of Van't Hoff plots, the thermodynamic parameters, ΔG, ΔH and ΔS of the complex formation were calculated using the relationships previously mentioned on the thermodynamic study of piroxicam. These parameters are summarized in Table 27.

Table 27 Thermodynamic parameters of meloxicam-CDs complexes in solution at pH 3.0 and at pH 6.0

pH	CDs	ΔH, kJ/mole	ΔG, kJ/mole	ΔS, J/mole/K	r^{2*}
3.0					
	BCD	-19.2	-14.1	-16.8	0.9482
	GCD	-10.5	-15.8	17.2	0.9990
	HPBCD	-13.8	-16.2	7.9	0.9403
	HPGCD	-4.3	-15.8	37.4	0.9961
6.0	BCD	-36.5	-13.1	-75.9	0.9998
	GCD	-21.1	-11.4	-31.5	0.9904
	HPBCD	-30.2	-13.5	-54.4	0.9833
	HPGCD	-23.0	-11.9	-36.2	0.9830

r^{2*} Linear regression coefficient of Van't Hoff plot

According to Table 27, the decrease in the free energy is signified by the negative ΔG values are observed in all cases. This strongly suggests that the inclusion processes take place spontaneously. The negative ΔH values also indicate that the

inclusion complex formation is exothermic and enthalpy-driven. This is a common situation for the formation of the inclusion complexes between CDs and various guest molecules.

Fundamentally, the entropy should increase upon the inclusion complex formation. The positive ΔS value essentially caused by the increase of the freedom of motion of the enthalpy-rich water molecules after being replaced from the CD cavity by the drug molecule. However, it is common to obtain negative ΔS values. The negative entropy change may be resulted by the following possibilities: firstly, due to the restricted motion of the guest molecule within the CD cavity after being included. This likely occurs either in the case when the CD cavity is quite limited for the quest molecule to reside or the existence of somewhat strong binding interaction between the guest and the CD molecule. Secondly, negative entropy change is contributed by enthalpy-entropy compensation phenomenon. This is a general feature when a specific linear relationship between the enthalpy change and entropy change exists. The change in entropy ultimately depends on the predominantly involved phenomenon.

At pH 6.0, the ΔS values are negative in all cases indicating the reduction of entropy upon the complex formation. In addition to enthalpy-entropy compensation phenomena, it is also suggested that the interaction between charged-drug and the hydroxyl group located at the periphery of CD cavity occurs which results in a decrease in freedom of motion of the guest molecule within the CD cavity.

3. 3 Preparation of solid complexes

The solid complexes of piroxicam and meloxicam were prepared by different methods using different CD types. In the case piroxicam, the CDs used were BCD, GCD HPBCD and MeBCD. The complexes were prepared at 1:1, 1:2 and 2:1 molar ratio. The CDs used for meloxicam-CD complex preparation were BCD, GCD, HPBCD and HPGCD. The complexes were prepared at 1:1 molar ratio only. The method of preparation applied for both drugs were physical mixing, kneading method, co-evaporation method and co-lyophilization method. The products obtained from each method were designated as PM, KN, COE and COL respectively.

The outer appearance the complexes obtained depends on the property of CD and the preparation methods as following

Complex	CDs	Description
PM	BCD, GCD	yellow, crystalline power
	HPBCD, MeBCD	yellow, amorphous-like powder
KN	All CDs	yellow, dense crystalline powder
COE	All CDs	yellow, crystalline powder
COL	All CDs	yellow, fluffy powder

The color intensity of piroxicam-CD complexes also depend on the molar ratio of the drug and CD. For instance, the 1:2 complex is more pale yellow powder than the 2:1 complex.

Among the methods of preparation, kneading is a simple and low cost method, because the process involves less sophisticated equipments and organic solvents. It

can be easily scaled up for industrial applications, using common mixing devices. However, this method is generally less effective than the others. The completeness of the inclusion complex formation depends on the mechanical stress and the time of mixing. The co-evaporation and co-lyophilization method provides higher extent of the drug-CD interaction. Moreover, low energetic crystalline product or in many cases, the amorphous complex is obtained. The dissolution rate and/or the solubility of the drug are therefore substantially improved by dual effects. These two methods possess main drawback of being rather expensive especially for mass production and in some cases organic solvents are needed. Therefore, it is not considered as a “Green method” for industrial application.

The percentages of yield of the solid complexes shown in Table 28 were satisfactory. The weight of the products was recorded after the sieving process. The percentage of recovery of the complexes is over 80 for all methods of preparation. However, these values obtained from laboratory scale of preparation, for which the process can be easily controlled.

Table 28 The percentage of yield of the solid complexes

Drug	Method	Molar ratio	% Yield of prepared complexes of CD type*				
			BCD	GCD	HPBCD	MeBCD	HPGCD
Prx	KN	1:1	86.74	83.64	83.86	82.76	-
		1:2	84.22	85.28	83.53	83.46	-
		2:1	84.53	85.86	84.22	85.50	-
	COE	1:1	83.45	82.67	81.89	82.45	-
		1:2	84.08	83.75	82.35	82.58	-
		2:1	82.54	82.72	83.26	82.74	-
	COL	1:1	82.11	83.34	81.15	80.45	-
		1:2	83.32	82.66	82.53	88.82	-
		2:1	80.44	81.37	80.59	80.76	-
Mlx	KN	1:1	88.64	81.15	83.78	-	84.18
	COE	1:1	87.89	82.74	86.48	-	83.84
	COL	1:1	81.00	86.32	82.16	-	83.23

* The weight was recorded after the complex was sieved.

3.4 Characterization of solid complexes

The inclusion complexes of piroxicam–CDs as well as meloxicam-CDs in the solid state was characterized by dissolution studies, powder X-ray diffractometry, differential scanning calorimetry, Fourier-transformed infrared spectroscopy and near infrared spectroscopy. These techniques could provide meaningful evidences of the existence of the inclusion complex formation.

3.4.1 Dissolution studies

The in vitro dissolution studies of the intact drugs, the physical mixtures and the complexes were performed at 37±0.5 °C using USP II, paddle method. The dissolution medium used for piroxicam and its complexes was distilled water, whereas the simulated gastric fluid without enzyme was used for meloxicam. The particle size of the samples was controlled within 150-180μm. The dissolution profile of each sample was followed up to 90 minutes.

In addition to dissolution profiles, the dissolution parameters used to characterize the dissolution behaviors of the complexes are the percentage of the dissolution efficiency up to 30 minutes (%DE30) and the time required for dissolving 50% of the drug ($t_{50\%}$).

The %DE30 was calculated from the area under the dissolution curve (AUC) at the corresponding time interval in this case up to 30 minutes of dissolution process. This parameter has been extensively applied in dissolution studies because it can represent the rate and the extent of dissolution which relates to the area under the curve of the drug concentration in plasma after being absorbed (Khan, 1975).

The dissolution profiles and the dissolution parameters were used to compare the CD types, the method of preparation, as well as the molar ratio on the dissolution behaviors of drug and the corresponding complexes.

3.4.1.1 Dissolution studies of piroxicam-CD inclusion complexes

A. Comparison of methods of preparation

The dissolution profiles of piroxicam compared to the physical mixture

and the piroxicam-BCD inclusion complexes prepared by different methods at 1:1, 1:2 and 2:1 molar ratio are shown in Figure 34-36. It is found that the dissolution behavior (the rate and the extent of dissolution of the drug) markedly increased by complex formation irrespective to the molar ratios and methods of preparation applied. Except, the 1:1 COE complex whose dissolution profile is comparable to that of the physical mixture as illustrated in Figure 34.

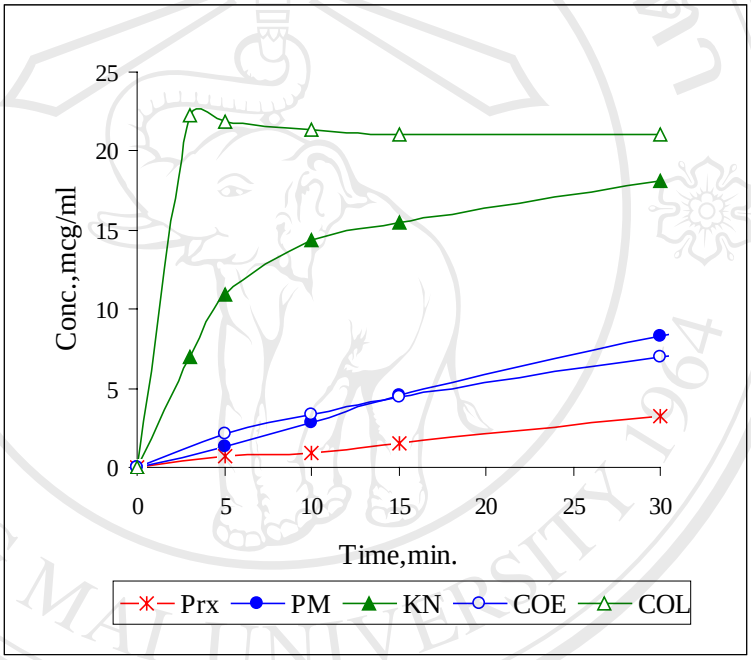

Figure 34 Dissolution profiles of piroxicam in distilled water From intact drug (Prx), 1:1 molar ratio of Prx: BCD physical mixture, PM and inclusion complexes prepared by kneading, KN; co-evaporation, COE and co-lyophilization, COL

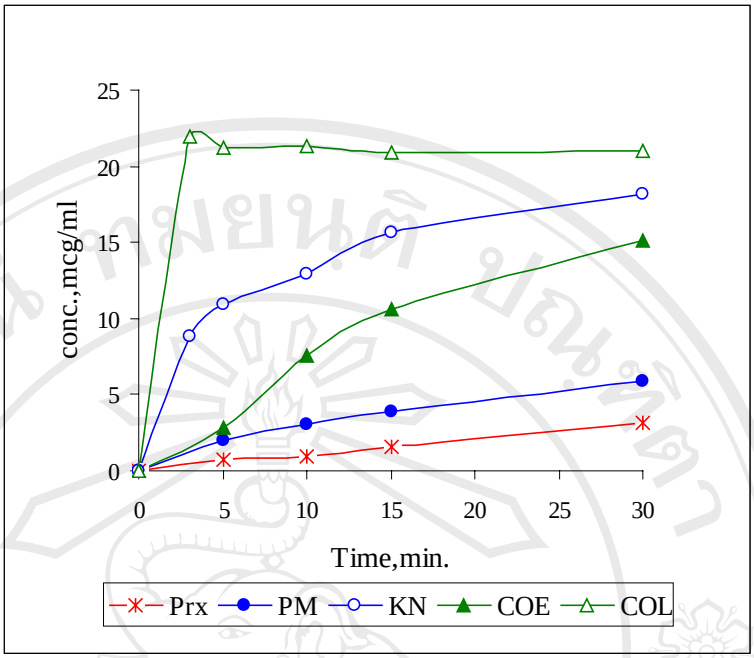

Figure 35 Dissolution profiles of piroxicam in distilled water from intact drug (Prx), 1:2 molar ratio of Prx:BCD physical mixture, PM and the inclusion complexes COE and co-lyophilization, COL

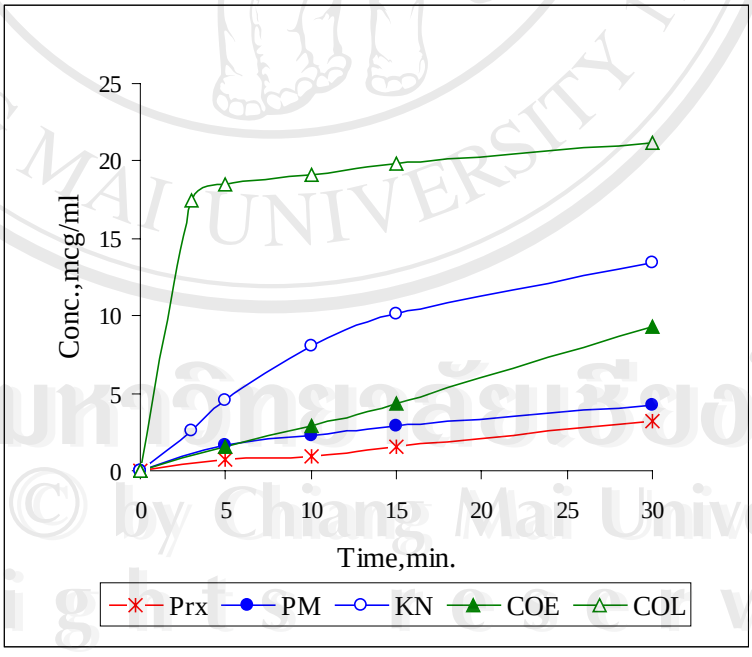

Figure 36 Dissolution profiles of piroxicam in distilled water from intact drug (Prx), 2:1 molar ratio of Prx:BCD physical mixture, PM and the inclusion complexes initially prepared by kneading, KN; co-evaporation, COE; and co-lyophilization, COL

The dissolution parameters of piroxicam-BCD inclusion complexes from the dissolution profiles shown in Figures 34-36 are illustrated in Table 29.

Table 29 Dissolution parameters of piroxicam in distilled water from intact drug (Prx), binary mixtures of Prx:BCD; physical mixture, PM and inclusion complexes initially prepared by kneading, KN; co-evaporation, COE and co-lyophilization, COL (Mean±SD; n=3)

	Prx:BCD	AUC 0-30min	%DE30	$t_{50\%}$ (min.)
Prx	1:0	214.9±7.57	7.17±0.25	>30
PM	1:1	577.2±21.04	19.24±0.70	>30
KN	1:1	1886.2±32.12	62.87±1.07	< 30
COE	1:1	558.5±34.5	18.62±1.15	>30
COL	1:1	2731.3±46.79	91.04±1.6	< 30
PM	1:2	489.4±18.80	16.31±0.63	>30
KN	1:2	1882.7±24.64	62.76±0.82	< 30
COE	1:2	1221.8±31.80	40.73±1.06	< 30
COL	1:2	2713.4±36.91	90.45±1.23	< 30
PM	2:1	359.2±19.64	11.98±0.66	>30
KN	2:1	1193.6±26.27	39.79±0.88	< 30
COE	2:1	613.3±27.73	20.44±0.92	>30
COL	2:1	2525.3±40.52	84.18±1.35	< 30

Based on the %DE30 values summarized in Table 29, it is clearly shown that all piroxicam-BCD binary mixtures exhibit the better dissolution behaviors than those of

the intact drug. The COL complex shows the highest dissolution efficiency. The %DE30 value is as high as 90% for 1:1 and 1:2 complexes, whereas it was only 60% and lower exhibited by KN and COE complexes respectively. The analysis of variances by LSD tests shows that the differences in the dissolution efficiency among the complex types are ranked in order of COL>KN>COE>PM. The $t_{50\%}$ also signifies that the COL and KN complexes dissolved faster than the other complexes when they have contact with the medium.

The enhancement of the dissolution resulted for the drug-CD-complexes is mainly due to the inclusion of the whole molecule or even the nonpolar part of the drug molecule in the CD cavity. Those hydrophobic parts are thus covered by the hydrophilic outer surface of CD molecules. As a consequence, the interaction between the drug and the aqueous medium is substantially increased. Moreover, the reduction of the crystallinity of the drug upon the complex formation process as well as the improvement of the wettability of the drug particles by the local solubilizing effect are responsible for the dissolution enhancement.

The method of complex preparation generally reduces the crystallinity of the drug to some extent. For instance, the complete loss of crystallinity of the drug by lyophilization process is well-documented. This is also evidenced in this study by the DSC and X-ray diffractometry. It is the explanation for the difference of the dissolution efficiency obtained from different complexes presented above.

It is worthy to note that the physical mixture, prepared by simple mixing could markedly increase the dissolution efficiency of the drug. The %DE30 of the intact drug and its physical mixture is statistically significantly different ($p<0.05$). As the inclusion phenomenon was not evidenced, the dissolution enhancement can be

explained by the following mechanisms: firstly, it was due to the local solubilizing effect of the CD when readily dissolved, which provides the hydrophilic microenvironment surrounding the drug particles. This leads to the improvement of the wettability as well as of the solubility of the drug. The second mechanism is due to the occurrence of the *in situ* complex formation when both are immediately soluble in the medium (Lin and Kao, 1989; Moyano et al., 1997).

The dissolution profiles of piroxicam-GCD complexes prepared by different methods at 1:1, 1:2 and 2:1 molar are illustrated in Figure 37-39 followed by the calculated dissolution parameters in Table 30.

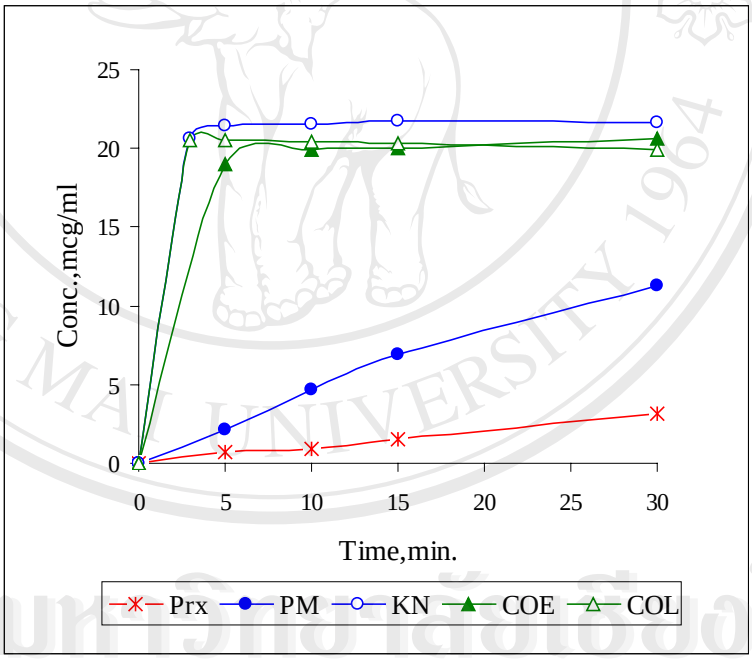

Figure 37 Dissolution profiles of piroxicam in distilled water from intact drug (Prx), 1:1 molar ratio of Prx: GCD physical mixture, PM; and the inclusion complexes initially prepared by kneading, KN; co-evaporation, COE and co-lyophilization, COL

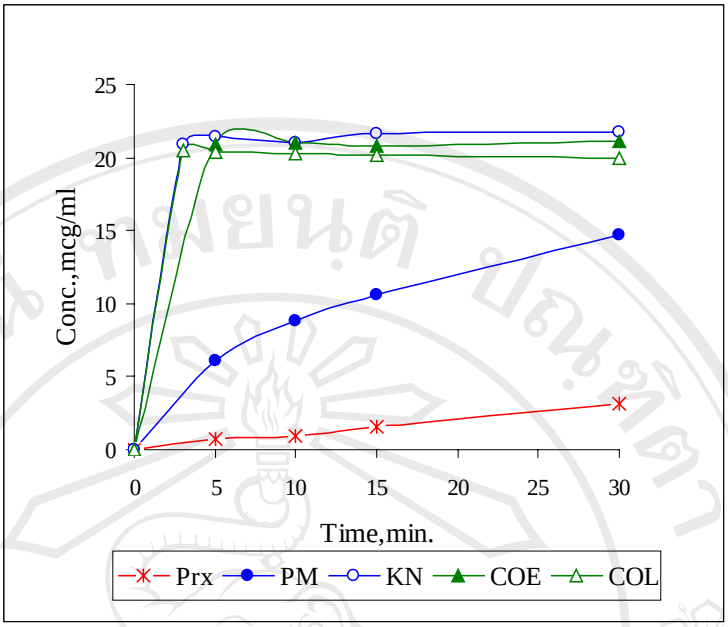

Figure 38 Dissolution profiles of piroxicam in distilled water from intact drug (Prx), 1:2 molar ratio of Prx: GCD physical mixture, PM and the inclusion complexes initially prepared by kneading, KN; co-evaporation, COE and co-lyophilization, COL

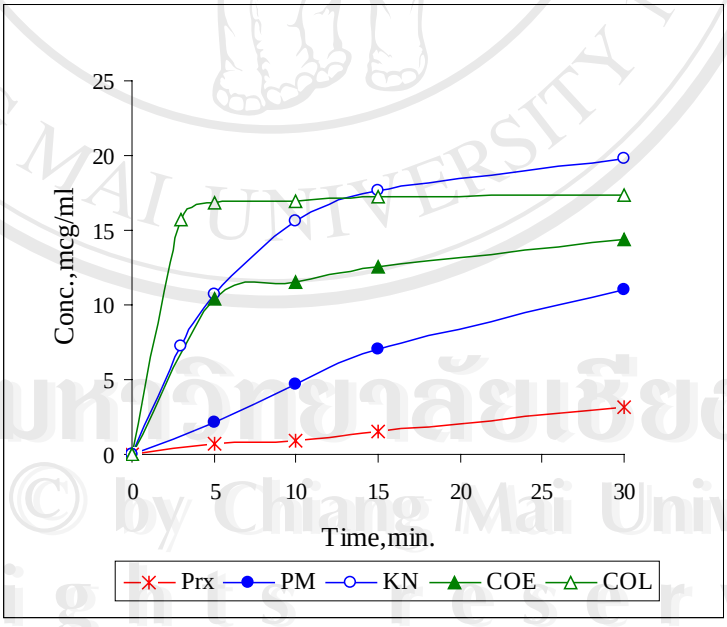

Figure 39 Dissolution profiles of piroxicam in distilled water from intact drug (Prx), 2:1 molar ratio of Prx: GCD physical mixture, PM and the inclusion complexes initially prepared by kneading, KN; co-evaporation, COE and co-lyophilization, COL

Table 30 Dissolution parameters of piroxicam in distilled water from intact drug (Prx), binary mixture of Prx: GCD; physical mixture, PM and inclusion complexes initially prepared by kneading, KN; co-evaporation, COE and co-lyophilization, COL (Mean±SD; n=3)

	Prx:GCD	AUC 0-30min	%DE30	$t_{50\%}$ (min.)
Prx	1:0	214.9±7.57	7.17±0.25	>30
PM	1:1	844.4±22.51	28.15±0.75	>30
KN	1:1	2762.5±43.96	92.08±1.46	< 30
COE	1:1	2471.1±37.45	82.37±1.25	< 30
COL	1:1	2600.4±44.45	86.68±1.48	< 30
PM	1:2	1308.8±33.04	43.63±1.10	< 30
KN	1:2	2753.3±37.81	91.78±1.26	< 30
COE	1:2	2589.8±36.72	86.33±1.22	< 30
COL	1:2	2587.1±41.69	86.24±1.39	< 30
PM	2:1	843.6±20.77	28.12±0.69	>30
KN	2:1	2064.7±33.94	68.82±1.13	< 30
COE	2:1	1544.6±30.02	51.49±1.00	< 30
COL	2:1	2183.9±34.32	72.80±1.14	< 30

The dissolution profiles illustrated in Figure 37-39 accompanied by the dissolution parameters in Table 30 shows that the method of preparation also plays an important role on the dissolution behaviors of the complexes prepared from GCD. The physical mixture, as well as the complexes showed substantially higher dissolution efficiency than the intact drug. The diversity in the dissolution efficiency

among the complexes still exists but in different order of piroxicam-BCD complexes. Using the same statistical technique of comparison as previous mentioned ($p<0.05$), the dissolution efficiency of the complexes is ranked as follows: KN >COL ~COE > PM. The complex prepared by kneading method shows the highest dissolution efficiency, whereas a non-significant difference was observed for COL and COE complexes. An interesting result is that the piroxicam-GCD complexes exhibit better drug dissolution than those prepared from BCD. This is evidenced by the higher value of %DE30 and $t_{50\%}$ which shows that the 50% of the drug dissolved could be attained before 30 minutes.

The dissolution profiles of piroxicam-HPBCD complexes prepared by different methods at 1:1, 1:2 and 2:1 molar are illustrated in Figure 40-42, respectively. The dissolution parameters obtained from these dissolution profiles are summarized in Table 31.

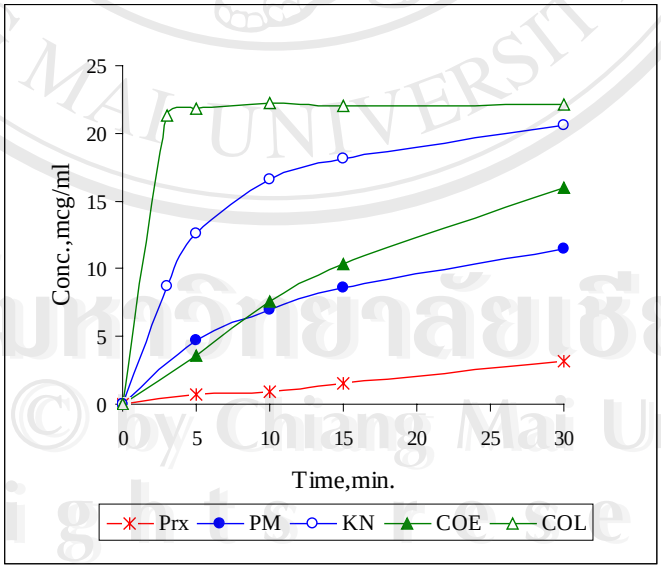

Figure 40 Dissolution profiles of piroxicam from intact drug (Prx), 1:1 molar ratio of Prx:HPBCD physical mixture, PM and the inclusion complexes prepared by kneading, KN; co-evaporation, COE and co-lyophilization, COL

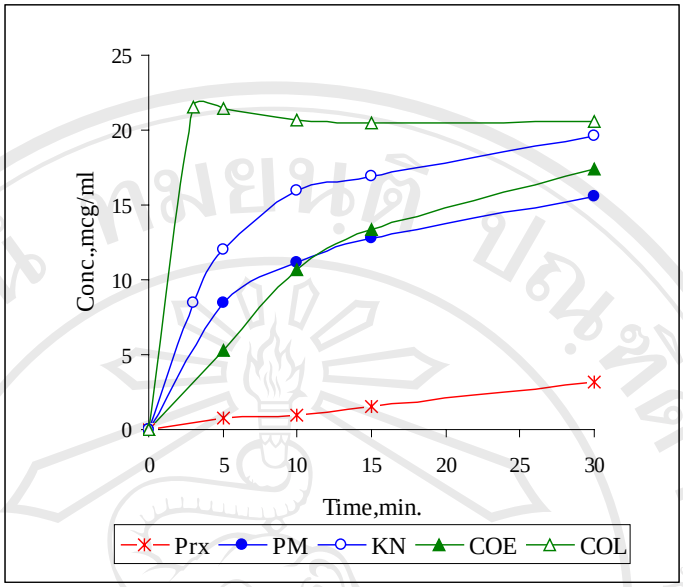

Figure 41 Dissolution profiles of piroxicam from intact drug (Prx), 1:2 molar ratio of Prx:HPBCD physical mixture, PM and the inclusion complexes prepared by kneading, KN; co-evaporation, COE and co-lyophilization, COL

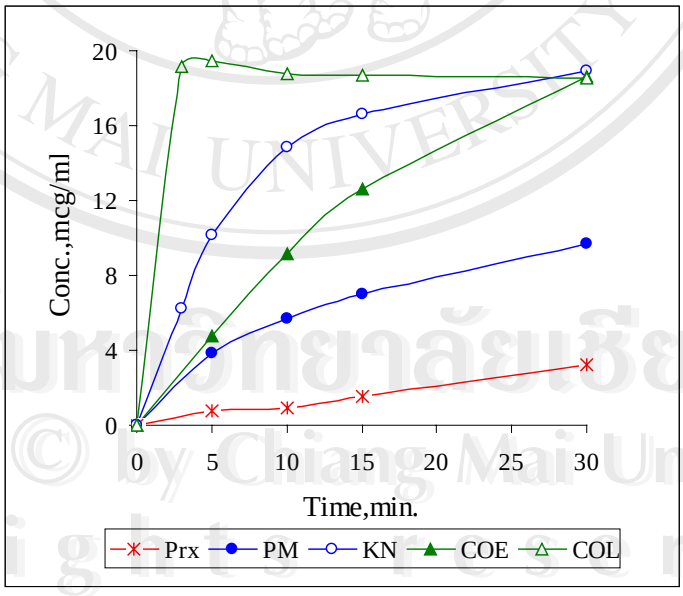

Figure 42 Dissolution profiles of piroxicam from intact drug (Prx), 2:1 molar ratio of Prx:HPBCD physical mixture, PM and the inclusion complexes prepared by kneading, KN; co-evaporation, COE and co-lyophilization, COL

Table 31 Dissolution parameters of piroxicam in distilled water from intact drug (Prx), binary mixtures of Prx: HPBCD; physical mixture, PM; and inclusion complexes initially prepared by kneading, KN; co-evaporation, COE and co-lyophilization, COL (Mean±SD; n=3)

	Prx:HPBCD	AUC 0-30min	%DE30	$t_{50\%}$ (min.)
Prx	1:0	214.98±7.57	7.17±0.25	>30
PM	1:1	1034.53±29.89	34.48±0.99	< 30
KN	1:1	2181.01±38.94	72.70±1.30	< 30
COE	1:1	1254.56±46.45	41.82±1.55	< 30
COL	1:1	2822.15±38.54	94.07±1.28	< 30
PM	1:2	1541.46±31.84	51.38±1.06	< 30
KN	1:2	1836.6±33.15	61.22±1.10	< 30
COE	1:2	1549.24±33.25	51.64±1.11	< 30
COL	1:2	2664.43±36.30	88.81±1.21	< 30
PM	2:1	855.58±25.68	28.52±0.86	>30
KN	2:1	1952.38±32.95	65.08±1.10	< 30
COE	2:1	1510.6±31.66	50.35±1.06	< 30
COL	2:1	2413.28±36.83	80.44±1.23	< 30

From the dissolution profiles illustrated in Figure 40-42 and the dissolution parameters shown in Table 31, it is demonstrated that the complex prepared by lyophilization method exhibits the highest dissolution efficiency followed by KN complex, COE complex and the physical mixture. The dissolution of the drug from these binary mixtures is significantly better than that of the intact drug. These findings

are essentially similar to those obtained from the prepared complexes using natural CDs. By statistical comparison, the rank on the dissolution efficiency of different complexes were COL>KN>COE>PM, respectively.

In the same pattern of presentation, the dissolution profiles of piroxicam-MeBCD complexes prepared by different methods at 1:1, 1:2 and 2:1 molar ratio are illustrated in Figure 43-45. The dissolution parameters obtained from these profiles are summarized in Table 32.

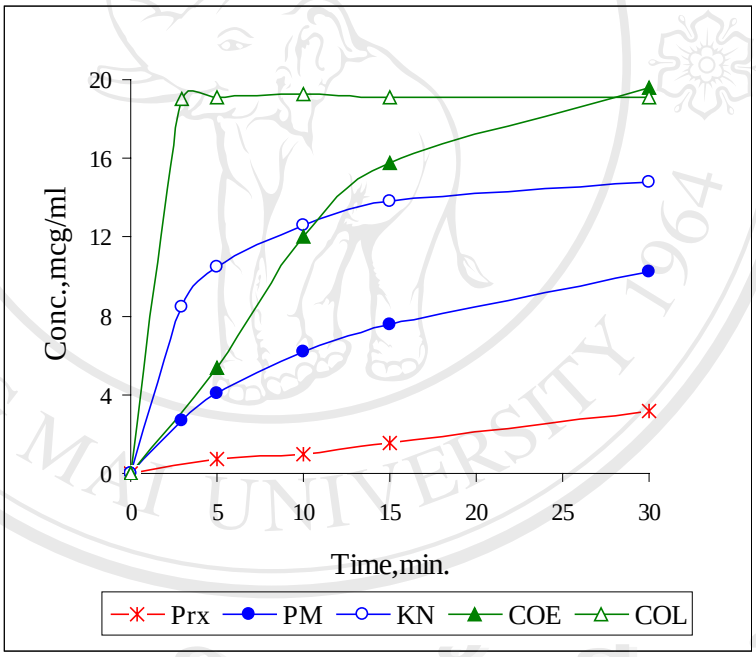

Figure 43 Dissolution profiles of piroxicam in distilled water from intact drug (Prx), 1:1 molar ratio of Prx:MeBCD physical mixture, PM and the inclusion complexes initially prepared by kneading, KN; co-evaporation, COE and co-lyophilization, COL

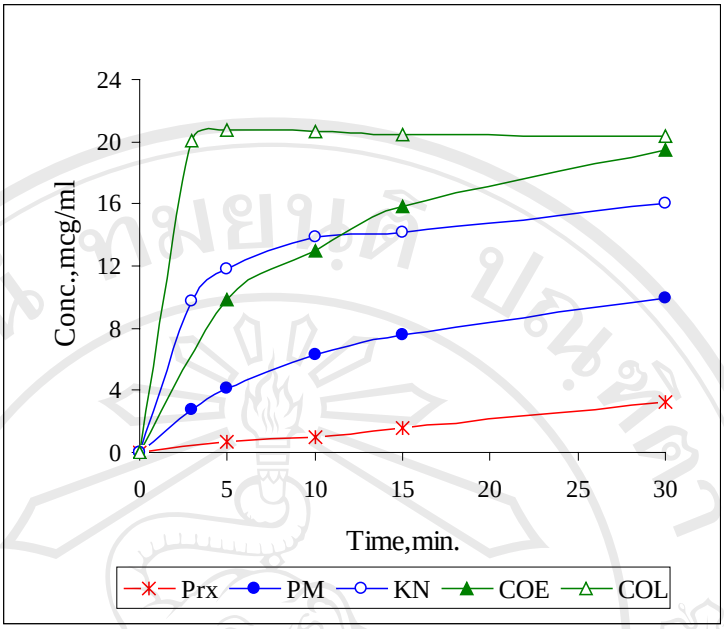

Figure 44 Dissolution profiles of piroxicam from intact drug (Prx), 1:2 molar ratio of Prx:MeBCD physical mixture, PM and the inclusion complexes prepared by kneading, KN; co-evaporation, COE and co-lyophilization, COL

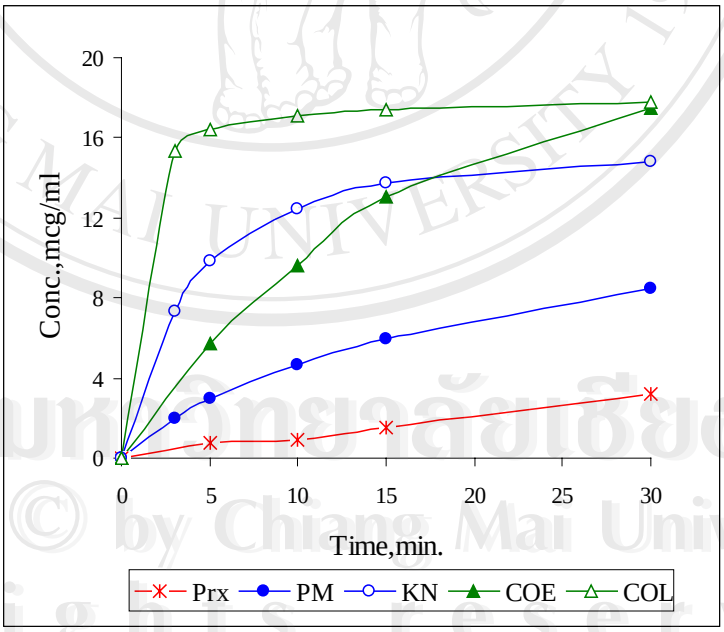

Figure 45 Dissolution profiles of piroxicam from intact drug (Prx), 2:1 molar ratio of Prx:MeBCD physical mixture, PM and the inclusion complexes prepared by kneading, KN; co-evaporation, COE and co-lyophilization, COL

Table 32 Dissolution parameters of piroxicam in distilled water from intact drug (Prx), binary mixtures of Prx:MeBCD; physical mixture, PM; and inclusion complexes initially prepared by kneading, KN;co-evaporation, COE and co-lyophilization, COL (Mean±SD; n=3)

	Prx:MeBCD	AUC 0-30min	%DE30	$t_{50\%}$ (min.)
Prx	1:0	214.9±7.57	7.17±0.25	>30
PM	1:1	920.9±31.88	30.70±1.06	>30
KN	1:1	1666.6±32.31	55.55±1.08	< 30
COE	1:1	1763.9±30.37	58.80±1.01	< 30.
COL	1:1	2456.0±34.53	81.87±1.15	< 30
PM	1:2	917.2±29.91	30.57±1.00	>30
KN	1:2	1786.5±45.27	59.55±1.51	< 30
COE	1:2	1882.3±48.25	62.74±1.61	< 30
COL	1:2	2621.7±57.86	87.39±1.93	< 30
PM	2:1	727.1±28.66	24.24±0.95	>30
KN	2:1	1634.5±33.35	54.48±1.11	< 30
COE	2:1	1524.9±38.66	50.83±1.29	< 30
COL	2:1	2200.47±35.64	73.35±1.19	< 30

According to the dissolution profiles in Figure 43-45 and the dissolution parameters shown in Table 32, it is evidenced that the piroxcam-MeBCD complex prepared by lyophilization method yields the highest dissolution enhancement for piroxicam. The dissolution enhancement resulted by KN complex and COE complex is not significantly different however, it is significantly higher than those of physical mixture and the intact drug. The rank of the dissolution efficiency is the same as that obtained from piroxicam-GCD complexes. That is COL >KN~COE >PM >Prx respectively.

. In order to substantiate the significance of the preparation method on the dissolution efficiency of piroxicam-CDs complexes, the regression models shown in Table 33 were developed from the %DE30 values collected from Table 29-32. It was clearly demonstrated that the method of preparation has a significant effect on the %DE30 of the complexes regardless of the CD type and the molar ratio of the drug to the CD. In the same Table, the dissolution efficiency ranks for all piroxicm-CDs complexes are summarily presented.

Table 33 Regression models of the %DE30 values and the method of preparation of piroxicam-CDs inclusion complexes at different molar ratios

CDs	Molar ratio	Model(R^2)	p-value
BCD	1:1	%DE30 = 0.730 method (0.534)	0.007
	1:2	%DE30 = 0.716 method (0.513)	0.009
	2:1	%DE30 = 0.729 method (0.531)	0.007
		Rank : COL>KN>COE>PM>Prx	
GCD	1:1	%DE30 = 0.635 method (0.403)	0.027
	1:2	%DE30 = 0.665 method (0.443)	0.018
	2:1	%DE30 = 0.645 method (0.416)	0.024
		Rank : COL>KN~COE>PM>Prx	
HPBCD	1:1	%DE30 = 0.730 method (0.533)	0.007
	1:2	%DE30 = 0.687 method (0.473)	0.013
	2:1	%DE30 = 0.717 method (0.513)	0.009
		Rank : COL>KN>COE>PM>Prx	
MeBCD	1:1	%DE30 = 0.931 method (0.867)	< 0.001
	1:2	%DE30 = 0.925 method (0.856)	< 0.001
	2:1	%DE30 = 0.930 method (0.865)	< 0.001
		Rank : COL>KN~COE>PM>Prx	

B. Comparison of CD types

Different types of CDs were used in the study in order to verify the suitable CD types for the dissolution enhancement of piroxicam. As previously shown the

method of preparation has a significant effect on the dissolution of the complexes. The comparison of the CD types was therefore carried out on the complexes prepared by the same method.

The dissolution profiles of piroxicam-CD physical mixtures prepared from different CD types at 1:1, 1:2 and 2:1 molar ratio are illustrated in Figure 46-48, respectively. The dissolution parameters calculated from these profiles were summarized in Table 34.

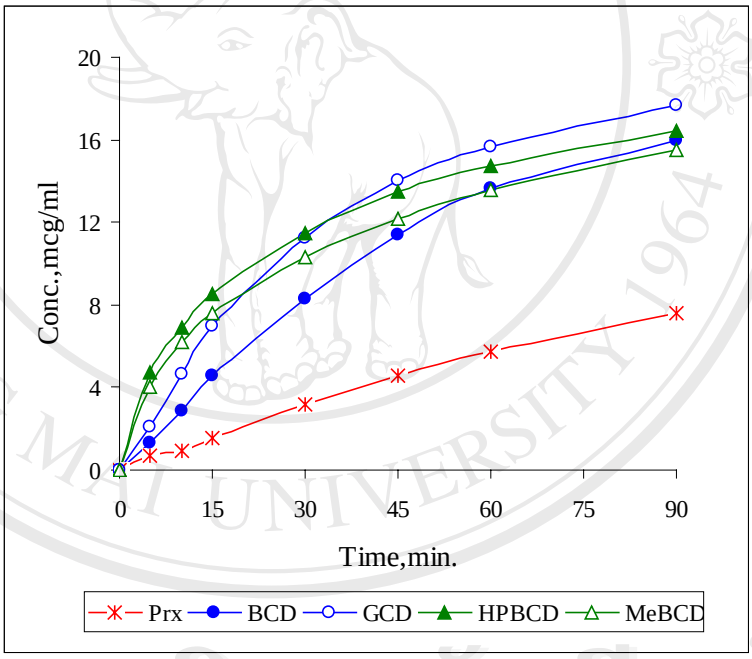

Figure 46 Dissolution profiles of piroxicam from intact drug (Prx), and 1:1 molar ratio of Prx:CDs physical mixture prepared; BCD, β-cyclodextrin; GCD, γ-cyclodextrin; HPBCD, hydroxypropyl-β-cyclodextrin and MeBCD, methylated-β-cyclodextrin.

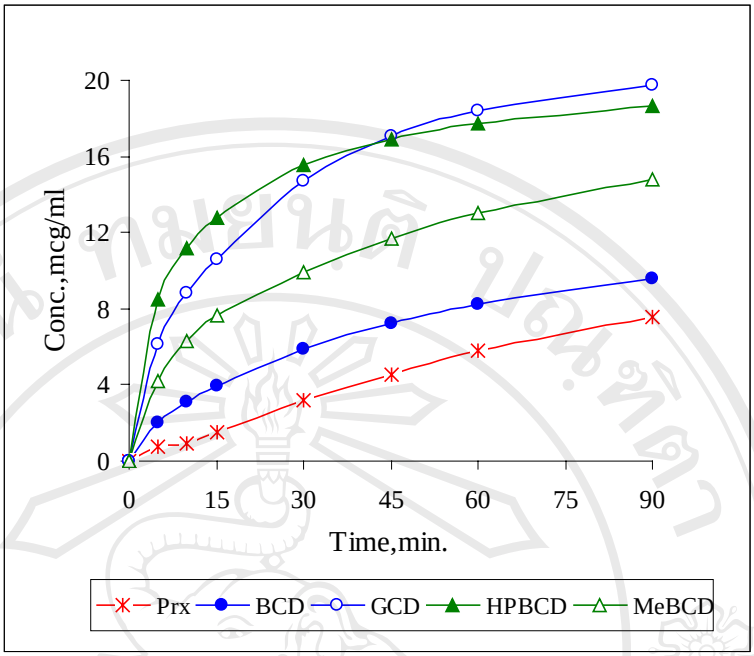

Figure 47 Dissolution profiles of piroxicam from intact drug (Prx), and 1:2 molar ratio of Prx:CDs physical mixture initially prepared

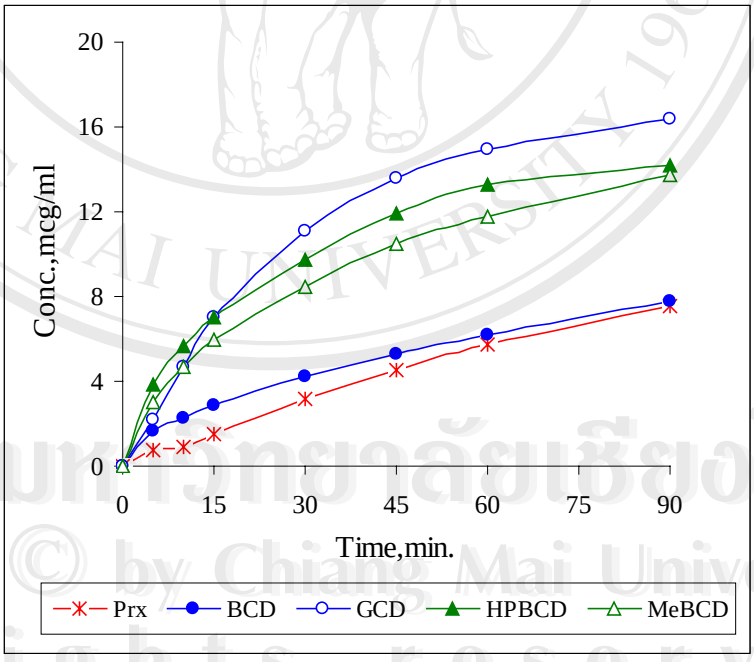

Figure 48 Dissolution profiles of piroxicam from intact drug (Prx), and 2:1 molar ratio of Prx:CDs physical mixture initially prepared

Table 34 Dissolution parameters of piroxicam in distilled water from intact drug (Prx) and Prx:CDs physical mixtures initially prepared (Mean± SD; n=3)

	Prx :CD	AUC 0-30min	%DE30	$t_{50\%}$ (min.)
Prx	-	214.9±7.57	7.17±0.25	>30
BCD	1:1	577.2±21.04	19.24±0.70	>30
GCD	1:1	844.4±22.51	28.15±0.75	>30
HPBCD	1:1	1034.5±29.89	34.48±0.99	<30
MeBCD	1:1	920.9±31.88	30.70±1.06	>30
BCD	1:2	489.4±18.80	16.31±0.63	>30
GCD	1:2	1308.8±33.04	43.63±1.10	<30
HPBCD	1:2	1541.5±31.84	51.38±1.06	<30
MeBCD	1:2	917.2±29.90	30.57±1.00	>30
BCD	2:1	359.25±19.64	11.98±0.66	>30
GCD	2:1	843.58±20.77	28.12±0.69	>30
HPBCD	2:1	855.58±25.68	28.52±0.86	>30
MeBCD	2:1	727.09±28.66	24.24±0.96	>30

The dissolution profiles in Figure 46-48 and the dissolution parameters in Table 34 provide the evidence that the physical mixtures of piroxicam and HPBCD show the highest dissolution enhancement. The solubilization effect of the CDs is more pronounced in the 1:2 mixtures where the excessive amount of CDs exists.

In Figure 46 the dissolution profiles obtained from 1:1 physical mixture of the drug and HPBCD, MeBCD and GCD look comparable at a glance, but the dissolution efficiencies calculated are significantly different ($p<0.05$) by the following rank, HPBCD> MeBCD> GCD> BCD> Prx. Similarly, the 1:2 physical mixtures shown in Figure 41, the %DE30 values could be ranked by HPBCD> GCD >MeBCD> BCD> Prx. The higher dissolution improvement is also demonstrated by CD derivatives namely HPBCD and MeBCD compared to the naturally occurring CDs. The piroxicam-BCD physical mixtures yield the lowest dissolution enhancement at all molar ratios.

Generally, the inclusion complex formation unlikely occurs in physical mixtures, the dissolution enhancement of the drug is attributed mainly by the local solubilization effect of the CDs as previously mentioned. This effect essentially depends on the intrinsic water solubility of the CD. The CD which is more readily dissolved when it has contacted with the medium could provide better local solubilizing effect.

Due to the amorphous nature of HPBCD and MeBCD the intrinsic water solubility is substantially higher than the natural CDs, which are normally in crystalline form. The greater intrinsic solubility of HPBCD and MeBCD is thus responsible for the higher dissolution rate of piroxicam obtained from piroxicam-HPBCD and piroxicam-MeBCD physical mixtures than those prepared using BCD.

The piroxicam-BCD complex shows the least dissolution improvement owing to the lowest water solubility of BCD compared to the others.

The dissolution profiles of piroxicam prepared by kneading method using different CD types at 1:1, 1:2 and 2:1 molar ratio are shown in Figure 49-51 respectively. The corresponding dissolution parameters are listed in Table 35.

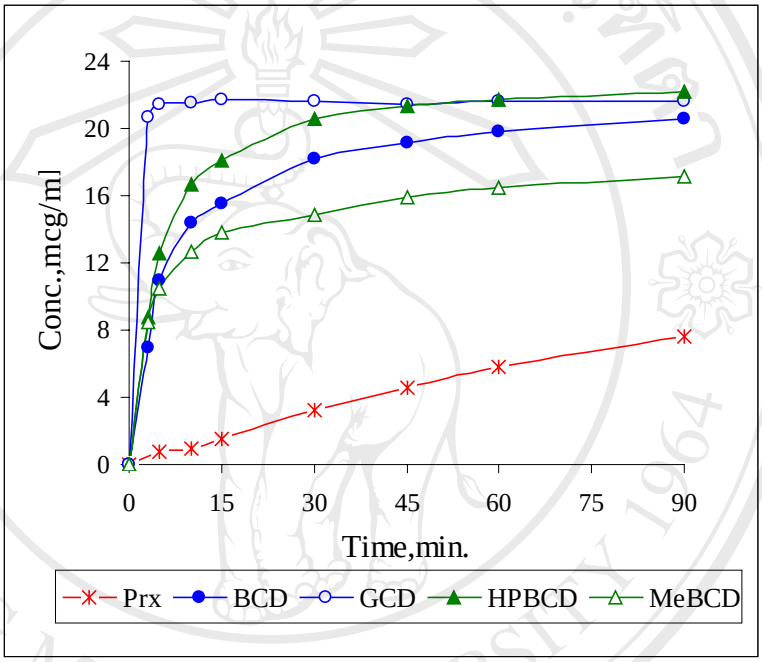

Figure 49 Dissolution profiles of piroxicam in distilled water from intact drug (Prx), and 1:1 molar ratio of Prx:CDs; inclusion complexes initially prepared by kneading method

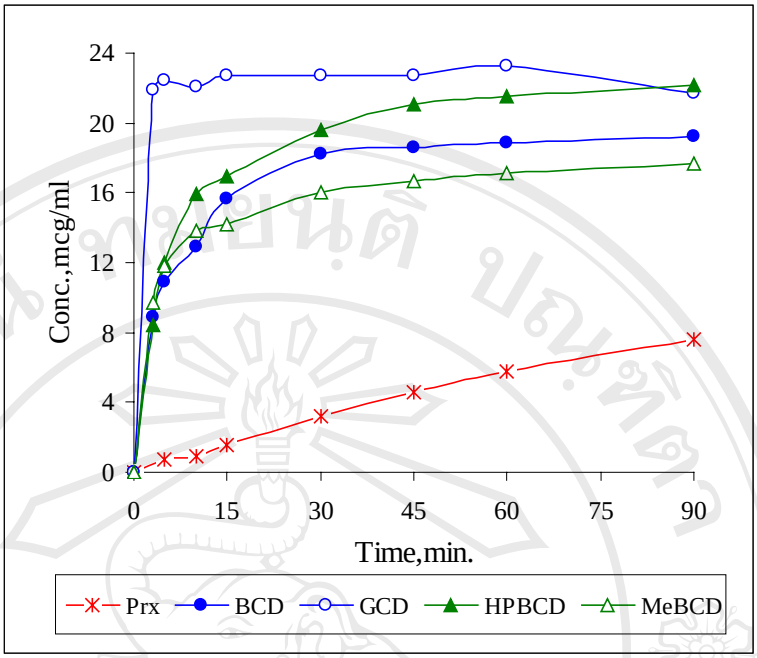

Figure 50 Dissolution profiles of piroxicam from intact drug (Prx), and 1:2 molar ratio of Prx:CDs; inclusion complexes initially prepared by kneading method

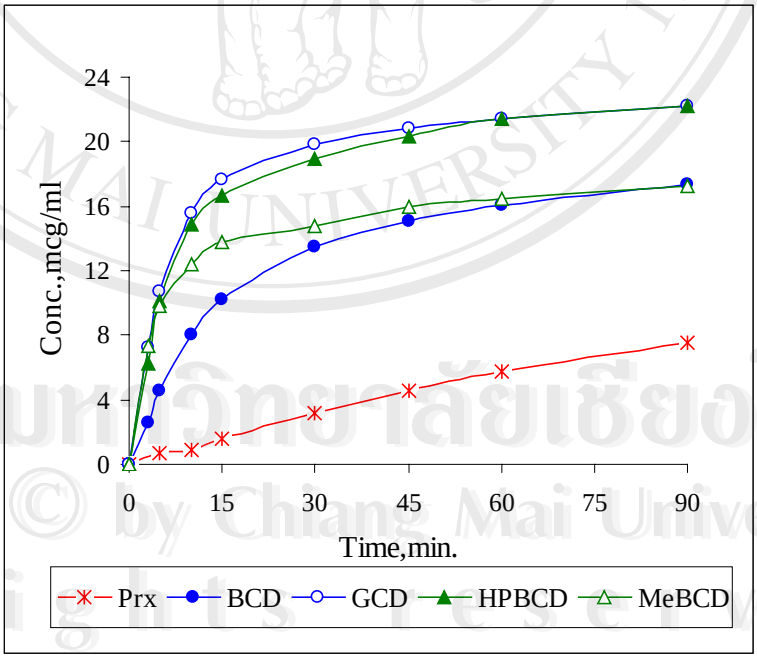

Figure 51 Dissolution profiles of piroxicam from intact drug (Prx), and 2:1 molar ratio of Prx:CDs; inclusion complexes initially prepared by kneading method

Table 35 Dissolution parameters of piroxicam in distilled water from intact drug (Prx), Prx:CDs inclusion complex initially prepared by kneading method (Mean±SD; n=3)

	Prx : CD	AUC 0-30min	%DE30	$t_{50\%}$ (min.)
Prx	1:0	214.9±7.57	7.17±0.25	>30
BCD	1:1	1886.2±32.12	62.87±1.07	<30
GCD	1:1	2762.5±43.96	92.08±1.47	<30
HPBCD	1:1	2181.0±38.94	72.70±1.30	<30
MeBCD	1:1	1666.6±32.31	55.55±1.08	<30
BCD	1:2	1882.7±24.64	62.76±0.82	<30
GCD	1:2	2753.3±37.81	91.78±1.26	<30
HPBCD	1:2	1836.6±33.15	61.22±1.11	<30
MeBCD	1:2	1786.5±45.27	59.55±1.51	<30
BCD	2:1	1193.6±26.27	62.76±0.82	<30
GCD	2:1	2064.7±33.94	68.82±1.13	<30
HPBCD	2:1	1952.4±32.95	65.08±1.10	<30
MeBCD	2:1	1634.5±33.40	54.48±1.11	<30

According to the dissolution profiles in Figure 49-51 and the dissolution parameters summarized in Table 35, it is demonstrated that the highest dissolution enhancement is obtained from the KN complex of piroxicam-GCD and then followed by those prepared from HPBCD, MeBCD and BCD, respectively. The %DE30 obtained from piroxicam-GCD at 1:1and 1:2 molar ratio is as high as 90% signifying

that the dissolution nearly completely occurs within half an hour. The greater effect on the solubility improvement by GCD than the others is attributed by the complete inclusion of piroxicam into GCD cavity which will be shown by X-ray diffractograms and FTIR spectra on further discussions.

Figure 52-54 illustrate the dissolution profiles of piroxicam-CD complexes prepared by co-evaporation method from different CD types at 1:1, 1:2 and 2:1 molar ratio. The dissolution parameters calculated from these profiles are summarized in Table 36.

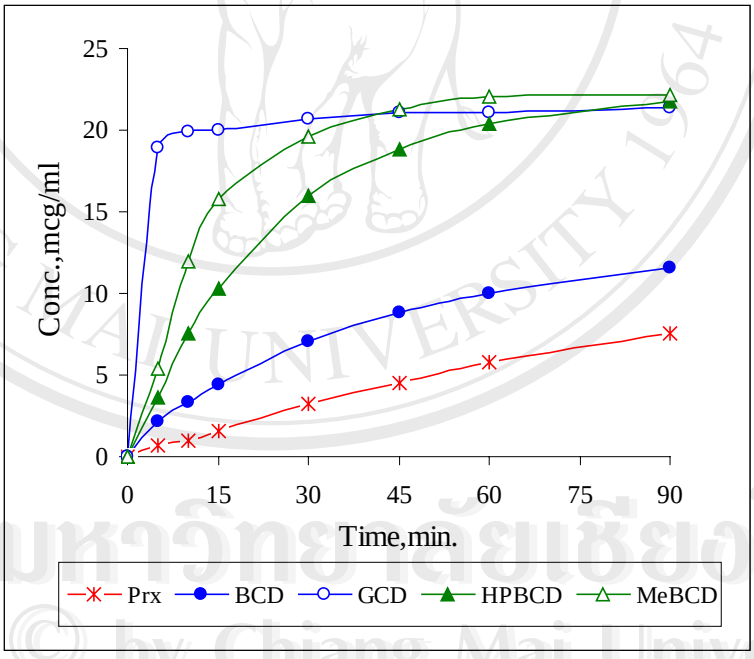

Figure 52 Dissolution profiles of piroxicam in distilled water from intact drug (Prx), and 1:1 molar ratio of Prx:CDs inclusion complexes initially prepared by co-evaporation method

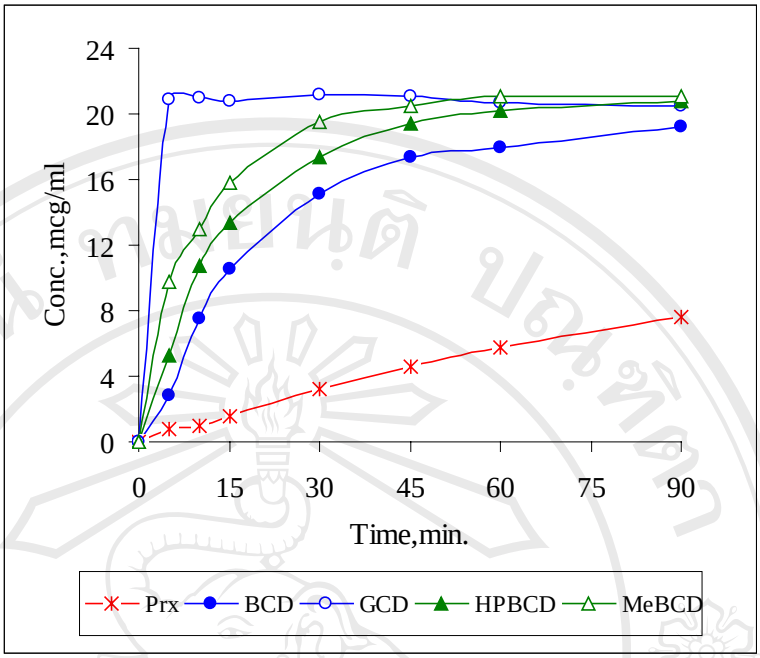

Figure 53 Dissolution profiles of piroxicam from intact drug (Prx), and 1:2 molar ratio of Prx:CDs inclusion complexes initially prepared by co-evaporation method

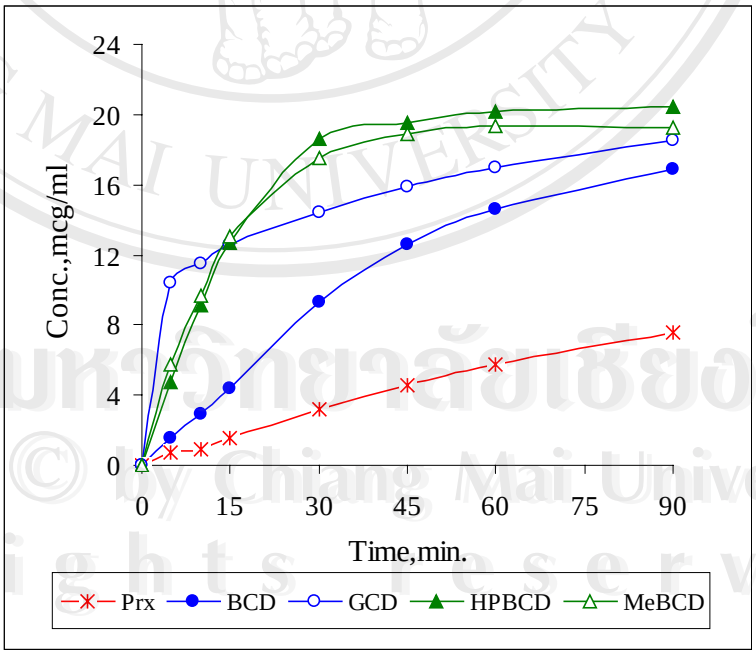

Figure 54 Dissolution profiles of piroxicam from intact drug (Prx), and 2:1 molar ratio of Prx:CDs inclusion complexes initially prepared by co-evaporation method

Table 36 Dissolution parameters of piroxicam in distilled water from intact drug (Prx), Prx:CDs inclusion complex initially prepared by co-evaporation method (Mean±SD; n=3)

	Prx: CD	AUC 0-30min	%DE30	$t_{50\%}$ (min.)
Prx	1:0	214.9±7.57	7.17±0.25	>30
BCD	1:1	558.5±34.52	18.62±1.15	>30
GCD	1:1	2471.1±37.45	82.37±1.25	>30
HPBCD	1:1	1254.6±46.45	41.82±1.55	<30
MeBCD	1:1	1763.9±30.37	58.80±1.01	<30
BCD	1:2	1221.8±31.80	40.73±1.06	<30
GCD	1:2	2589.8±36.72	86.33±1.22	<30
HPBCD	1:2	1549.2±33.25	51.64±1.11	<30
MeBCD	1:2	1882.3±48.25	62.74±1.61	<30
BCD	2:1	613.3±27.73	20.44±0.92	>30
GCD	2:1	1544.6±30.02	51.49±1.00	<30
HPBCD	2:1	1510.6±31.66	50.35±1.06	<30
MeBCD	2:1	1524.9±38.66	50.83±1.29	<30

The dissolution profiles presented in Figures 52-54 in addition to the dissolution parameters listed in Table 36 shows that the COE complexes of piroxicam and all CD types markedly increase the dissolution of the drug. The results are somewhat similar to those obtained from KN complexes that the complex prepared from GCD yields the highest dissolution enhancement followed by MeBCD, HPBCD

and BCD. The explanation for the dissolution improvement is attributed by the inclusion complex formation associated by the decrease in crystallinity of the drug and the CD during the complex preparation by evaporation under reduced pressure. The latter mechanism is supported by the considerable increase in the dissolution of 2:1 complexes. The local solubilizing effect of CD still predominantly exhibited in 2:1 complexes that the complexes prepared from CD derivatives showed higher dissolution profiles than those prepared from natural CDs (Figure 54).

The dissolution profiles of COL complexes of piroxicam prepared from different CD types at 1:1, 1:2 and 2:1 are respectively shown in Figure 55-57. The corresponding dissolution parameters of these profiles are presented in Table 37.

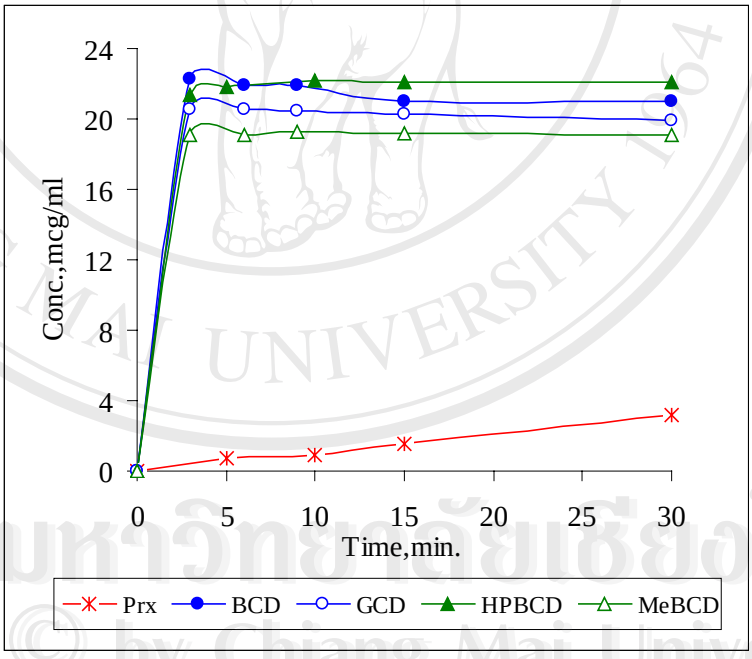

Figure 55 Dissolution profiles of piroxicam in distilled water from intact drug (Prx), and 1:1 molar ratio inclusion complexes initially prepared by co-lyophilization method

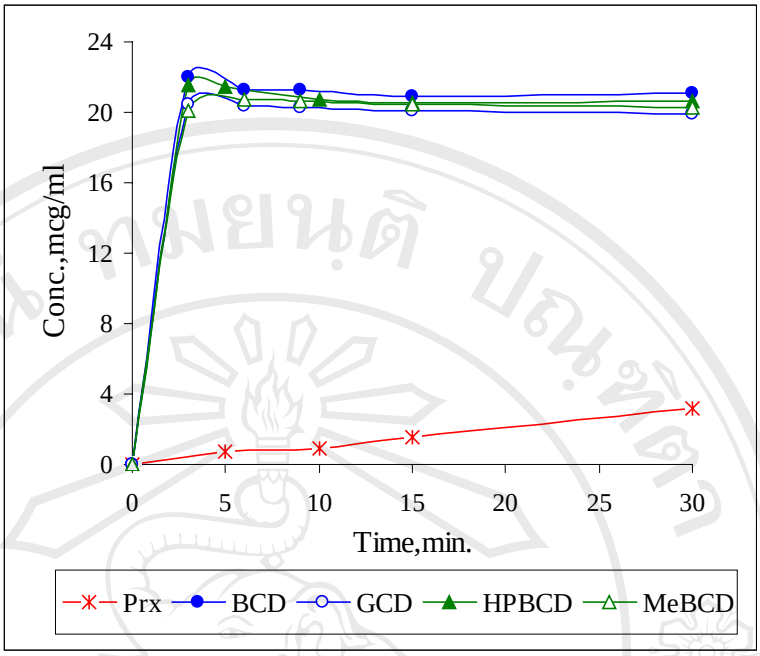

Figure 56 Dissolution profiles of piroxicam from intact drug (Prx), and 1:2 molar ratio of Prx:CDs inclusion complexes initially prepared by co-lyophilization method

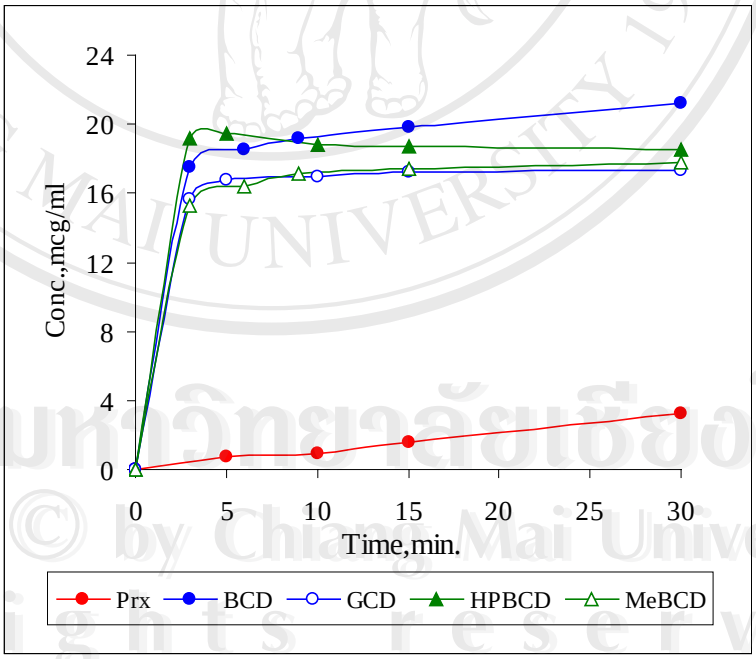

Figure 57 Dissolution profiles of piroxicam from intact drug (Prx), and 2:1 molar ratio of Prx:CDs inclusion complexes initially prepared by co-lyophilization method

Table 37 Dissolution parameters of piroxicam in distilled water from intact drug (Prx) and Prx:CDs inclusion complex initially prepared by co-lyophilization method. (Mean±SD; n=3)

	Prx: CD	AUC 0-30min	%DE30	$t_{50\%}$ (min.)
Prx	1:0	214.9±7.57	7.17±0.25	>30
BCD	1:1	2731.3±46.79	91.04±1.56	<30
GCD	1:1	2600.4±44.45	86.68±1.48	<30
HPBCD	1:1	2822.2±38.54	94.07±1.28	<30
MeBCD	1:1	2456.0±34.53	81.87±1.15	<30
BCD	1:2	2713.4±36.91	90.45±1.23	<30
GCD	1:2	2587.1±41.69	86.24±1.39	<30
HPBCD	1:2	2664.4±36.30	88.81±1.21	<30
MeBCD	1:2	2621.7±57.86	87.39±1.93	<30
BCD	2:1	2525.3±40.52	84.18±1.35	<30
GCD	2:1	2183.90±34.32	72.80±1.14	<30
HPBCD	2:1	2413.3±36.83	80.44±1.23	<30
MeBCD	2:1	2200.5±35.64	73.35±1.19	<30

The effect of CD types on the dissolution of the COL complexes is shown in Figures 55-57 and in Table 37. It was clearly demonstrated that the dissolution of the drug was extremely increased by co-lyophilization method. The dissolution of the

intact drug increases more than 10-folds by the complex formation irrespective to the CD types and the molar ratio of the complexes. The CDs showing greater effect are ranked by HPBCD> BCD> MeBCD >GCD. The formation of the inclusion complex between the drug and CDs is responsible for the enhancement. It is well-documented that the inclusion complex is obtained by lyophilization process. Additionally, the drug and the CD are completely changed to amorphous form when subjected to the same process. This is an explanation for the considerable increase in the drug dissolution observed in 2:1 complexes. The excessive amount of the crystalline drug that might exist in 2:1 complex was entirely changed to the amorphous form. This resulted in the higher extent of the dissolution increasing compared to 2:1 complexes prepared by the other method. The higher solubilizing effect of BCD on the COL complexes than those prepared by the other methods can be explained by the same fact. This suggestion was evidenced by X-ray diffractograms and DSC thermograms. The FTIR spectra also provide information confirm the existence of the inclusion complexes. These evidences will be further presented.

The effect of CD types of the dissolution of piroxicam from drug-CD inclusion complexes is summarized and demonstrated in Table 38. The statistical comparison was based on the mean values of %DE30 obtained from any particular complex in order to exclude the effect of the preparation method. The Table 38 shows not only the effect of CD types but also the effect of the method of preparation.

Table 38 Comparison of %DE30 of piroxicam-CD inclusion complexes prepared from different CD types (n=9)

Complex	CD type	%DE30 (Mean ± SD)	Statistical comparison of %DE30	p-value
PM	BCD	15.84±3.22	GCD ~ HPBCD	0.145
	GCD	33.30±7.78	GCD ~ MeBCD	0.148
	HPBCD	38.13±10.30	HPBCD > MeBCD	0.005
	MeBCD	28.50± 3.32	**HPBCD ~ GCD ~ MeBCD > BCD**	
KN	BCD	55.14±11.54	GCD > HPBCD > BCD	<0.001
	GCD	84.45±11.80	GCD > HPBCD > MeBCD	<0.001
	HPBCD	66.33±5.16	BCD ~ HPBCD	0.738
	MeBCD	56.53±2.55	**GCD > HPBCD ~ BCD > MeBCD**	
COE	BCD	26.60±10.67	GCD >MeBCD	<0.05
	GCD	73.40±16.55	GCD >HPBCD	<0.001
	HPBCD	47.94±4.75	MeBCD ~HPBCD	0.061
	MeBCD	57.57±5.55	**GCD> HPBCD~ MeBCD > BCD**	
COL	BCD	88.56±3.51	BCD> GCD	<0.05
	GCD	81.90±6.93	BCD> HPBCD	<0.05
	HPBCD	83.23±4.32	BCD> MeBCD	<0.05
	MeBCD	81.09±5.96	**BCD> GCD ~HPBCD ~MeBCD**	

In Table 38, the one-way analysis of variance followed by LSD test was applied for the comparison of %DE30 values obtained from different CD types. The overall comparison is presented by the bold-typed letters. In the dissolution improvement point of view, the proper CD type for preparing the physical mixture should be HPBCD, MeBCD or GCD. In the case when the substantial increase in the dissolution is needed, the complex formation should be taken into consideration. In such case, when either the kneading of the co-evaporation method is chosen, the preferable CD type should be GCD and HPBCD. BCD shows appreciable increase in the drug dissolution when the complex is prepared by lyophilization method.

C. Comparison of the molar ratios

The inclusion complex of piroxicam-CDs were prepared at different molar ratios at 1:1, 1:2 and 2:1 in order to determine the appropriate molar ratio for achieving the maximum dissolution enhancement. As previously presented, the method of preparation has a great effect on the dissolution of the complexes. The comparison of the molar ratio was thus conducted on the complexes of the same CD types and the same method of preparation.

The dissolution profiles of the physical mixture and the inclusion complexes of piroxicam-CDs at different molar ratios and the dissolution parameters calculated from these profiles are shown in Appendix A. The dissolution profiles of 1:1 and 1:2 complexes molar ratios are comparable however, they are rather higher than those of 2:1 complexes. In order to verify the significant effect of the molar ratio on the dissolution of the complexes, the regression models of the dissolution efficiency, %DE30 values and the molar ratio were developed as shown in Table 39. According

to the models, it can be pointed out that the molar ratio has no effect on the dissolution of the complexes irrespective of the CD types and the method of preparations. In other words, it is insignificant difference in the dissolution of the complexes prepared from different molar ratios ($p > 0.05$). The negative regression coefficient of the models signifies that the dissolution efficiency decreases when the molar ratio are in order of 1:1, 1:2 and 2:1, respectively.

The effect of all factors on the dissolution efficiency of piroxicam-CD complexes could be confirmed by the following regression model.

$$\%DE30 = 0.694Method^{*} + 0.087CDtype - 0.007Ratio$$

$$R^2 = 0.489; \ ^{*}p<0.001$$

The model was obtained when all factors were taken into account simultaneously in order to weigh the significance of each factor.

It is signified that all factors influence the dissolution behavior of the complexes, but at different degree of impact. The larger value of the regression coefficient reflects the relatively high impact of the factor. The significant effect was exhibited by the method of preparation ($p<0.001$) while the CD types and the molar ratio factor shows insignificant effects. The regression coefficient of each factor was nearly 10 times different. The dissolution efficiency of the complexes is in order of COL >KN> COE> PM.

When all factors were considered simultaneously, the effect of the CD type was negligible due to the more pronounced effect shown by the method of preparation. Nevertheless, it is prominent when the consideration is taken with the particular method of preparation. The effect of the CD type on complexes prepared by definite method is clearly demonstrated in Table 38. In contrast to the effect of molar ratio, it

insignificantly affects the dissolution efficiency of the complexes shown by the regression models in Table 39.

According to this finding, these methods of preparation were used for meloxicam-CD complexes however, only 1:1 molar ratio.

Table 39 Regression models of the %DE30 values of Prx-CD inclusion complexes

Method	CDs	Model (R^2)	p-value
PM	BCD	%DE30 = 0.032 ratio (0.001)	0.934
	GCD	%DE30 = - 0.039ratio (0.001)	0.922
	HPBCD	%DE30 = -0.024 ratio (0.001)	0.951
	MeBCD	%DE30 = -0.040 ratio (0.002)	0.919
KN	BCD	%DE30 = -0.008 ratio (0.0)	0.984
	GCD	%DE30 = -0.048 ratio (0.002)	0.903
	HPBCD	%DE30 = -0.040 ratio (0.002)	0.918
	MeBCD	%DE30 = 0.022 ratio (0.0)	0.955
COE	BCD	%DE30 = 0.009 ratio (0.0)	0.981
	GCD	%DE30 = -0.001 ratio (0.0)	0.998
	HPBCD	%DE30 = -0.101 ratio (0.010)	0.796
	MeBCD	%DE30 = 0.119 ratio (0.014)	0.761
COL	BCD	%DE30 = -0.22 4 ratio (0.050)	0.563
	GCD	%DE30 = -0.037 ratio (0.001)	0.924
	HPBCD	%DE30 = -0.237 ratio (0.056)	0.539
	MeBCD	%DE30 = 0.034 ratio (0.001)	0.931

3.4.1.2 Dissolution studies of meloxicam-CD inclusion complexes (initially prepared)

The dissolution studies of meloxicam-CD complexes were carried out by the same procedures used for piroxciam-CD complexes except the simulated gastric fluid without enzyme was used as the dissolution medium of meloxicam-CD complexes in stead of distilled water. The dissolution parameters, %DE30 value and $t_{50\%}$ obtained from the particular dissolution profiles were used as the indicators for comparison.

A. Comparison of method of preparations

The meloxicam-CD inclusion complexes were prepared at 1:1 molar ratio by kneading method, co-evaporation method and by simple mixing resulting in products designated as KN complex, COE complex, COL complex and PM, respectively. The CDs used in the case of meloxicam were BCD, GCD HPBCD and HPGCD.

The dissolution profiles of meloxicam compared to the physical mixture and the inclusion complexes prepared by different methods are respectively shown in Figure 58-61. The dissolution parameters obtained from these profiles are shown in Table 39. The statistical comparison of %DE30 are summarized in Table 41.

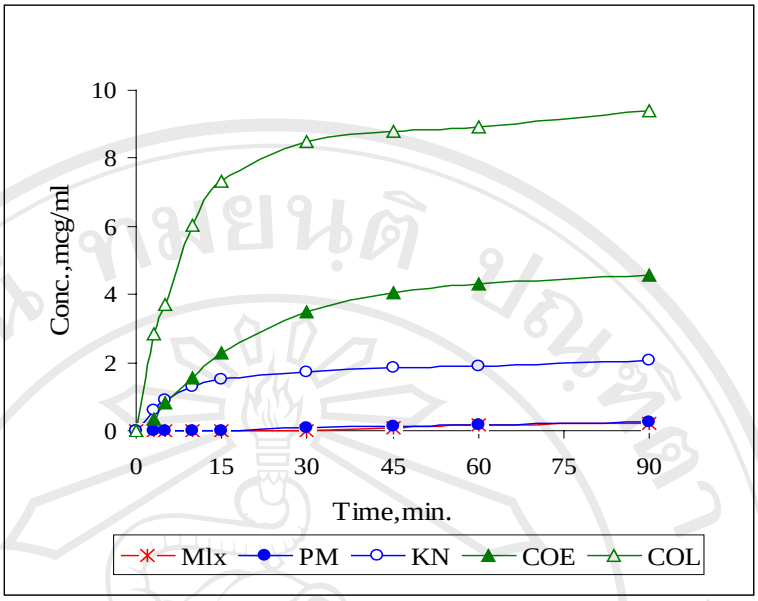

Figure 58 Dissolution profiles of meloxicam from intact drug (Mlx), 1:1 molar ratio of Mlx:BCD physical mixture, PM; and the inclusion complexes initially prepared by kneading, KN; co-evaporation, COE and co-lyophilization, COL

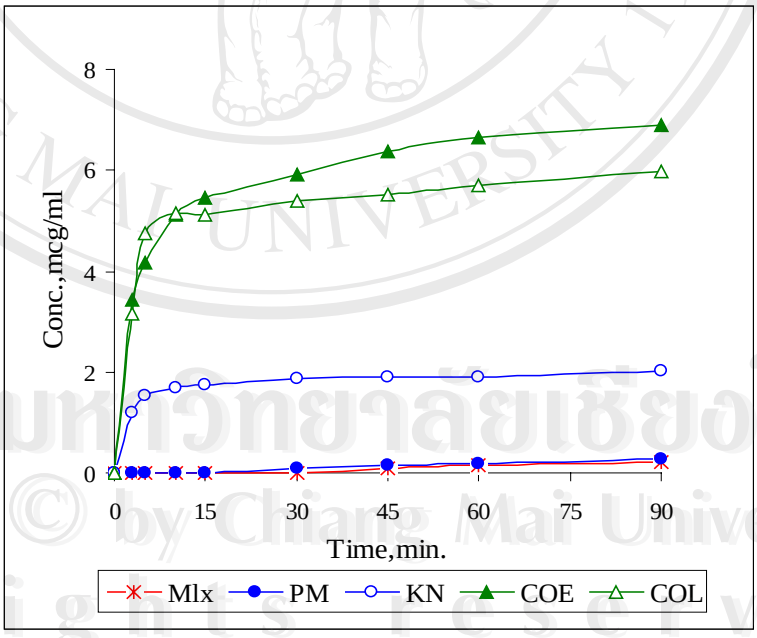

Figure 59 Dissolution profiles of meloxicam from intact drug (Mlx), 1:1 molar ratio of Mlx:GCD physical mixture, PM; and the inclusion complexes initially prepared by kneading, KN; co-evaporation, COE and co-lyophilization, COL

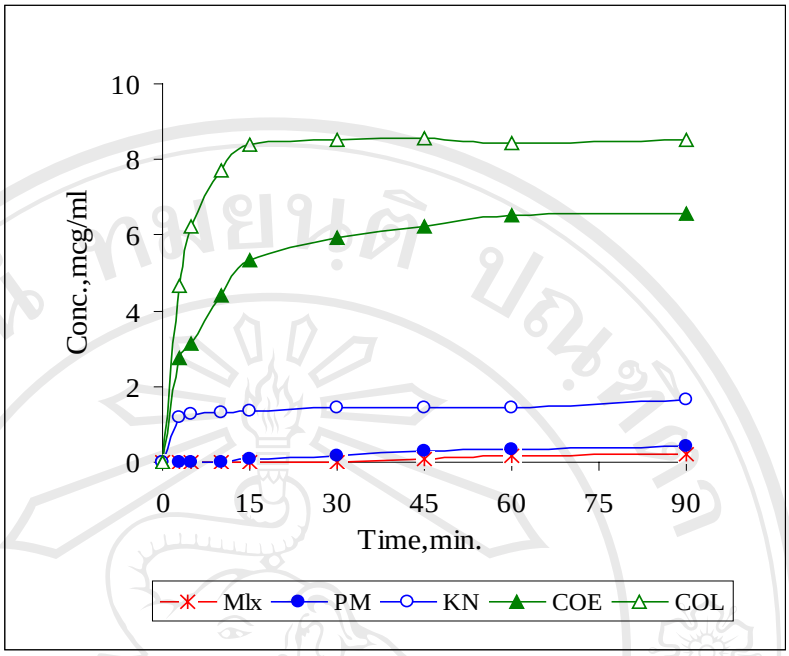

Figure 60 Dissolution profiles of meloxicam from intact drug (Mlx), 1:1 molar ratio of Mlx:HPBCD physical mixture, PM; and the inclusion complexes initially prepared by kneading, KN; co-evaporation, COE and co-lyophilization, COL

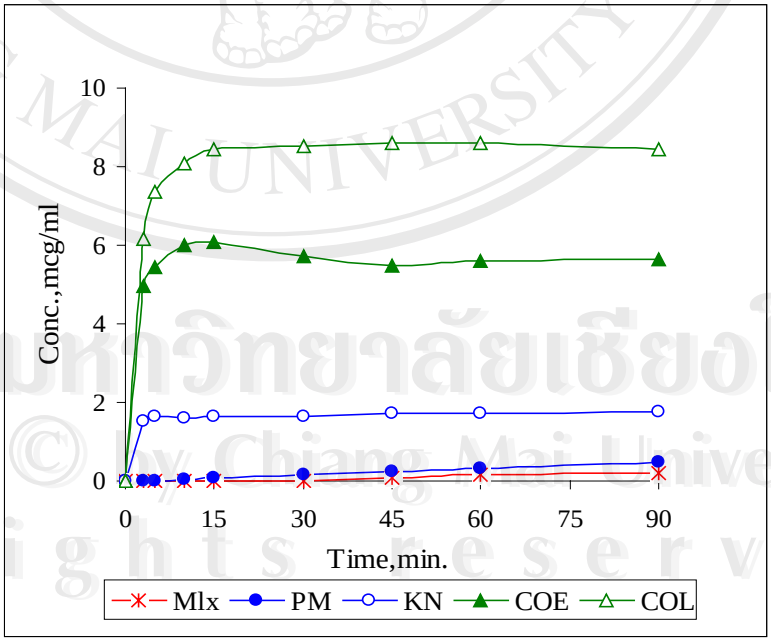

Figure 61 Dissolution profiles of meloxicam from intact drug (Mlx), 1:1 molar ratio of Mlx:HPGCD physical mixture, PM; and the inclusion complexes initially prepared by kneading, KN; co-evaporation, COE and co-lyophilization, COL

The dissolution profiles in Figures 58-61 show the consistent results that the dissolution of meloxicam is substantially increased by complex formation irrespective to the CD types used. The physical mixture evidently increases the dissolution of the drug. However, it is more pronounced in the case of CD derivatives than for the natural CDs. The method of preparation markedly affects the dissolution efficiency of the drug from the complexes. The quantitative comparison based on the %DE30 values will be discussed later.

Compared to the dissolution profiles of piroxicam and its inclusion complexes, it is noted that the amount of meloxicam dissolved is relatively lower. This was attributed by the different dissolution medium used. In fact, the intrinsic solubility of both drugs is pH-dependent exhibiting the U-shaped pH-solubility profile. Compared to piroxicam, the solubility of meloxicam is not only lower but more sensitive to pH change. Its U-shaped solubility profile exhibits a narrow bottom at pH range of 2-3. The solubility changes drastically from pH 3 to pH 10 presenting the steepest portion of the solubility curve. This pH range is coincident to pH of the distilled water. The relatively small variation in the pH of the distilled water generally induces the high fluctuation of the dissolved amount of the drug. The simulated gastric fluid without enzyme was then chosen as the dissolution medium for meloxicam. In addition to its inherent property of being able to simulate the in vivo environment, the pH of the medium can be well-controlled providing the less pH-sensitive medium for the dissolution of the drug. Unfortunately, the solubility of the drug in this pH is very low. The solubility of meloxicam obtained in this study was 0.47 mcg/ml and 22.4 mcg/ml at pH 3.00 and pH 6.00 respectively. Accordingly, it

was unable to detect the dissolved amount of meloxicam up to 30 minutes of the dissolution process. As a consequence, the %DE30 value of the intact drug could not be obtained. However, the overall results can be used satisfactorily for the purpose of comparison.

Table 40 shows the dissolution parameters obtained from dissolution profiles in Figures 58-61. The area under the dissolution profiles are also presented for comparison. From this parameter, the %DE30 values were calculated and used for statistical comparison shown in Table 41. The $t_{50\%}$ values are valuable for comparison especially in the application point of view. It can be pointed out that although the dissolution efficiency of the drug from the complexes was substantially higher than the intact drug, it was not possible to obtain the amount of drug absorbed by 50% within 30 minutes.

The extent of the increase in the dissolution efficiency was obviously influenced by the method of preparation. The rank of the method of preparation based on the %DE30 is shown in Table 41. For all CDs, the co-lyophilization exhibited as the most powerful method for improving the dissolution of meloxicam followed by co-evaporation and kneading method.

Table 40 Dissolution parameters of meloxicam from intact drug (Mlx), 1:1 physical mixture, PM and inclusion complexes initially prepared by kneading, KN; co-evaporation, COE and co-lyophilization, COL (Mean±SD; n=3)

	Method	AUC 0-30min	%DE30	$t_{50\%}$ (min.)
Mlx	-	0	0	>30 min
BCD	PM	0.66±0.037	0.022±0.001	>30 min
	KN	235.2±16.408	7.84±0.547	>30 min
	COE	362.6±18.225	12.09±0.608	>30 min
	COL	1133.7±13.617	37.79±0.454	30 min.
GCD	PM	0.70±0.043	0.023±0.001	>30 min
	KN	288.5±19.924	9.62±0.664	>30 min
	COE	876.1±18.074	29.20±0.602	>30 min
	COL	852.6±22.02	28.42±0.734	>30 min.
HPBCD	PM	13.3±1.374	0.44±0.046	>30 min
	KN	229.5±13.836	7.65±0.461	>30 min
	COE	825.9±27.927	27.53±0.931	>30 min
	COL	1318.5±25.297	43.95±0.843	<30 min.
HPGCD	PM	11.3±0.957	0.38±0.032	>30 min
	KN	275.6±9.616	9.19±0.320	>30 min
	COE	934.3±21.196	31.14±0.706	>30 min
	COL	1380.0±28.446	46.00±0.948	<30 min.

Table 41 Comparison of %DE30 values of meloxicam-CD inclusion complexes prepared by different methods

CD type	Method	%DE30 (Mean±SD)	Statistical comparison of %DE30	p-value
BCD	PM	0.02±0.001	COL >COE >KN > PM	<0.001
	KN	7.8±0.569		
	COE	12.1±0.610		
	COL	37.8±0.452		
GCD	PM	0.02±0.001	COL ~COE	0.139
	KN	9.6±0.662	COL, COE >KN > PM	<0.001
	COE	29.2±0.602		
	COL	28.4±0.735		
HPBCD	PM	0.4±0.046	COL >COE >KN > PM	<0.001
	KN	7.6±0.459		
	COE	27.5±0.927		
	COL	43.9±0.843		
HPGCD	PM	0.4±0.032	COL >COE >KN > PM	<0.001
	KN	9.2±0.319		
	COE	31.1±0.704		
	COL	46.0±0.944		

Different methods of preparation could provide the inclusion complex formation at varying degrees of completeness. It was reported that kneading method was less successfully introduced to the complete inclusion of the drug molecule into the CD cavity compared to the co-evaporation or co-lyophilization method. The additional factor generated by different method of preparation is the successive reduction of the drug and/or CD crystallinity during the process. This is why lyophilization displays as the most powerful method for the dissolution improvement. However, the increase in the dissolution could be detected even when the drug and the CD particles were intimately contacted such as those found in the physical mixture. This is due to the local effect of CD as previously discussed

B. Comparison of CD types

The meloxicam-CD inclusion complexes were prepared using different CD types. Two natural CDs, BCD and GCD and their hydroxypropyl derivatives were included in this study.

Figure 62 shows the dissolution profiles of the intact drug compared to those of meloxicam-CD physical mixtures of different CD types. The dissolution profiles displayed by the intact drug, by the natural CDs and by the CD derivatives were simply differentiated. The highest enhancement is exhibited by the CD derivatives. This is due to their higher solubility which introduces greater local solubilization effect on the drug.

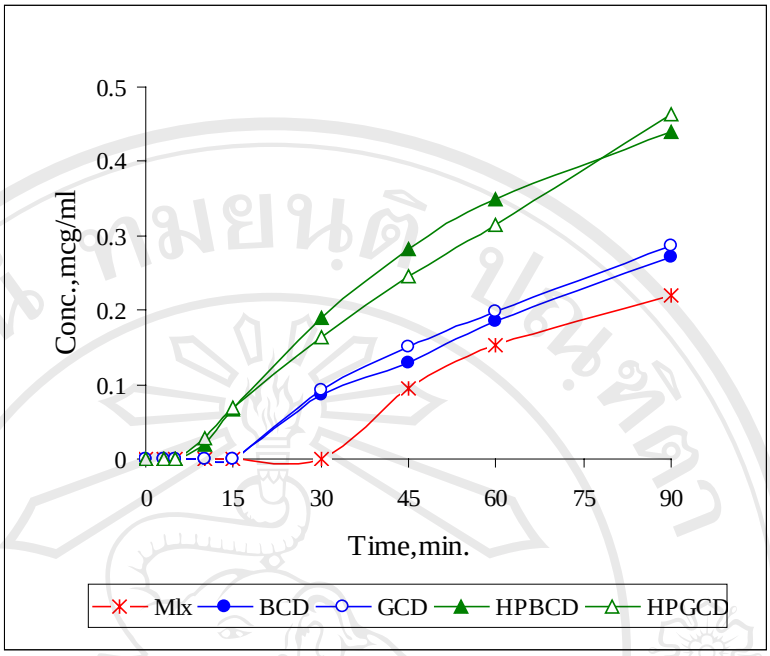

Figure 62 Dissolution profiles of meloxicam from intact drug (Mlx) and 1:1 physical mixture of Mlx:CDs initially prepared

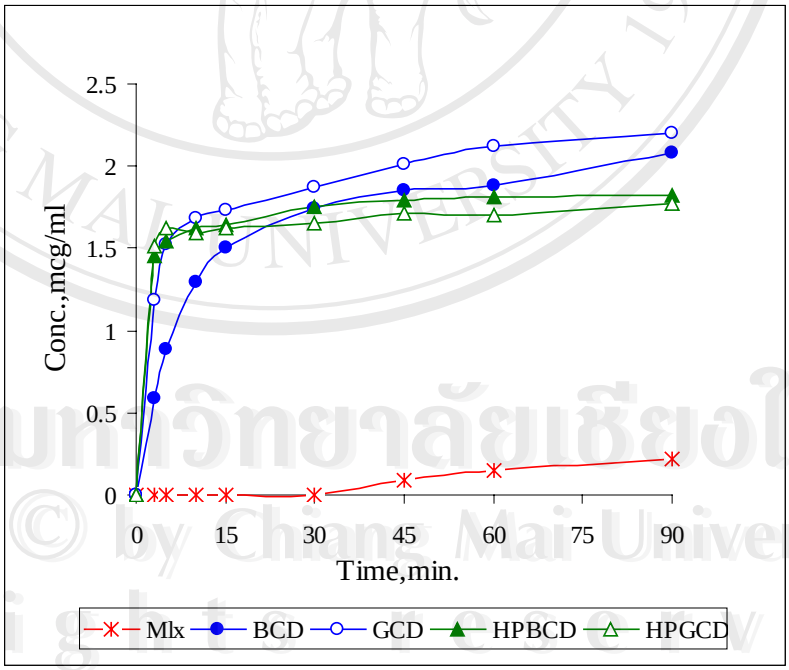

Figure 63 Dissolution profiles of meloxicam from intact drug (Mlx) and 1:1 inclusion complexes of Mlx:CDs; initially prepared by kneading method

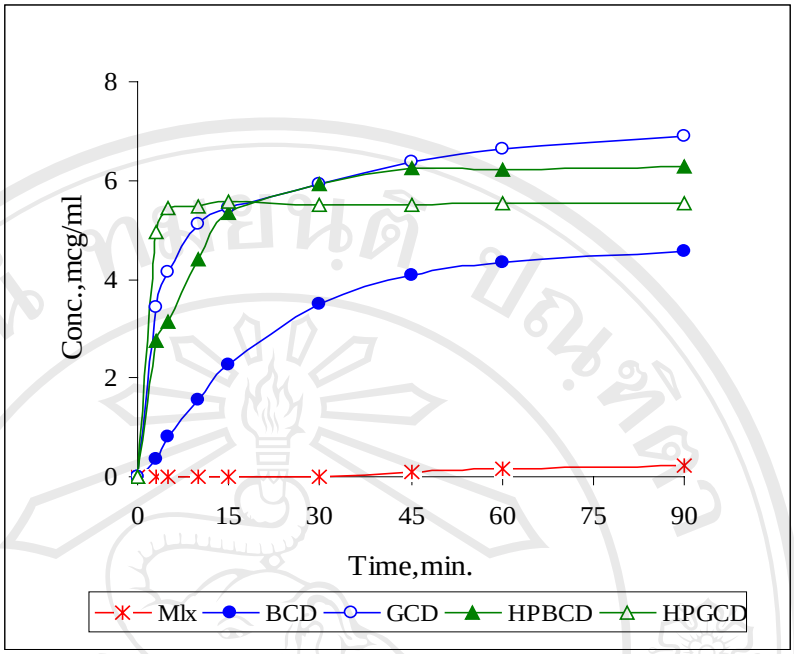

Figure 64 Dissolution profiles of meloxicam from intact drug (Mlx) and 1:1 inclusion complexes of Mlx:CDs; initially prepared by co-evaporation method

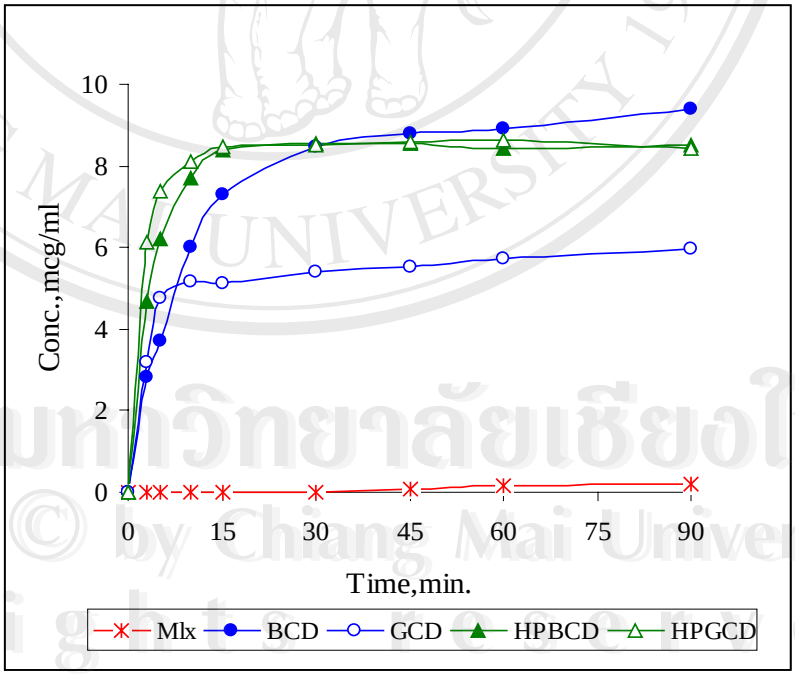

Figure 65 Dissolution profiles of meloxicam from intact drug (Mlx) and 1:1 inclusion complexes of Mlx:CDs; initially prepared by co-lyophilization method

Table 42 Dissolution parameters of meloxicam in simulated gastric fluid from intact drug (Mlx), 1:1 Mlx:CDs physical mixtures initially prepared using different CD types (Mean±SD; n=3)

Method	CDs	AUC 0-30min	%DE30	t 50% (min.)
Mlx		0	0	>30
PM	BCD	0.66±0.037	0.022±0.001	>30
	GCD	0.69±0.043	0.023±0.001	>30
	HPBCD	13.3±1.374	0.44±0.046	>30
	HPGCD	11.9±0.957	0.40±0.032	>30
KN	BCD	235.2±16.408	7.84±0.547	>30
	GCD	288.5±19.924	9.62±0.664	>30
	HPBCD	229.5±13.836	7.65±0.461	>30
	HPGCD	275.6±9.616	9.19±0.320	>30
COE	BCD	362.6±18.225	12.09±0.608	>30
	GCD	876.1±18.074	29.20±0.602	>30
	HPBCD	825.9±27.927	27.53±0.931	>30
	HPGCD	934.3±21.196	31.14±0.706	>30
COL	BCD	1133.7±13.617	37.79±0.454	30
	GCD	852.6±22.017	28.42±0.734	>30
	HPBCD	1318.5±25.297	43.95±0.843	<30
	HPGCD	1380.0±28.446	46.00±0.948	<30

Table 43 Comparison of %DE30 values of meloxicam-CD inclusion complexes prepared from different CD types

Method	CD type	%DE30 (Mean ±SD)	Statistical comparison of %DE30	p-value
PM	BCD	0.02±0.001	HPBCD >HPGCD	0.021
	GCD	0.02±0.001	BCD ~GCD	0.958
	HPBCD	0.44±0.046	**HPBCD,HPGCD >BCD,GCD**	<0.001
	HPGCD	0.38±0.032		
KN	BCD	7.81±0.569	HPGCD ~GCD	0.339
	GCD	9.62±0.662	HPBCD ~BCD	0.710
	HPBCD	7.65±0.459	**GCD,HPGCD >BCD,HPBCD**	<0.05
	HPGCD	9.19±0.319		
COE	BCD	12.09±0.610	**HPGCD >GCD >HPBCD >**	<0.05
	GCD	29.20±0.602	**BCD**	
	HPBCD	27.53±0.927		
	HPGCD	31.14±0.704		
COL	BCD	37.79±0.452	**HPGCD >HPBCD >GCD >**	<0.05
	GCD	28.42±0.735	**BCD**	
	HPBCD	43.95±0.843		
	HPGCD	46.0±0.944		

Figures 63-65 illustrate the dissolution profiles of meloxicam-CD complexes of different CD types prepared by kneading method, co-evaporation method and co-

lyophilization method respectively. The dissolution parameters obtained from these profiles were listed in Table 42 and compared as shown in Table 43.

According to Table 43, it is showed that the dissolution efficiency of the drug is also influenced by the CD type. The extent of the dissolution enhancement depends on the properties of the CDs. Amorphous CD derivatives are show higher water solubility thus providing greater local solubilizing effect than the two natural CDs. This effect is evident in the case of the physical mixtures. In the cases where the inclusion complex formation occurs, the GCD and its derivative show higher effects on the dissolution enhancement. This might be due to the better fit of the drug molecule into the larger cavity of GCD and HPGCD.

The following MLR regression model was developed based on the %DE30 values to verify the significant effect of the factors on the dissolution of drug from complexes.

MLR regression model, $\%DE30 = 0.939Method^* + 0.175CDType^*$

$R^2 = 0.912, \quad p<0.001$

The model shows that the method of preparation and the CD types significantly affect the dissolution behaviors of the drug in the complexes. The higher regression coefficient value exhibit by the factor method signifies that the method of preparation has greater influence than the CD type. The positive regression coefficient value reveals the increasing trend of %DE30 from the method of preparation by PM <KN<COE<COL. Similarly, the order of CD type is HPGCD>HPBCD>GCD>BCD. This rank is in good agreement with the complexation efficiency of meloxicam-CD at pH 3.0.

3.4.2 Differential scanning calorimetry

The existence of inclusion complexation can be proven by thermal analysis. When the guest molecule is enclosed in CD cavities or in the crystal lattice, its melting point is generally shifted to lower temperatures or disappeared within the melting temperature range. On the other hand, when the inclusion complexation does not likely occur the characteristic thermograms of the individual component are still detectable (Marques et al., 1990).

3.4.2.1 DSC of piroxicam-CD complxes

DSC thermograms of piroxicam compared to those of physical mixtures and the inclusion complexes in different CD types prepared by different method of preparation are illustrated in Figures 66-76.

Piroxicam showed a sharp endothermic peak at 201.6°C which was assigned to its melting peak. The heat of fusion is 107.4 J/g. The value is in good agreement with that previously documented.

The physical mixtures of piroxicam and BCD exhibit no evidence of interaction between the drug and BCD. The melting peak of the drug in physical mixtures is nearly unchanged from that of the intact drug. The onset and peak maximum of endothermic peaks shown in complexes prepared by kneading and co-evaporation method are somewhat lower than that of the drug (Figures 66-68 and Table 44). This finding was contributed by many factors: the formation of the inclusion complex between the drug and BCD, some extent of drug-CD interaction, however, not true inclusion complex formation (Fernandes et al., 2002). The reduction in the crystallinity and/or the modification of the crystal structures of the

drug and BCD during the preparation process might be responsible for the findings. The disappearance of the melting peak observed in co-lyophilized complexes at 1:1 and 1:2 molar ratios (Figure 69), could signify the complete inclusion of the drug molecule into the BCD cavity (Babu and Pandit, 2004; Jug and Becirevic-Lacan, 2004) . The lack of the melting peak is also attributed to the entire amorphous state of the drug and BCD obtained from lyophilization process (Fernandes et al., 2002; Cerchiara et al., 2003). The characteristic peak of the drug still exists in 2:1 co-lyophilized complex however, at lower onset and peak temperature. It is of interested that this peak resembles to the melting point of the metastable form of piroxicam (Reynolds et al., 1989). Thus, it might be suggested that only one molecule of the drug could fit well in BCD cavity. The excessive, noncomplexed drug then exhibits an endothermic peak of the less stable modification. In a particular complex, the heat of fusion of the complexes changes according to the molar ratio of the drug to CD. The complexes containing higher drug content, as shown in 2:1 molar ratio requires more energy than the lower drug-containing complexes for achieving complete melting, thus exhibiting the higher ΔH values. However, the slight difference in enthalpy values of the complexes prepared by different methods could be ascribed to an interaction between the drug and CD (Filipovic-Grcic et al., 2000; Bayomi et al., 2002).

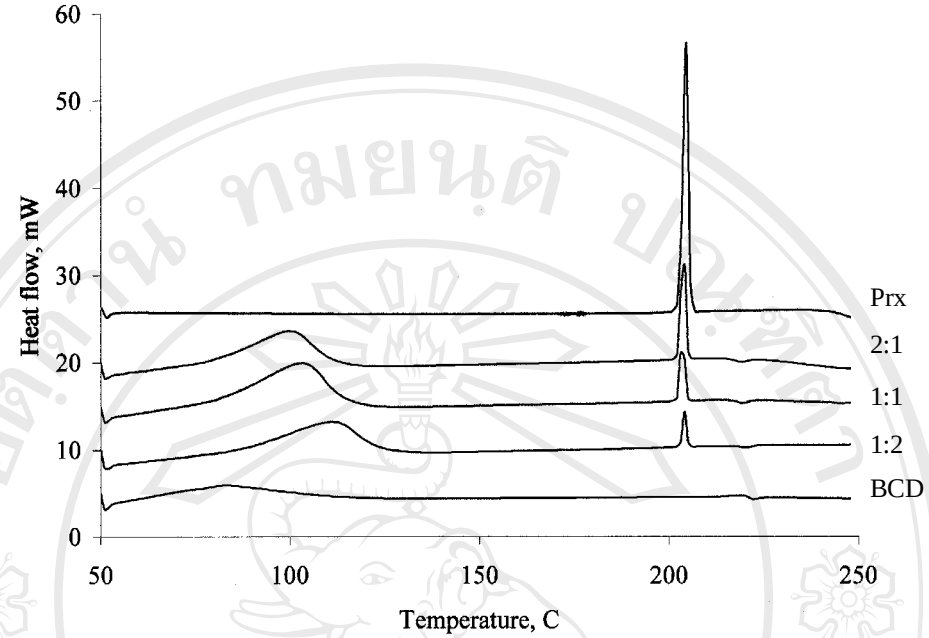

Figure 66 DSC thermograms of piroxicam , piroxicam-BCD physical mixtures of various molar ratios and BCD.

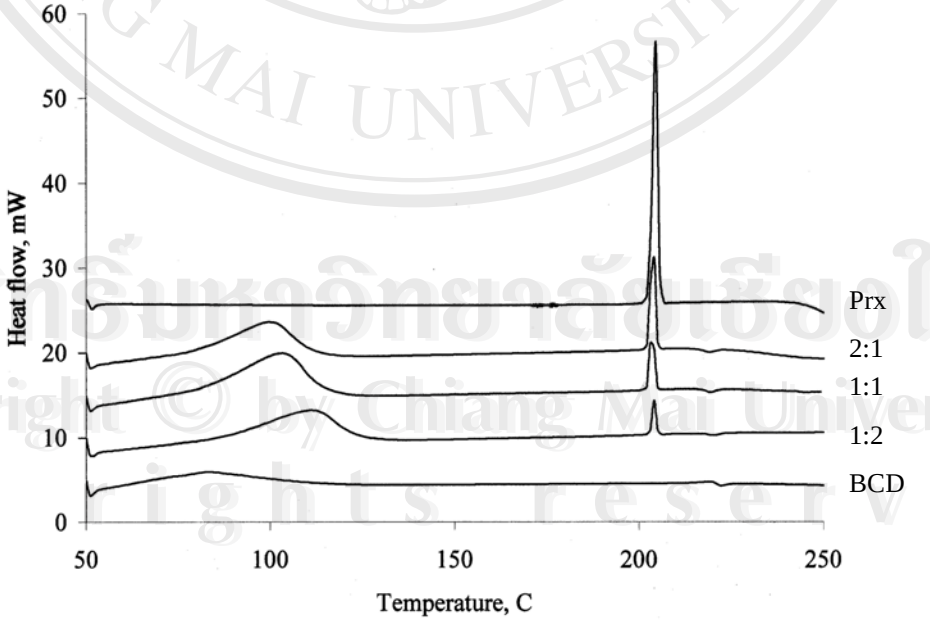

Figure 67 DSC thermograms of piroxicam , piroxicam-BCD inclusion complexes of various molar ratios prepared by kneading method and BCD.

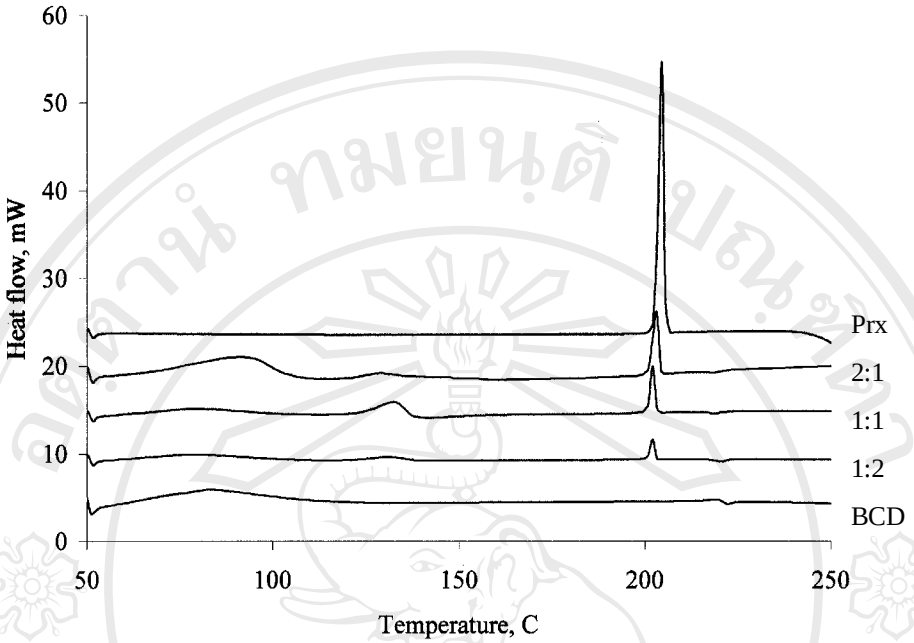

Figure 68 DSC thermograms of piroxicam , piroxicam-BCD inclusion complexes of various molar ratios prepared by co-evaporation method and BCD.

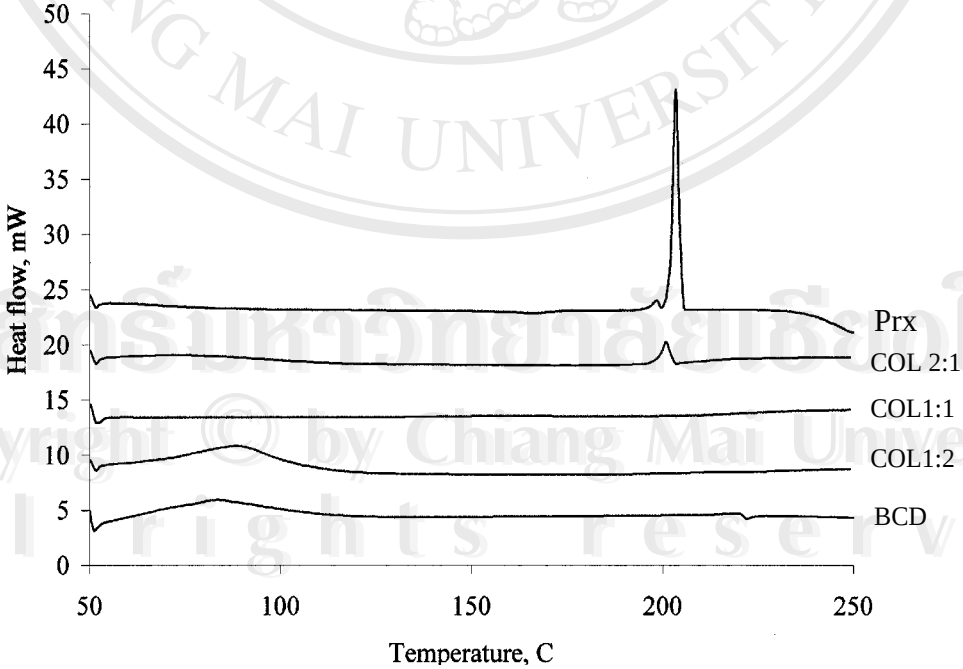

Figure 69 DSC thermograms of piroxicam , piroxicam-BCD inclusion complexes of various molar ratios prepared by co-lyophilization method and BCD.

Table 44 DSC parameters of piroxicam intact, piroxicam lyophilization and piroxicam-BCD inclusion complexes of various molar ratios initially prepared

	Initial		
	Onset,°C	Peak,°C	ΔH, J/g
Prx, intact	201.60	202.89	107.2
Prx, lyo	201.90	203.59	95.5
PM 1:1	202.43	203.47	19.3
1:2	203.03	203.95	10.8
2:1	202.42	203.62	34.8
KN 1:1	201.30	202.74	19.8
1:2	201.45	202.70	8.8
2:1	201.38	202.75	27.7
COE 1:1	200.81	202.04	14.6
1:2	200.80	201.96	7.0
2:1	201.30	202.75	32.8
COL 1:1		No peak	
1:2		No peak	
2:1	198.34	201.20	15.2

The DSC thermograms shown by physical mixtures and the inclusion complexes of piroxicam and GCD at various molar ratios are similar to those of piroxicam-BCD complexes (Figures 70-73). Moreover, the DSC parameters listed in Table 44 were comparable to those of piroxicam-BCD complexes. Upon the thermal behaviors of DSC, it could be suggested that the two parent CDs have very similar interactions with piroxicam.

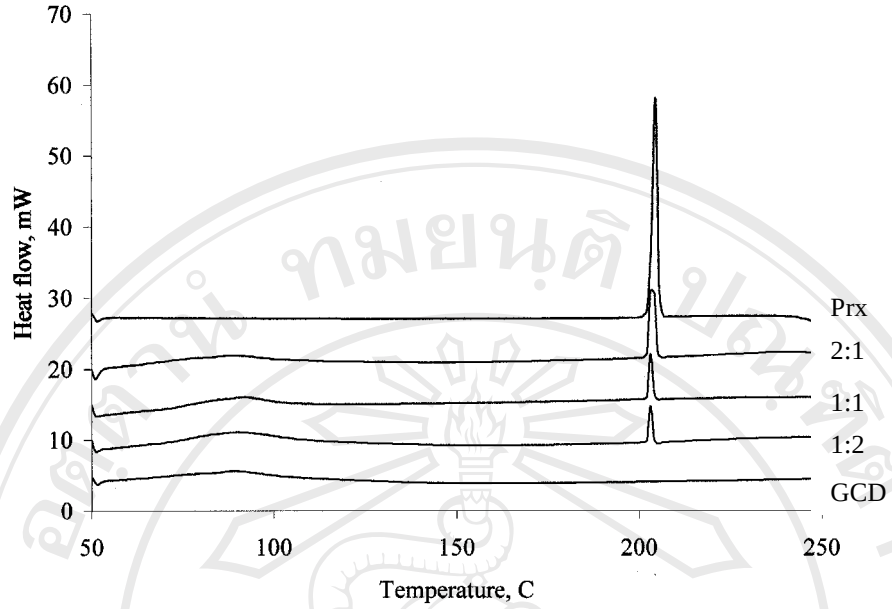

Figure 70 DSC thermograms of piroxicam, piroxicam-GCD physical mixtures of various molar ratios initially prepared and GCD.

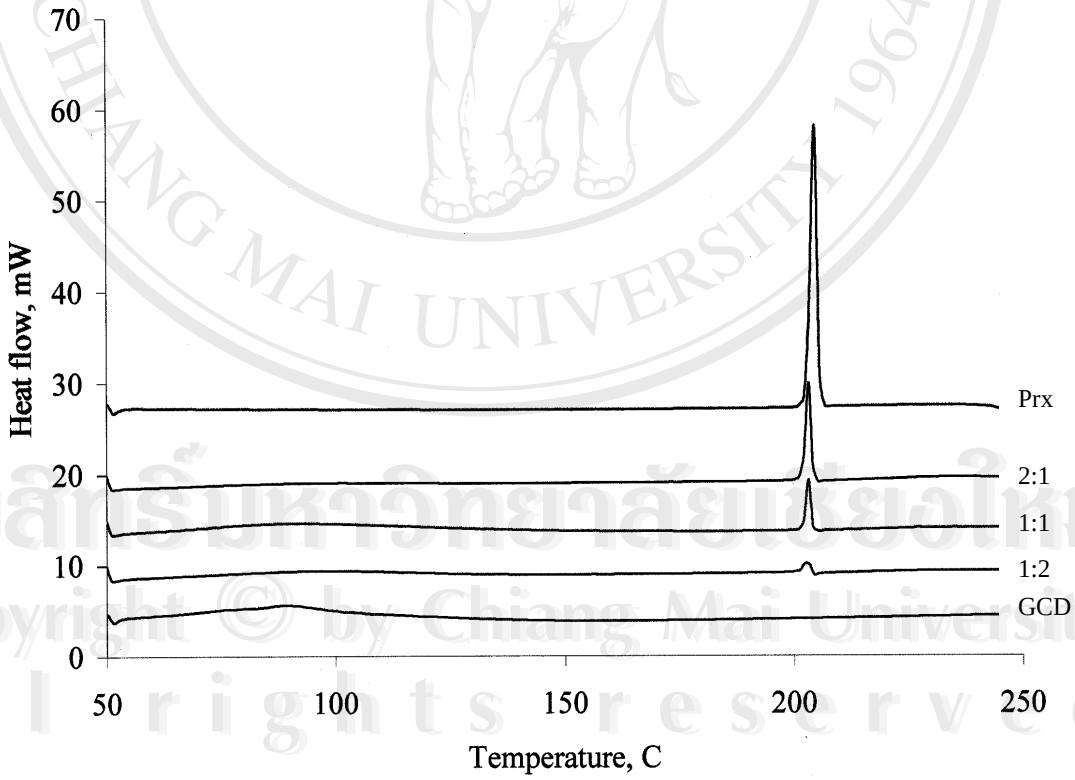

Figure 71 DSC thermograms of piroxicam, piroxicam-GCD inclusion complexes of various molar ratios initially prepared by kneading method and GCD.

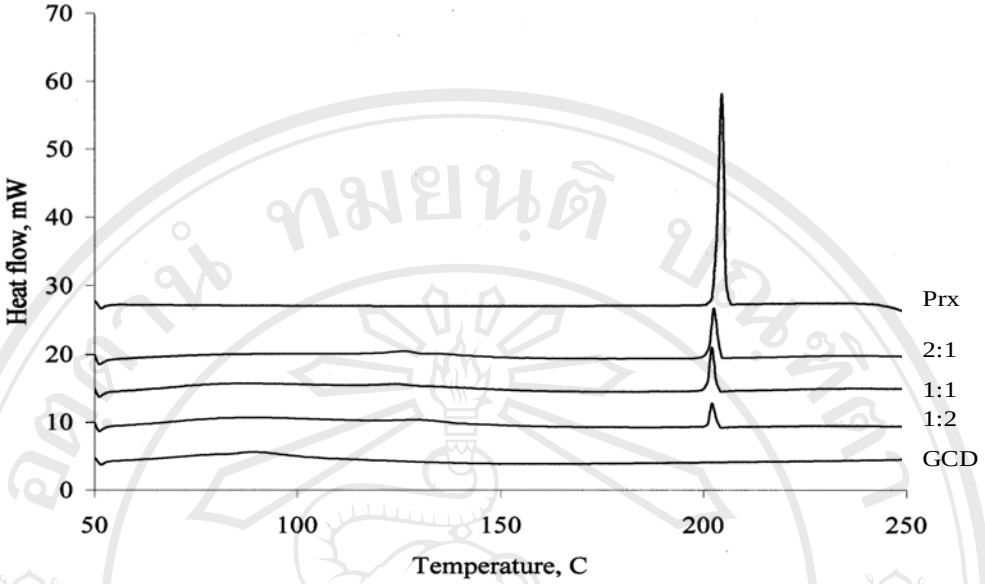

Figure 72 DSC thermograms of piroxicam, piroxicam-GCD inclusion complexes of various molar ratios initially prepared by co-evaporation method and GCD.

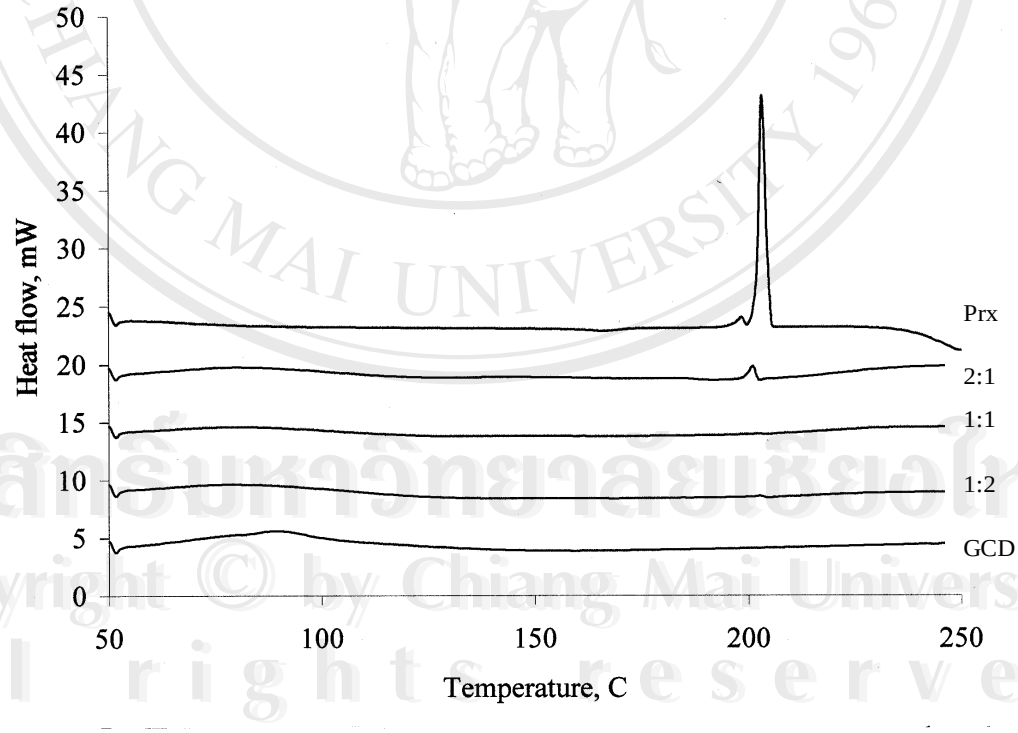

Figure 73 DSC thermograms of piroxicam, piroxicam-GCD inclusion complexes of various molar ratios initially prepared by co-lyophilization method and GCD.

Table 45 DSC parameters of piroxicam, intact; piroxicam, lyophilization and piroxicam-GCD inclusion complexes of various molar ratios

	Initial		
	Onset, °C	Peak, °C	ΔH, J/g
Prx, intact	201.60	202.89	107.2
Prx, lyo	201.90	203.59	95.5
PM 1:1	202.43	203.47	19.3
1:2	203.03	203.95	10.8
2:1	202.42	203.62	34.8
KN 1:1	201.71	202.37	13.7
1:2	201.82	202.74	5.6
2:1	201.82	203.03	30.6
COE 1:1	200.92	202.17	17.7
1:2	201.22	202.29	10.3
2:1	201.21	202.63	29.6
COL 1:1		No peak	
1:2		No peak	
2:1	199.12	200.93	4.6

In the case of piroxicam-HPBCD complexes, their DSC thermograms were similar to those of piroxicam-BCD and piroxicam-GCD except the onset temperatures of the COE and KN complexes were some lower due to non-crystalline nature of HPBCD. The DSC parameters were summarized in Table 46.

Table 46 DSC parameters of piroxicam, intact; piroxicam, lyophilization and piroxicam-HPBCD inclusion complexes of various molar ratios

Samples		Initial		
		Onset,° C	Peak,° C	ΔH, J/g
Prx, intact		201.60	202.89	107.2
Prx, lyo		201.90	203.59	95.5
PM	1:1	201.73	202.64	15.1
	1:2	201.85	202.74	8.2
	2:1	201.74	202.74	25.1
KN	1:1	200.62	201.27	13.7
	1:2	200.24	201.74	5.6
	2:1	200.12	201.63	30.6
COE	1:1	199.95	202.17	11.2
	1:2	199.81	201.02	7.0
	2:1	199.69	200.92	20.4
COL	1:1		No peak	
	1:2		No peak	
	2:1	198.94	201.23	13.1

Table 47 DSC parameters of piroxicam, intact; piroxicam, lyophilization and piroxicam-MeBCD inclusion complexes of various molar ratios initially prepared

Samples	Initial		
	Onset,°C	Peak,°C	ΔH, J/g
Prx, intact	201.60	202.89	107.2
Prx, lyo	201.90	203.59	95.5
PM 1:1		No peak	
1:2		No peak	
2:1		No peak	
KN 1:1		No peak	
1:2		No peak	
2:1		No peak	
COE 1:1	159.72	161.56	13.3
1:2	151.33	159.89	6.9
2:1	159.30	160.85	26.8
COL 1:1		No peak	
1:2		No peak	
2:1		No peak	

Table 47 illustrates DSC parameters of physical mixtures and inclusion complexes of piroxicam and MeBCD at varying molar ratios. It is very interesting that the characteristic melting peak in the drug alters significantly in all mixtures. The peaks could not be unable detected even in the physical mixtures at 2: 1 molar ratio. The lack of melting peak in physical mixtures has been reported in piroxicam and HPBCD complexes (Jug and Becirevic-Lacan, 2004). The thermogram of KN complex of piroxicam-MeBCD is illustrated in Figure 74. In the case of COE complexes, the melting peak shifts to the lower temperature. This could be ascribed to drug-MeBCD interaction (Fernandes et al., 2002), the inclusion of the drug to MeBCD cavity (Dollo

et al., 1996) or the existence of the new crystal modification. However, the latter suggestion can be confirmed by XPD diffractograms, FTIR spectra and NIR spectra which will be shown further.

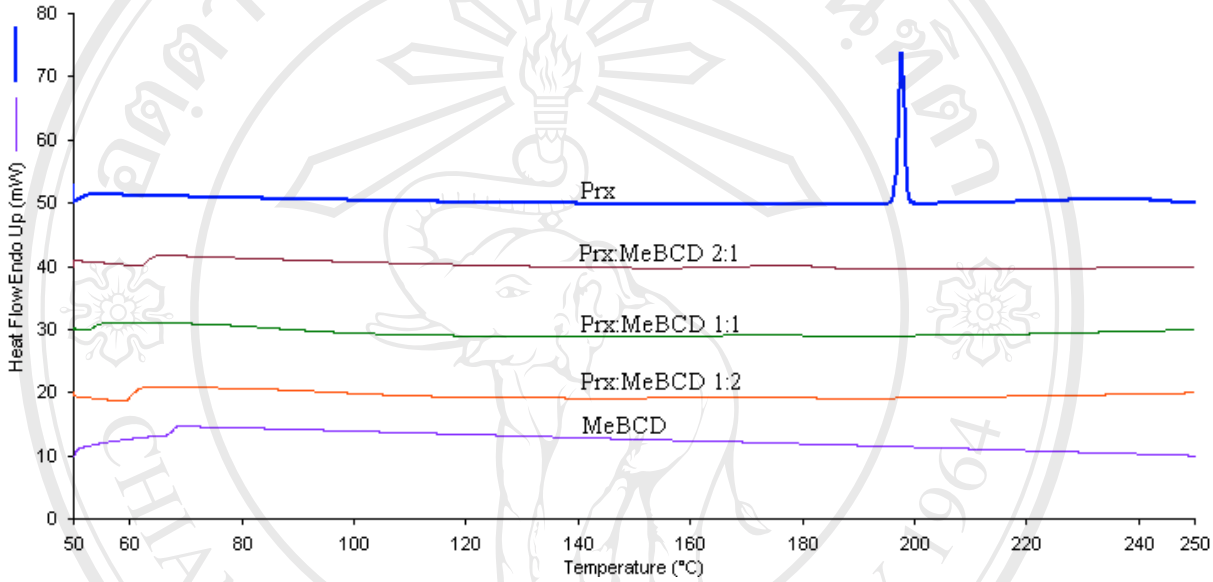

Figure 74 DSC thermograms of piroxicam, intact and piroxicam-MeBCD inclusion complexes prepared by kneading method at various drug to MeBCD molar ratios initially prepared.

3.4.2.2 DSC thermograms of meloxicam-CDs complexes

DSC thermograms of 1:1 inclusion complexes of meloxicam in BCD, GCD, HPBCD and HPGCD, prepared by different methods are given in Figures 75-78, respectively. The DSC parameters of the complexes are illustrated in Table 46.

The characteristic melting peak of meloxicam was exhibited at 253.53°C with the enthalpy of fusion 132.50 J/g. The lowering of the melting peak in accompanied by the reduction of the enthalpy of fusion is observed in all binary mixtures

irrespectively to the method of preparation. This signifies the interaction occurring between the drug and CDs.

The endodermic peaks shift in meloxicam-BCD complexes (Figure 76) are not distinctly different from each other compared to meloxicam-GCD complexes (Figure 76). The COE of meloxicam-GCD shows a large change compared to those meloxicam-BCD complexes. This finding could suggest that the interaction between meloxicam and GCD is stronger than between the drug and BCD.

In the cases of meloxicam-HPBCD and meloxicam-HPGCD complexes, the interaction between the drug and these hosts is much stronger than those with the parent CDs. The changes of the thermal behavior of the drug are evident even in their physical mixtures (Figure 77-78 and Table 48). The lack of an endothermic peak of the drug in the case of COE and COL meloxicam-HPGCD complexes signifies the complete inclusion of the drug into HPGCD cavity. The evidences depicted from DSC study correlate well with the results obtained from dissolution studies. For instance, the %DE30 of meloxicam-CD physical mixtures, prepared from different CD types, was ranged as HPBCD>HPGCD>GCD~BCD. This rank is in agreement with the rank of the degree of melting point lowering detected in their thermograms. Similarly, the corresponding order between %DE30 and the extent of melting lowering in the case of COL complexes was evidence.

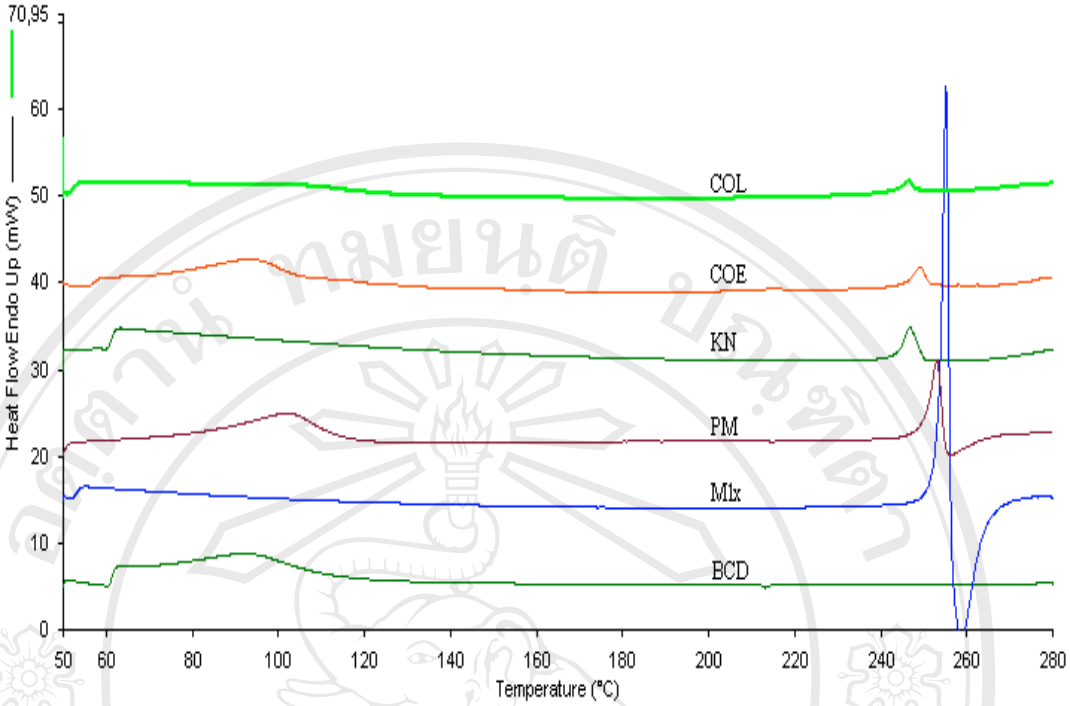

Figure 75 DSC thermograms of meloxicam, Mlx ; BCD ; 1:1 physical mixture, PM ; the inclusion complexes initially prepared by kneading, KN ; co-evaporation, COE and co-lyophilization method, COL.

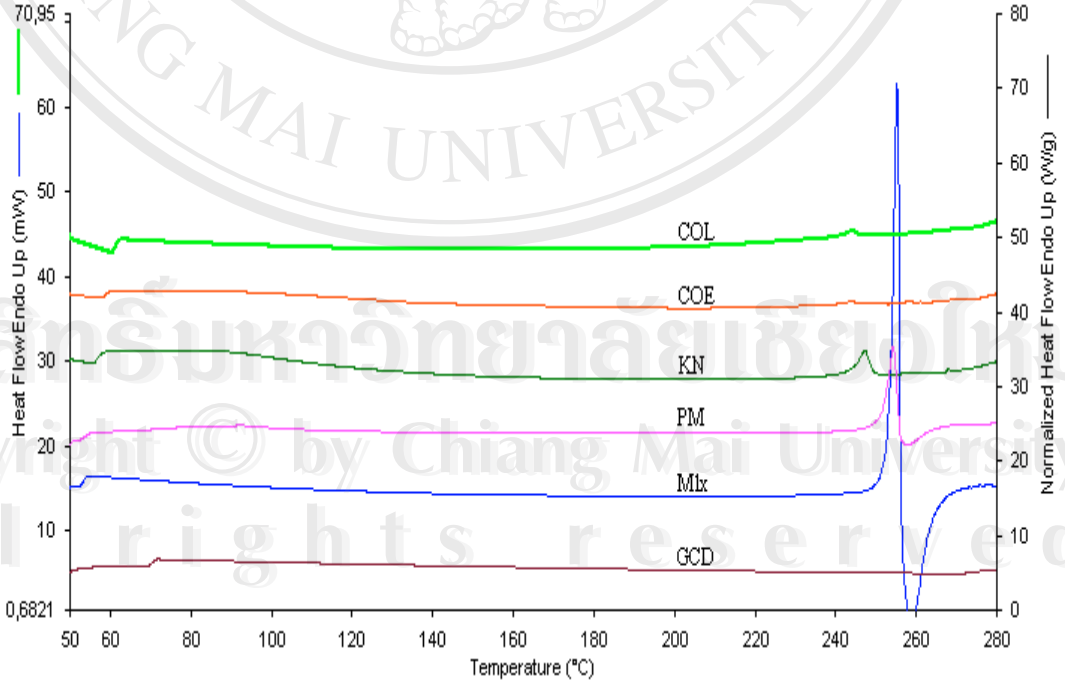

Figure 76 DSC thermograms of meloxicam, Mlx ; GCD ; 1:1 physical mixture, PM ; the inclusion complexes initially prepared by kneading, KN ; co-evaporation, COE and co-lyophilization method, COL.

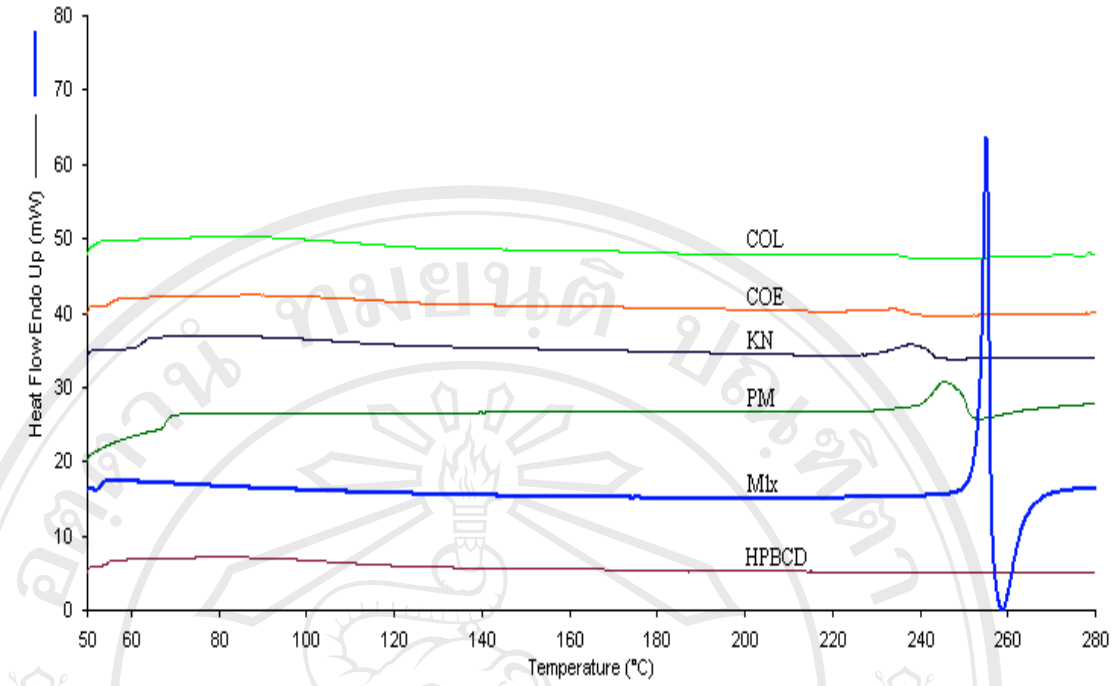

Figure 77 DSC thermograms of meloxicam, Mlx ; HPBCD ; 1:1 physical mixture, PM ; the inclusion complexes initially prepared by kneading, KN ; co-evaporation, COE and co-lyophilization method, COL.

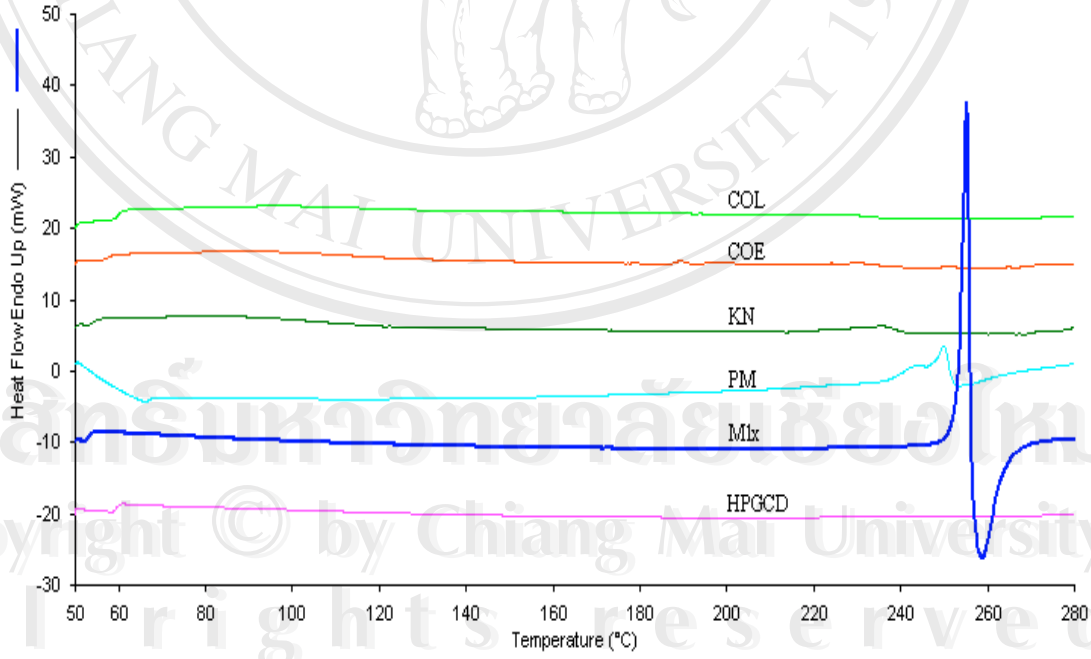

Figure 78 DSC thermograms of meloxicam , Mlx ; HPGCD ; 1:1 physical mixture, PM ; the inclusion complexes initially prepared by kneading, KN ; co-evaporation , COE and co-lyophilization method, COL.

Table 48 DSC parameters of meloxicam, intact; 1:1 meloxicam-CDs physical mixtures and inclusion complexes prepared by different methods

	Initial		
	Onset,°C	Peak,°C	ΔH, J/g
Mlx, intact	253.53	255.20	132.5
Mlx:BCD			
PM	248.20	252.17	35.5
KN	243.74	246.87	28.4
COE	245.93	249.20	20.4
COL	243.25	246.53	20.9
Mlx:GCD			
PM	249.62	253.03	27.6
KN	243.87	247.33	24.5
COE	238.98	244.03	6.3
COL	240.30	244.20	12.6
Mlx:HPBCD			
PM	227.63	245.33	33.3
KN	229.13	237.83	31.5
COE	224.65	234.50	13.5
COL	228.36	232.83	4.2
Mlx:HPGCD			
PM	232.18	240.67	23.1
KN	213.38	235.83	24.9
COE	No peak	No peak	-
COL	No peak	No peak	-

3.4.3 X-ray powdered diffraction (XPD)

Further evidence used for supporting the formation of inclusion complex was obtained from the X-ray diffraction studies. XPD is recognized as a very powerful

technique for the identification of crystalline and non-crystalline compounds. Moreover, lack of a diffraction peak of the drug can be attributed to the complete inclusion complex formation. This technique has been extensively used to verify the occurrence of the inclusion complex between the drug and the CDs (Bayomi et al., 2002; Babu and Pandit 2004; Jug and Becirevic-Lacan, 2004; Sinha et al., 2005).

3.4.3.1 XPD of piroxicam- BCD inclusion complexes

The diffactograms of piroxicam, the intact CDs, the physical mixtures and corresponding complexes of the drug and CDs at varying molar ratios are illustrated in Figures 79-90.

XPD diffractograms of piroxicam-BCD systems prepared at 1:1, 1:2 and 2:1 drug to BCD molar ratio are illustrated in Figures 79-81, respectively. It is shown that piroxicam exhibits its characteristic diffraction peaks at 2θ angle of 27.26 and 17.51, which was designated herein as the major and minor peaks, respectively. Due to the crystalline character, BCD shows its predominant peak at 12.33, and a less dominant one at 22.70. It is beneficial for the characterization that these indicative peaks are not superimposed.

Regardless of the molar ratios between drug to BCD, the XPD diffraction patterns of the physical mixtures are apparently superimposed with those of the components in the mixtures, indicating that the drug and BCD remained their crystallinity state upon simple mixing. The position and intensity of the characteristic peaks were changed slightly. However, no significant interaction is observed.

The KN complex shows spectra somewhat similar to those of the physical mixture but less intense, diffused peaks, due to the reduction in drug and BCD

crystallinity during kneading process. However, the appearance of the major characteristic peaks of the drug and BCD signifies the incomplete phase transition and that of inclusion of the drug into BCD cavity does not occur.

The prominent change in the diffraction pattern is observed in the case of COE and COL complexes. It is of interest that a new peak was observed in COE complexes. This peak is pronounced in the complexes of 1:1 and 2:1 molar ratio which were shown at 25.99 and 26.09, respectively. It is diminished in 1:2 molar ratio complexes due to the high content of BCD. This new peak could be attributed to the formation of new crystals (Veiga et al,. 1996) that might be formed during the evaporation process. The existence of BCD in crystalline state could be supported by its major characteristic peak in the XPD pattern. The evidence of a new peak from XPD was in good agreement with the dissolution study results. The dissolution efficiency of COE complex of piroxicam-BCD is lower than that of KN complexes, due to the existence of a new crystalline compound. The formation of this new peak can be confirmed by FTIR spectra and NIR spectra, which will be further demonstrated.

The complete diffused peak, which is so called halo diffractogram, was evident in COL complex, indicating the complete transformation of the drug and BCD from the crystalline state into the amorphous state. Additionally, the complete inclusion of the crystalline drug into BCD cavity could be suggested.

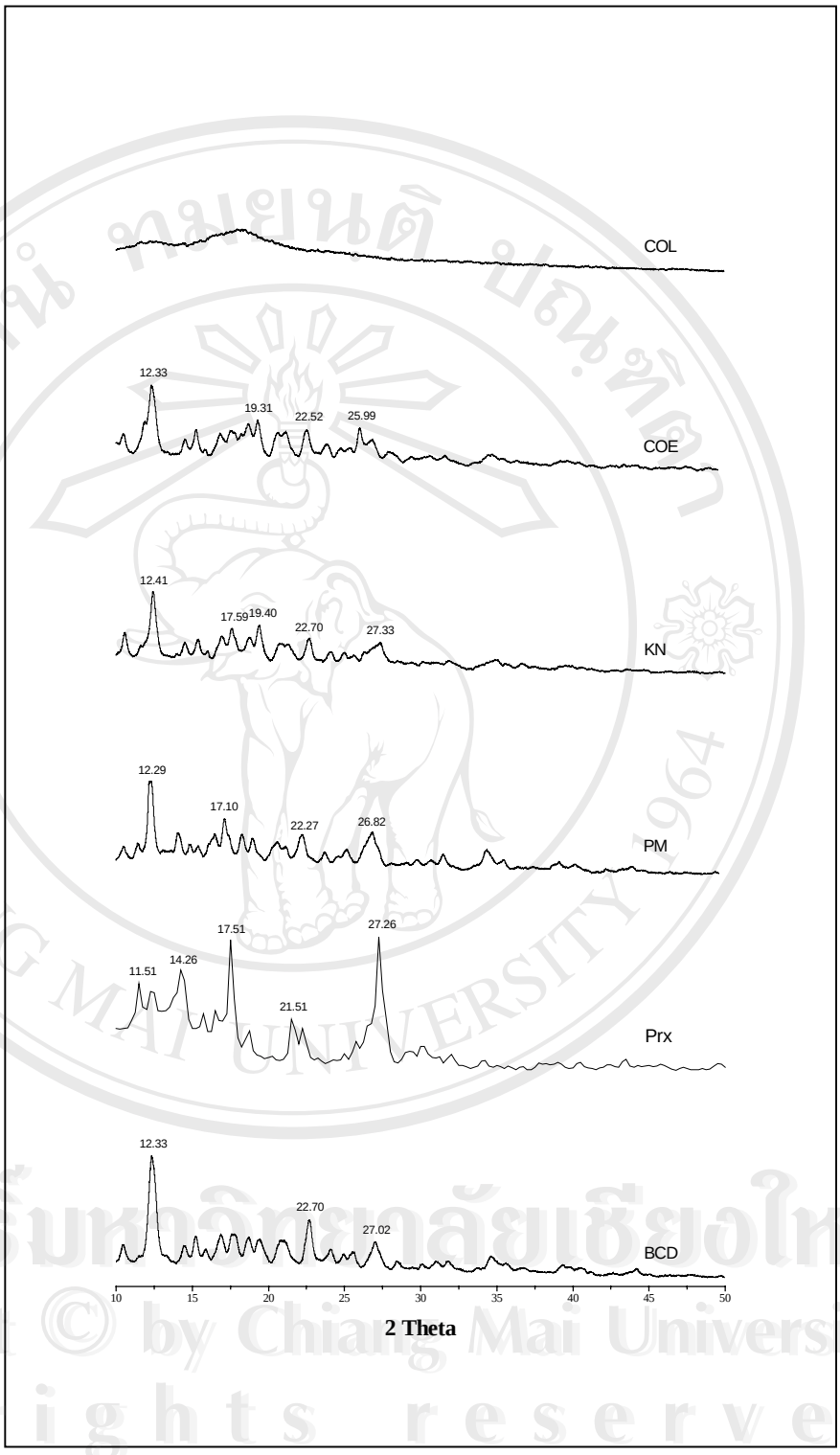

Figure 79 X-ray diffractograms of BCD, piroxicam (Prx), 1:1 physical mixture (PM), and inclusion complexes prepared by kneading method (KN), co-evaporation method (COE) and co-lyophilization method

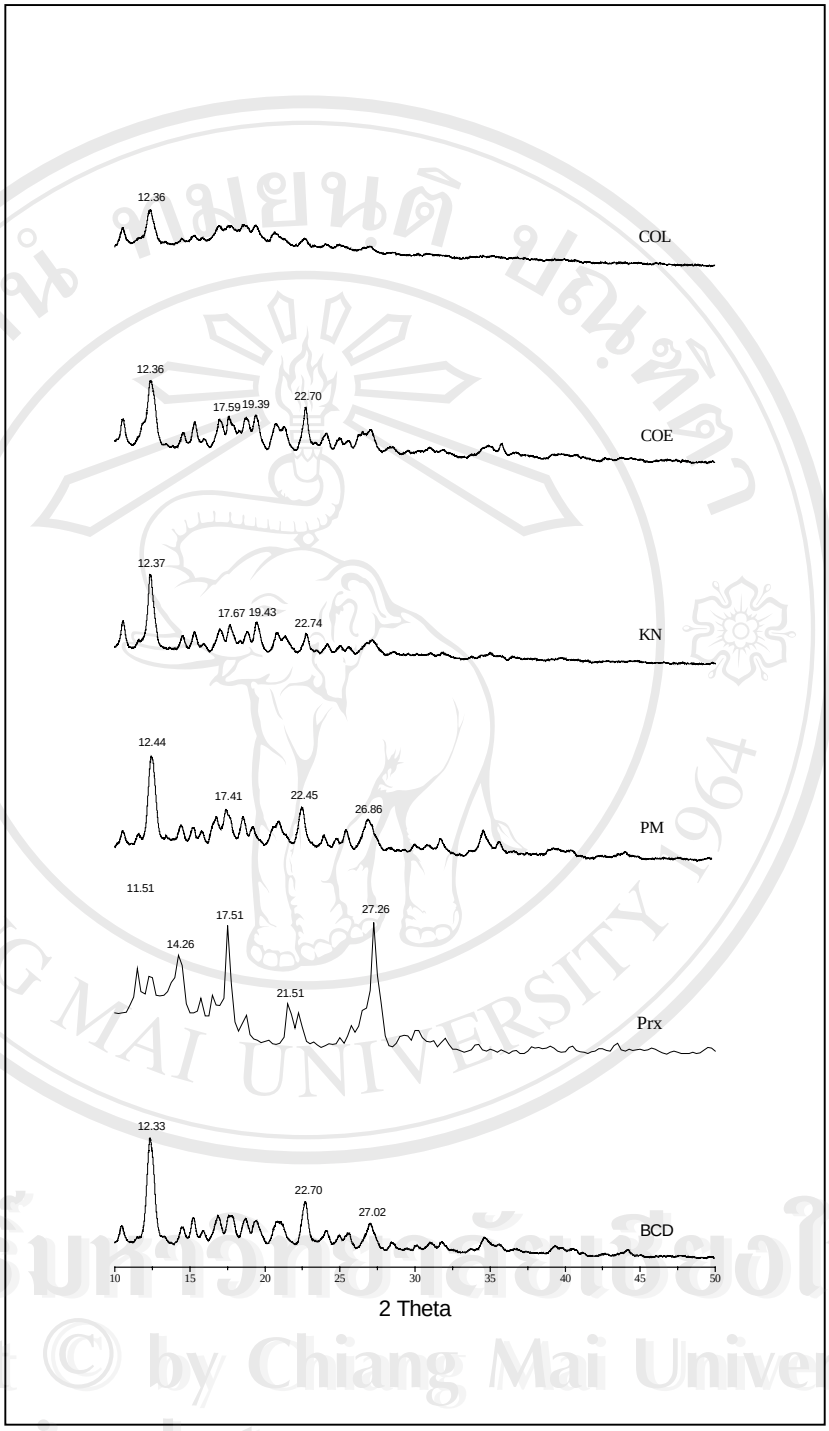

Figure 80 X-ray diffractograms of BCD, piroxicam (Prx), 1:2 physical mixture (PM), and inclusion complexes prepared by kneading method (KN), co-evaporation method (COE) and co-lyophilization (COL) method

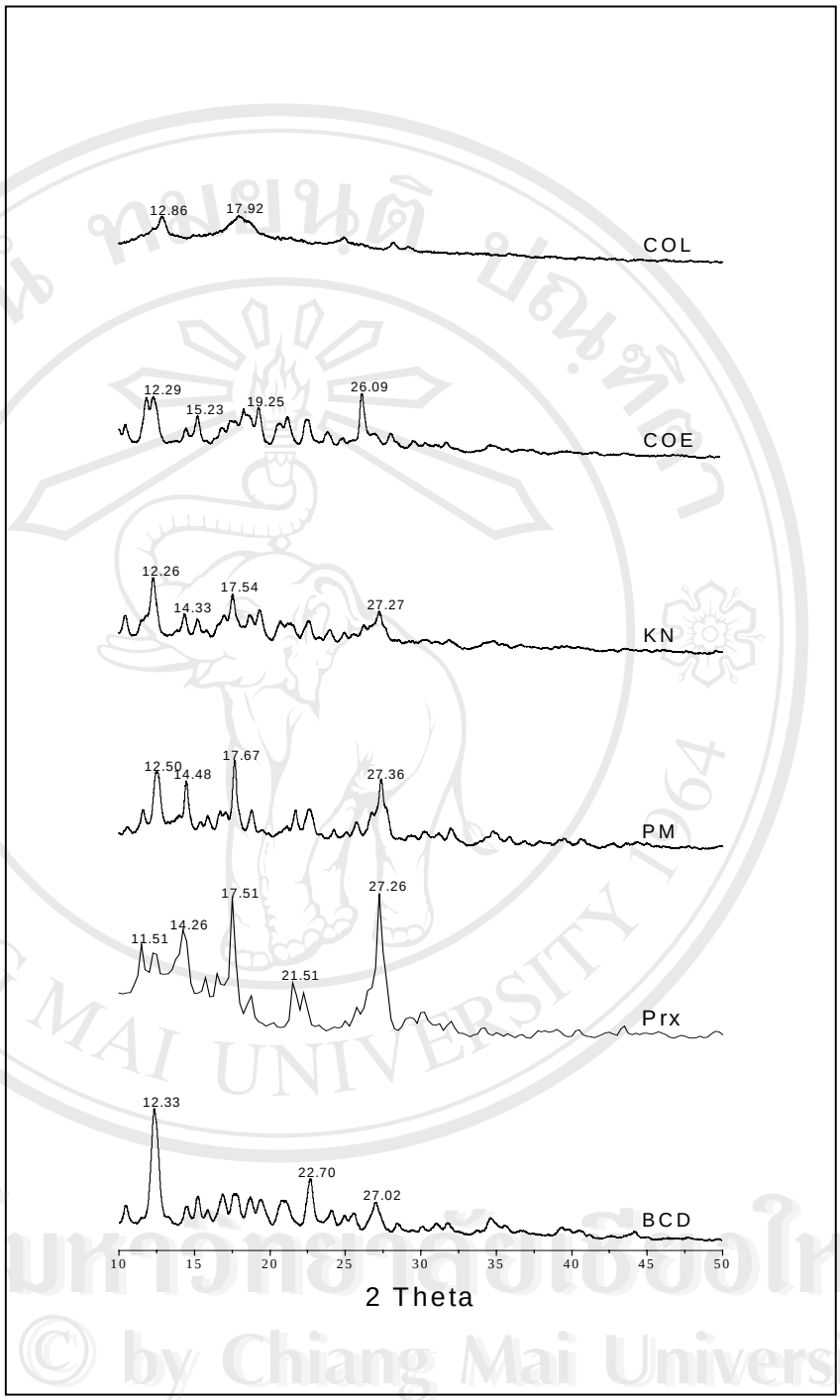

Figure 81 X-ray diffractograms of BCD, piroxicam (Prx), 2:1 physical mixture (PM), and inclusion complexes prepared by kneading method (KN), co-evaporation method (COE) and co-lyophilization (COL) method

The similar XPD evidence is observed in the case of piroxciam-GCD binary mixtures (Figure 82-84). Summarily, the physical mixtures and KN complexes exhibit the broader; less intense peaks, which are however, nearly superimposed to the combination peaks of the drug and GCD. The new peak assigned to the new crystalline form of the drug was detected in COE complexes at 26.28 and 26.03 for 1:1 and 2:1 complexes respectively. The peak position of the new crystal form is slightly different from those observed in piroxicam-BCD complexes, however; it points out the same crystal structure. The halo pattern is shown by COL complexes at all molar ratios, signifying the amorphous state of the complexes.

Figures 85-87 illustrates the XPD diffractograms of piroxicam-HPBCD physical mixtures and the corresponding inclusion complexes at 1:1, 1:2 and 2:1 molar ratio, respectively. Similar XPD behaviors to those of BCD and GCD are observed. The physical mixtures and KN complexes exhibited broader, less intense peaks. The major characteristic peak of the drug was detected in 1:1 and 2:1 complex. These peaks are diminished or likely disappear in 2:1 complexes. This is due to the dilution effect of the HPBCD. New diffraction peaks are also denoted at 25.64 and 25.46 for 1:1 and 2:1 COE complexes. They were in the same range of those observed in the case of BCD and GCD. The halo pattern was obtained in COL complexes irrespective to the molar ratio.

The XPD diffractograms of piroxicam-MeBCD complexes are shown in Figure 88-90. The XPD evidences are similar to the other CDs previously demonstrated. The new peak position in COE complexes are depicted at 25.38 and 25.30 for 1:1 and 2:1 complexes, respectively.

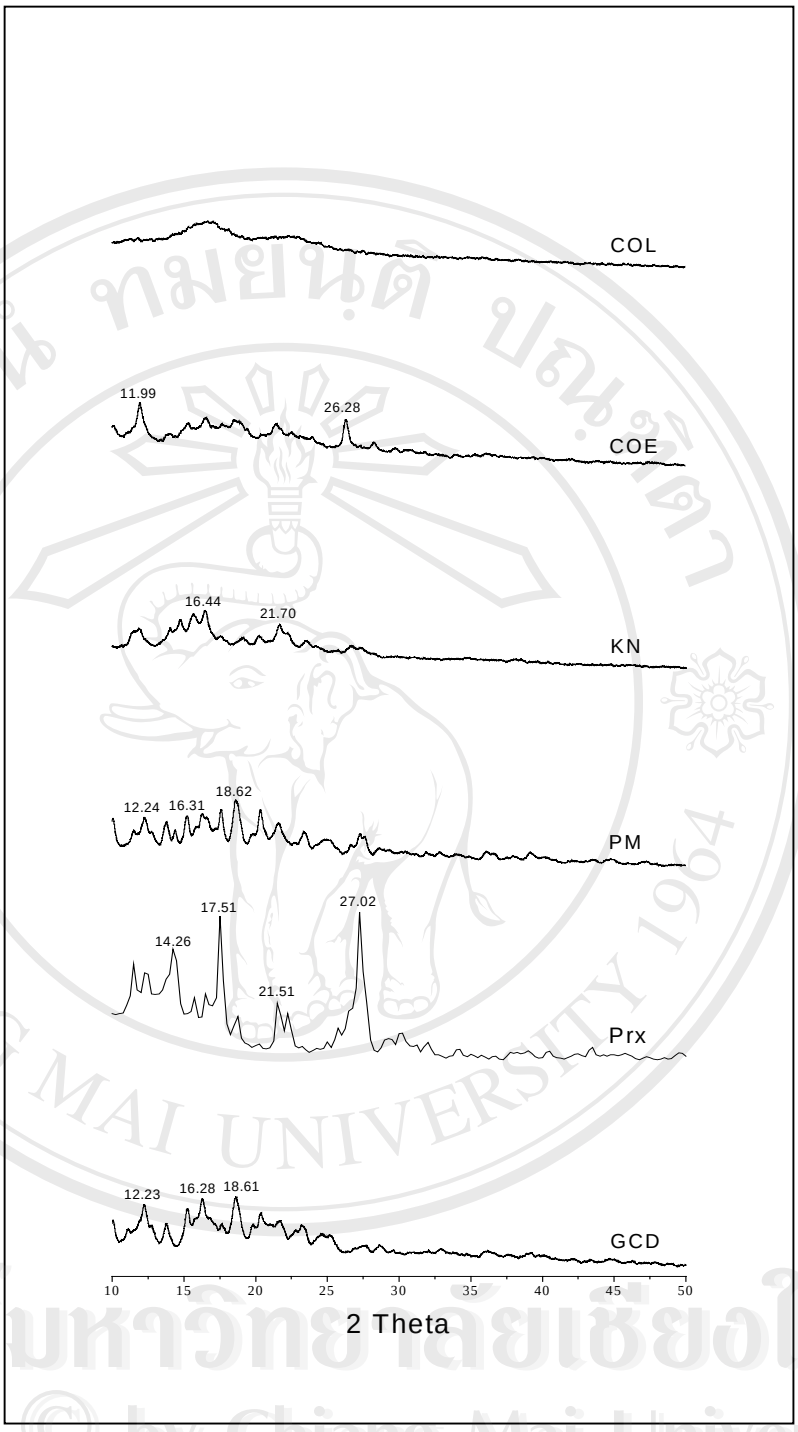

Figure 82 X-ray diffractograms of GCD, piroxicam (Prx), 1:1 physical mixture (PM), and inclusion complexes prepared by kneading method (KN), co-evaporation method (COE) and co-lyophilization (COL) method

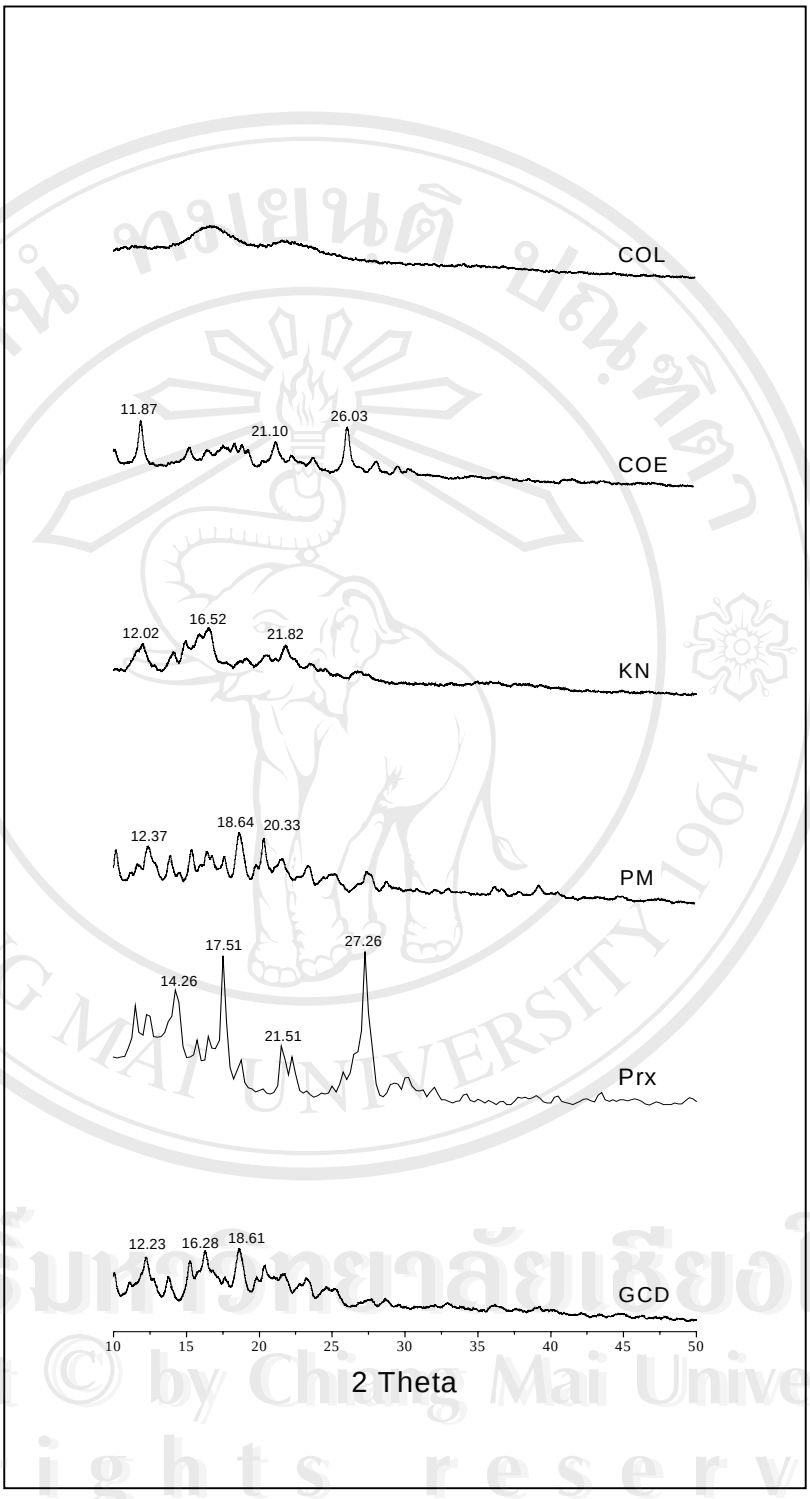

Figure 83 X-ray diffractograms of GCD, piroxicam (Prx), 1:2 physical mixture (PM), and inclusion complexes prepared by kneading method (KN), co-evaporation method (COE) and co-lyophilization (COL) method

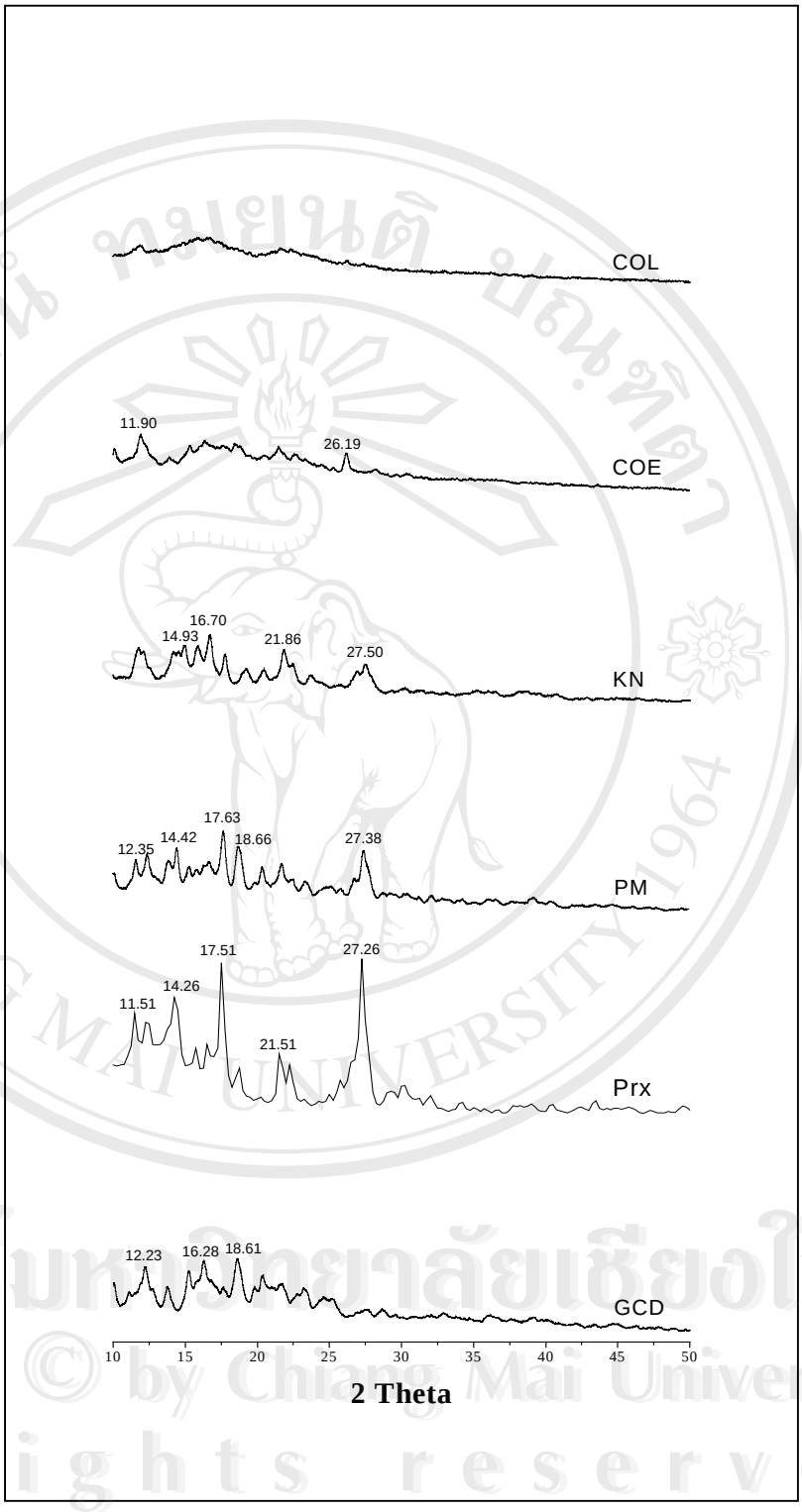

Figure 84 X-ray diffractograms of GCD, piroxicam (Prx), 2:1 physical mixture (PM), and inclusion complexes prepared by kneading method (KN), co-evaporation method (COE) and co-lyophilization (COL) method

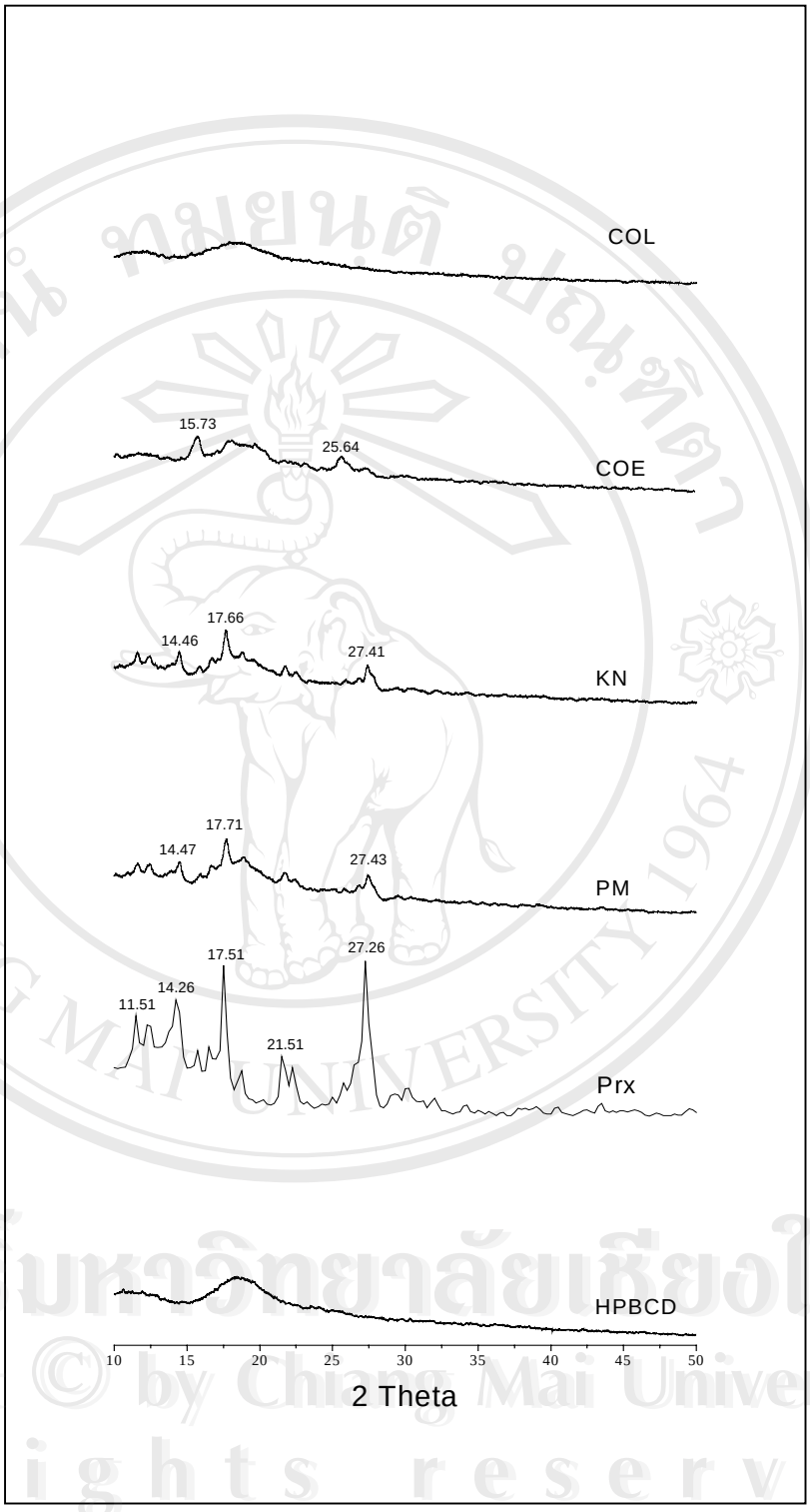

Figure 85 X-ray diffractograms of HPBCD, piroxicam (Prx), 1:1 physical mixture (PM), and inclusion complexes prepared by kneading method (KN), co-evaporation method (COE) and co-lyophilization (COL) method

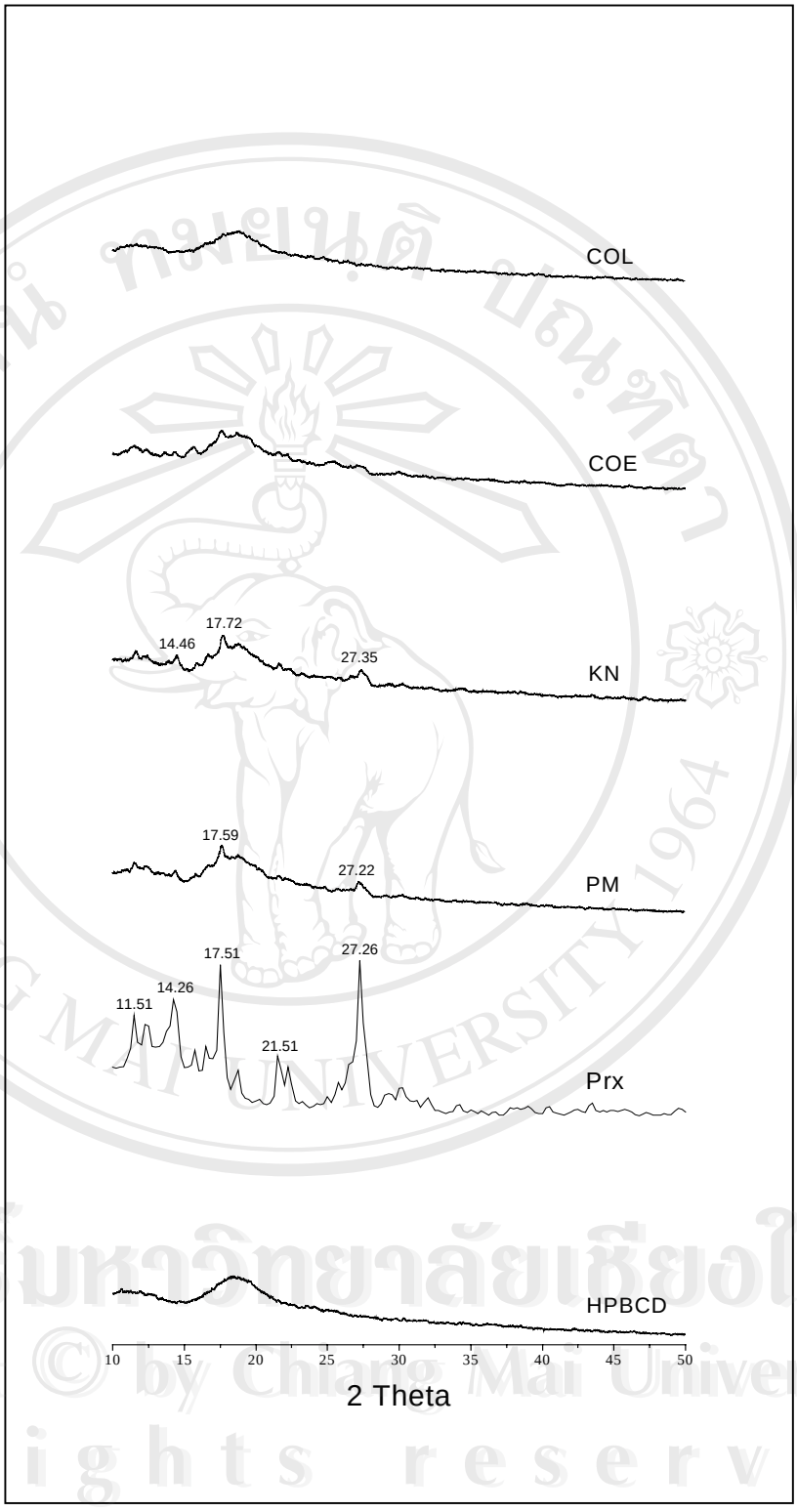

Figure 86 X-ray diffractograms of HPBCD, piroxicam (Prx), 1:2 physical mixture (PM), and inclusion complexes prepared by kneading method (KN), co-evaporation method (COE) and co-lyophilization (COL) method

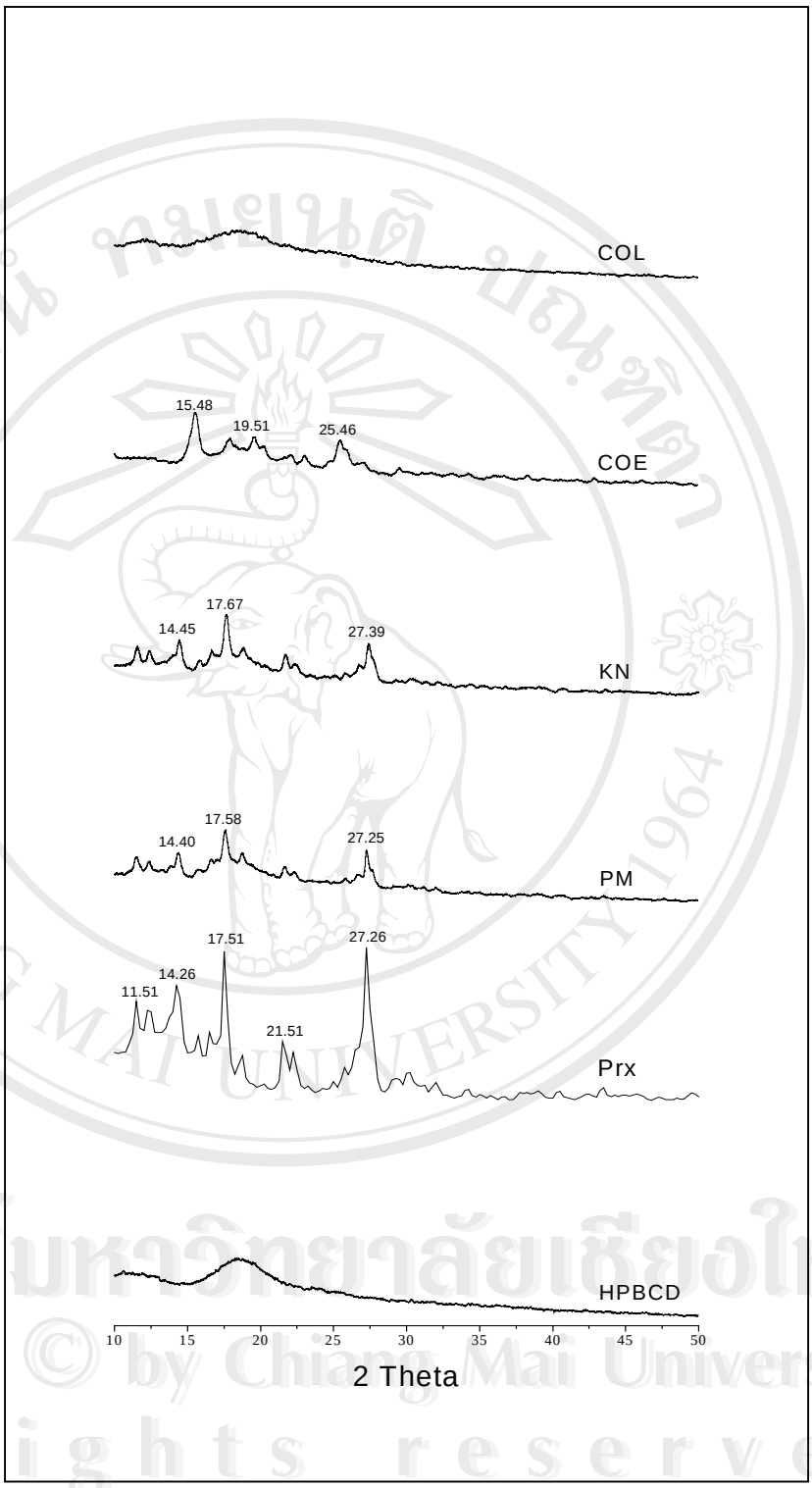

Figure 87 X-ray diffractograms of HPBCD, piroxicam (Prx), 2:1 physical mixture (PM), and inclusion complexes prepared by kneading method (KN), co-evaporation method (COE) and co-lyophilization (COL) method

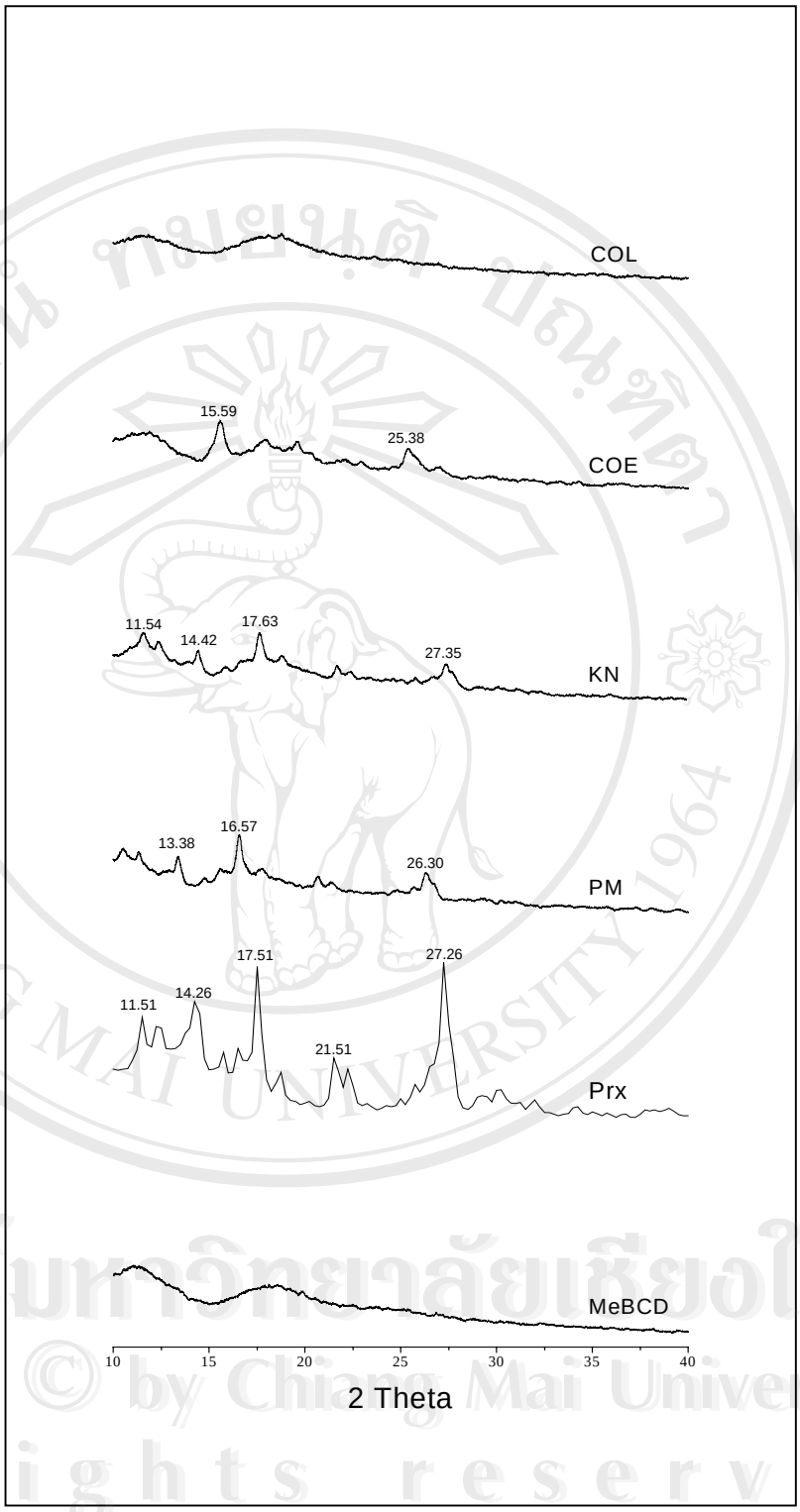

Figure 88 X-ray diffractograms of MeBCD, piroxicam (Prx), 1:1 physical mixture (PM), and inclusion complexes prepared by kneading method (KN), co-evaporation method (COE) and co-lyophilization (COL) method

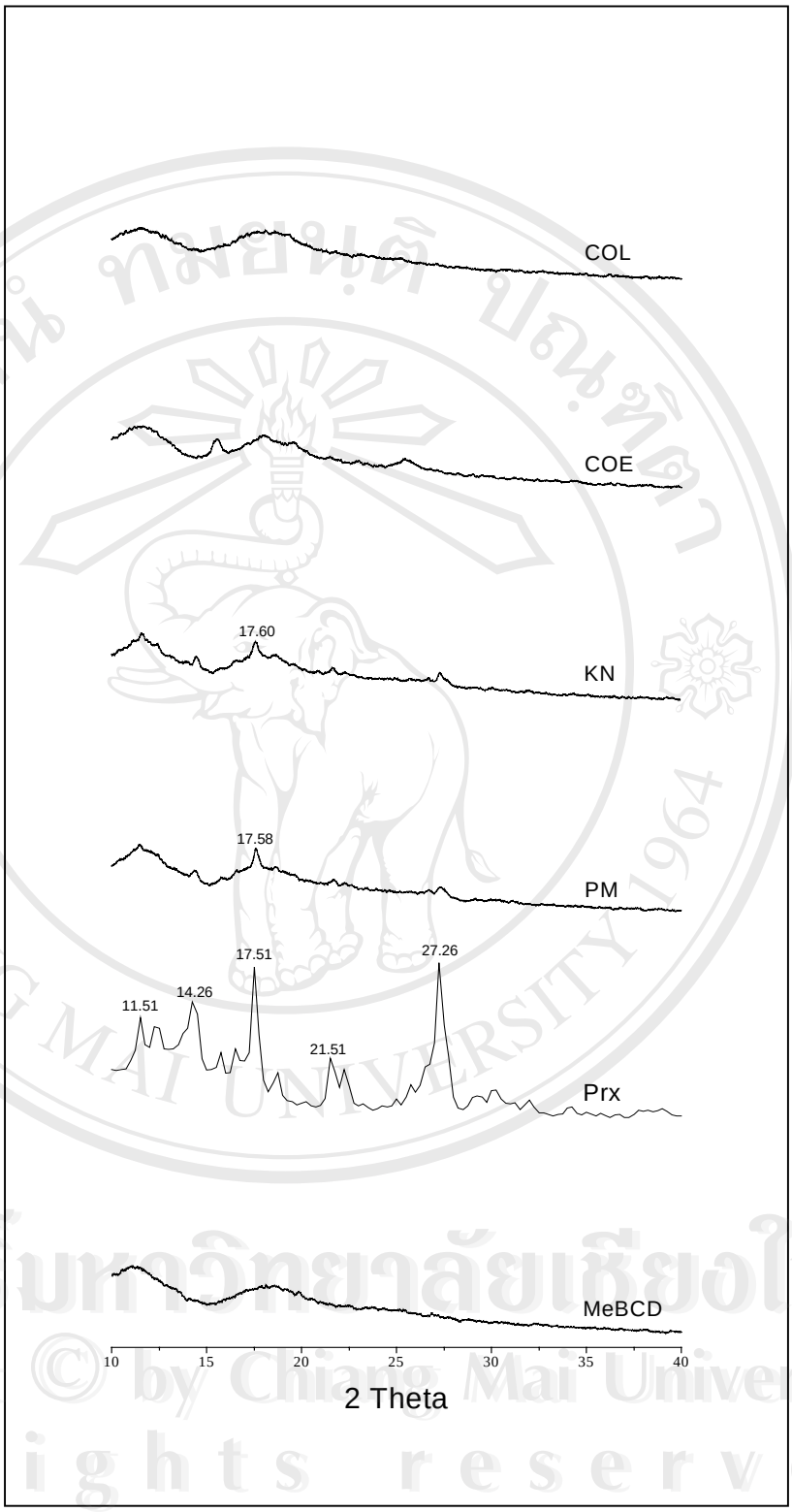

Figure 89 X-ray diffractograms of MeBCD, piroxicam (Prx), 1:2 physical mixture (PM), and inclusion complexes prepared by kneading method (KN), co-evaporation (COE) and co-lyophilization (COL) method

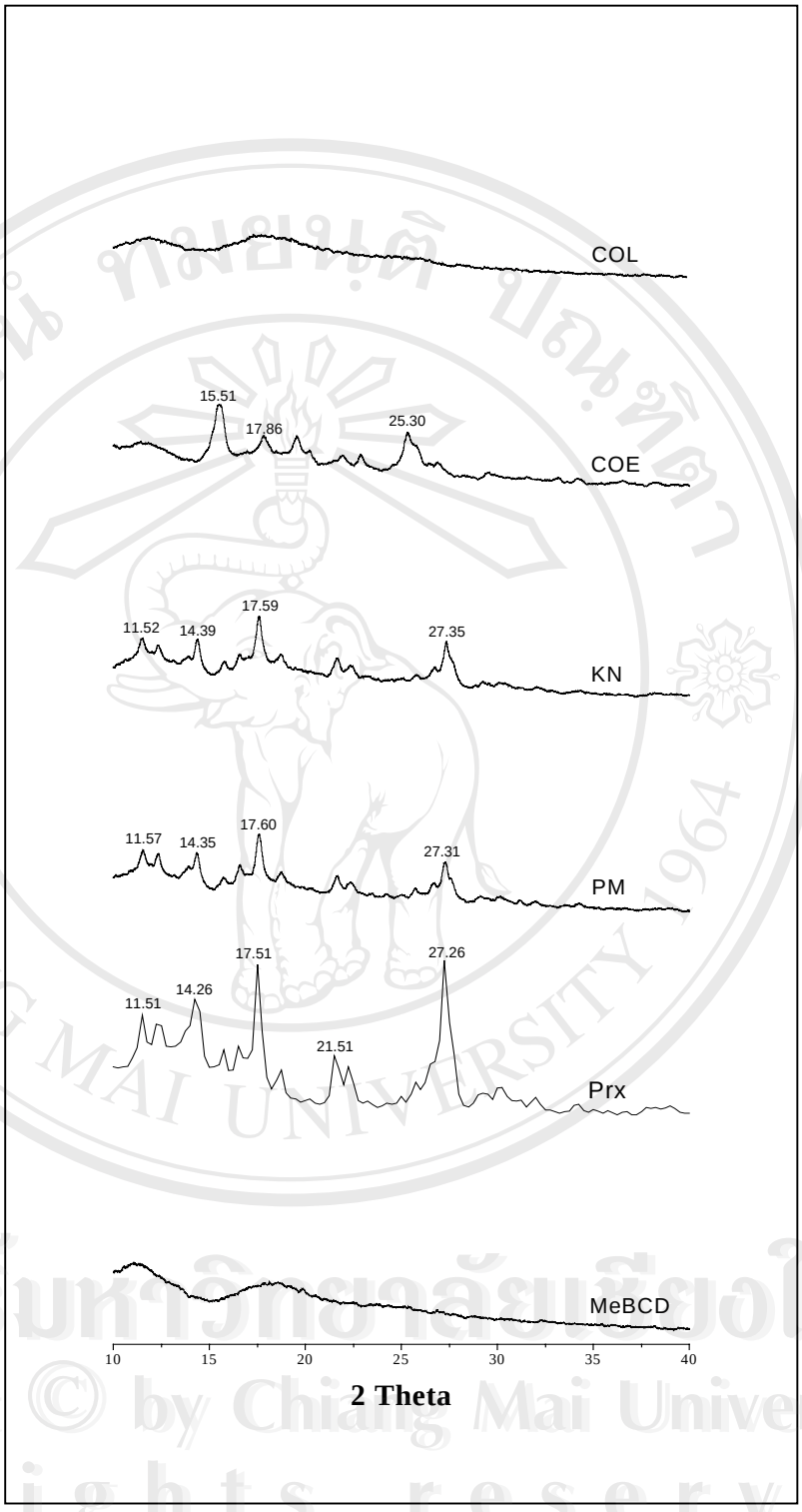

Figure 90 X-ray diffractograms of MeBCD, piroxicam (Prx), 2:1 physical mixture (PM), and inclusion complexes prepared by kneading method (KN), co-evaporation (COE) and co-lyophilization (COL) method

3.4.3.2 XPD of meloxicam- BCD inclusion complexes

The XPD diffractograms of meloxicam, CDs, 1:1 physical mixtures and their inclusion complexes are illustrated in Figures 91-94 for BCD, GCD HPBCD and HPGCD, respectively.

Meloxicam shows a well-defined intense peaks at 25.70 and 14.72 which are ascribed to its characteristic peaks. The physical mixtures of meloxicam in BCD, GCD and HPBCD exhibit similar XPD pattern. It consists of broader and less intense peaks which are somewhat superimposed to those of the drug. The shift of major peak of the drug and the lower peak intensity is more pronounced in the physical mixture of the drug and HPGCD. The finding is corresponding to the evidence obtained from DSC thermograms and the dissolution studies. The KN complexes shows more diffused peaks compared to the corresponding physical mixtures, but the major characteristic peak of the drug is still detectable. The COE and COL complexes of the drug and GCD, HPBCD and HPGCD show halo patterns implying the amorphous state of the complex as well as the complete inclusion complex formation whereas these complexes between the drug and BCD exhibit some diffused peaks. This finding is corresponding to the dissolution study which demonstrates that the lowest %DE30 value is obtained from meloxicam-BCD complexes.

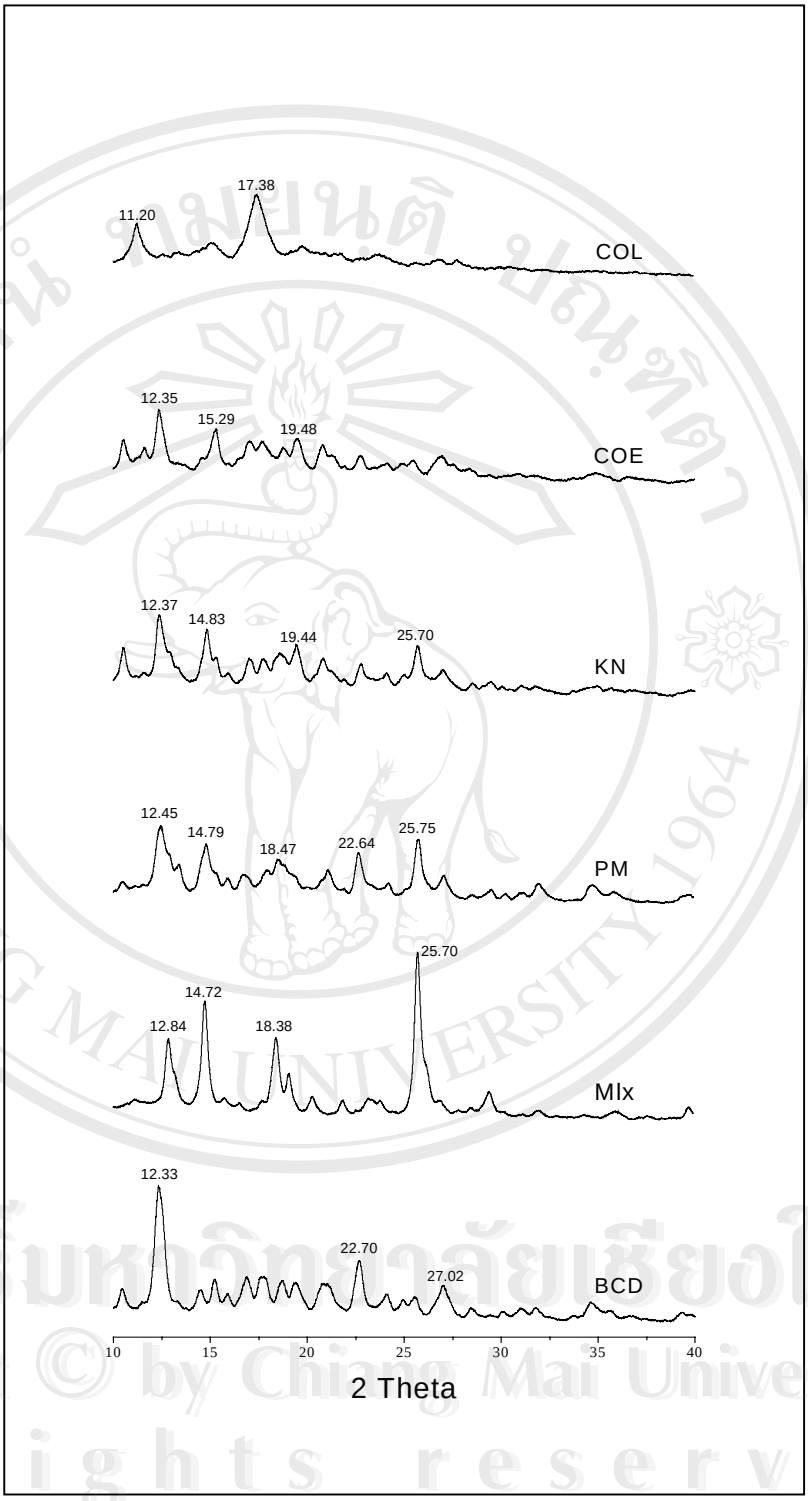

Figure 91 X-ray diffractograms of BCD, meloxicam (Mlx), 1:1 Physical mixture (PM), and inclusion complexes prepared by kneading (KN), co-evaporation (COE) and co-lyophilization (COL) method

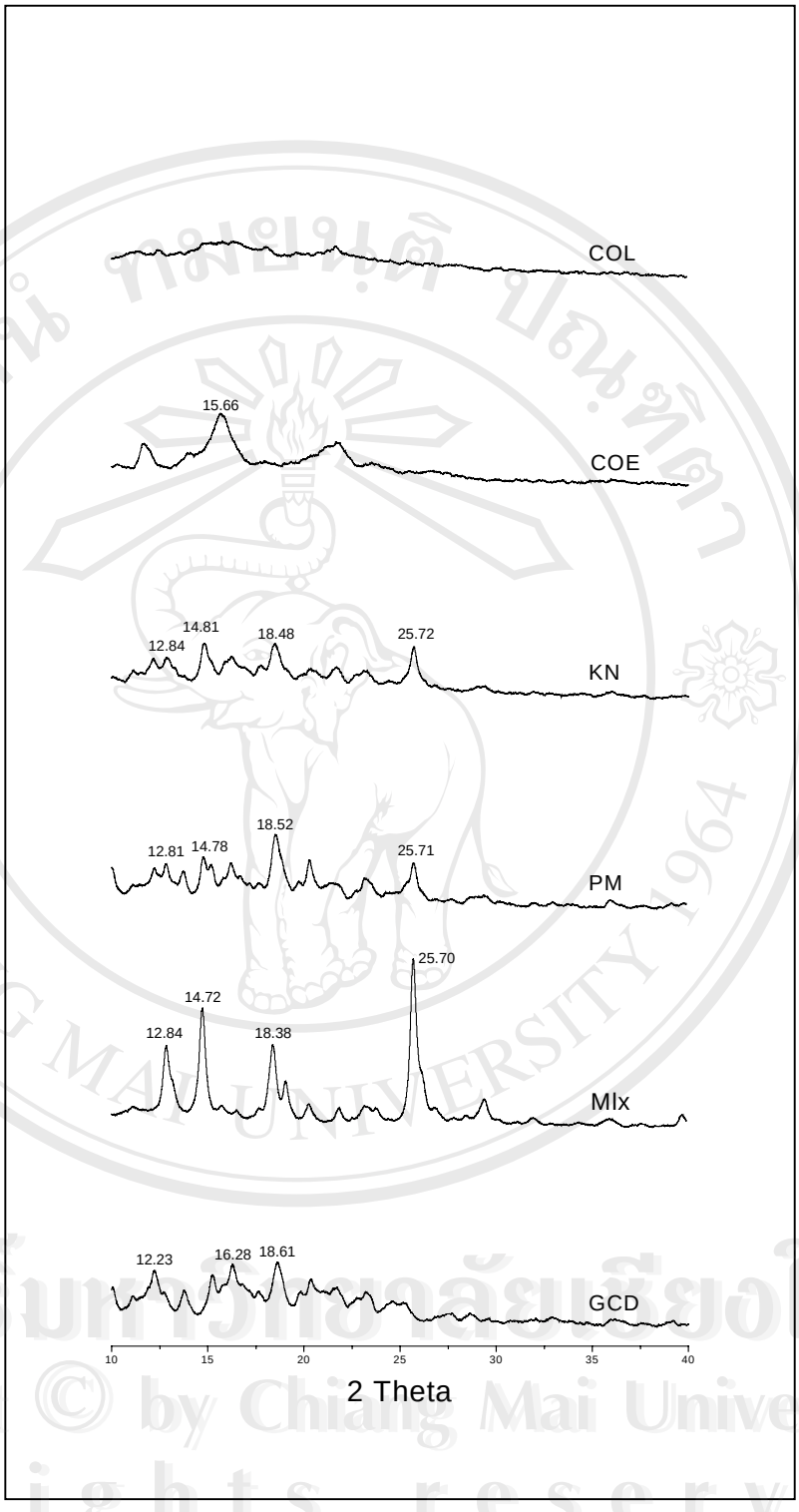

Figure 92 X-ray diffractograms of GCD, meloxicam (Mlx), 1:1 Physical mixture (PM), and inclusion complexes prepared by kneading (KN), co-evaporation (COE) and co-lyophilization (COL) method

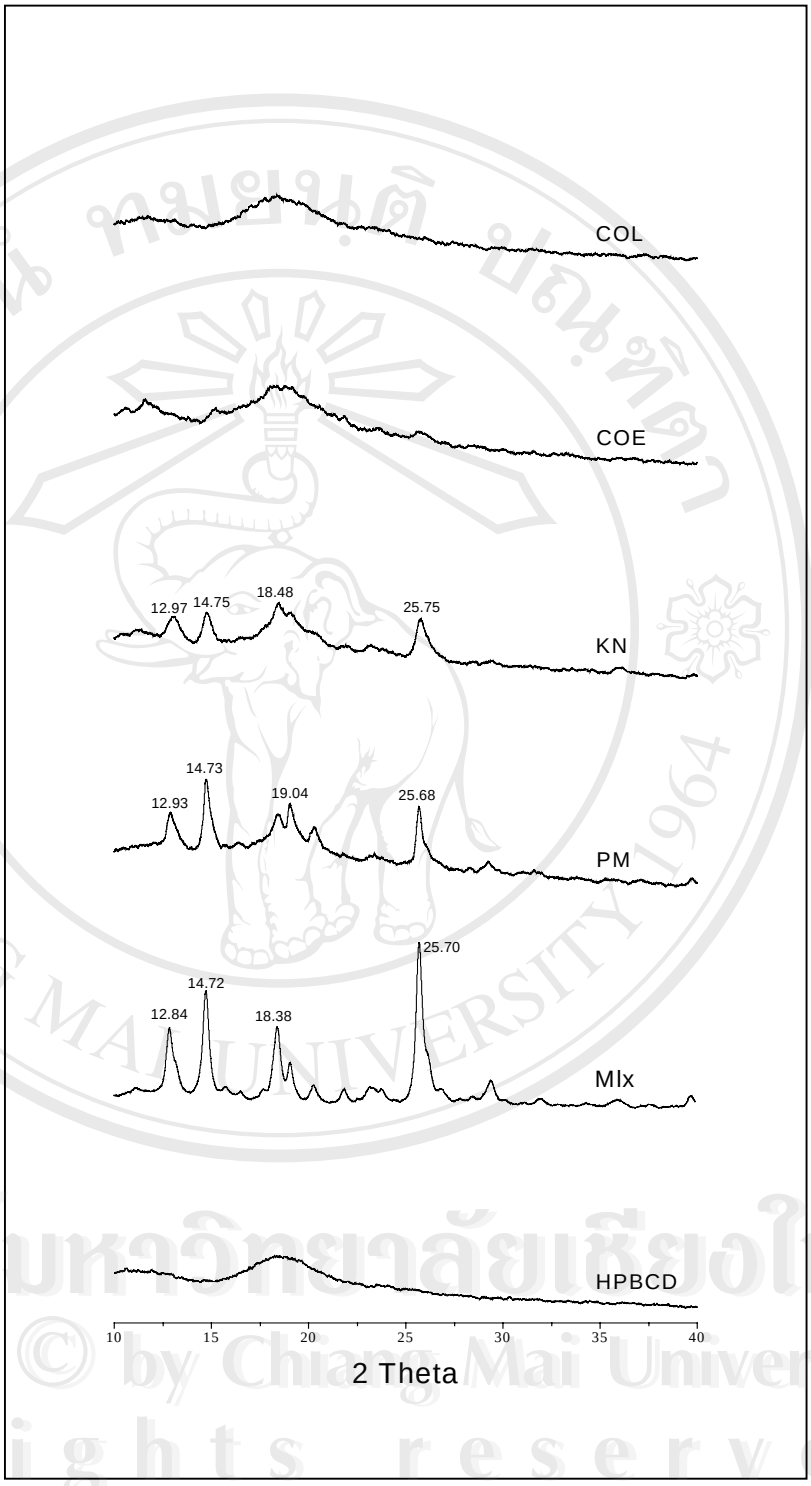

Figure 93 X-ray diffractograms of HPBCD, meloxicam (Mlx), 1:1 Physical mixture (PM), and inclusion complexes prepared by kneading (KN), co-evaporation (COE) and co-lyophilization (COL) method

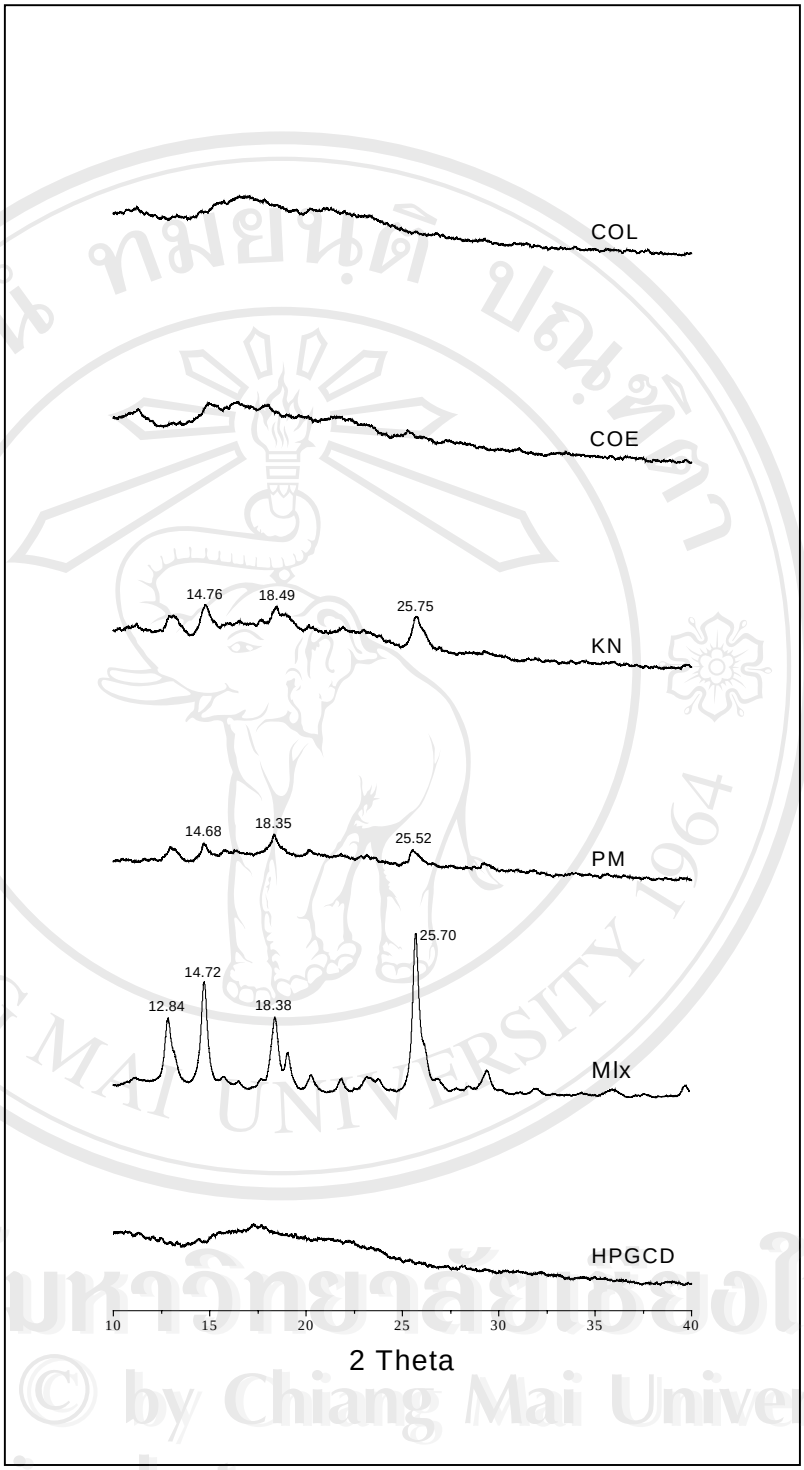

Figure 94 X-ray diffractograms of HPGCD, meloxicam (Mlx), 1:1 Physical mixture (PM), and inclusion complexes prepared by kneading (KN), co-evaporation (COE) and co-lyophilization (COL) method

3.4.4 Fourier transform infrared spectroscopy (FTIR)

FTIR studies can provide useful evidence of the drug-CD complex formation by exploring the functional groups involved in the complex formation process. Accordingly, a significant shift of the characteristic peaks belonging to the involved functional group to either higher or lower frequency could signify the interaction between the drug and CDs (Dollo et al., 1996; Mura et al., 1998; Fernandes et al., 2002; Perdomo-Lopez et al., 2002). The disappearance and broadening of the peaks indicates the inclusion of the drug into the cavity of CD (Guyot et al., 1995).

3.4.4.1 FTIR spectra of piroxicam-CD inclusion complexes

FTIR spectrum of the intact piroxicam shown in Figure 95 exhibits a strong absorption peak at 3330 cm^{-1} belonging to –NH and –OH stretching vibrations. The other characteristic peaks appear at 1630 cm^{-1} and 1528 cm^{-1} which were assigned to the first and the second amide- carbonyl stretching vibrations.

The FTIR spectra of pure CDs (Figure 96-100) are characterized by the broad intense absorption band at 3374-3392 cm^{-1} which is assigned to stretching vibration of free –OH groups. The absorption bands corresponding to the vibration of –CH and –CH_2 groups appear at 2916-2925 cm^{-1} (Perdomo-Lopez et al., 2002).

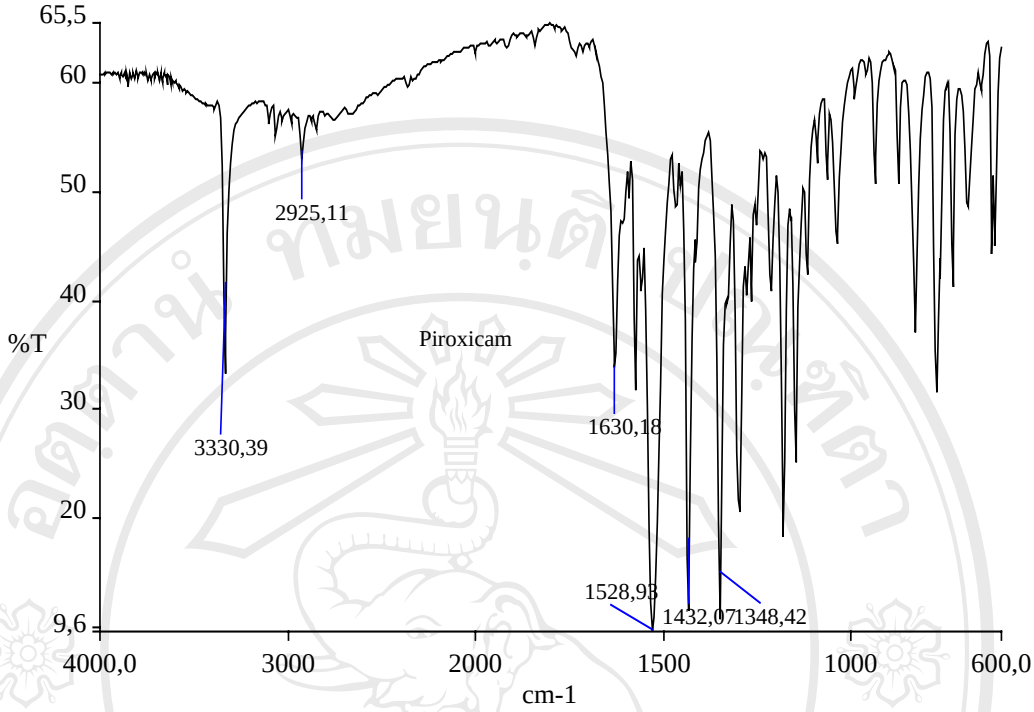

Figure 95 FTIR spectrum of piroxicam , intact

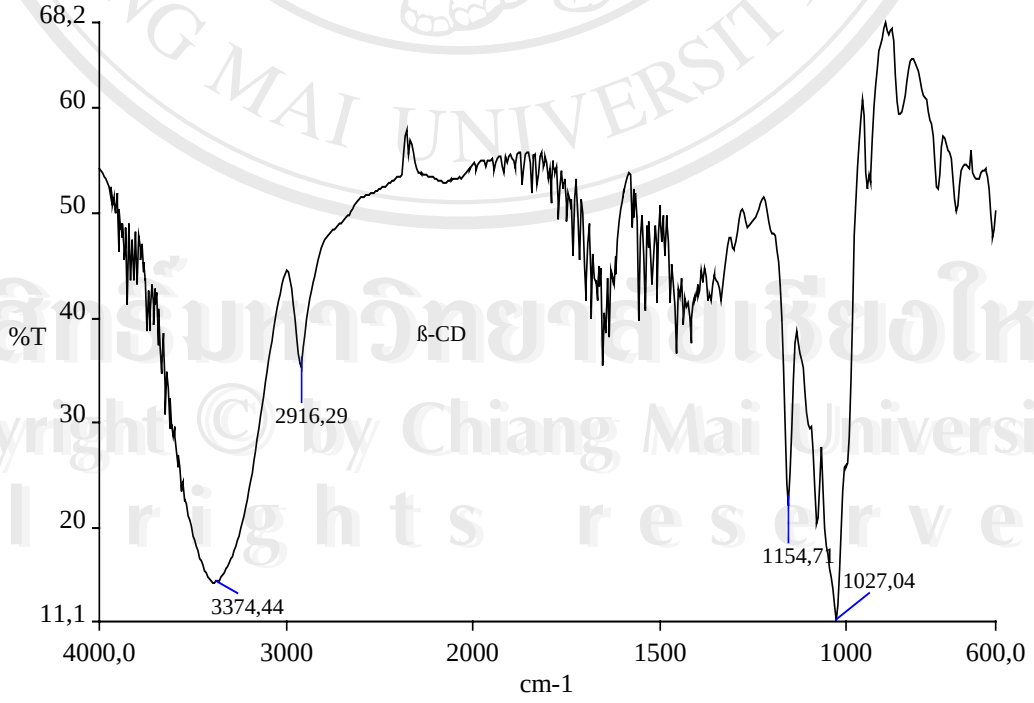

Figure 96 FTIR spectrum of β-cyclodextrin (BCD) , intact

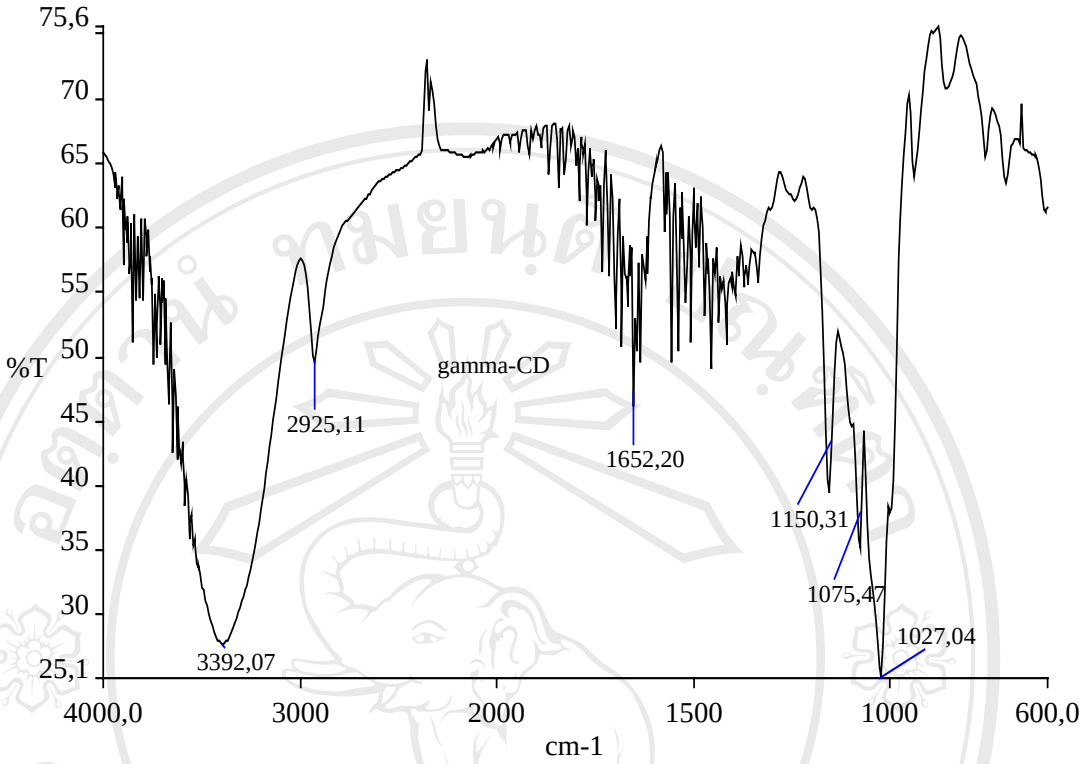

Figure 97 FTIR spectrum of gamma-cyclodextrin (GCD) , intact

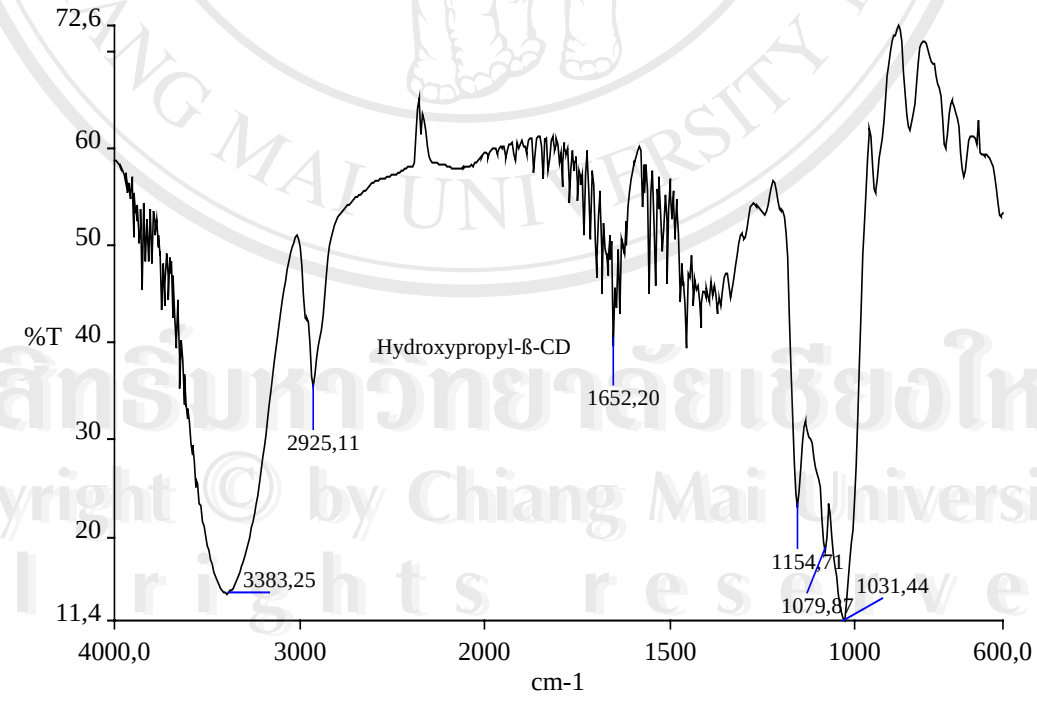

Figure 98 FTIR spectrum of hydroxypropyl-β-cyclodextrin

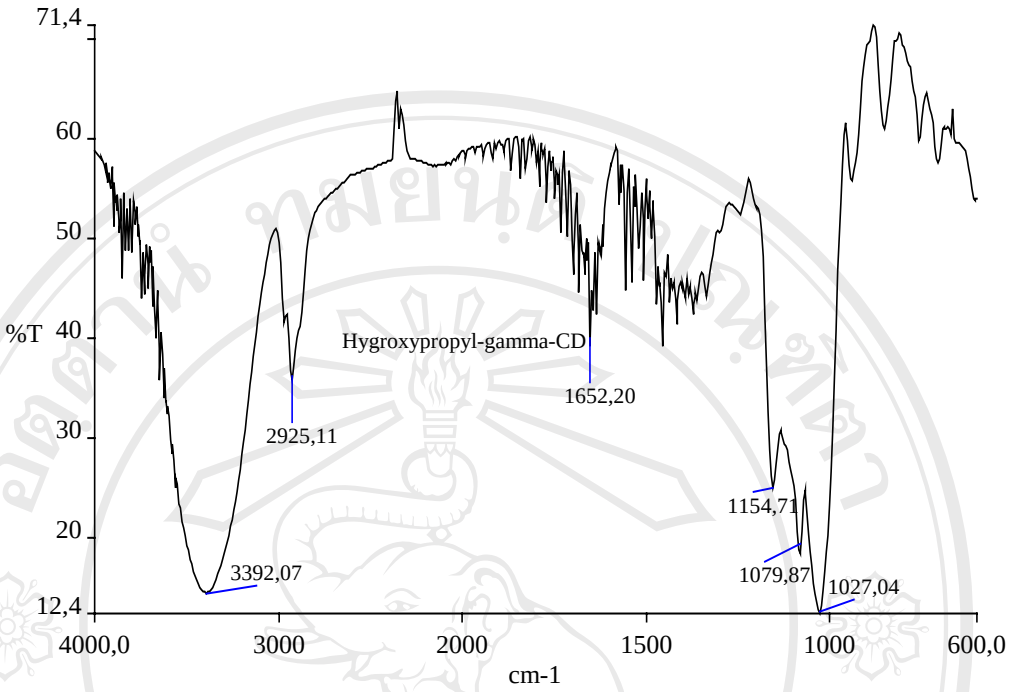

Figure 99 FTIR spectrum of hydroxypropyl-gamma cyclodextrin (HPGCD) , intact

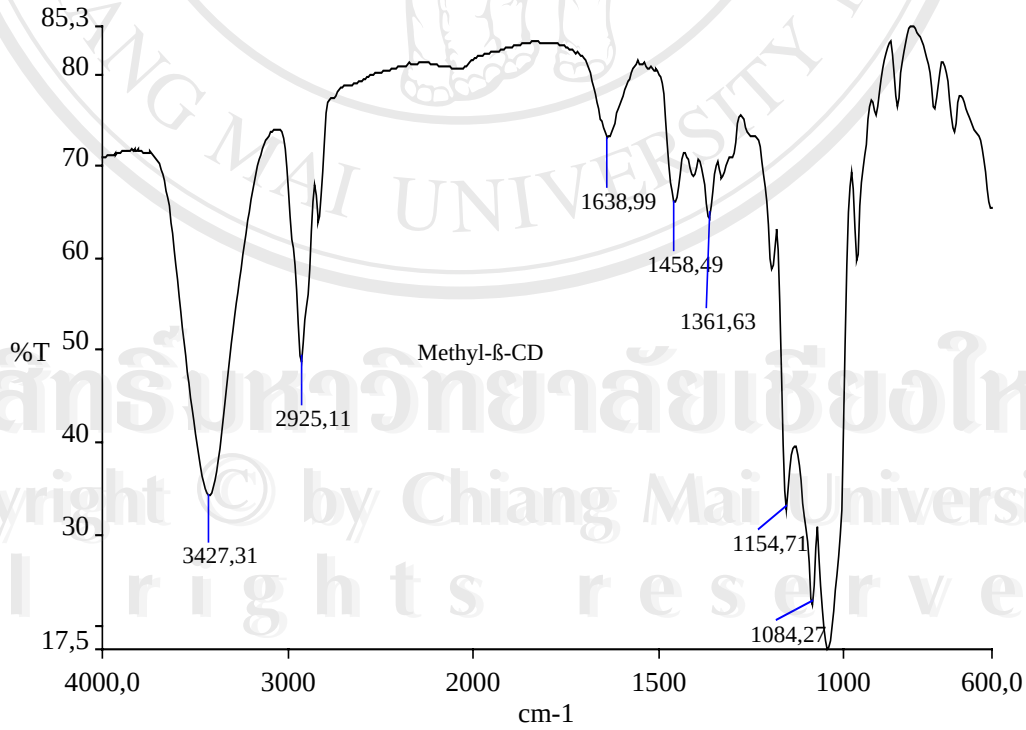

Figure 100 FTIR spectrum of methylated -β-cyclodextrin (MeBCD) , intact

The FTIR spectrum of the physical mixture of piroxicam with BCD (Figure 101) shows no significant difference from the respective spectra of the pure components indicated that no interaction occurs between the drug and BCD. This finding corresponds to the DSC and XPD studies. For KN complex of piroxicam-BCD which is illustrated in Figure 102, the sharp peaks at 3330, 1630 and 1528 cm^{-1} are slightly shifted to higher wave numbers i.e., 3339, 1634 and 1537 cm^{-1}. This could signify the occurrence of the interaction between the drug and BCD. The shift of the peaks corresponding to –OH groups and carbonyl group to the higher wave number is ascribed to the opening of the intramolecular hydrogen bonding of the drug molecule and the formation of strong intermolecular hydrogen bonding with BCD (Dollo et al., 1996).

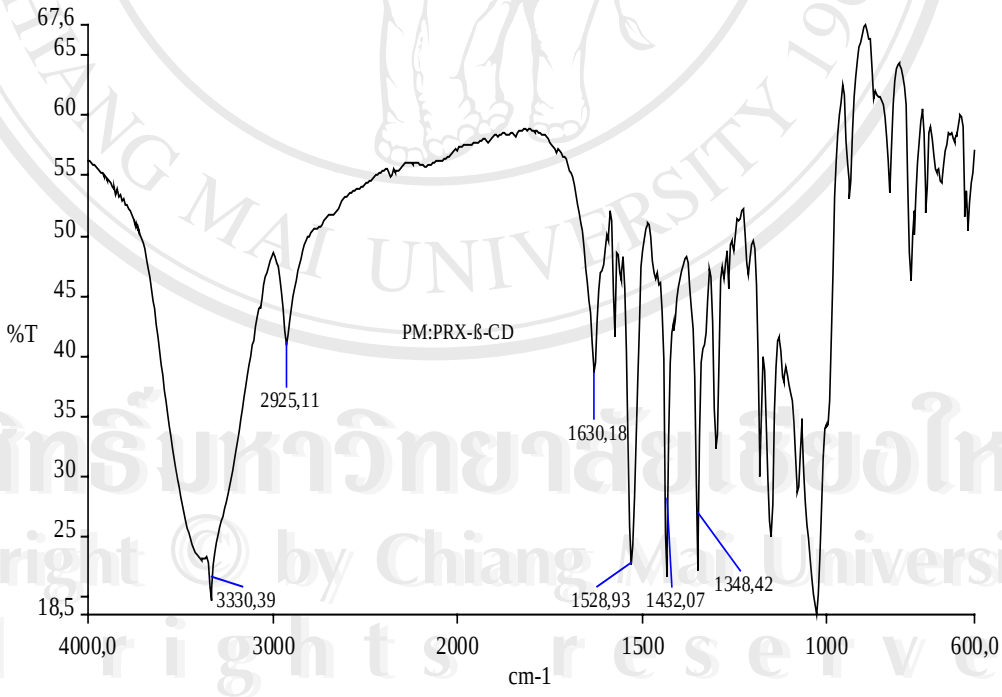

Figure 101 FTIR spectrum of 1:1 piroxicam –BCD physical mixture

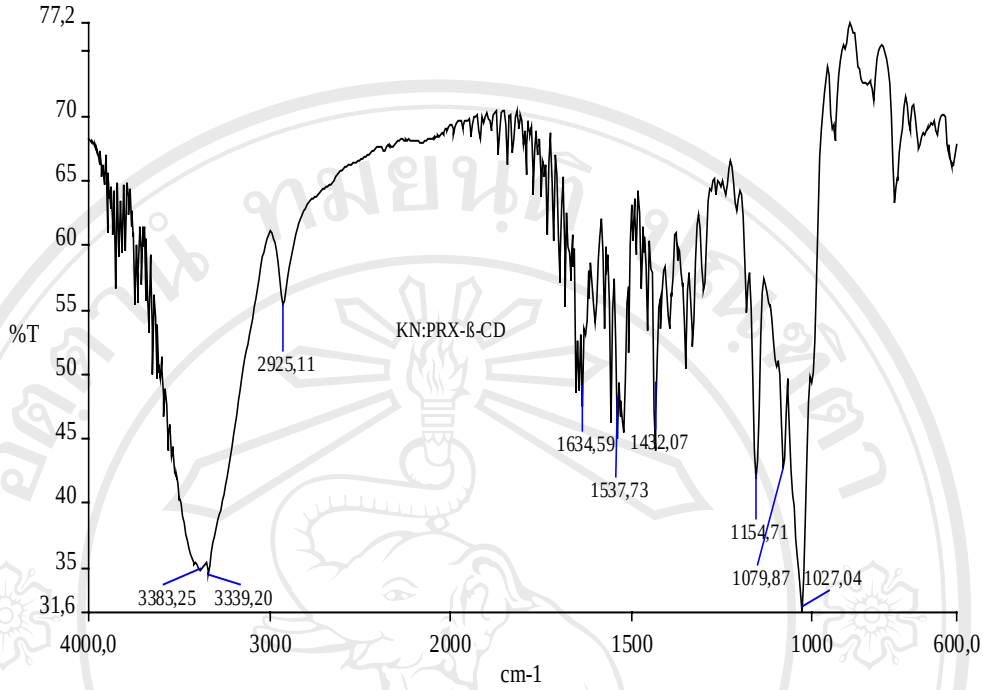

Figure 102 FTIR spectrum of 1:1 piroxicam-BCD inclusion complex prepared by kneading method

A significant change in FTIR spectra is observed in COE and COL complexes of piroxicam-BCD (Figure 103-104). The sharp peak of the drug at 3330 cm^{-1} disappears completely in both complexes. Additionally, the new absorption peak at 1555 cm^{-1} was denoted in COE complexes. It did not belong to any peak of the drug and BCD, thus, it might be attributed to the new crystalline complex of the drug, formed during evaporation process. This suggestion is also supported by the results obtained from DSC and XPD studies. The interaction between the drug and BCD in COE complex is indicated by the shift of the BCD peak from 3374 cm^{-1} to 3418 cm^{-1}. The shift of the carbonyl amide peak towards lower wave numbers, i.e. 1528 cm^{-1} to 1520 cm^{-1} evidences the interaction between the drug and BCD in COL complexes. When the carbonyl group binds to a hydroxylic compound via hydrogen bonding, the

stretching vibration peak is displaced to lower wave numbers due to a weakening of the carbonyl double bonds (Fernandes et al., 2002).

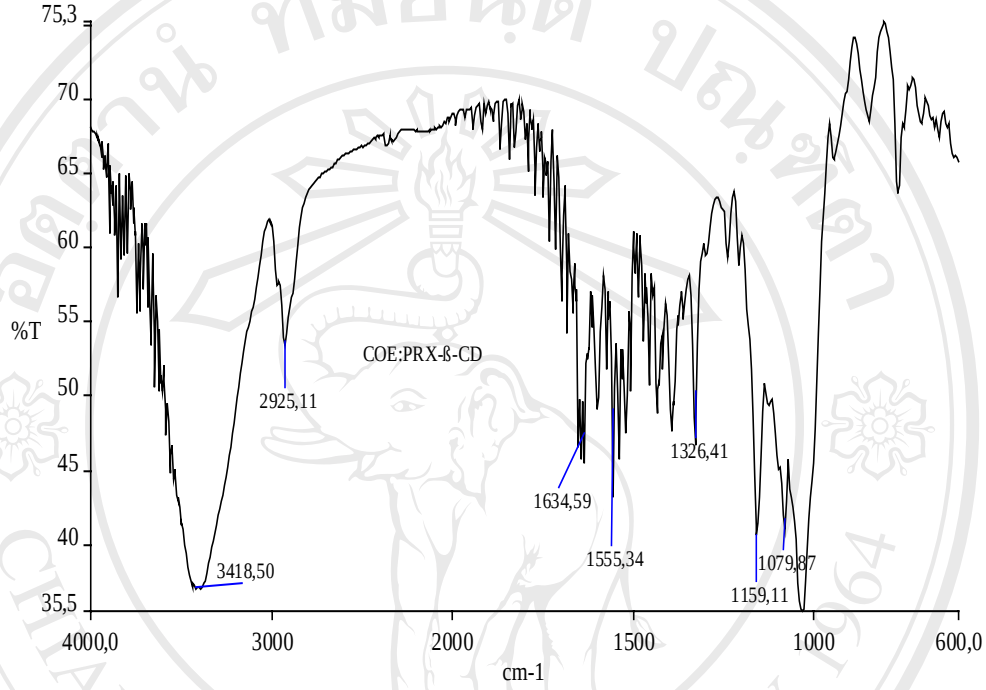

Figure 103 FTIR spectrum of 1:1 piroxicam-BCD inclusion complex prepared by co- evaporation method

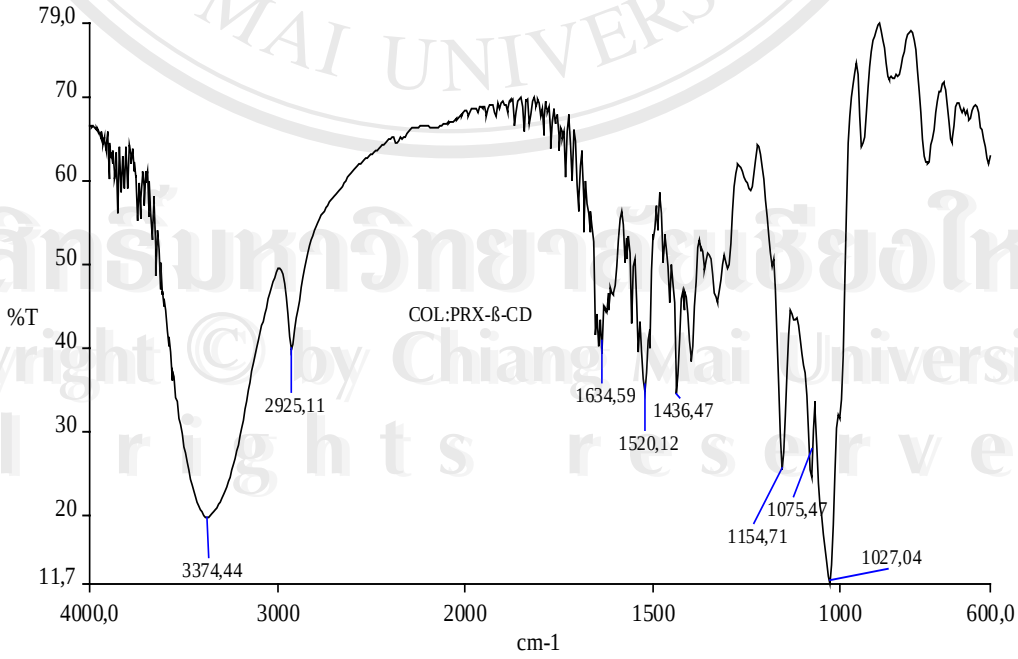

Figure 104 FTIR spectrum of 1:1 piroxicam-BCD inclusion complex prepared by co-lyophilization method

The FTIR spectrum of the physical mixture of piroxicam and GCD, illustrated in Figure 105 exhibits the absorption peaks assigned by the drug and GCD. No significant change is observed on each peak indicating that no interaction exists between the drug and GCD. The interaction between the drug and GCD in KN, COE and COL complexes is evidenced by the disappearance of the peak at 3330 cm^{-1} , and the shift of the carbonyl amide peak from 1528 cm^{-1} to 1520 cm^{-1} . In addition to these finding, the new absorption peak at 1555 cm^{-1} is observed in COE complex.

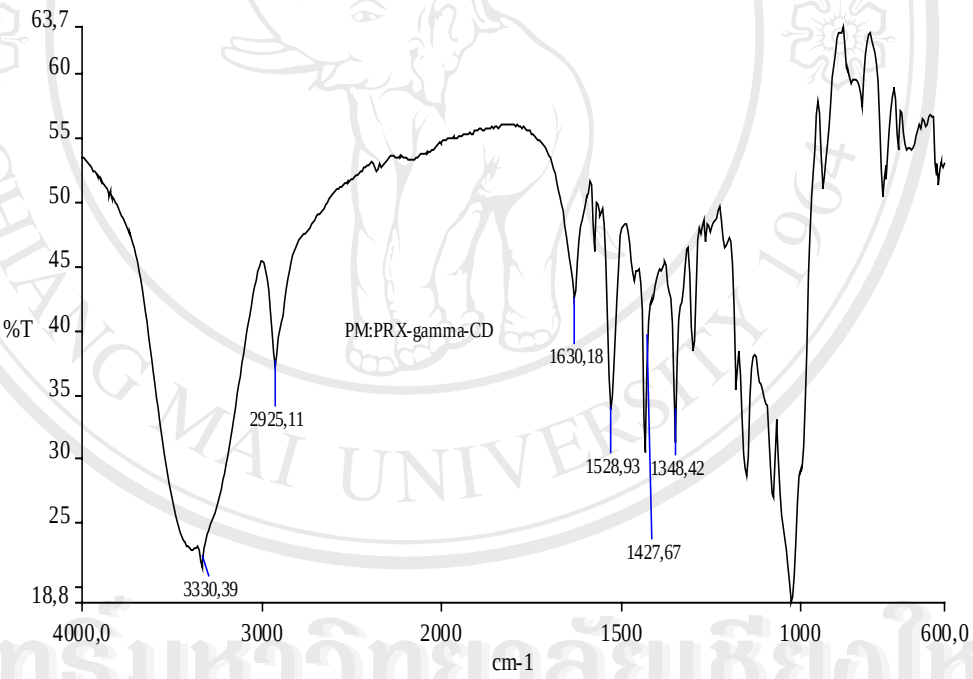

Figure 105 FTIR spectrum of 1:1 piroxicam-GCD physical mixture

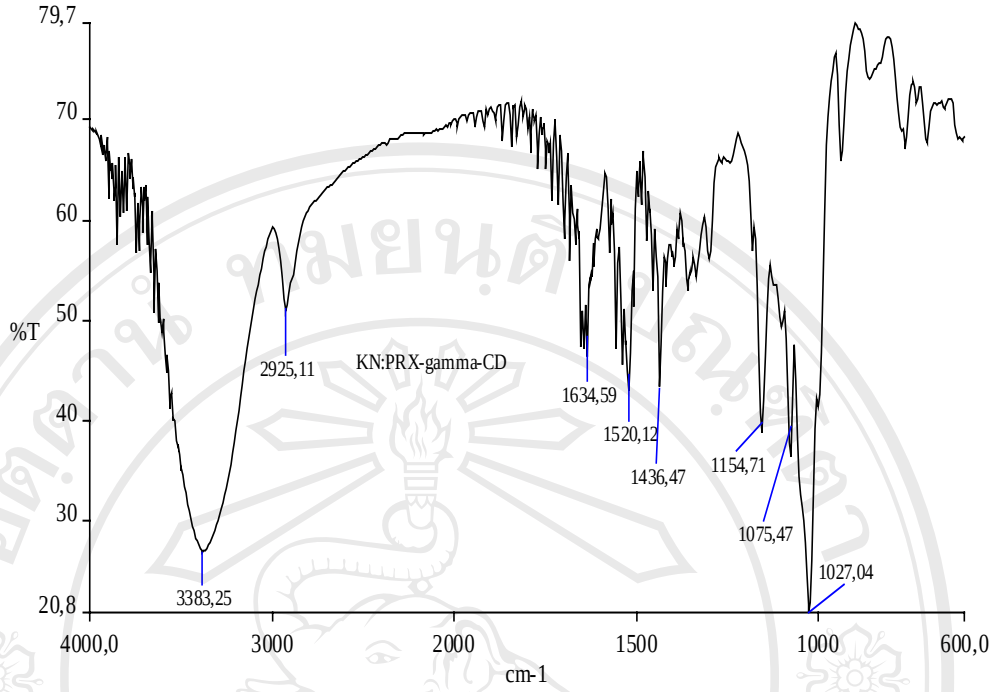

Figure 106 FTIR spectrum of 1:1 piroxicam-GCD inclusion complex prepared by kneading method

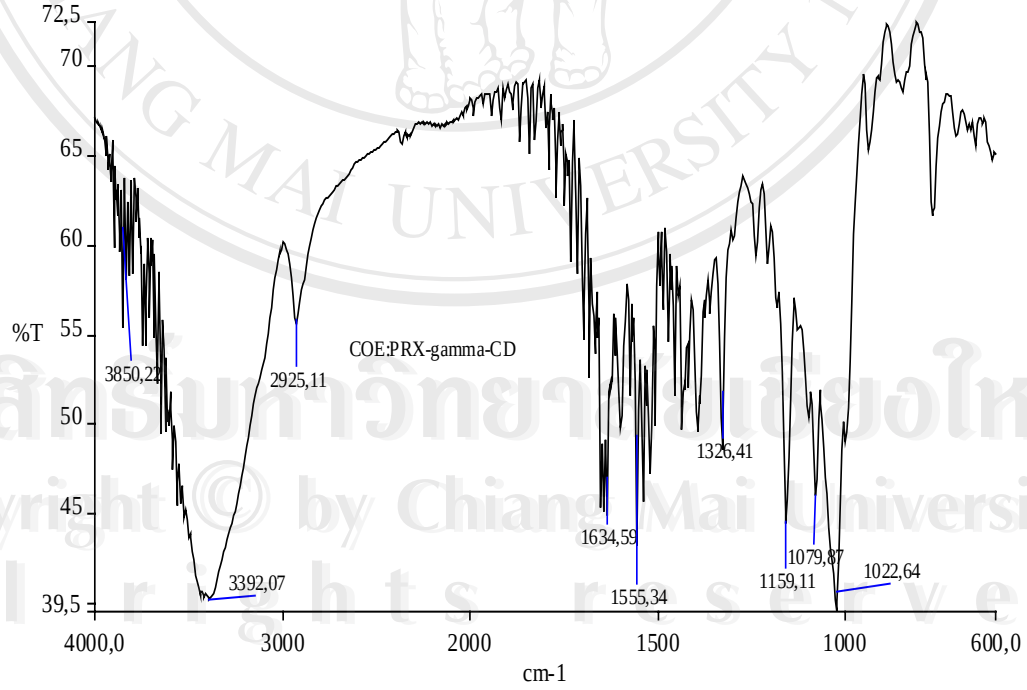

Figure 107 FTIR spectrum of 1:1 piroxicam-GCD inclusion complex prepared by co-evaporation method

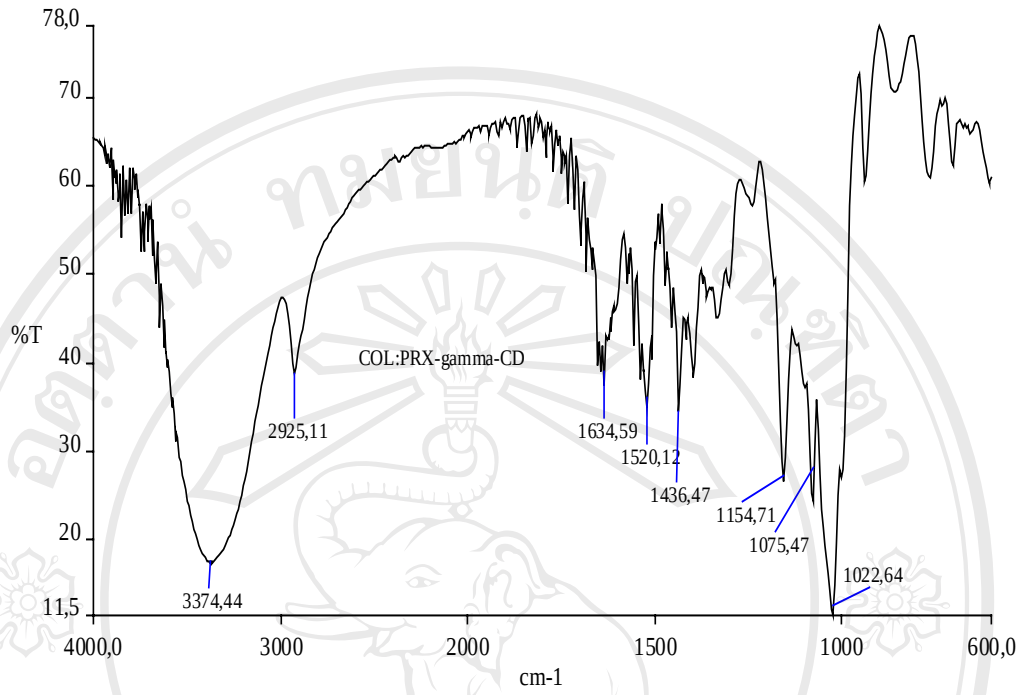

Figure 108 FTIR spectrum of 1:1 piroxicam-GCD inclusion complex prepared by co-lyophilization method

the corresponding complexes are shown in Figure 109-112. It is interesting to note the disappearance of the absorption at 3330 cm^{-1} in the physical mixture. Although, the other characteristic peaks do not unchanged it could be implied, that there is interaction to some extent. This finding is consistent to the dissolution studies which could find the increase in the %DE30 value from the physical mixture. The interaction between the drug and HPBCD in KN, COE and COL complexes is evidenced by the same change which is observed in the case of the other CDs.

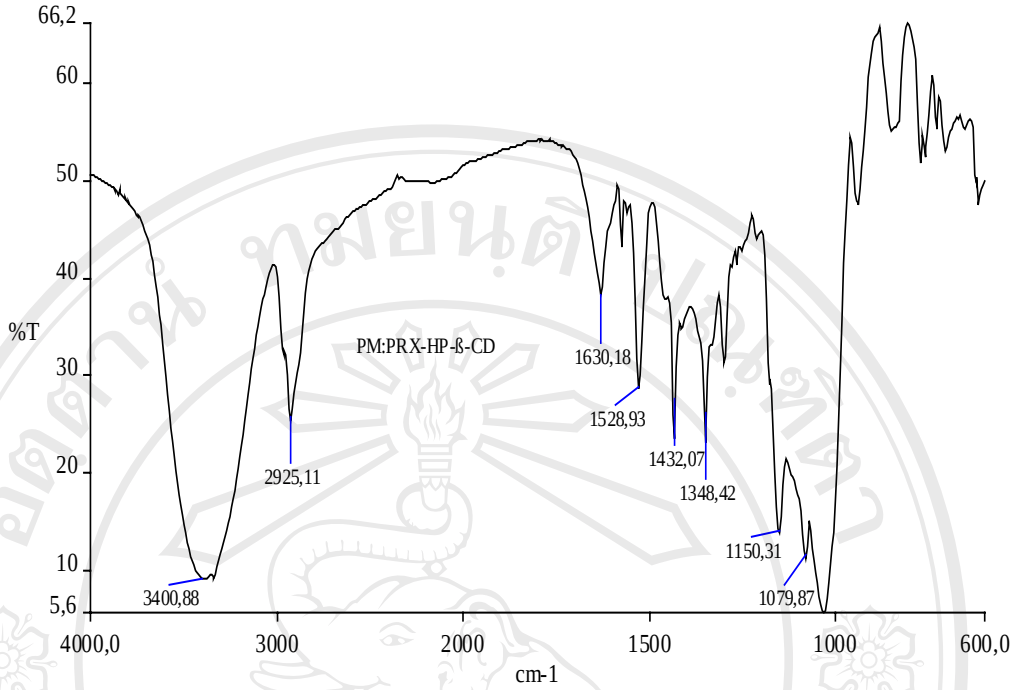

Figure 109 FTIR spectrum of 1:1 piroxicam-HPBCD physical mixture

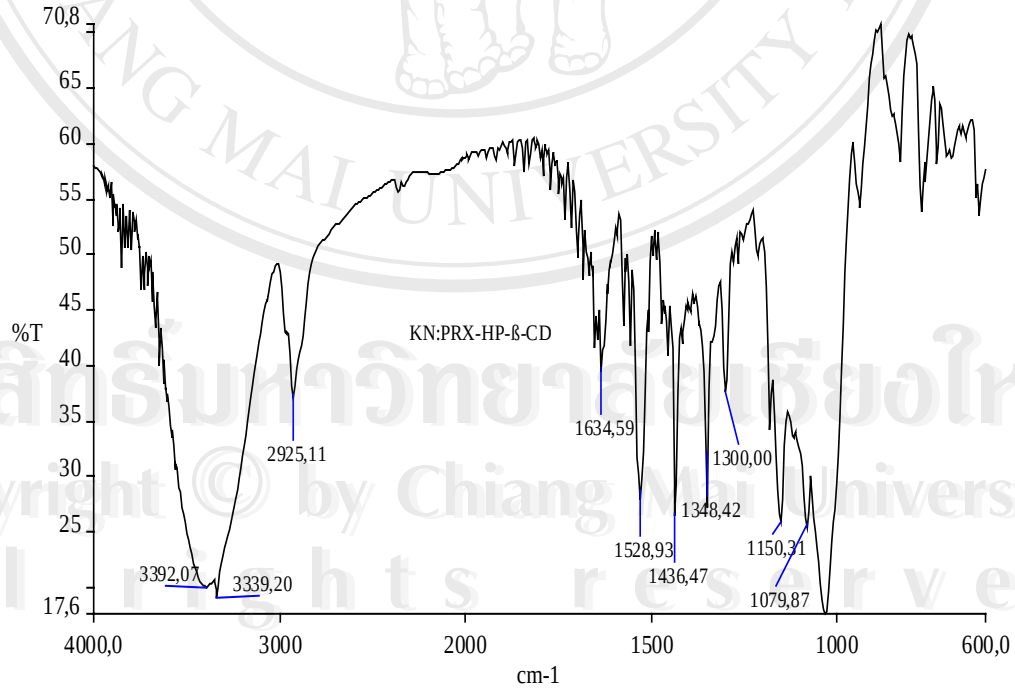

Figure 110 FTIR spectrum of 1:1 piroxicam-HPBCD inclusion complex prepared by kneading method

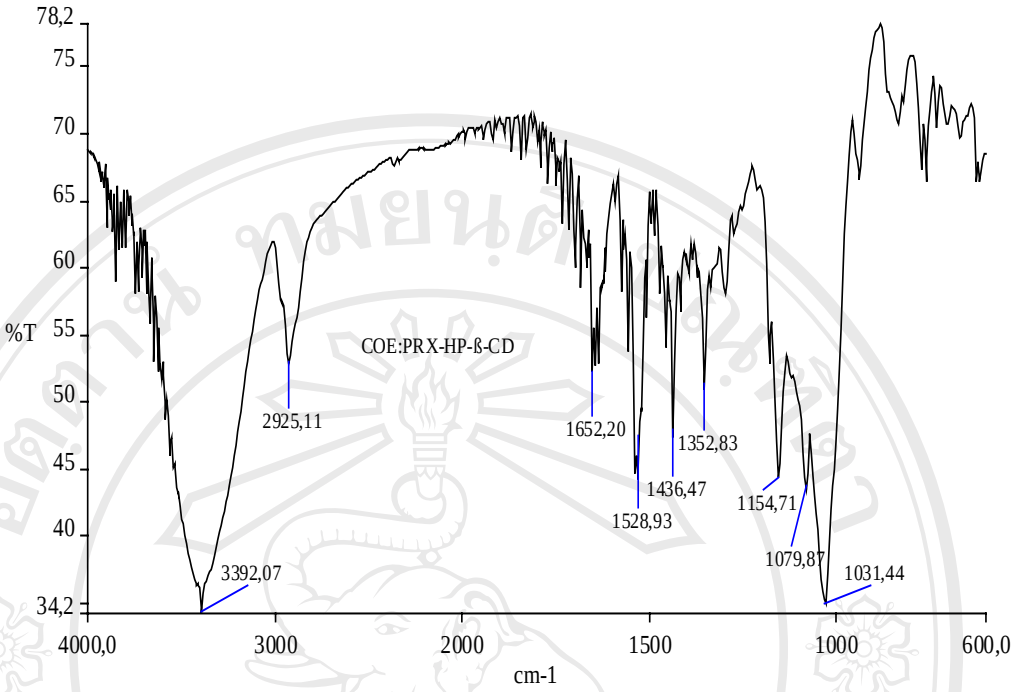

Figure 111 FTIR spectrum of 1:1 piroxicam-HPBCD inclusion complex prepared by co-evaporation method

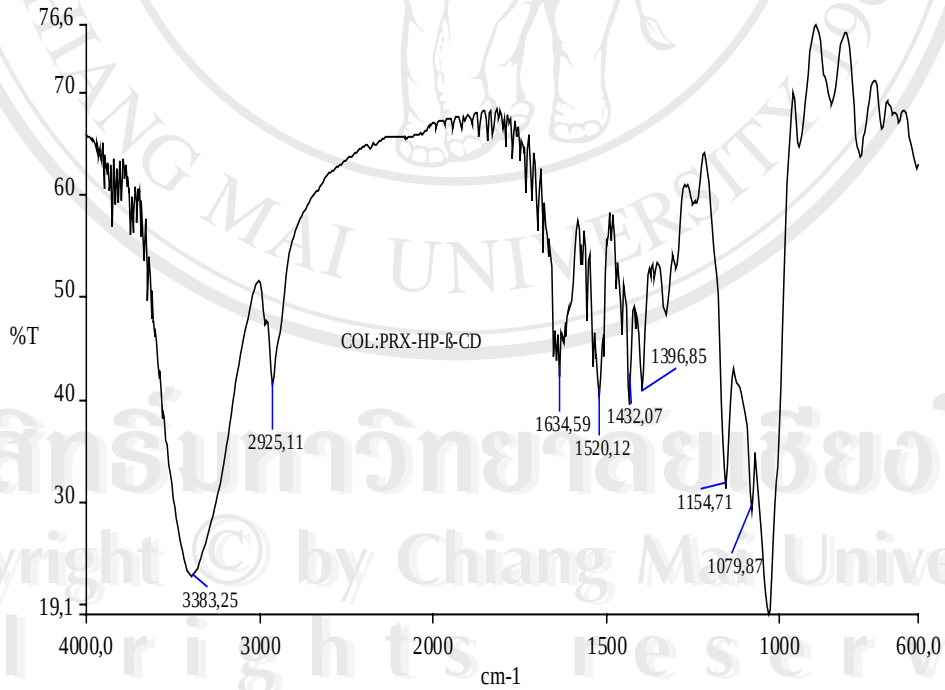

Figure 112 FTIR spectrum of 1:1 piroxicam-HPBCD inclusion complex prepared by co-lyophilization method

The FTIR spectra of piroxicam-MeBCD physical mixture and the corresponding complexes are shown in Figure 113-116. The evidences substantiate that the interaction between the drug and MeBCD are similar to those ascribed to HPBCD. The complete disappearance of the peak at 3330 cm^{-1} is observed in all complexes, including the physical mixture. The shift of the carbonyl amide peaks to either higher or lower wave numbers is also detected.

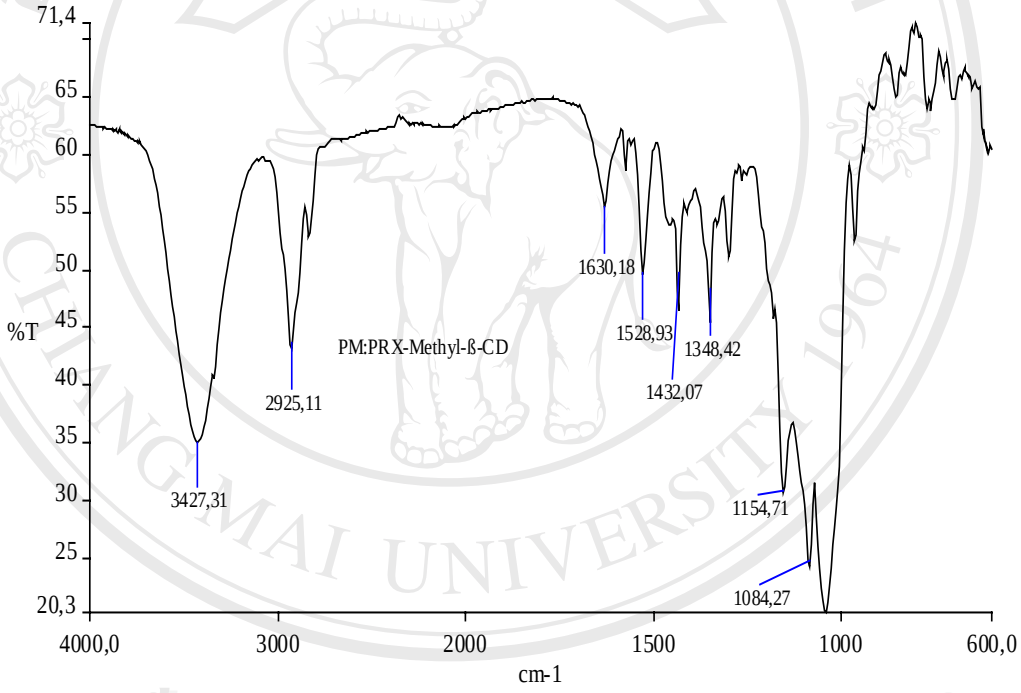

Figure 113 FTIR spectrum of 1:1 piroxicam-MeBCD physical mixture

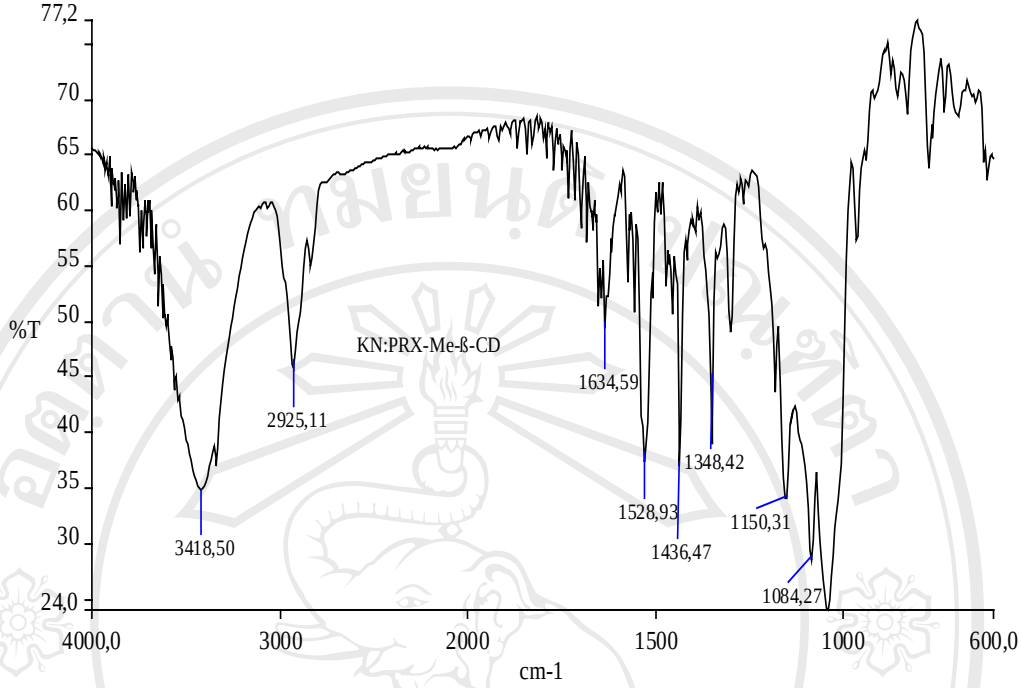

Figure 114 FTIR spectrum of 1:1 piroxicam-MeBCD inclusion complex prepared by kneading method

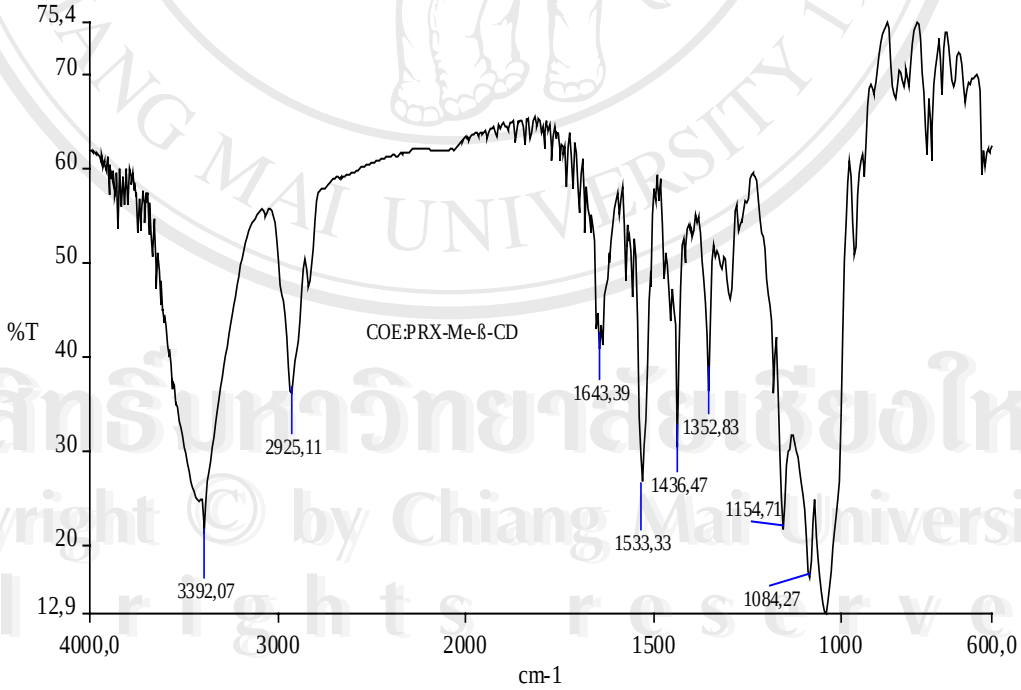

Figure 115 FTIR spectrum of 1:1 piroxicam-MeBCD inclusion complex prepared by co-evaporation method

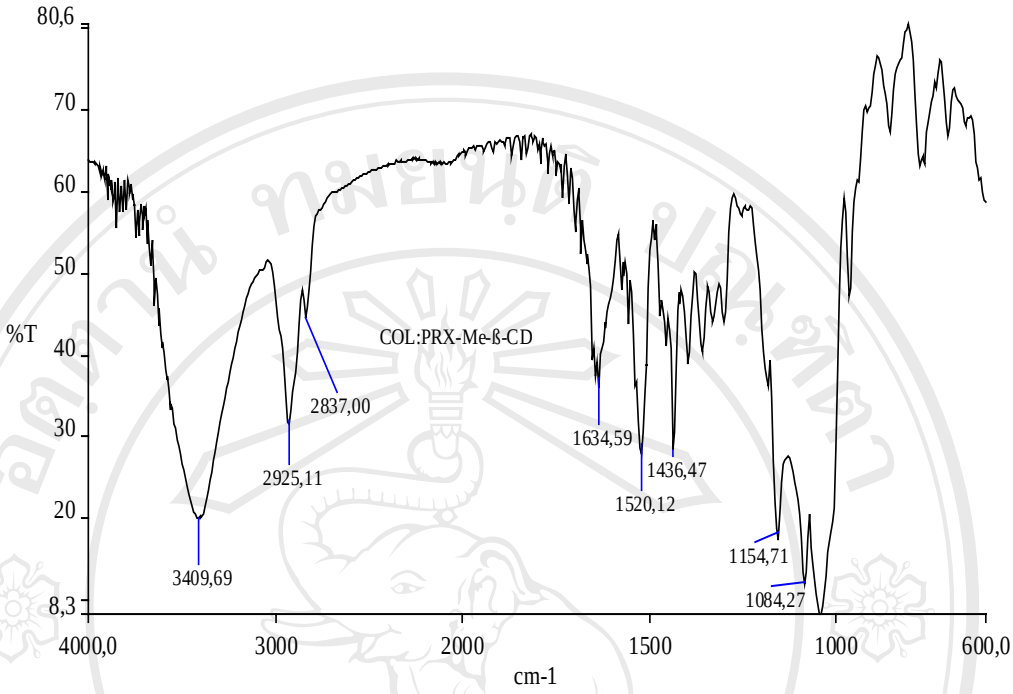

Figure 116 FTIR spectrum of 1:1 piroxicam-MeBCD inclusion complex prepared by co-lyophilization method

3.4.4.2 FTIR spectra of meloxicam-CDs inclusion complexes

Similar to piroxicam, FTIR spectrum of the intact meloxicam, shown in Figure 117 exhibits a strong absorption peak at 3286 cm^{-1} belonging to –NH and –OH stretching vibrations. The characteristic peaks appear at 1616 cm^{-1} and 1546 cm^{-1} were assigned to the first and the second amide- carbonyl stretching vibration.

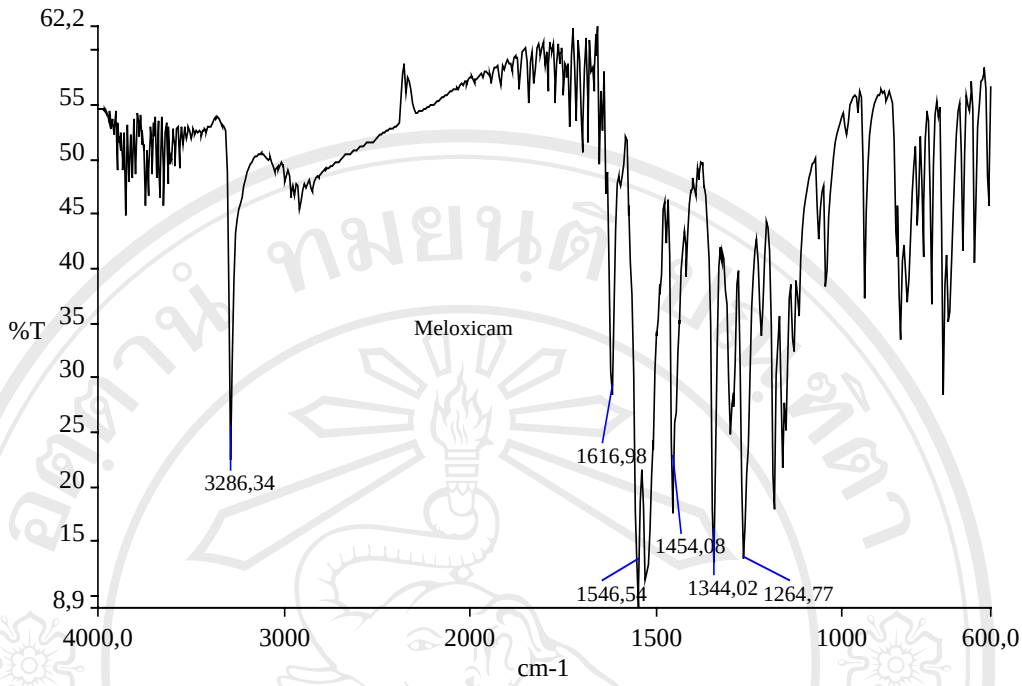

Figure 117 FTIR spectrum of meloxicam, intact

FTIR spectra of meloxicam-BCD physical mixture and the corresponding complexes prepared by kneading, co-evaporation and co-lyophiliazation method are illustrated in Figure 118-121, respectively. The physical mixture and KN complex exhibits spectra containing the characteristic peaks of the drug. This observation could imply that there is negligible interaction between the drug and BCD. In the case of COE and COL complexes, the interaction between the drug and BCD is evidenced by the disappearance of the peak at 3286 cm^{-1} and 1616 cm^{-1} . The second amide peak at 1546 cm^{-1} is shifted to a lower wave number at 1520 cm^{-1}. It is very interesting that the peak is shifted to the same position as observed in piroxicam-CDs complexes.

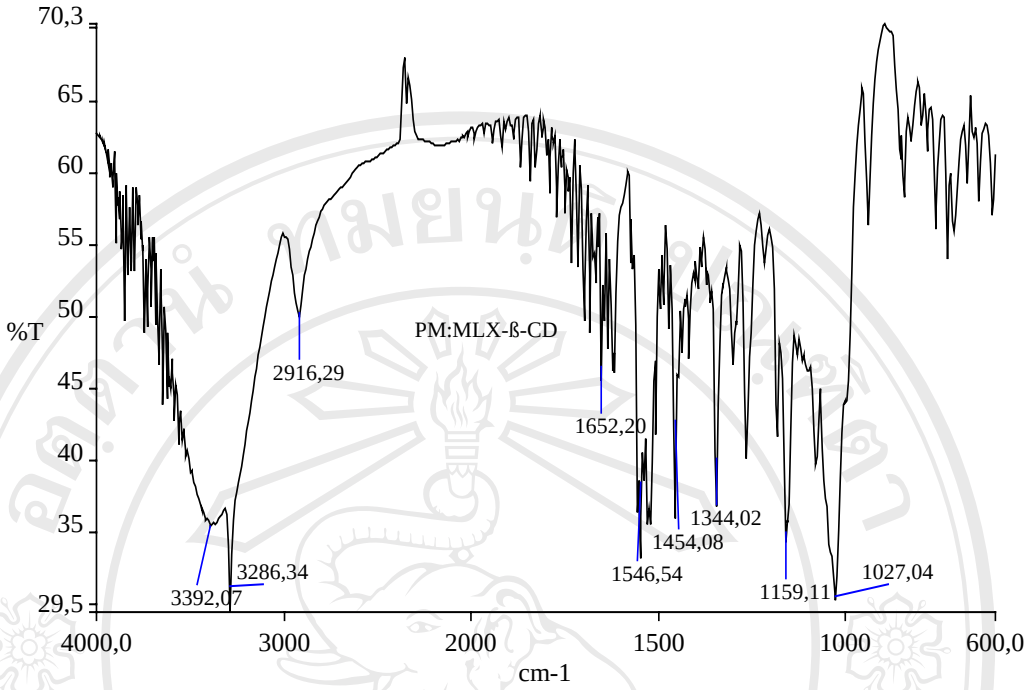

Figure 118 FTIR spectrum of 1:1 meloxicam-BCD physical mixture

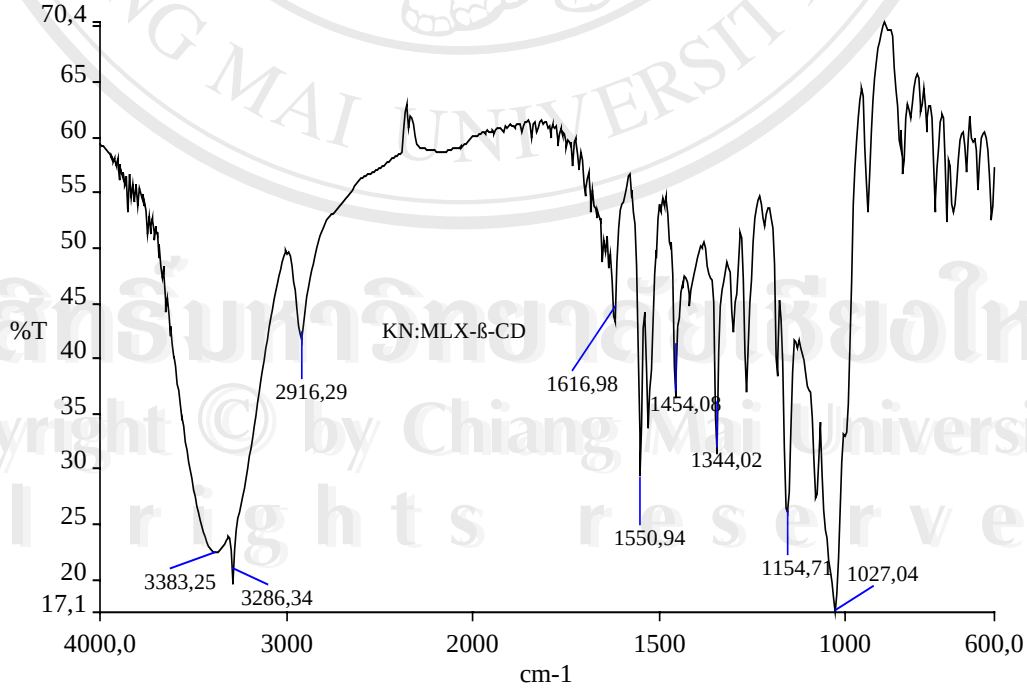

Figure 119 FTIR spectrum of 1:1 meloxicam-BCD inclusion complex prepared by kneading method

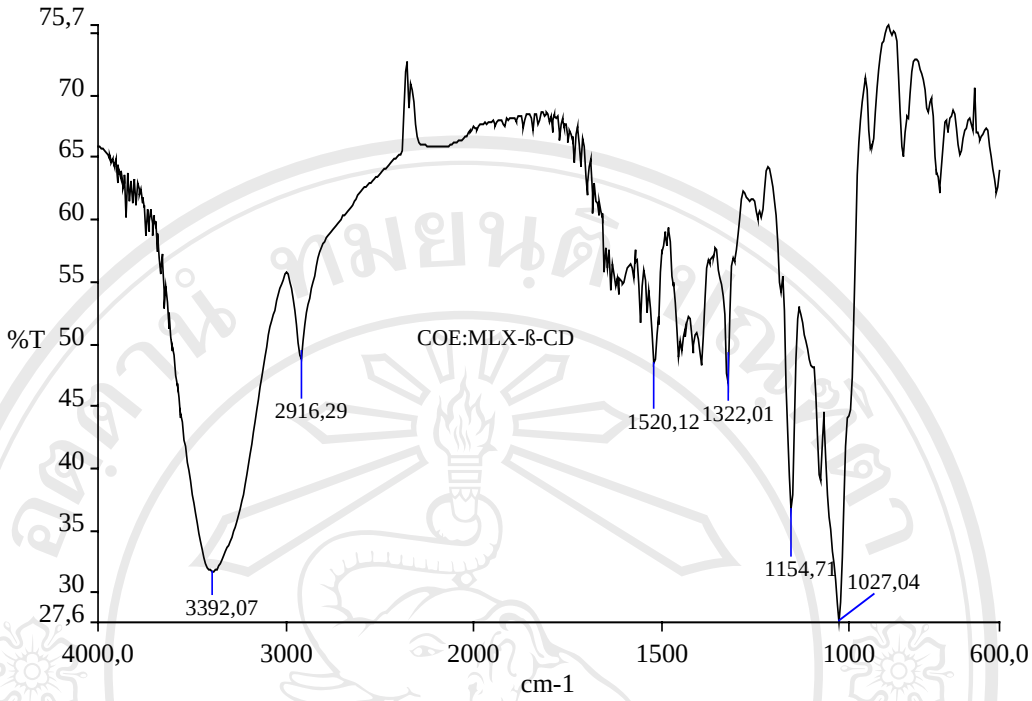

Figure 120 FTIR spectrum of 1:1 meloxicam-BCD inclusion complex prepared by co-evaporation method

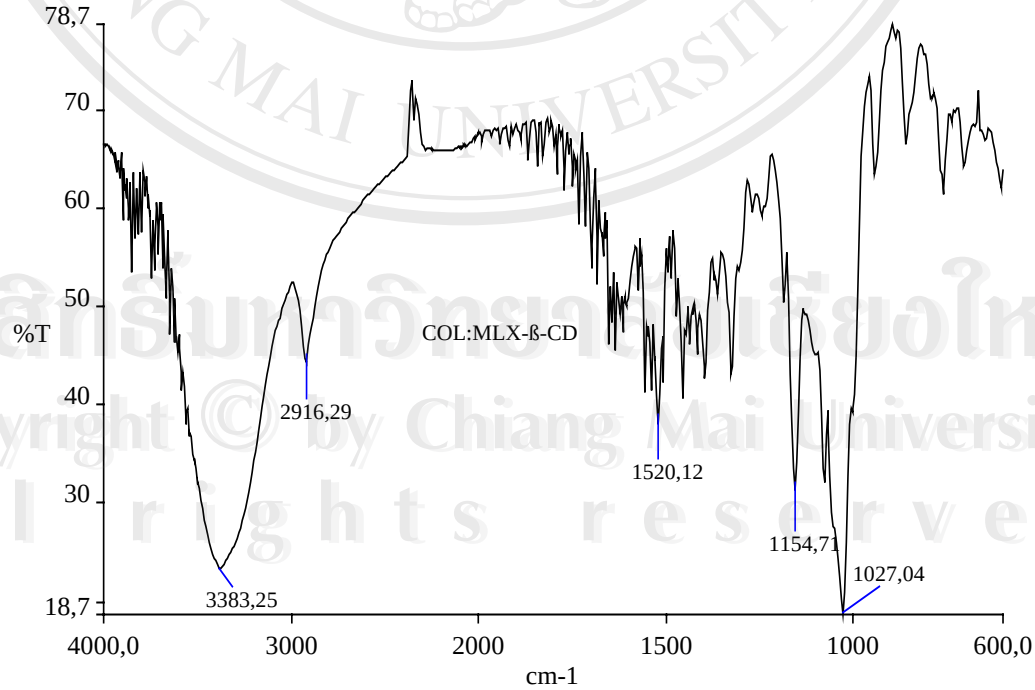

Figure 121 FTIR spectrum of 1:1 of meloxicam-BCD inclusion complex prepared by co-lyophilization method

FTIR spectra of meloxicam-GCD physical mixture and the complexes illustrated in Figure 122-125 demonstrates similar evidences to those observed in the drug and BCD systems. The physical mixtures and KN complex show no interaction between the drug and GCD whereas the existence of the interaction in COE and COL complexes is indicated by the disappearance of the peak at 3286 cm^{-1}. and the diminishing of the peaks which correspond to the carbonyl amide stretching.

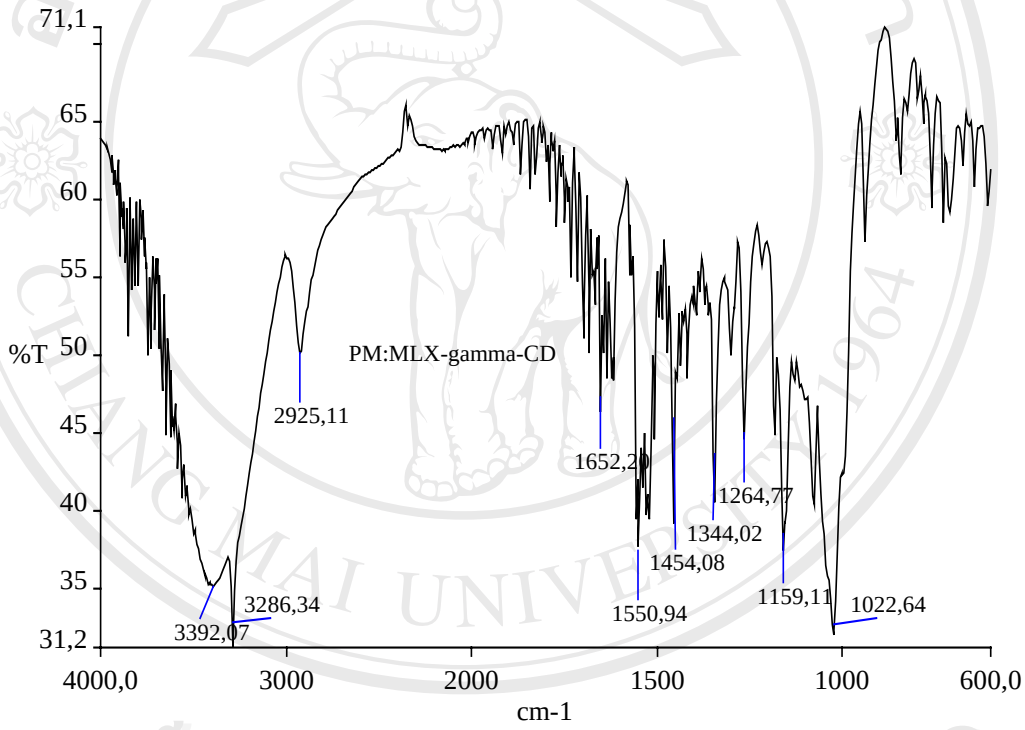

Figure 122 FTIR spectrum of 1:1 meloxicam-GCD physical mixture

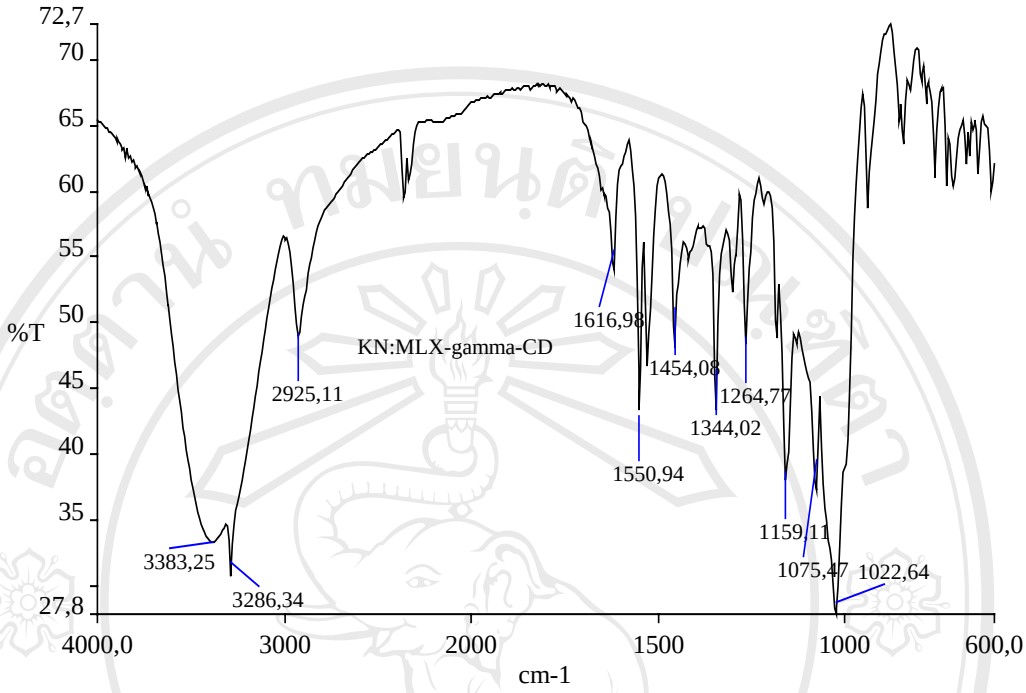

Figure 123 FTIR spectrum of 1:1 meloxicam-GCD inclusion complex prepared by kneading method

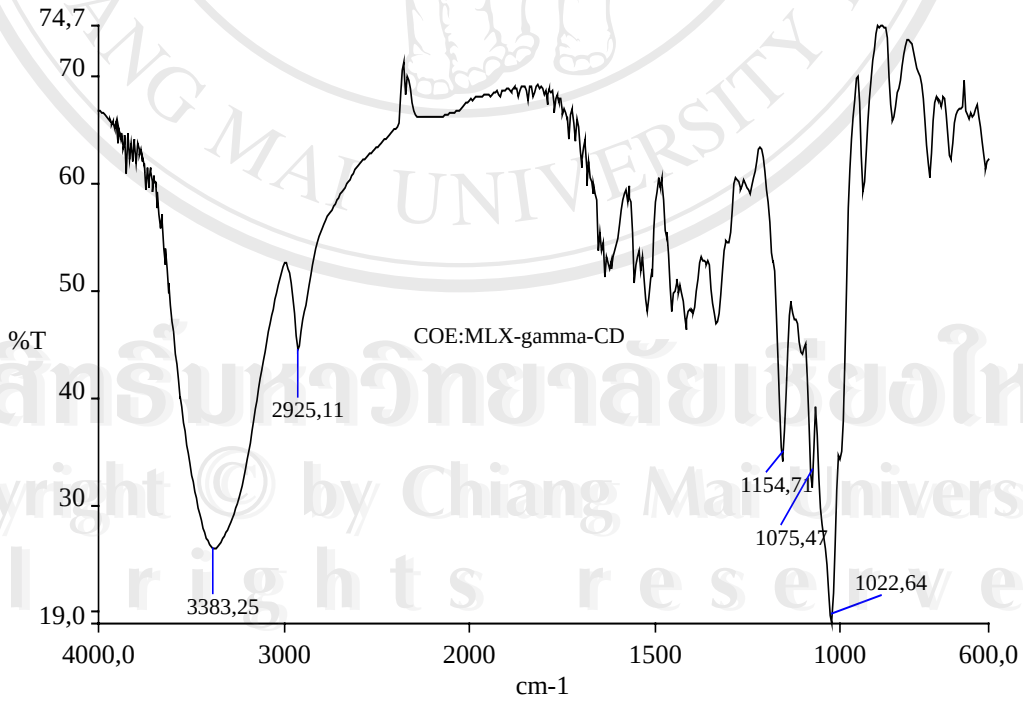

Figure 124 FTIR spectrum of 1:1 meloxicam-GCD inclusion complex prepared by co-evaporation method

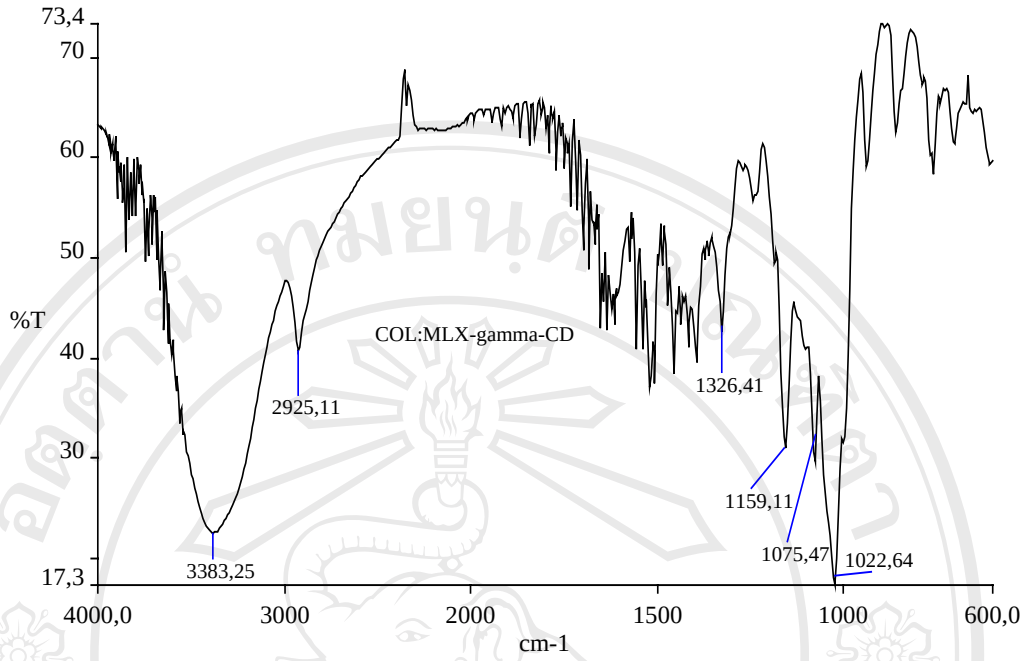

Figure 125 FTIR spectrum of 1:1 meloxicam-GCD inclusion complex prepared by co-lyophilization method

Figure 126-129 show the FTIR spectra of meloxicam-HPBCD physical mixture and the complexes prepared by kneading, co-evaporation and co-lyophilization method. Although the peak of the drug at 3286 cm^{-1} still exists, the interaction between the drug and HPBCD in physical mixture and KN mixtures can be detected by the shift of the peak of HPBCD at 3383 cm^{-1} to 3400 cm^{-1}. Furthermore, those peaks responsible for the carbonyl group, are diminished and shifted to lower wave numbers.

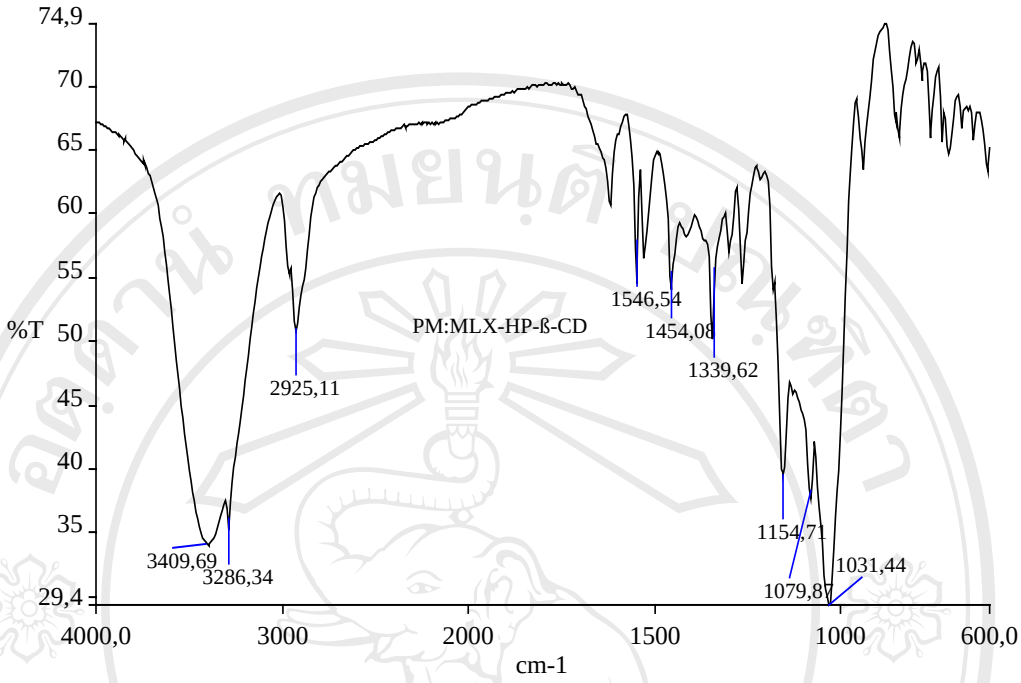

Figure 126 FTIR spectrum of 1:1 meloxicam-HPBCD physical mixture

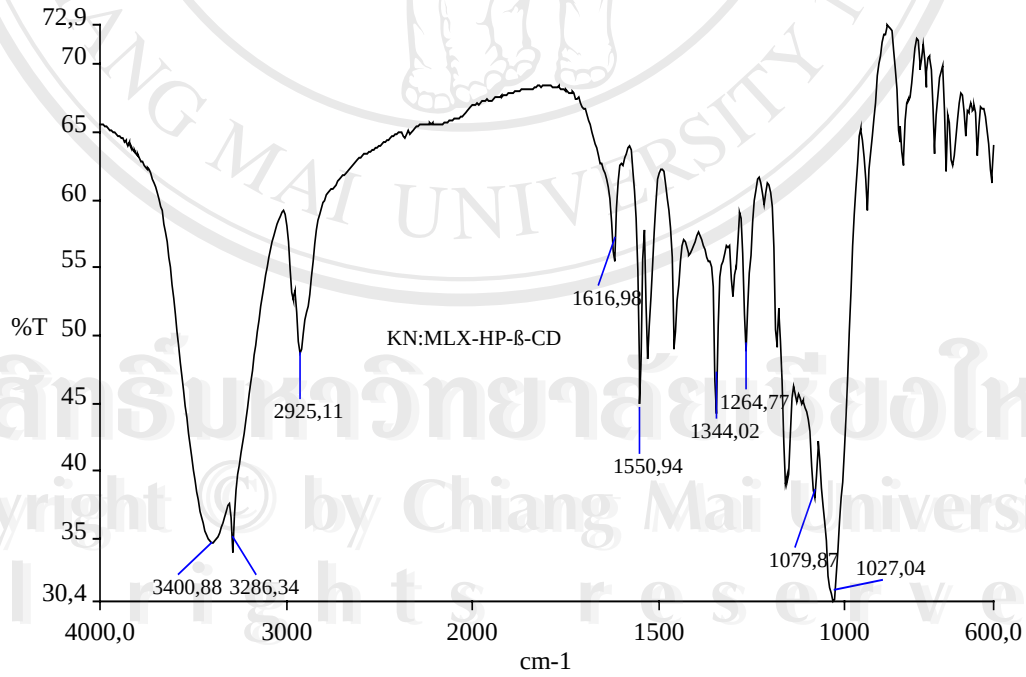

Figure 127 FTIR spectrum of 1:1 meloxicam-HPBCD inclusion complex prepared by kneading method

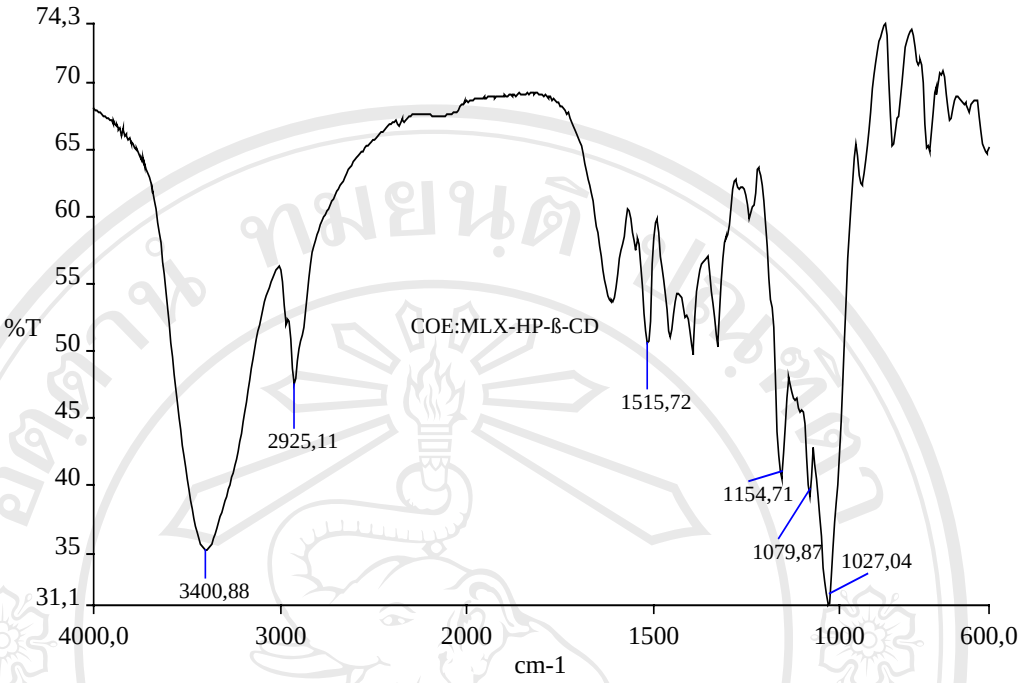

Figure 128 FTIR spectrum of 1:1 meloxicam-HPBCD inclusion complex prepared by co-evaporation method

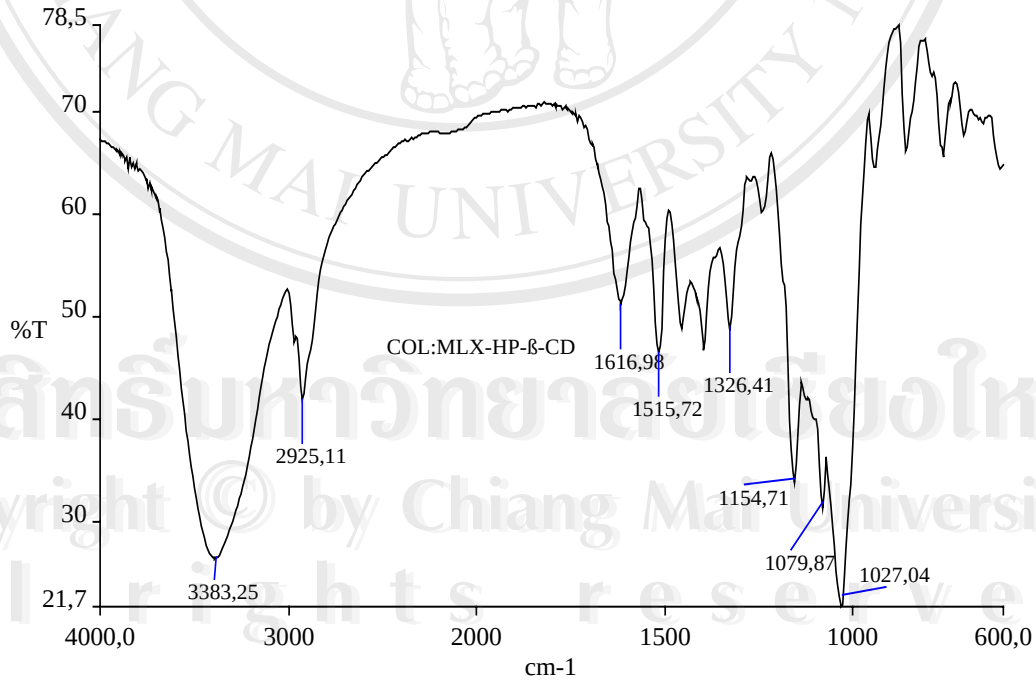

Figure 129 FTIR spectrum of 1:1 meloxicam-HPBCD inclusion complex prepared by co-lyophilization method

The FTIR spectra of meloxicam-HPGCD physical mixture and the complexes prepared by kneading, co-evaporation and co-lyophilization method are shown in Figure 130-133, respectively. Similar evidence to those HPBCD complexes is observed. The interaction between the drug and HPGCD in the physical mixture and KN complexes is implemented by the shift of the peak of the drug at 3286 cm^{-1}. Higher extent of interaction is observed in COE and COL complexes by the complete disappearance of the peak at 3286 $cm^{-1}$and the diminishing of the peaks which correspond to the carbonyl amide stretching vibration.

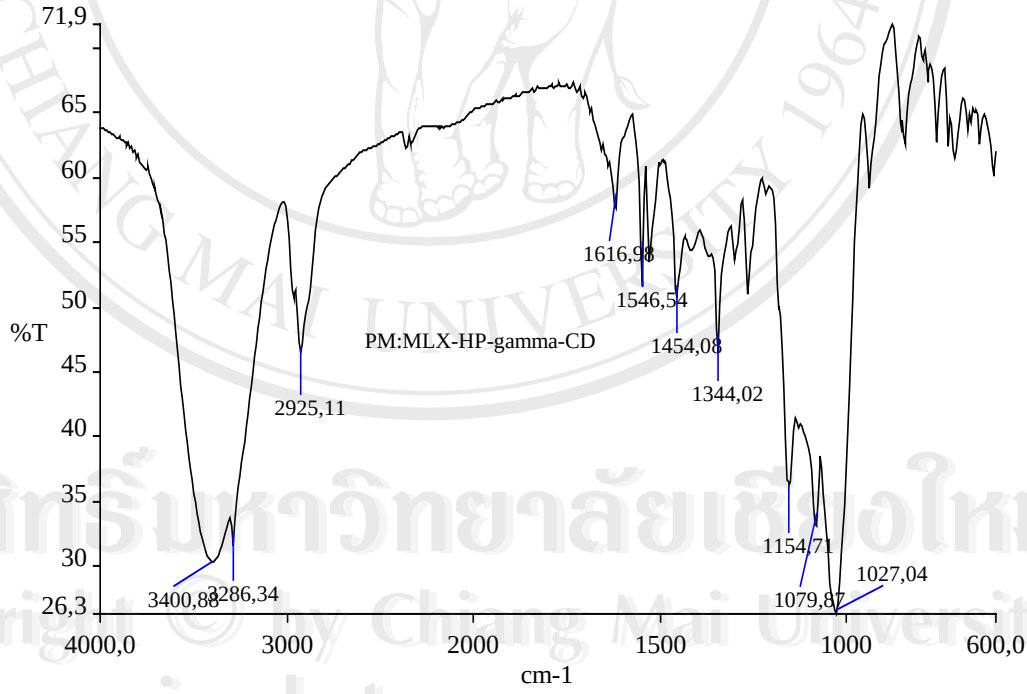

Figure 130 FTIR spectrum of 1:1 meloxicam HPGCD physical mixture

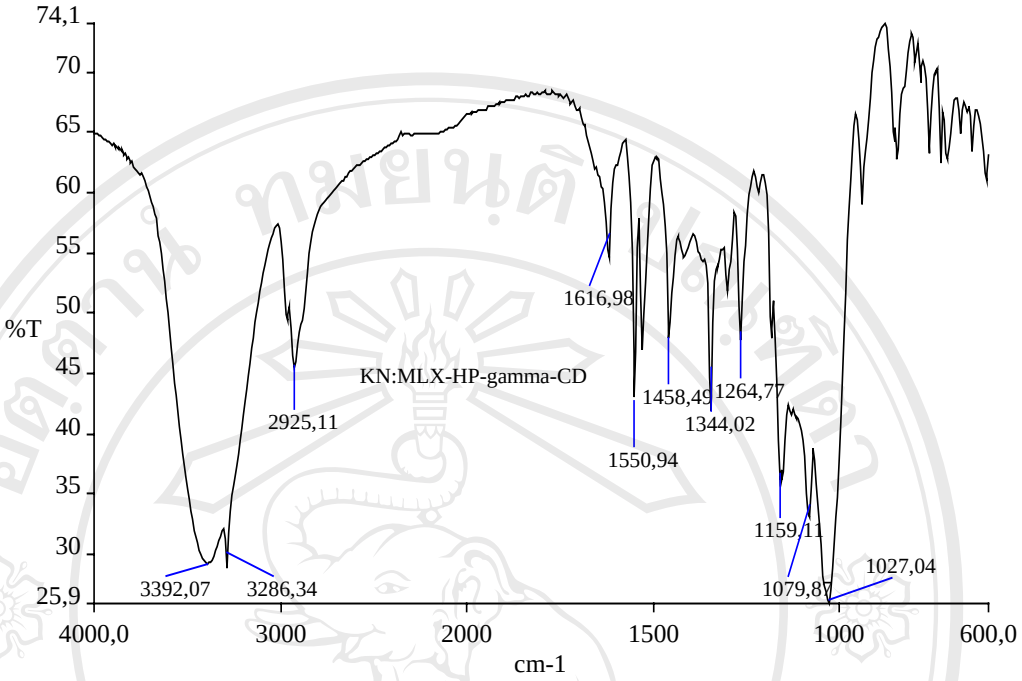

Figure 131 FTIR spectrum of 1:1 meloxicam-HPGCD inclusion complex prepared by kneading method

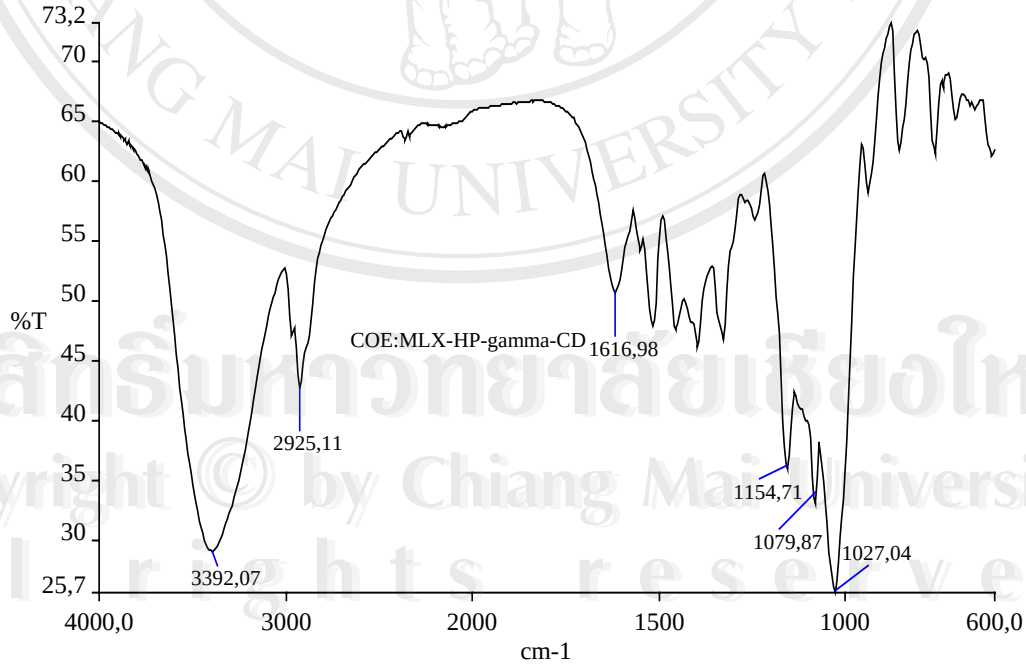

Figure 132 FTIR spectrum of 1:1 meloxicam-HPGCD inclusion complex prepared by co-evaporation method

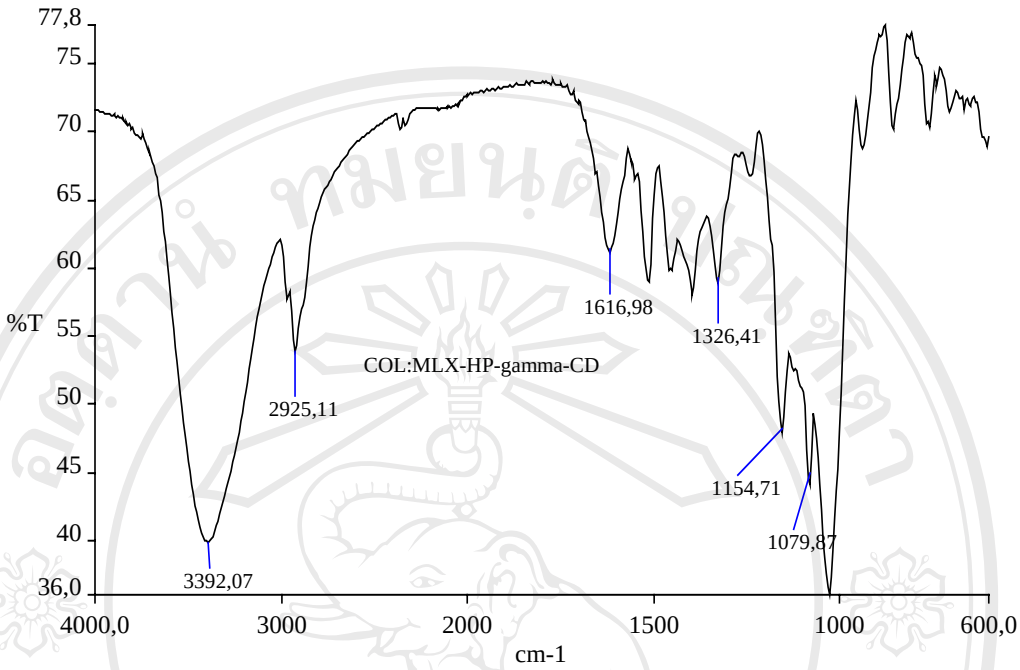

Figure 133 FTIR spectrum of 1:1 meloxicam-HPGCD inclusion complex prepared by co-lyophilization method

In summary, FTIR spectroscopy can provide meaningful information for supporting the interactions between the drug and CDs. However, they can not be used as the indicative evidence for the true inclusion complex formation.

3.4.5 Near infrared spectroscopy (NIR)

NIR spectroscopy has been used to characterize the complex formation between drugs and CDs. The significant difference in NIR spectra indicates the existence of complex formation (Viernstein, 1994).

3.4.5.1 NIR spectra of piroxicam-CDs inclusion complexes

The original and the first derivative NIR spectra of piroxicam, the physical mixture of piroxicam-BCD and the corresponding inclusion complexes prepared by

kneading, co-evaporation and co-lyophilization method are illustrated in Figure 134. From the original spectra, piroxicam intact shows characteristic band at 4800, 6000 and 6500 cm^{-1} whereas at these regions, BCD exhibits less intense peaks. The physical mixture and KN complex shows NIR bands consistent with those of the drug at 6000 and 6500 cm^{-1} but to some lower extent. The COE and COL complexes show only the NIR band at 6000 cm^{-1}. This can suggest that the interaction between the drug and BCD occurs to a different extent. The derivative spectra were generated in order to correct the shift effect in the data caused by different particle size of the sample. The amount of light absorbed by the reflecting sample generally depends on the depth of the light penetration which is consequently depending on the particle size of the sample. In the first derivative spectra, the significant differences in NIR spectra between the drug and those of complexes are clearly depicted.

The NIR spectra of the drug compared to those of piroxcam-BCD physical mixture and COL complex are shown in Figure 135. The spectra of the physical mixture are similar to that of the intact drug and BCD indicating that the drug and BCD exist independently. In contrast, the NIR spectra of COL complexes are resembling to BCD, but without the bands of the drug. This could point out the complete inclusion of the drug in the CD cavity.

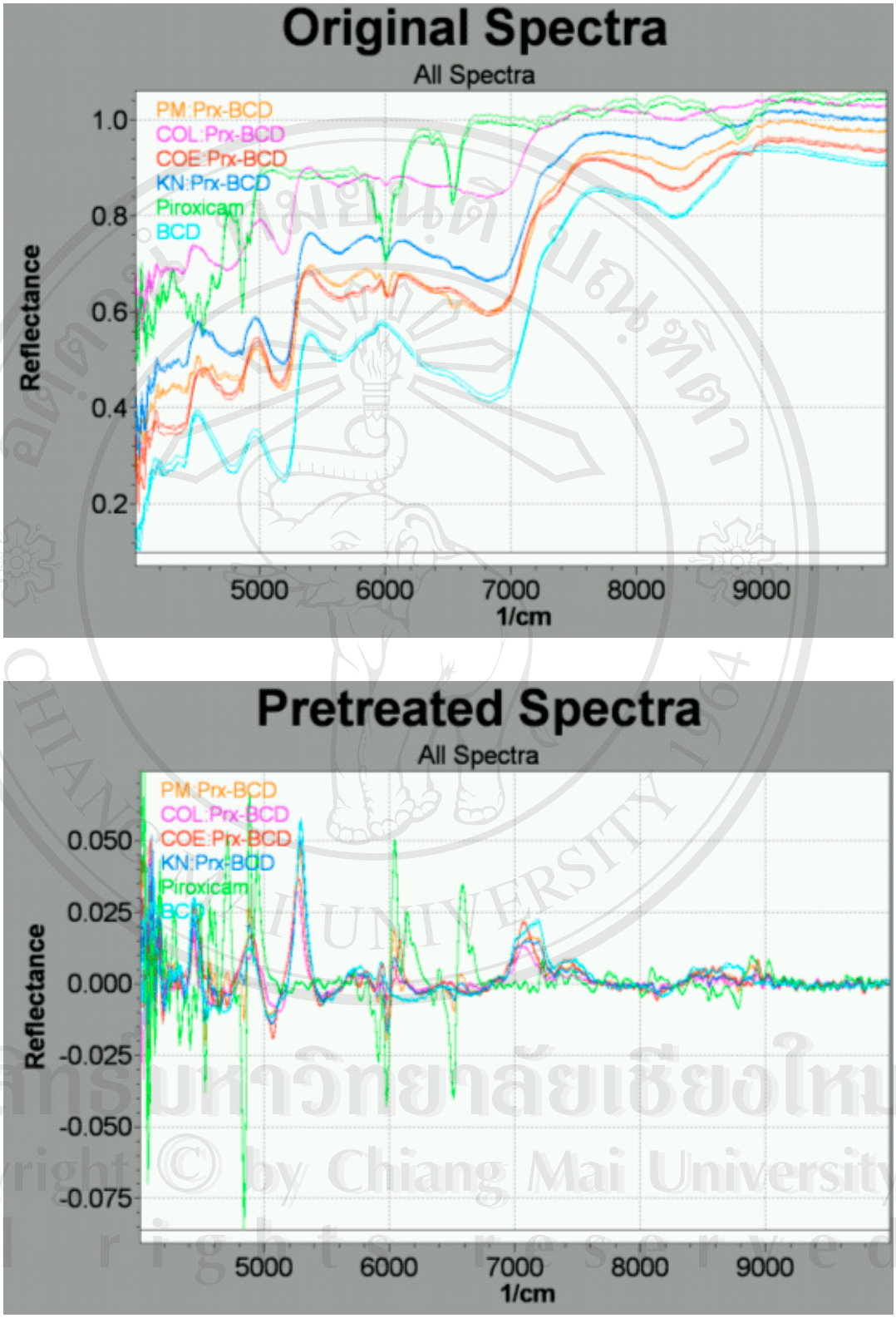

Figure 134 NIR Spectra of piroxicam; BCD; 1:1 physical mixture, PM and the inclusion complexes prepared by kneading, KN; co-evaporation, COE and co-lyophilization, COL method. Upper: original spectra, lower: first derivative spectra.

Figure 136 illustrates the NIR spectra of piroxicam, piroxicam-GCD physical mixture and the inclusion complexes prepared by kneading, co-evaporation and co-lyophilization method. The spectra are similar to those of piroxicam-BCD complexes. In physical mixtures, the absorption bands of the drug at 6000 and 6500 cm^{-1} exist. For COE complexes, only the band at 6000 cm^{-1} could be detected. These absorption bands nearly disappear in KN and COL complexes. The disappearance of these bands is attributed to the complete inclusion of the drug into the GCD cavity. This suggestion is supported by the DSC thermograms and FTIR spectra. The dissolution study also shows that the KN complex has higher dissolution efficiency than COE complexes. The difference in NIR spectra of the physical mixture and COL complex of piroxicam-GCD is clearly demonstrated in Figure 137.

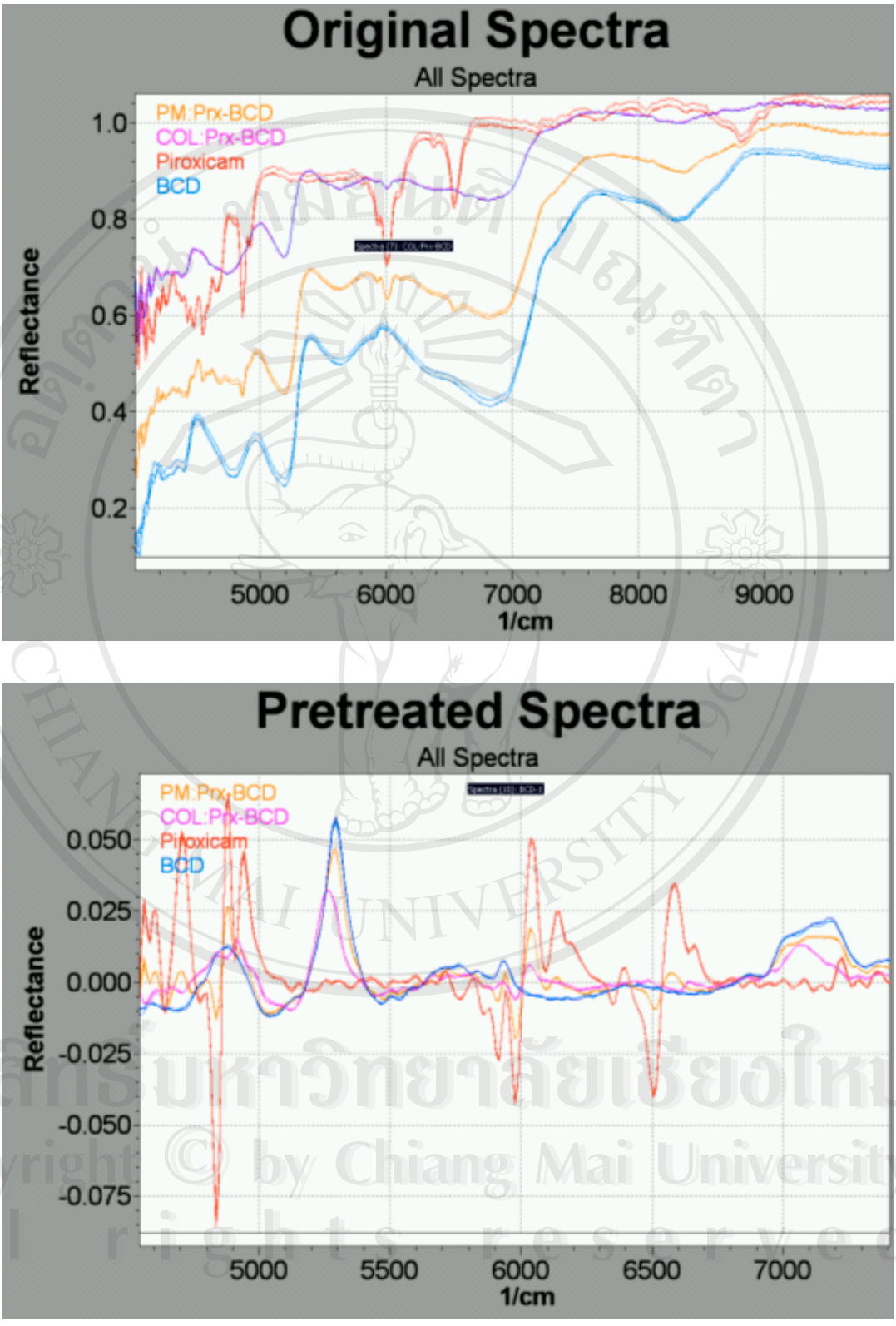

Figure 135 NIR Spectra of piroxicam; BCD; 1:1 physical mixture, PM and the inclusion complexes prepared by co-lyophilization method, COL. Upper: original spectra, lower: first derivative spectra.

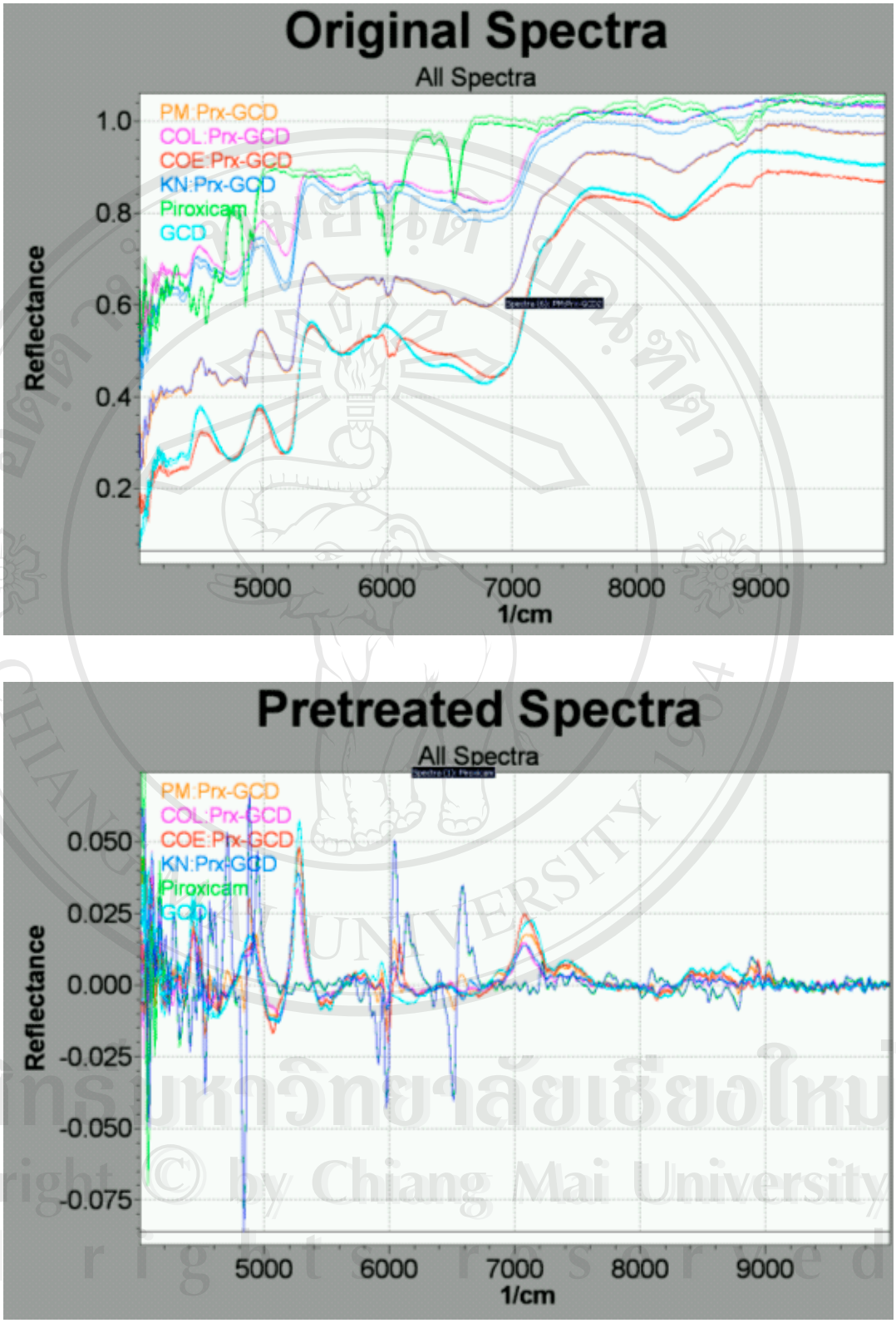

Figure 136 NIR Spectra of piroxicam; GCD; 1:1 physical mixture, PM and the inclusion complexes prepared by kneading, KN; co-evaporation, COE and co-lyophilization, COL method. Upper: original spectra, lower: first derivative spectra.

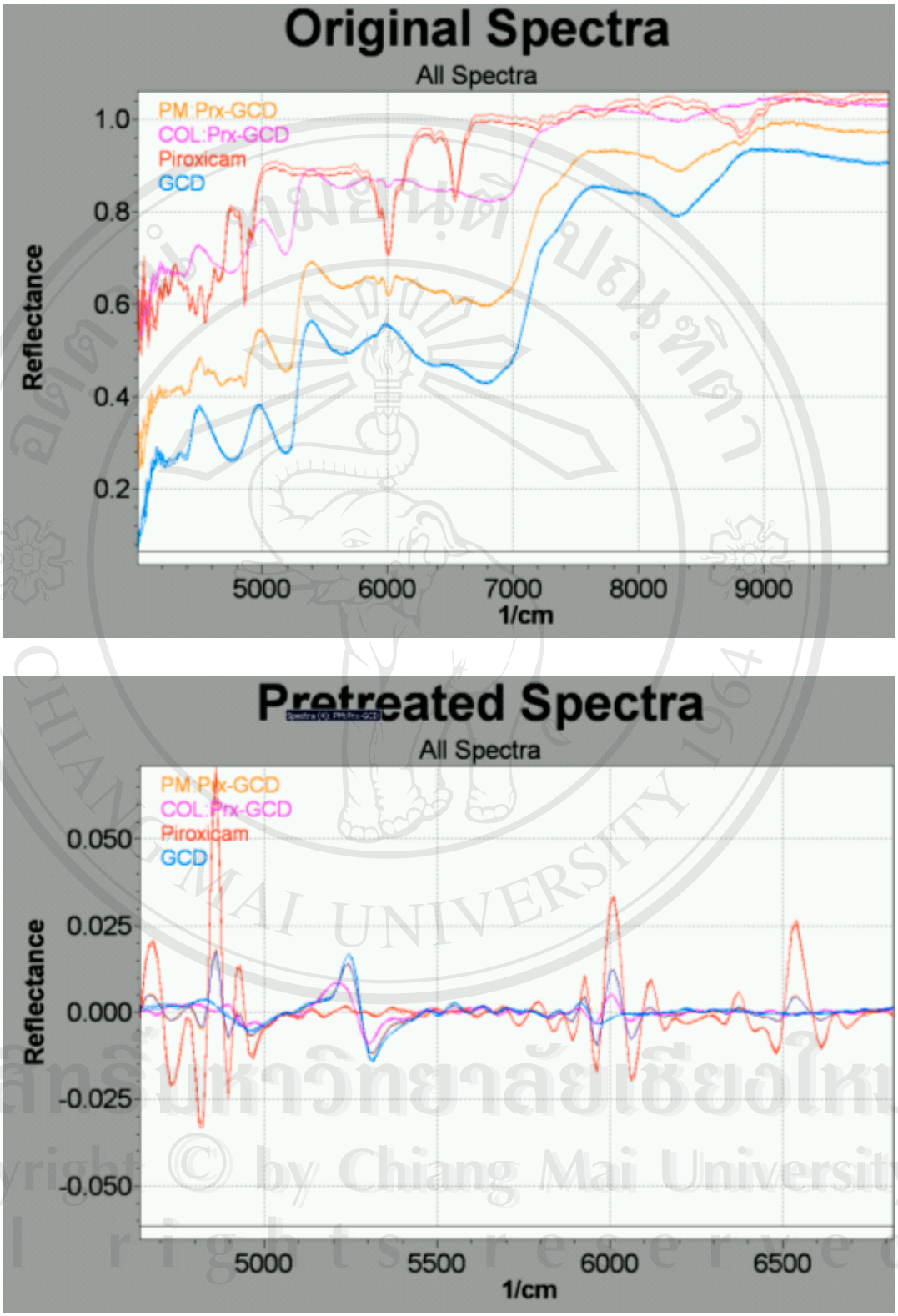

Figure 137 NIR Spectra of piroxicam; GCD; 1:1 physical mixture, PM and the inclusion complexes prepared by co-lyophilization method, COL. Upper: original spectra, lower: first derivative spectra.

The original and the first derivative NIR spectra of the NIR spectra piroxicam-HPBCD physical mixture and the inclusion complexes prepared by kneading, co-evaporation and co-lyophilization method are shown in Figure 138. It is very interesting that the physical mixture exhibits the spectra which are superimposed to those of HPBCD and COL complexes.

The original and the first derivative NIR spectra of piroxicam-HPBCD physical mixture and the inclusion complexes prepared by kneading, co-evaporation and co-lyophilization method are shown in Figure 138. The physical mixture exhibits the spectra which were superimposed to those of the COL complex. This is consistent with the lowering of the absorption peak at 1630 cm^{-1} in FTIR spectra. These findings support the better dissolution of the physical mixture of piroxicam-HPBCD compared to the other CDs. The first derivative NIR spectra demonstrate clearly the difference in the spectra of the drug and the physical mixture to those of the other complexes. It is of interest that the COE complex shows a new absorption band at 6600 cm^{-1} which does not belong to either the drug or HPBCD. The existence of the new peak is also confirmed by XPD and FTIR techniques, suggesting the formation of a new crystal of drug during the preparation process. The similarity of NIR spectra of the physical mixture to the COL complex of piroxicam-HPBCD is shown in Figure 139.

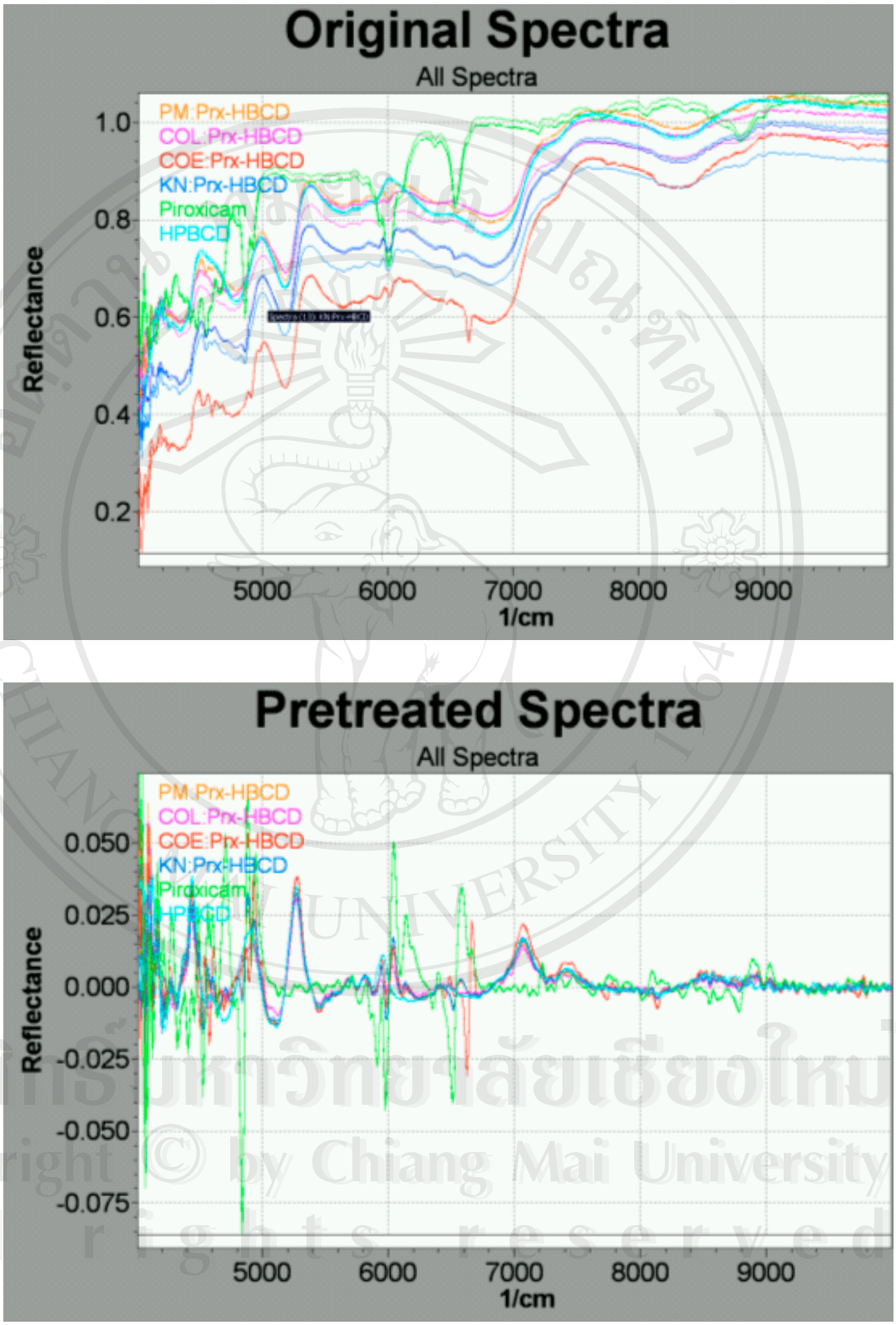

Figure 138 NIR Spectra of piroxicam; HPBCD; 1:1 physical mixture, PM and the inclusion complexes prepared by kneading, KN; co-evaporation, COE and co-lyophilization, COL method. Upper: original spectra, lower: first derivative spectra.

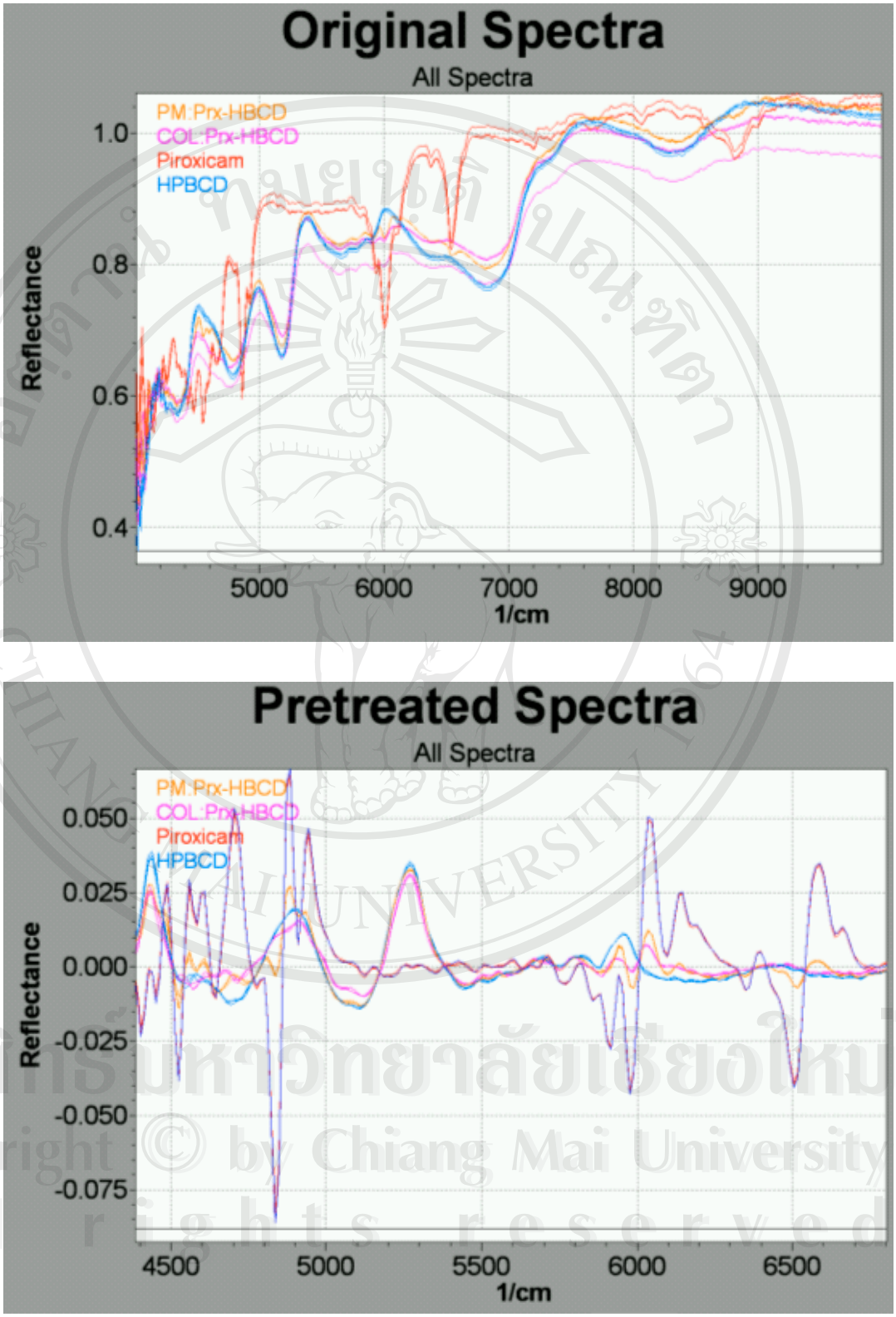

Figure 139 NIR Spectra of piroxicam; HPBCD; 1:1 physical mixture, PM and the inclusion complexes prepared by co-lyophilization method, COL. Upper: original spectra, lower: first derivative spectra.

NIR spectra of the physical mixture and the complexes of piroxicam-MeBCD are shown in Figure 140. These spectra provide evidences which are similar to piroxicam-HPBCD binary mixtures. The absorption bands of the drug in physical mixture, KN and COL complexes nearly disappear, meanwhile a new distinct peak is shown in the COE complex. These evidences could help supporting the other characterizing methods for the interaction between the drug and MeBCD. Figure 141 illustrates the significant changes in NIR spectra of the physical mixture and COL complex to those of the drug.

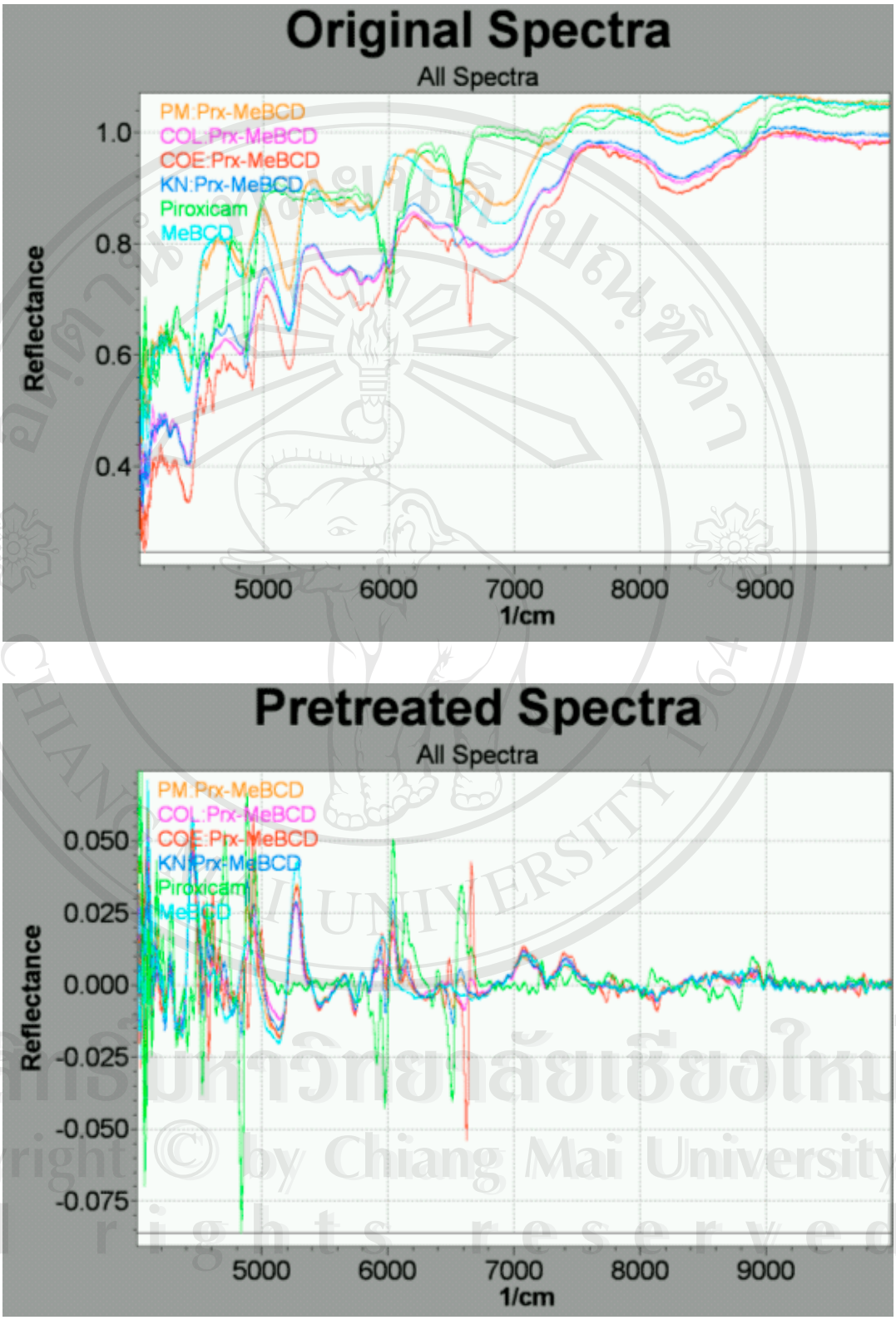

Figure 140 NIR Spectra of piroxicam; MeBCD; 1:1 physical mixture, PM and the inclusion complexes prepared by kneading, KN; co-evaporation, COE and co-lyophilization, COL method. Upper: original spectra, lower: first derivative spectra.

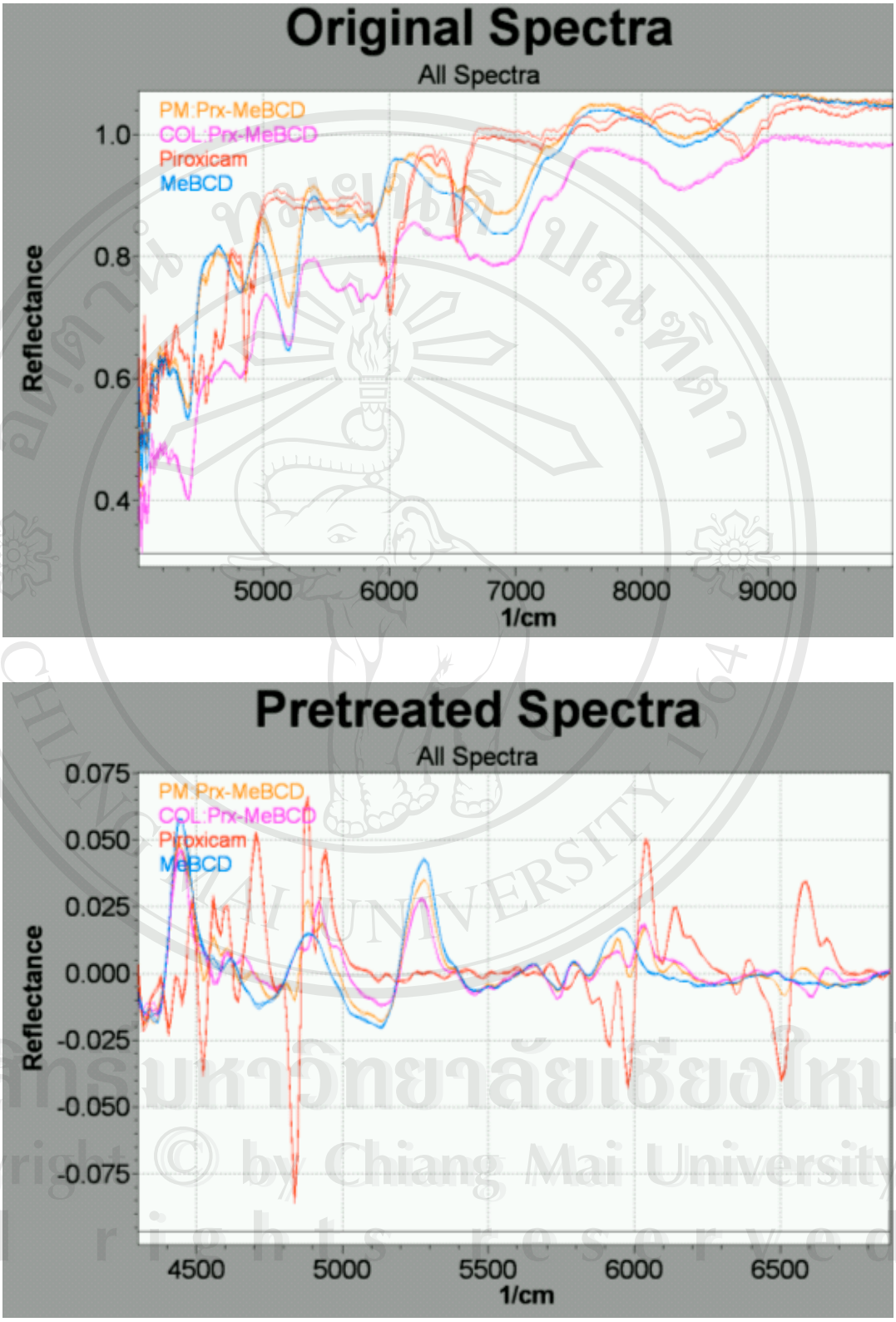

Figure 141 NIR Spectra of piroxicam; MeBCD; 1:1 physical mixture, PM and the inclusion complexes prepared by co-lyophilization method, COL. Upper: original spectra, lower: first derivative spectra.

3.4.5.2 NIR spectra of meloxicam-CDs complexes

The original and the first derivative NIR spectra of meloxicam-BCD physical mixture and the inclusion complexes prepared by kneading, co-evaporation and co-lyophilization method are shown in Figure 142.

Due to their structural relation, the NIR spectra of meloxicam are similar to those of piroxicam. However, there are some significant difference. The absorption bands at 6000 cm^{-1}, exhibited by piroxicam, is a sharp single band compared to a triplet, less intense band shown by meloxicam. The absorption band at 6500 cm^{-1} characterized by the pure drug is completely disappears in COE and COL complexes, whereas it could be detected in physical mixture and KN complex. These evidences support the other techniques used to point out the interaction between the drug and BCD.

Figure 143 shows the spectra of the drug compared to the physical mixture and COL complex to demonstrate the change in absorption band at 6500 cm^{-1} in these samples.

The NIR spectra of meloxicam-GCD physical mixture and the complexes illustrated in Figure 144 and 145 are very similar to those of piroxicam-BCD binary mixtures. Thus, they provide evidence supporting the interaction between the drug and GCD.

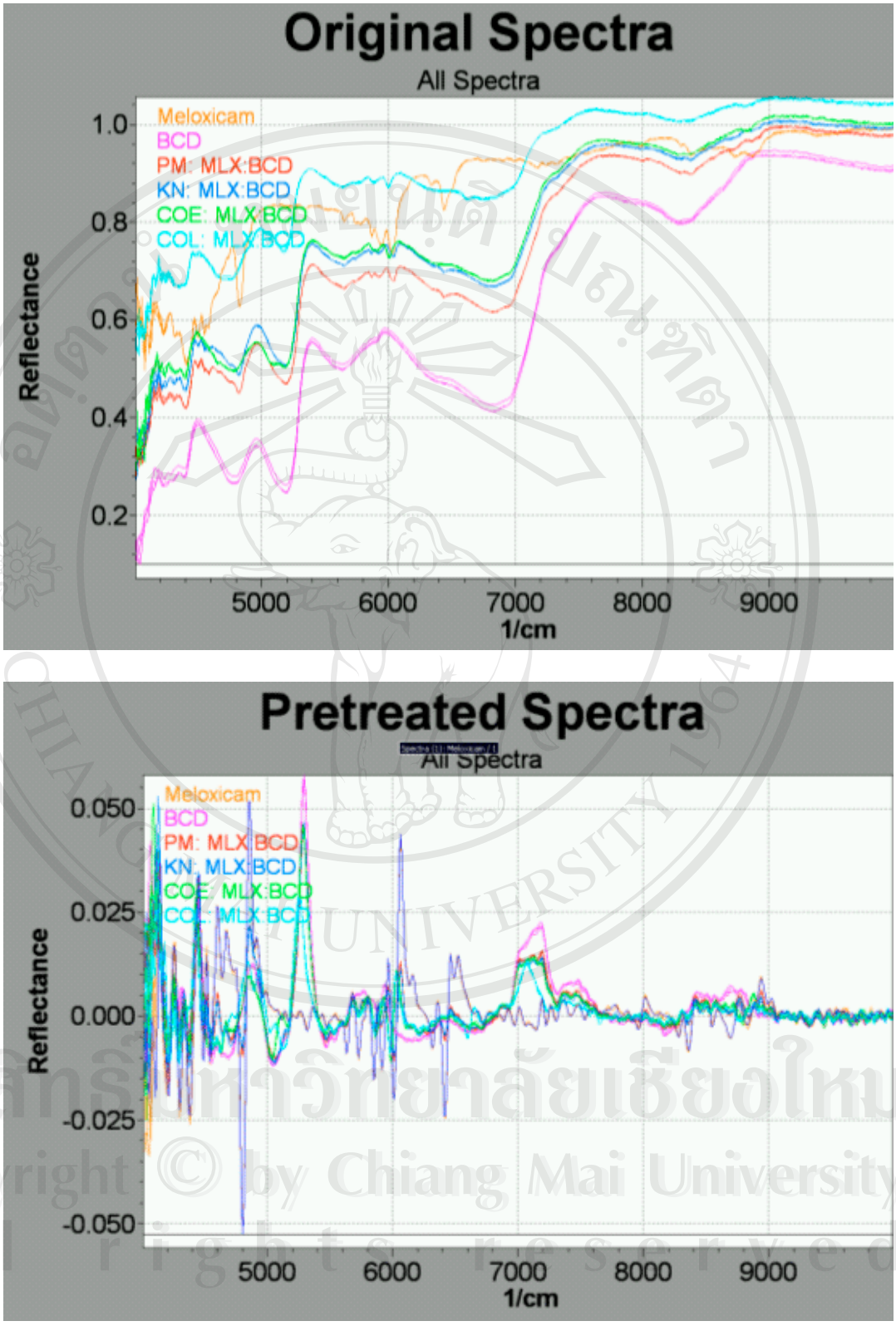

Figure 142 NIR Spectra of meloxicam; BCD; 1:1 physical mixture, PM and the inclusion complexes prepared by kneading, KN; co-evaporation, COE and co-lyophilization, COL method. Upper: original spectra, lower: first derivative spectra.

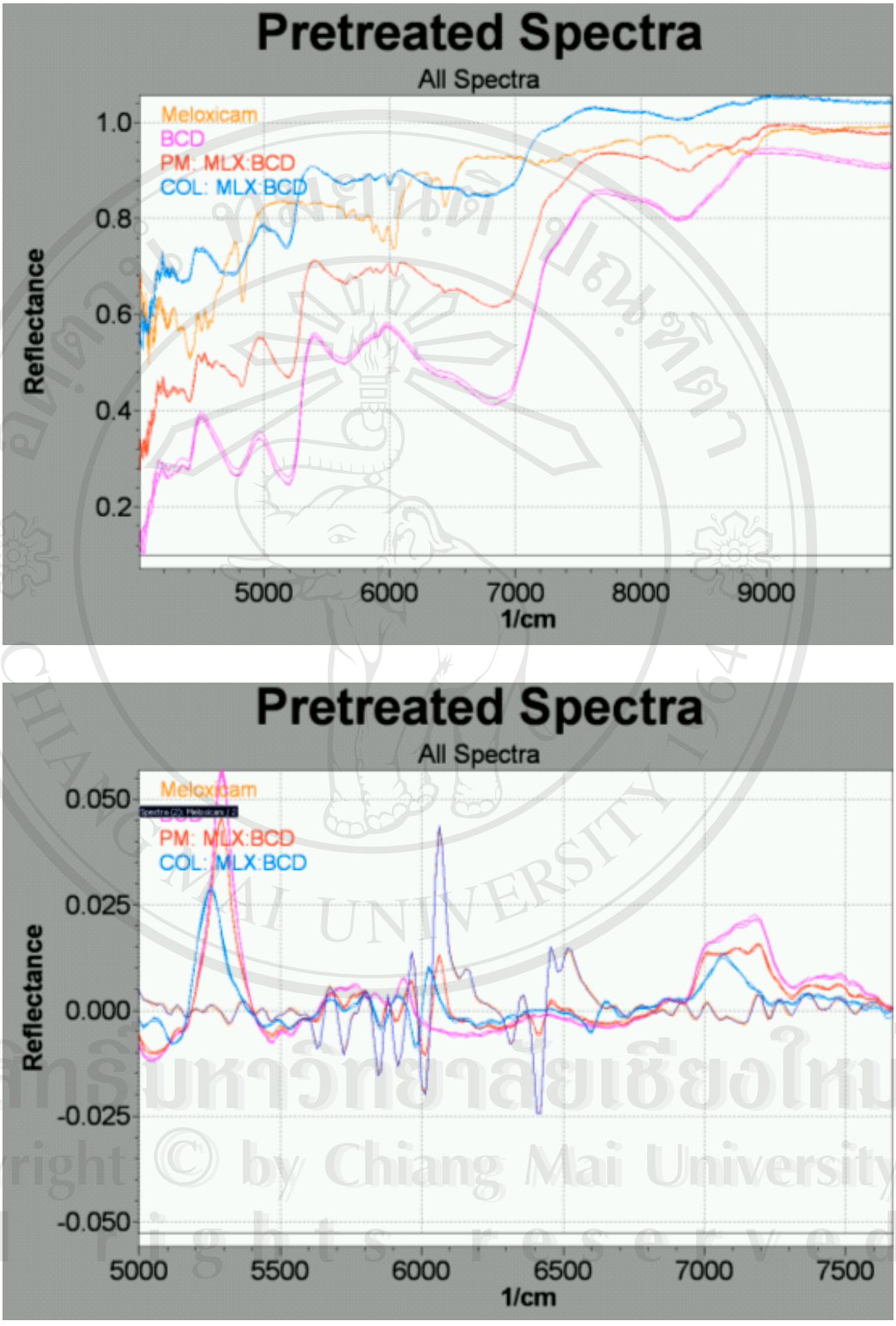

Figure 143 NIR Spectra of meloxicam; BCD; 1:1 physical mixture, PM and the inclusion complexes prepared by co-lyophilization method, COL. Upper: original spectra, lower: first derivative spectra.

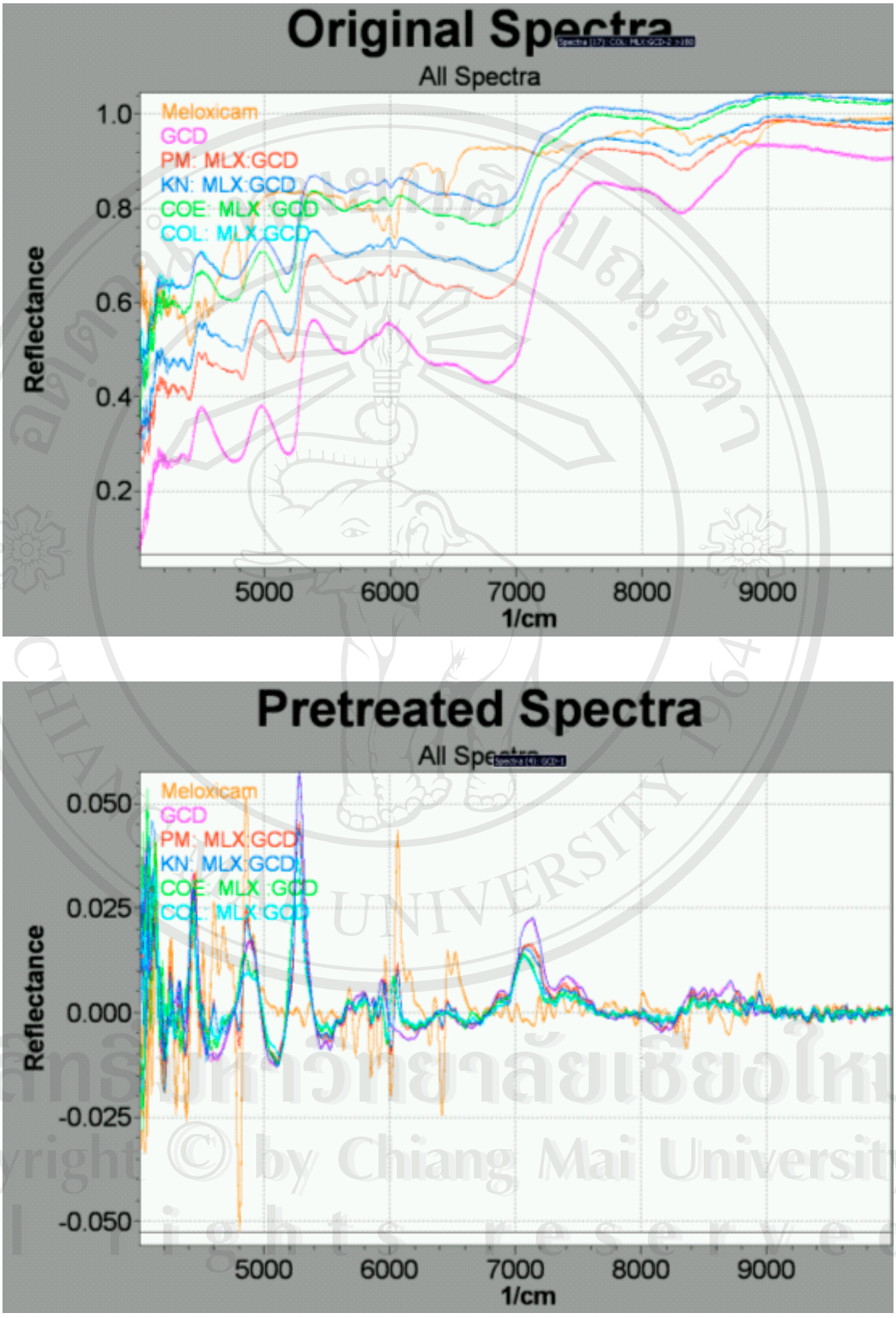

Figure 144 NIR Spectra of meloxicam; GCD; 1:1 physical mixture, PM and the inclusion complexes prepared by kneading, KN; co-evaporation, COE and co-lyophilization, COL method. Upper: original spectra, lower: first derivative spectra.

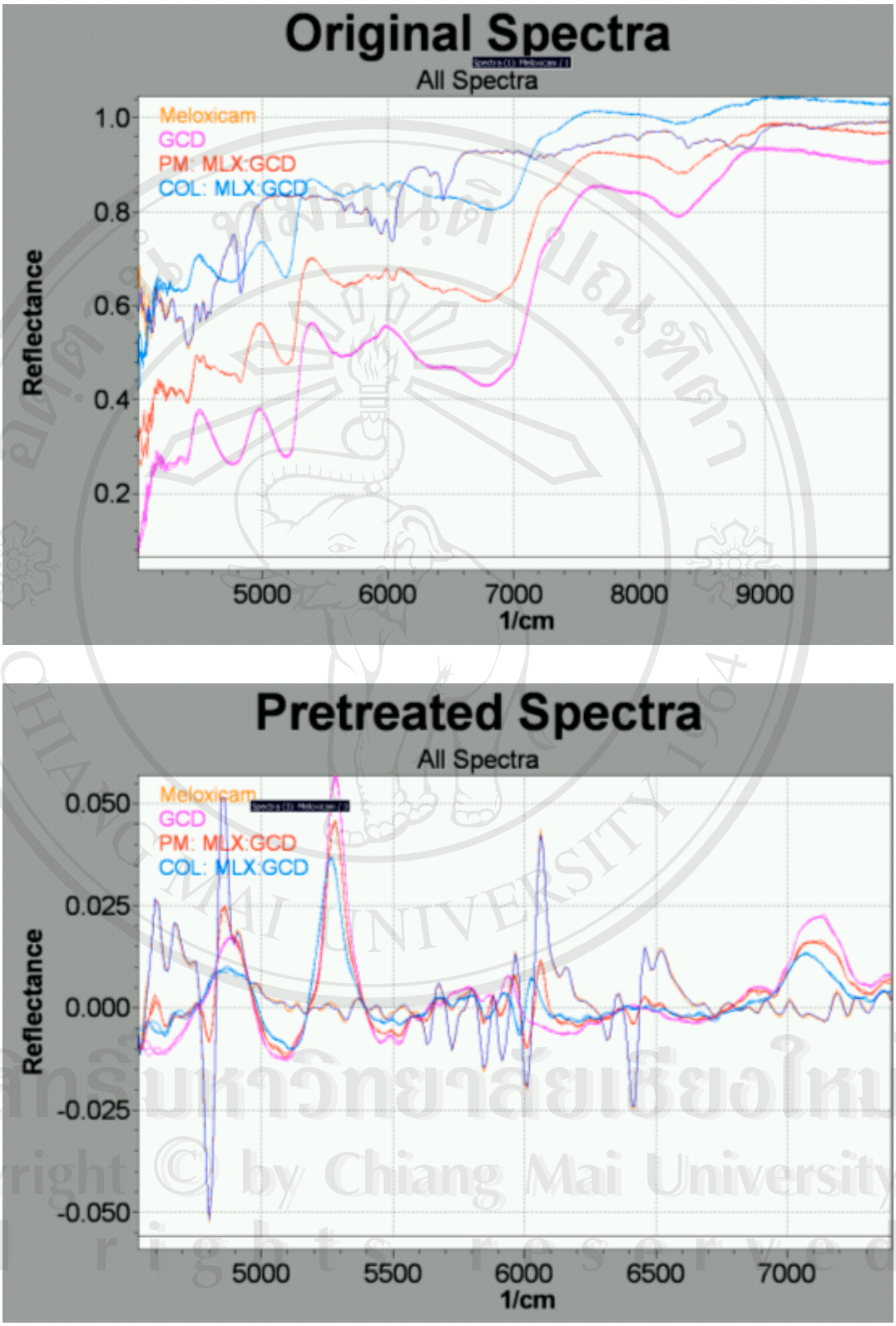

Figure 145 NIR Spectra of meloxicam; GCD; 1:1 physical mixture, PM and the inclusion complexes prepared by co-lyophilization method, COL. Upper: original spectra, lower: first derivative spectra.

Figure 146 illustrates NIR spectra of meloxicam compared to the physical mixture and inclusion complexes in HPBCD. The spectra of these binary mixtures are closely related to the spectra of HPBCD. The characteristic band of the drug, especially at 6500 cm^{-1} nearly disappears. This supports the interaction of the drug and HPBCD in the physical mixture and complexes which was suggested by DSC and XPD.

NIR spectra of meloxicam compared to meloxicam-HPGCD physical mixture and the inclusion complexes are shown in Figure 147 and Figure 148. The same evidence as meloxicam-HPBCD binary mixtures could be depicted. The spectra of the mixtures are totally different to the spectra of the drug. The completely disappearance of the absorption bands of the drug might be caused by the inclusion of the drug into the HPGCD cavity.

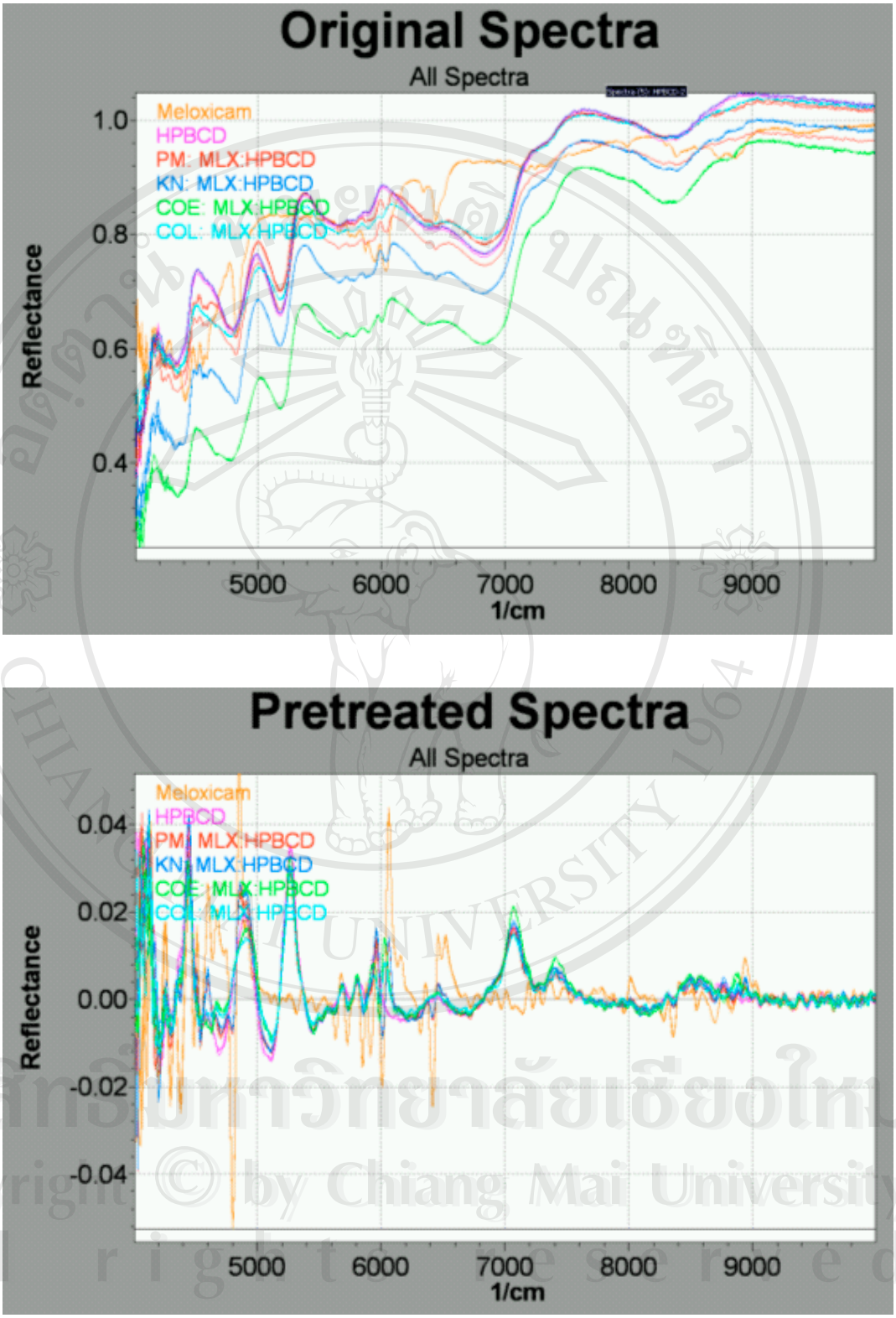

Figure 146 NIR Spectra of meloxicam; HPBCD; 1:1 physical mixture, PM and the inclusion complexes prepared by kneading, KN; co-evaporation, COE and co-lyophilization, COL method. Upper: original spectra, lower: first derivative spectra.

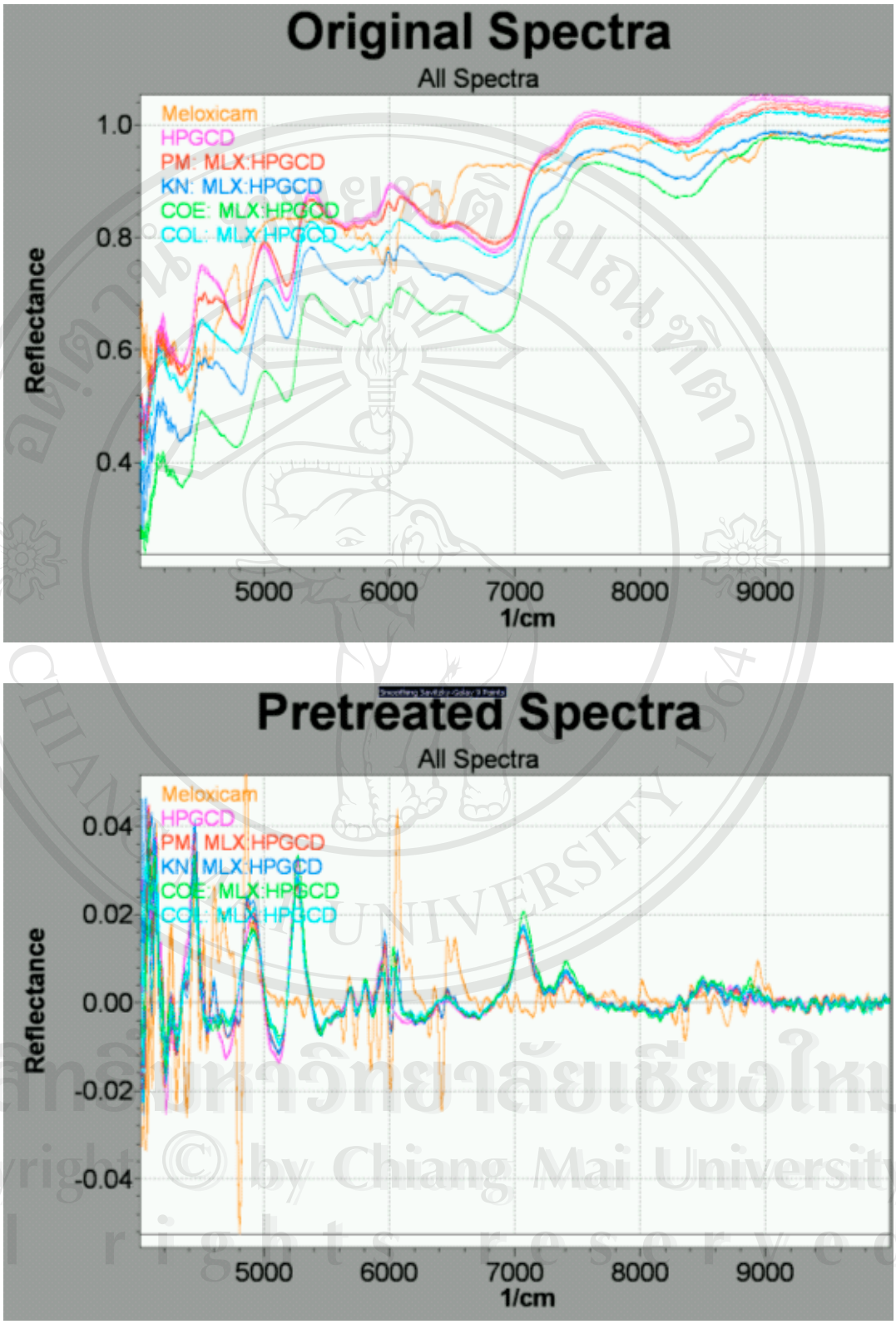

Figure 147 NIR Spectra of meloxicam; HPGCD; 1:1 physical mixture, PM and the inclusion complexes prepared by kneading, KN; co-evaporation, COE and co-lyophilization, COL method. Upper : original spectra, lower : first derivative spectra.

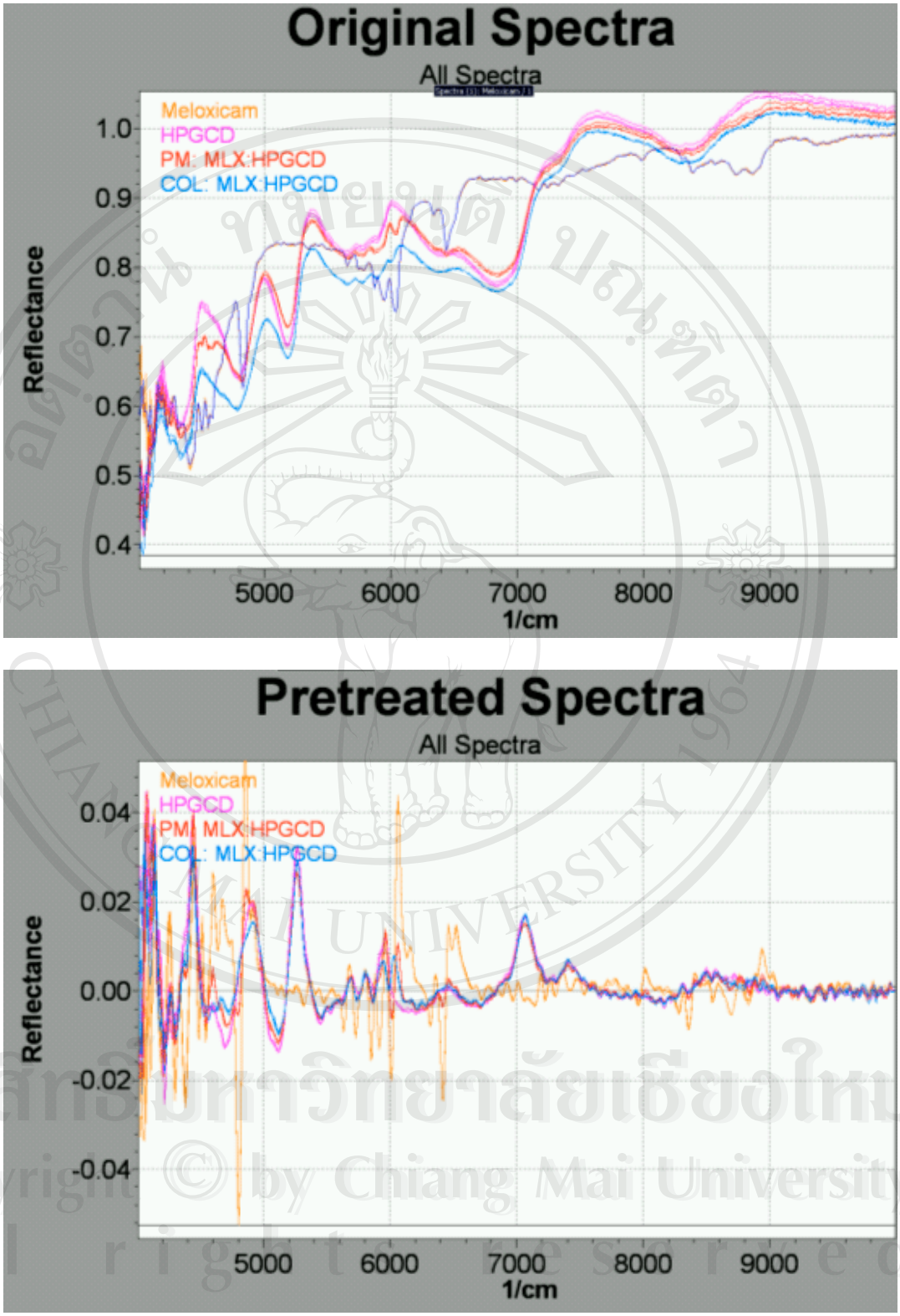

Figure 148 NIR Spectra of meloxicam; HPGCD; 1:1 physical mixture, PM and the inclusion complexes prepared by co-lyophilization method, COL. Upper: original spectra, lower: first derivative spectra.

3.5 Storage-stability studies

After the end of storage, the complexes were re-characterized by dissolution studies, DSC and XPD analyses in order to investigate whether the drug is being entrapped within the CDs cavity upon storage under the test conditions.

3.5.1 Dissolution studies

3.5.1.1 Dissolution studies of piroxicam-BCD complexes

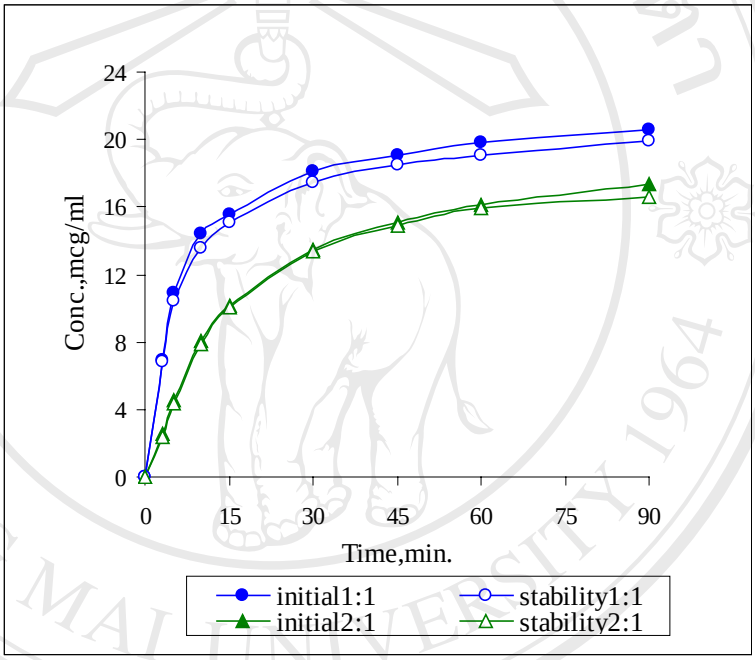

Figure 149 Dissolution profiles of piroxicam from 1:1 and 2:1 KN piroxicam-BCD inclusion complexes initially prepared and after stored at 30°C for 1 year

Figure 149-151 show the comparison dissolution profiles of piroxicam-BCD complexes prepared by kneading, co-evaporation and co-lyophilization methods between the initially prepared and the stored complexes. These profiles are nearly superimposed. From Table 49, the % DE30 values of the complexes at the end of storage are slightly lower than the initial values; however they are no-significantly different.

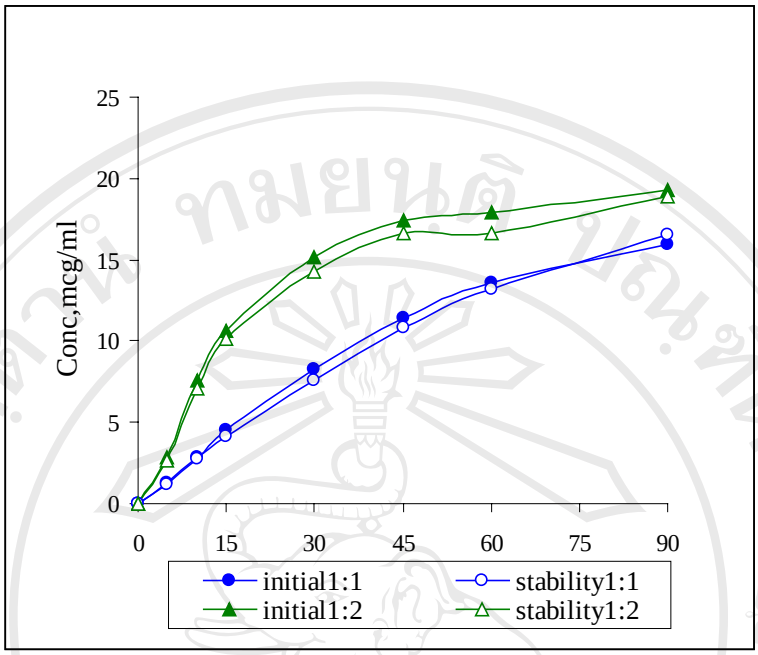

Figure 150 Dissolution profiles of piroxicam from 1:1 and 1:2 COE piroxicam-BCD inclusion complexes initially prepared and after stored at 30°C for 1 year.

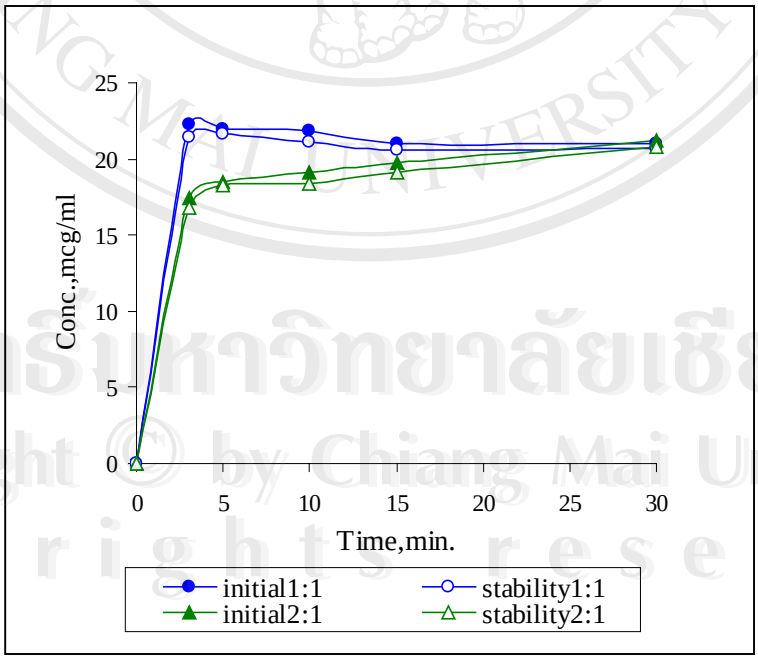

Figure 151 Dissolution profiles of piroxicam from 1:1 and 2:1 COL piroxicam-BCD inclusion complexes initially prepared and after stored at 30°C for 1 year

Table 49 Dissolution parameters of piroxicam in distilled water from intact drug (Prx) and 1:1 and 1:2 KN, COE and COL Prx:BCD inclusion initially prepared and after stored at 30°C for year.(Mean±SD)

	%DE		t50%, min.	
	Initial	Stability	Initial	Stability
Prx	7.17±0.25	-	>30	-
KN 1:1	62.87±1.07	60.55±1.52	< 30	< 30
KN 2:1	39.79±0.88	39.12±1.24	< 30	< 30
COE 1:1	18.62±1.15	17.75±1.10	< 30	< 30
COE 1:2	40.73±1.06	38.61±1.17	< 30	< 30
COL 1:1	91.04±1.56	89.38±1.40	< 30	< 30
COL 2:1	84.18±1.35	81.72±1.63	< 30	< 30

3.5.1.2 Dissolution studies of meloxicam-BCD complexes

Similar to piroxicam-BCD complexes, the dissolution profiles of meloxicam-BCD complexes initially prepared and after stored at specified temperature shown in Figure 152-154 are superimposed, indicating that the drug is entrapped within the BCD cavity throughout the storage time. The comparable %DE30 values in Table 50 support this suggestion.

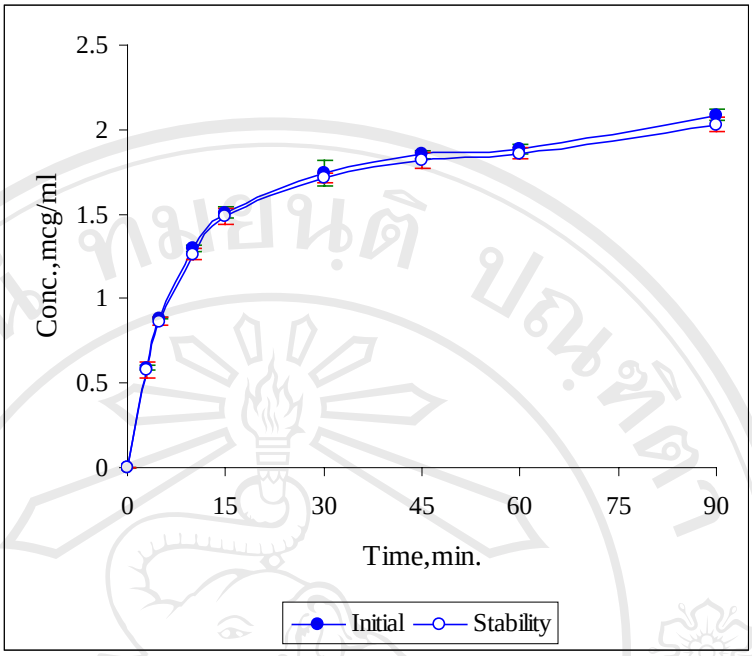

Figure 152 Dissolution profiles of meloxicam from 1:1 KN meloxicam: BCD inclusion complex initially prepared and after stored at 45°C for 4 months.

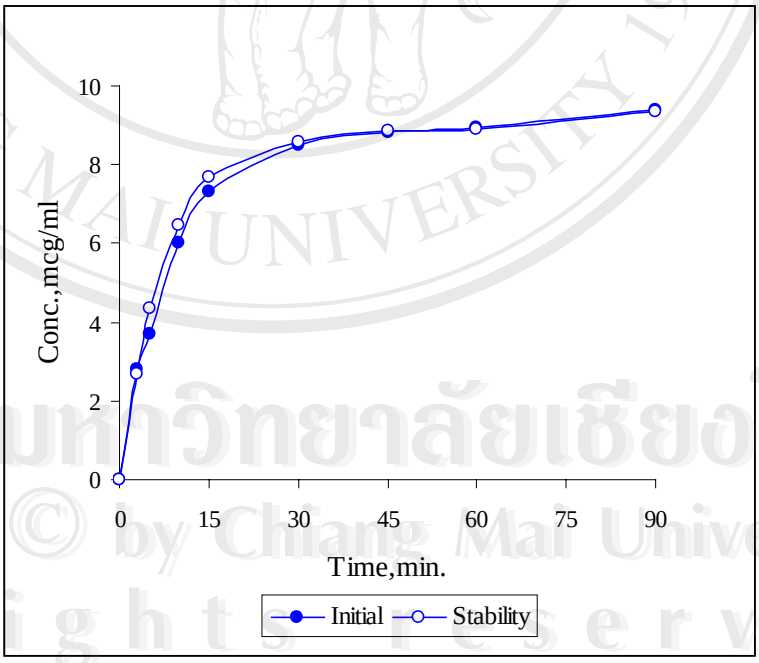

Figure 153 Dissolution profiles of meloxicam in from 1:1 COL meloxicam: BCD inclusion complex initially prepared and after stored at 45°C for 4 months

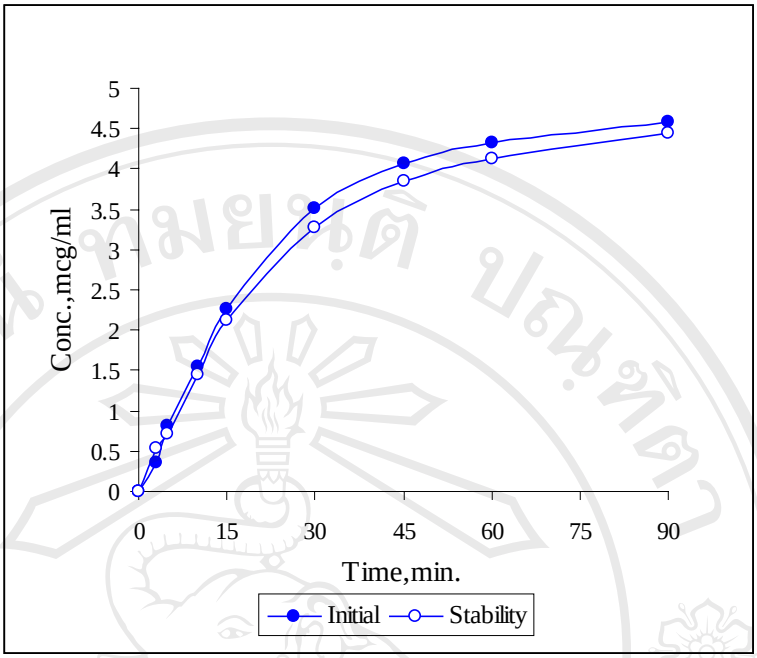

Figure 154 Dissolution profiles of meloxicam from 1:1 COE meloxicam: BCD inclusion complex initially prepared and after stored at 45°C for 4 months.

Table 50 Dissolution parameters of meloxicam from intact drug (Mlx) and binary mixtures of 1:1 Mlx:BCD; PM, KN, COE, COL. (Mean±SD)

	%DE30		t50%, min.	
	Initial	Stability	Initial	Stability
Mlx	0	0	>30	>30
PM	0.22±0.01	-	>30	-
KN	7.84±0.55	7.69±0.38	>30	>30
COE	12.09±0.61	11.38±0.39	>30	>30
COL	37.79±0.45	38.03±1.96	<30	<30

3.5.2 DSC studies of the stored complexes

3.5.2.1 DSC of piroxicam-CDs complexes

The DSC parameters of piroxicam intact, lyophilized piroxicam and piroxicam-BCD complexes initially prepared by different methods and after stored at

45°C for 4 months are shown in Table 51. At the end of storage, the onset and the temperature peak of piroxicam intact do not change significantly, indicating the stability of the pure drug upon storage. Thus, it is used as a positive control for checking the stability of the complexes. In the case of lyophilized piroxicam, the onset and the peak temperature are somewhat lower compared to the initial values; this is attributed to the alteration of the internal structure of the drug to some extent. The parameters of all complexes differ from those initially prepared, but they are not significantly difference.

Table 51 DSC parameters of piroxicam, intact; piroxicam, lyophilization and piroxicam-BCD inclusion complexes of various molar ratios initially prepared and at the end of storage

		Initial			End of storage		
		Onset,°C	Peak,°C	ΔH, J/g	Onset,°C	Peak, °C	ΔH, J/g
Prx, intact		201.06	202.89	107.18	201.62	202.70	107.36
Prx, lyo		201.90	203.59	95.53	200.71	201.70	74.35
PM	1:1	202.43	203.47	19.30	-	-	-
	1:2	203.03	203.95	10.76	-	-	-
	2:1	202.42	203.62	34.82	-	-	-
KN	1:1	201.30	202.74	19.81	200.16	201.33	20.78
	1:2	201.45	202.70	8.76	200.29	201.53	12.04
	2:1	201.38	202.75	27.67	200.24	201.37	35.74
COE	1:1	200.81	202.04	14.56	200.55	202.03	17.71
	1:2	200.80	201.96	7.00	200.84	202.03	12.12
	2:1	201.30	202.75	32.78	200.65	202.37	38.94
COL	1:1		No peak			No peak	
	1:2		No peak			No peak	
	2:1	198.34	201.20	15.24	198.53	200.84	14.51

3.5.2.1 DSC of meloxicam-CDs complexes

The DSC parameters of meloxicam-BCD complexes illustrate in Table 52 signify the stability of the complexes after the end of storage.

Table 52 DSC parameters of meloxicam intact, Mlx and meloxicam-CDs inclusion complexes prepared by different methods initially prepared and at the end of storage

	Initial			End of storage		
	Onset,°C	Peak,°C	ΔH, J/g	Onset,°C	Peak, °C	ΔH, J/g
Mlx, intact	253.53	255.20	132.50	-	-	-
Mlx:BCD						
PM	248.20	252.17	35.54	-	-	-
KN	243.74	246.87	28.43	244.68	247.67	24.78
COE	245.93	249.20	20.44	246.34	249.67	20.91
COL	243.25	246.53	20.08	243.49	246.83	24.93
Mlx:GCD						
PM	249.62	253.03	27.63	-	-	-
KN	243.87	247.33	24.54	245.96	249.00	28.96
COE	238.98	244.03	6.28	239.06	243.67	7.87
COL	240.30	244.20	12.59	240.64	245.00	13.93
Mlx:HPBCD						
PM	227.63	245.33	33.30	237.37		33.70
KN	229.13	237.83	31.46	228.28		32.44
COE	224.65	234.50	13.46	223.08		8.90
COL	228.36	232.83	4.17	222.51		11.60
Mlx:HPGCD						
PM	232.18	240.67	23.10	230.69		26.02
KN	213.38	235.83	24.91	224.88		26.19
COE		No peak			No peak	
COL		No peak			No peak	

3.5.3 XPD studies of the stored complexes

3.5.3.1 XPD of piroxicam-CDs complexes

3.5.3.2 XPD of meloxicam-CDs complexes

XPD diffractograms of piroxicam-BCD and meloxicam-BCD complexes shown in Figure 155 and Figure 156 support the evidences obtained from dissolution study and DSC investigations that the complexes are stable upon storage. The drug is still entrapped in BCD cavity showing the similar dissolution profiles, DSC thermograms and XPD diffractograms.

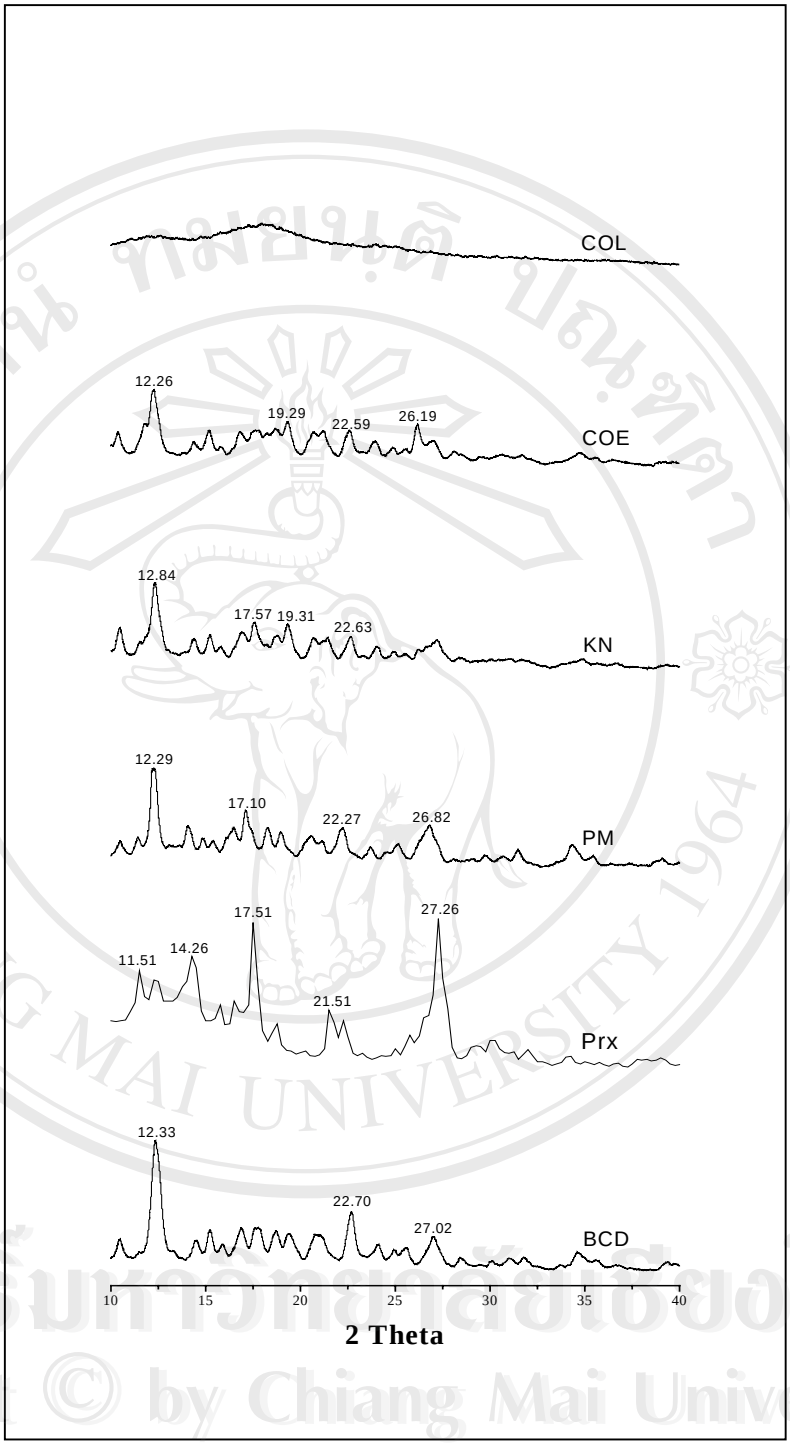

Figure 155 X-ray diffractograms of BCD, piroxicam (Prx), physical mixture, PM and the inclusion complexes prepared by kneading, KN, co-evaporation, COE and co-lyophilization, COL after stored at 30C° for 1 year

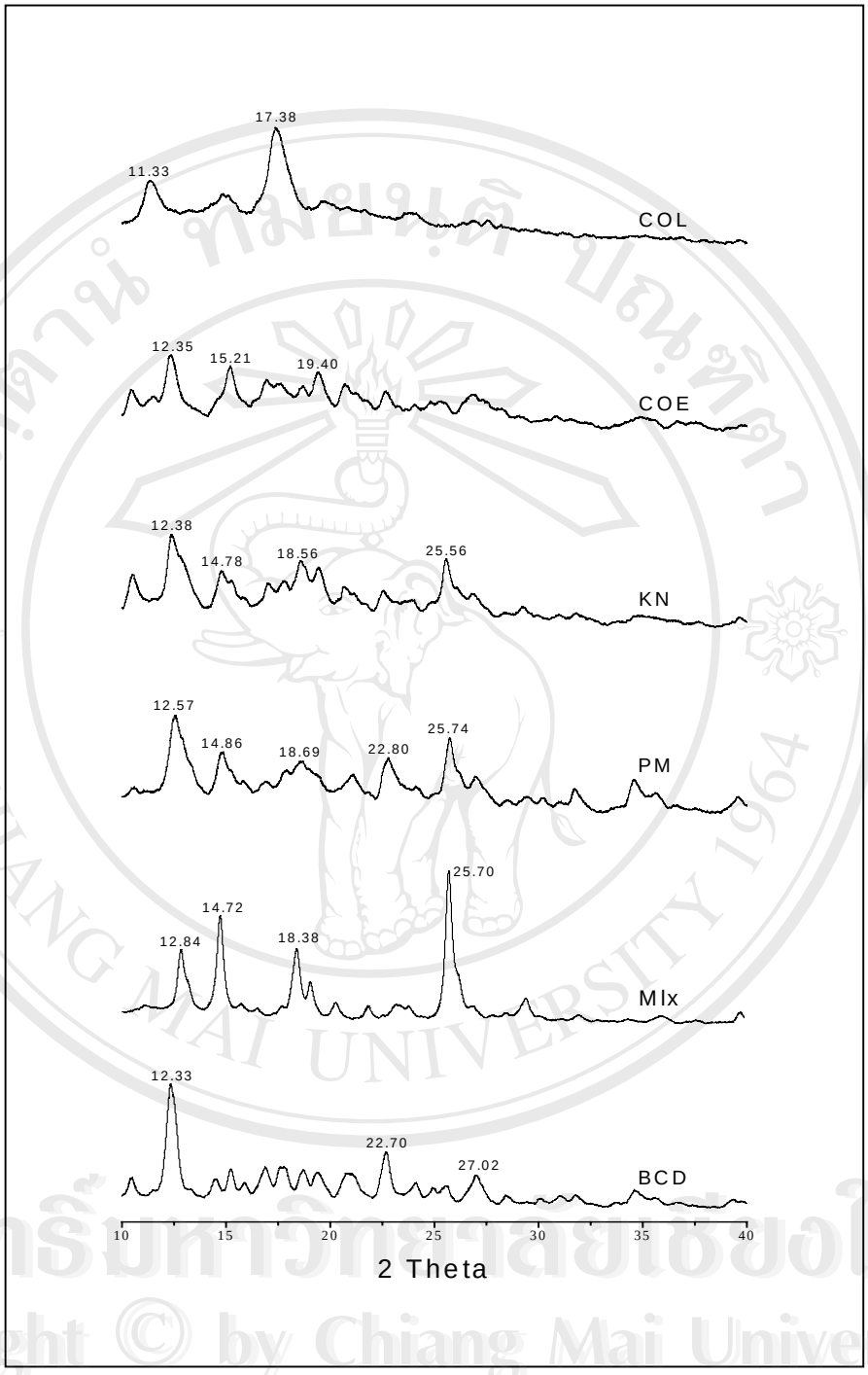

Figure 156 X-ray diffractograms of BCD, meloxicam (Mlx), physical mixture, PM and the inclusion complexes prepared by kneading, KN, co-evaporation, COE and co-lyophilization, COL after stored at 45C° for 3 months

3.6. Molecular modeling

3.6.1 Construction of Quantitative Structure Property relationship (QSPR) model

The QSPR model was constructed using the stability constants of 22 guests complexed with HPBCD as a training data set. Two QSPR models, model A and model B with respect to high r^2 values were obtained. The values of model A and model B are illustrated in Table 53 and Table 54, respectively.

Model: A

log k= -1.07672 – 0.00186* vdw.vol – 0.05910*PEOE_VSA+6
+ 0.02240*PEOE_VSA_NEG + 0.02564*ASA_P

r^2 = 0.91222; r = 0.9551; RMSE = 0.33100

r^2cv = 0.8584; s = 0.47883 (s^2= 0.2288); F = 28.31

n, dependent variables (observations) = 22

k, independent variables (descriptors) = 4

Model: B

log k= -1.52286 – 0.06527*PEOE_VSA+6
+ 0.02010*PEOE_VSA_NEG + 0.02745*ASA_P

r^2 = 0.90655; r = 0.9521; RMSE = 0.34154

r^2cv = 0.8659; s = 0.4423 (s^2= 0.2046); F = 41.67

n = 22, k = 3

Table 53 Training Sets (Model A)

Drugs	Log k (observed)	$ PRED	$ RES	$Z-Score	$X PRED	$X RES	$XZ-Score
Barbituric acid	3.9395	3.8971	0.0424	0.1281	3.8381	0.1014	0.2997
Barbital	3.9740	3.9186	0.0554	0.1675	3.9077	0.0663	0.1960
Amobarbital	4.1246	4.2723	-0.0577	0.1744	4.2818	-0.0672	0.1986
Pentobarbital	4.3228	3.9163	0.4065	1.2282	3.8615	0.4613	1.4180
Secobarbital	4.6169	5.2031	-0.5862	1.7709	5.4829	-0.8660	2.8772
Cyclobarbital	4.7773	4.1922	0.5851	1.7677	4.0912	0.6861	2.2183
Phenobarbital	4.8600	4.7979	0.0621	0.1877	4.7785	0.0815	0.2409
Lidocaine	1.2989	1.6428	-0.3440	1.0391	1.7187	-0.4198	1.2781
Ethidocaine	1.3838	1.6741	-0.2903	0.8770	1.7620	-0.3781	1.1425
Prilocaine	1.4771	1.5655	-0.0884	0.2671	1.6303	-0.1532	0.4535
Mepivacaine	1.5798	2.1202	-0.5404	1.6325	2.2125	-0.6327	2.0159
Bupivacaine	1.9782	1.6540	0.3241	0.9793	1.5737	0.4045	1.2277
Methyl paraben	2.9863	3.3598	-0.3735	1.1285	3.4688	-0.4825	1.4804
Ethyl paraben	2.9768	3.0425	-0.0657	0.1984	3.0608	-0.0840	0.2482
Propyl paraben	3.1898	3.1267	0.0631	0.1906	3.1131	0.0766	0.2264
Butyl paraben	3.5253	3.2250	0.3003	0.9072	3.1701	0.3552	1.0724
Amyl paraben	3.6776	3.4114	0.2662	0.8041	3.3630	0.3146	0.9452
Benzyl paraben	3.7810	3.7971	-0.0161	0.0488	3.8031	-0.0222	0.0655
Artemisinin	2.6767	3.0324	-0.3557	1.0745	3.1252	-0.4485	1.3700
Dihydroartemisinin	2.6075	2.8904	-0.2829	0.8548	2.9883	-0.3808	1.1500
Artether	2.5145	1.9597	0.5549	1.6764	1.7932	0.7214	2.3316
10-Deoxyartemisinin	2.1644	1.8236	0.3407	1.0293	1.7339	0.4305	1.3111

Table 54 Training Sets (Model B)

Drugs	Log k (observed)	$ PRED	$ RES	$ Z - Score	$ X PRED	$X RES	$ X Z - Score
Barbituric acid	3.9395	3.8749	0.0646	0.1892	3.7860	0.1535	0.4399
Barbital	3.9740	3.8794	0.0946	0.2771	3.8621	0.1119	0.3209
Amobarbital	4.1246	4.2976	-0.0830	0.2430	4.3108	-0.0962	0.2756
Pentobarbital	4.3228	3.9164	0.4064	1.1899	3.8616	0.4612	1.3703
Secobarbital	4.6169	5.2695	-0.6527	1.9109	5.5424	-0.9255	3.0277
Cyclobarbital	4.7773	4.2429	0.5344	1.5647	4.1626	0.6147	1.8831
Phenobarbital	4.8600	4.7887	0.0713	0.2086	4.7666	0.0934	0.2675
Lidocaine	1.2989	1.5917	-0.2929	0.8576	1.6492	-0.3504	1.0229
Ethidocaine	1.3838	1.6647	-0.2809	0.8225	1.7495	-0.3657	1.0676
Prilocaine	1.4771	1.4548	0.0224	0.0655	1.4430	0.0341	0.0975
Mepivacaine	1.5798	2.2019	-0.6221	1.8215	2.2734	-0.6936	2.1753
Bupivacaine	1.9782	1.7085	0.2696	0.7895	1.6495	0.3287	0.9568
Methyl paraben	2.9863	3.2746	-0.2883	0.8441	3.3376	-0.3512	1.0252
Ethyl paraben	2.9768	2.9107	0.0661	0.1936	2.9028	0.0740	0.2120
Propyl paraben	3.1898	3.0158	0.1740	0.5094	2.9969	0.1929	0.5555
Butyl paraben	3.5253	3.1359	0.3894	1.1401	3.0909	0.4344	1.2857
Amyl paraben	3.6776	3.3504	0.3272	0.9579	3.3015	0.3761	1.1027
Benzyl paraben	3.7810	3.7253	0.0556	0.1629	3.7079	0.0731	0.2092
Artemisinin	2.6767	3.1598	-0.4831	1.4145	3.2152	-0.5385	1.6250
Dihydroartemisinin	2.6075	3.0450	-0.4375	1.2811	3.0956	-0.4881	1.4584
Artether	2.5145	2.0979	0.4167	1.2200	2.0473	0.4673	1.3904
10-Deoxyartemisinin	2.1644	1.9161	0.2482	0.7268	1.8711	0.2933	0.8511

Model prediction, **$ PRED** = value of the model

Model residual, **$ RES** = Difference between the value of the model and the activity field; log k (observed) - $ PRED

Model Z-Score, **$Z-Score** = Absolute difference between the value of the model and the activity field divided by the square root of the mean square error of data test; [$ RES/RMSE]

Cross prediction, **$X PRED =** value of the model under a leave-one out cross validation scheme

Cross residual, **$X RES** = Difference between the value of the model under a leave-one out cross validation scheme and the activity field

Cross Z-Score, **$XZ-Score** = Absolute difference between the value of the model under a leave-one out cross validation scheme and the activity field divided by the square root of the mean square error of data test; [$X RES/RMSE]

The r^2cv value represents the internal predictivity of the model and is obtained by successively leave-one-out a compound from the model as the following relationship:

$$r^2cv = 1- PRESS/SSY$$

where, the predictive residual sum of squares, PRESS = $\Sigma^n_{i=1} = (yi – y')^2$

the sum squares of the observations, SSY = $\Sigma^n_{i=1} = (yi – y'')^2$

yi = the experimental log k values

y′ = the predicted log k values obtained from the QSPR model under a leave-one-out cross validation

y′′= the mean experimental log k values

r (r^2) is the correlation coefficient. This is a measure of how well the equation fits the data. It is a measure for the quality of the correlation.

s is the standard deviation of the regression line. It measures how well the function derived by the QSPR analysis predicts the observed activity. The smaller the value of s the better is the QSPR model.

$$s = \sqrt{\sum (yi - y')^2 \cdot 1/(n - k - 1)}$$

F is a value derived from the F-test indicating the probability of a true relationship or the significance level of the model. The F-value is the ratio between the explained and the unexplained variance for a given number of degrees of freedom. The larger the F value the greater the probability that the QSPR equation is significant. Usually, comparisons are made of the F value between different models until a model is obtained that shows no further improvement in the F value.

t, the t-statistic calculated for regression coefficients, compares each coefficient with its standard error. To be significant, the regression coefficient should be about twice as big as its standard error, at the 5% level for five or more degrees of freedom.

Model A and Model B and of same quality with respect to the comparability of the linear correlation coefficient of the model, r^2 , the standard deviation, s, and the cross-validation r^2 values. The two models consist of three common molecular descriptors, ASA_P, PEOE_VSA+6, and PEOE_VSA_NEG indicating the significance of these molecular properties on the complex formation between most drugs in training set and HPBCD. These descriptors represent charge-related van der Waals surface area of the guest molecules. ASA_P is the water accessible surface area of all polar atoms, representing the hydrophobicity of a compound. PEOE_VSA+6 is the sum of vi (van der Waals surface area) when qi > 0.30 and PEOE_VSA_NEG is total negative van der Waals surface area (sum of vi, when qi is negative), where qi stands for the partial charge of atom i. In model A, the vdw.vol represents the van der Waals volume.

The contribution of these molecular descriptors in the model was as followed:

Descriptor	Regression coefficient	Contribution
vdw.vol	-0.00186*	retardation
ASA_P	+0.02564* +0.02745	augment
PEOE_VSA+6	-0.05910* -0.06527	retardation
PEOE_VSA_NEG	+0.02240 * +0.02010	augment

*Model A

The most important properties of the guest molecules contributing to the complexation is PEOE_VSA+6, however, it exhibits negative effect. The higher van der Waals surface area when qi >0.30 results in the lower K value of the complex. In contrarily, PEOE_VSA_NEG, the total negative van der Waals surface area and the water accessible surface area of all polar atoms, ASA_P enhances the complexation efficiency between the guest molecules and HPBCD. It could be suggested in addition to the classic mechanism of van der Waals interaction, the inclusion complex formation between the guests in the training data set and HPBCD is a charge-involved interaction.

The role of charge on complex formation between seven drugs and HPBCD and sulfobutylether BCD has been demonstrated (Okimoto et al., 1996). The charge-transfer interaction has been proved as a driving force for cyclodextrin inclusion complexes (Liu and Guo, 2004). The van der Waals volume has less effect on the complexation as shown in Model A.

Model A and B were used to predict the K values of the test set, the 22 compounds rest. The predicted values and the experimental values are illustrated in Table 55 using model A and Table 56 using model B, respectively.

Table 55 Test set using Model A

Drugs	yi	y'	(yi-y')	$(yi-y')^2$
Bupranolol	2.4687	2.3394	0.1293	0.01672
Harmine	2.5478	1.7979	0.7499	0.56235
Tetracaine	3.1166	2.907	0.2096	0.04393
Diphenhydramine	2.6937	2.1919	0.5018	0.2518
Ibuprofen	3.7324	3.8978	-0.1654	0.02736
Naproxen	3.8129	4.2276	-0.4147	0.17198
Haloperodol	3.3247	3.0809	0.2438	0.05944
Flurbiprofen	4.2625	3.9816	0.2809	0.0789
Carbamazepine	2.8163	2.8486	-0.0323	0.00104
DTT	2.3522	2.4667	-0.1145	0.01311
DMDTT	2.8156	3.3268	-0.5112	0.26133
5PDTT	3.4568	3.4152	0.0416	0.00173
ATT	3.7943	4.0477	-0.2534	0.06421
Sertaconazole	3.8961	3.5444	0.3517	0.12369
Neutral Red	2.0792	2.0684	0.0108	0.00012
Deltametrin	2.918	2.7915	0.1265	0.016
AR	3.3802	3.7394	-0.3592	0.12902
Cryptotanshinone	3.5101	3.6259	-0.1158	0.01341
Oxazepam	2.6776	3.0548	-0.3772	0.14228
Metoprolol	2.3222	2.6073	-0.2851	0.08128
Ephedrine prodrug	3.1111	3.0201	0.091	0.00828
Oxybenzone	3.7663	3.7589	0.0074	5.5E-05

yi= log k, experiment
y'= log k, predicted

Table 56 Test set using Model B

Drugs	yi	y'	(yi-y')	$(yi-y')^2$
Bupranolol	2.4687	2.2592	0.2095	0.04389
Tetracaine	3.1166	3.1259	-0.0093	8.6E-05
Diphenhydramine	2.6937	2.2507	0.443	0.19625
Ibuprofen	3.7324	3.8068	-0.0744	0.00554
Naproxen	3.8129	4.2838	-0.4709	0.22175
Haloperodol	3.3247	3.2753	0.0494	0.00244
Flurbiprofen	4.2625	3.919	0.3435	0.11799
Carbamazepine	2.8163	2.733	0.0833	0.00694
DTT	2.3522	2.2272	0.125	0.01563
DMDTT	2.8156	3.205	-0.3894	0.15163
5PDTT	3.4568	3.2804	0.1764	0.03112
ATT	3.7943	4.0656	-0.2713	0.0736
Sertaconazole	3.8961	3.6863	0.2098	0.04402
Neutral Red	2.0792	2.2015	-0.1223	0.01496
Deltametrin	2.918	2.6322	0.2858	0.08168
AR	3.3802	3.8711	-0.4909	0.24098
Cryptotanshinone	3.5101	3.7856	-0.2755	0.0759
Oxazepam	2.6776	2.9757	-0.2981	0.08886
Metoprolol	2.3222	2.7537	-0.4315	0.18619
Ephedrine prodrug	3.1111	3.1791	-0.068	0.00462
Oxybenzone	3.7663	3.8048	-0.0385	0.00148

The correlation between the predicted K values using Model A and Model B to those of the observed K values from the test set are illustrated in Figure 158 and Figure 159, respectively.

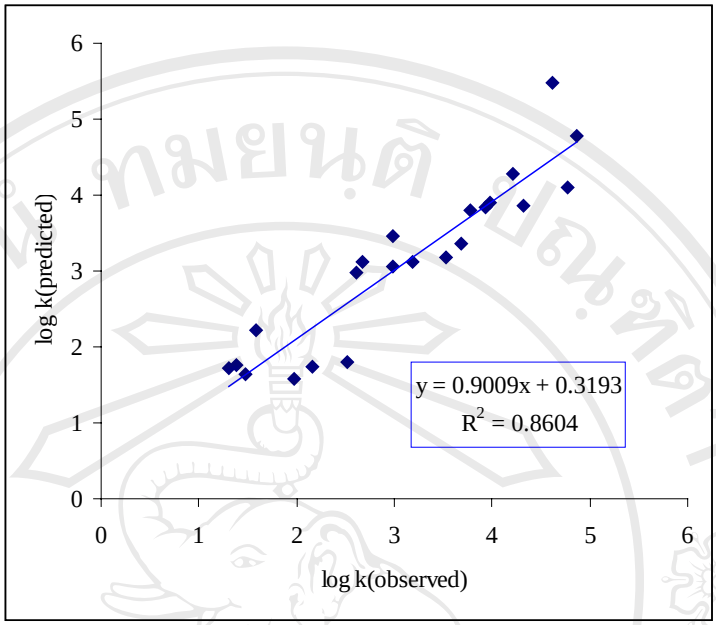

Figure 157 Correlation Plot between log k(observed) and log k(predicted) of the test set using Model A

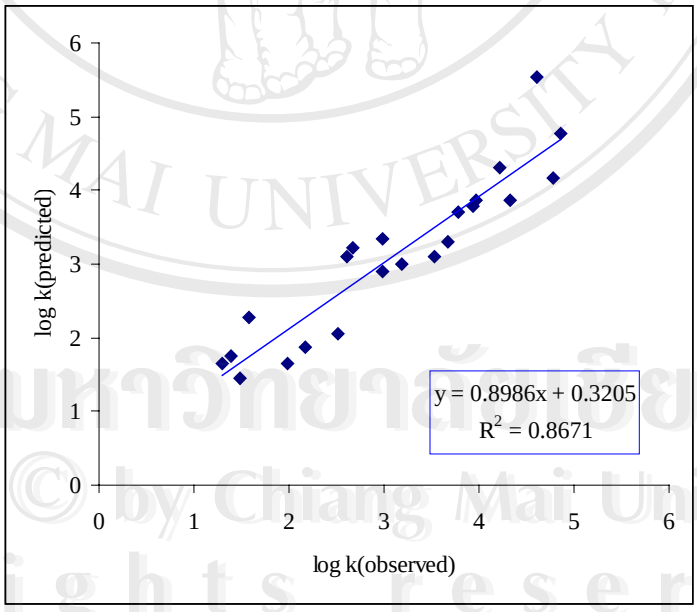

Figure 158 Correlation Plot between log k(observed) and log k(predicted) of the test set using Model B

The high value of the linear regression coefficients of the correlation plots signifies that both models have high predictive ability. Theoretically, these models can anticipate the stability constants of the complexes between the new compound and HPBCD, by calculating the molecular descriptors involved in the models and substituting the calculated values into the model to obtain the predicted K value.

This procedure was performed in order to obtain the K value of piroxicam-HPBCD complex and meloxicam-HPBCD complex as the predictive values and compared to the experimental values. Unfortunately, the K values obtained from both models are not in agreement with the experimental values, indicating low predictive ability of the model for these drugs. This might be due to large diversity of the molecular structures of the guest compounds in the training set to that of piroxicam and meloxicam. The QSPR model can predict properties of the unknown compound, which is structurally similar to those used to build the model. Poor predictive ability of the model is commonly obtained when a specific chemotype or functional groups of the unknown compound are not covered in the model. The existing data obtained from literature review is restricted to provide such information.

Basically, the molecular structure of the compounds in the training set should be diverse in order to obtain a model of wide predictive range. But, in this case, the compound in the training set composed of four main groups with their structures closely related. The data are shown in Appendix E. Additionally, the methods and conditions of determining the K values in the training set were different from the experiment in this study. It is a crucial factor to obtain un-correlated K values for piroxicam and meloxicam with HPBCD.

3.6.2 Conformational study of piroxicam-BCD complex

3.6.2.1 Energy optimization of piroxicam

Piroxicam is a drug which can exist in several prototropic species depending on the pH of the medium. Structurally, it is an amphoteric drug containing two ionizable moieties, the enolic and 2-pyridyl group. The pH of the medium has pronounced effect on its ionization. In aqueous solution of pH 0.9-7.0 the drug exists as zwitterion of very low solubility. In alkaline solution (pH> 7.0) the anionic species is predominant (Rozou et al., 2004). In addition to the difference orientation of the 2-pyridyl group, the amide group and the hydroxyl group, the 20 possible piroxicam conformations can be obtained. They are presented in Figure 160.

Structures (1)-(6) are neutral form with different conformations, (1) and (2) are closed conformations, (4)-(6) are opened conformations. Structures (7)-(10) represent zwitterionic conformations. Structures (11)-(14) are those of anionic species and structures (15)-(20) are conformations of cationic.

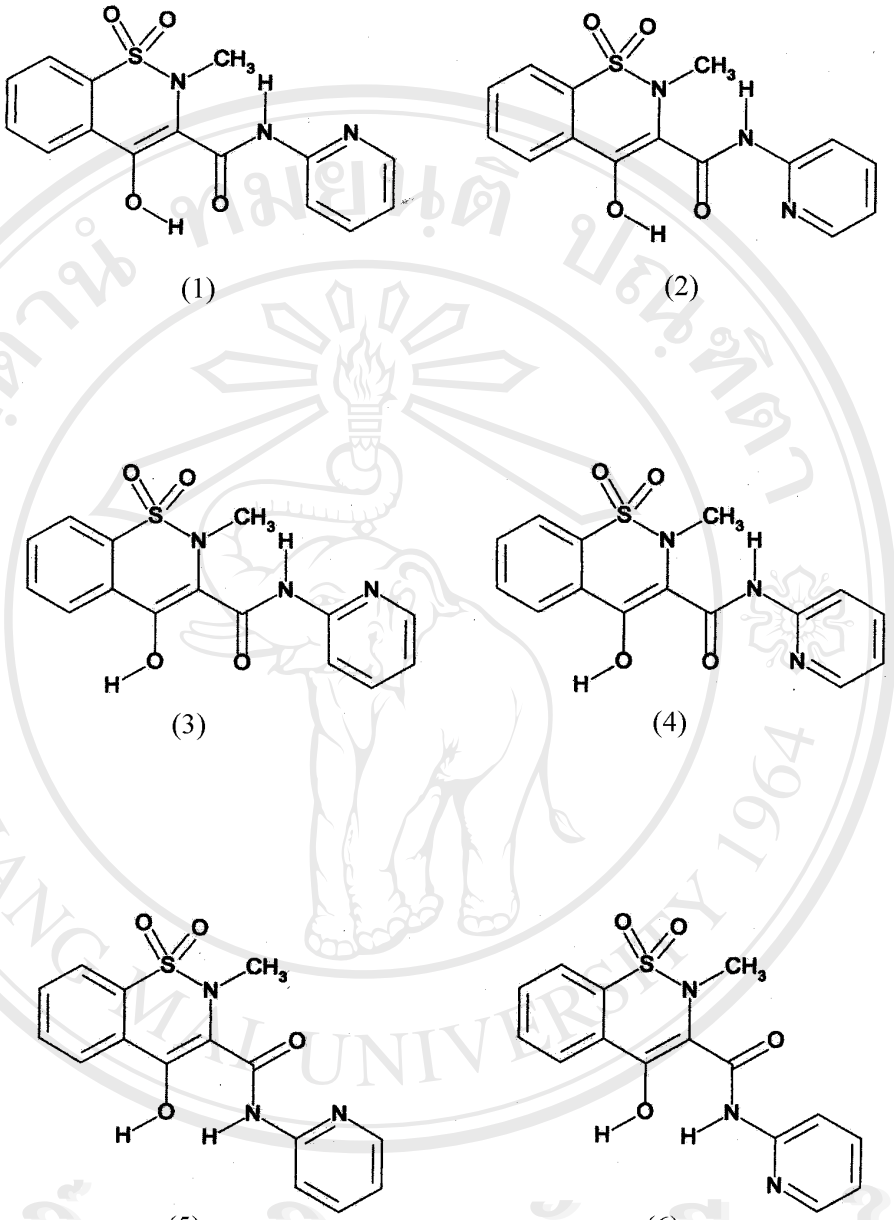

Figure 159 Conformation of piroxicam

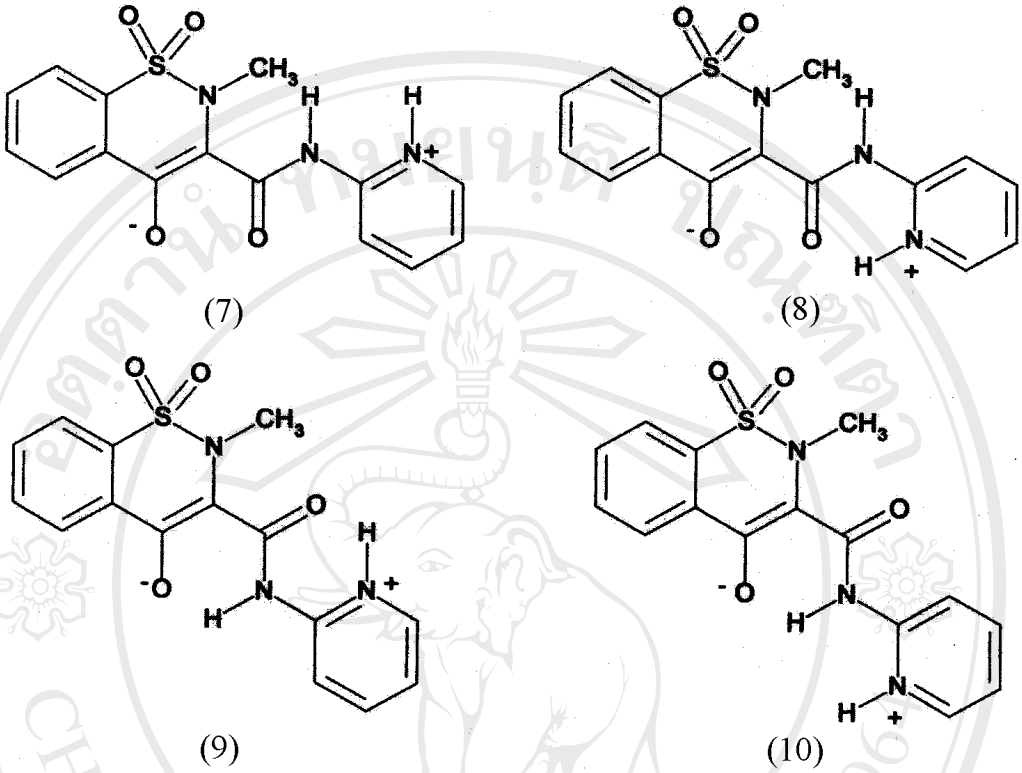

(7) (8)

(9) (10)

Figure 159 (cont.) Conformation of piroxicam

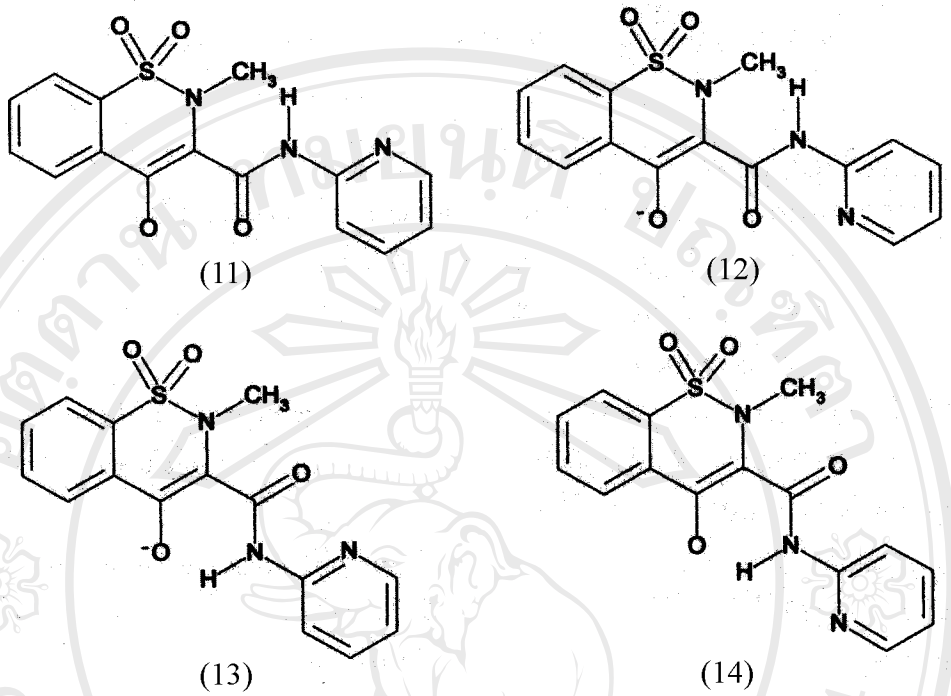

(11) (12)

(13) (14)

Figure 159 (cont.) Conformation of piroxicam

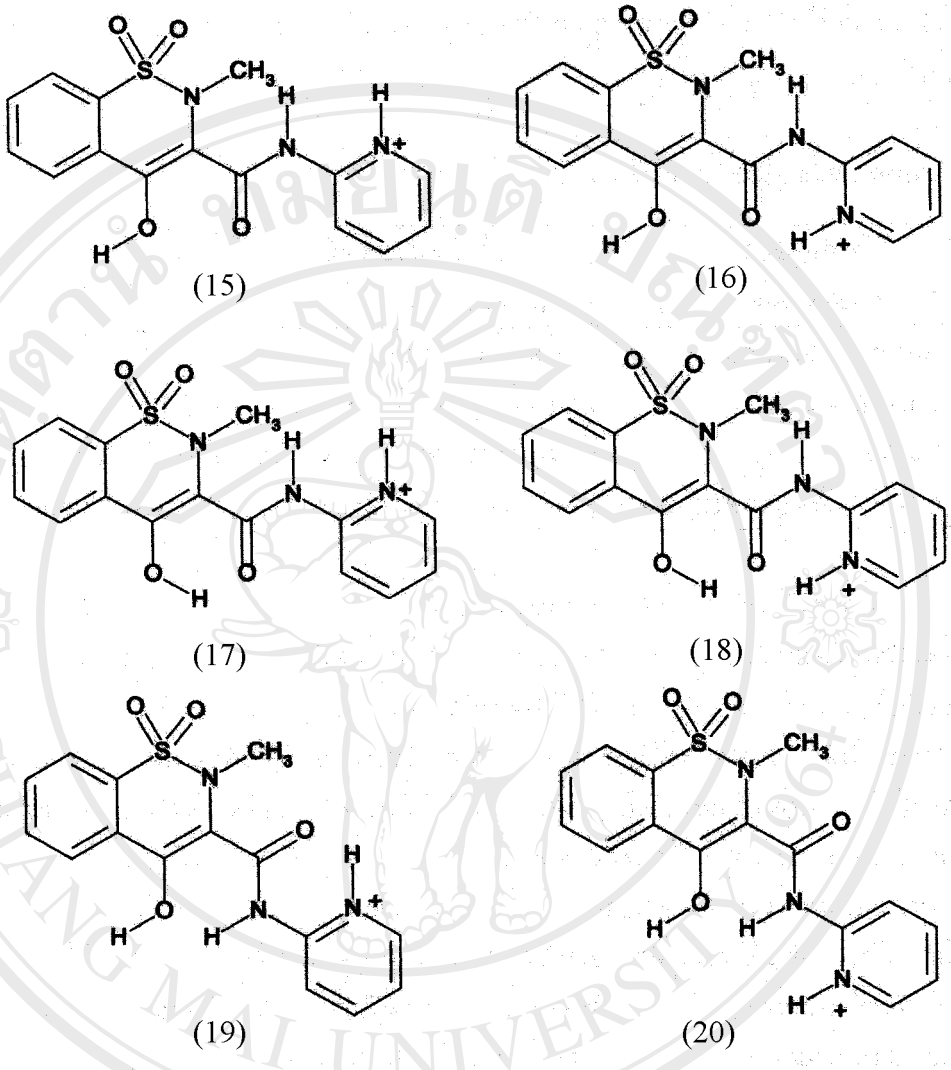

(15) (16)

(17) (18)

(19) (20)

Figure 159 (cont.) Conformation of piroxicam

The energy of optimization of these conformations using semiempirical method by PM3 method, AM1 method and the Density Function Theory method by B3LYP/6-31G** were shown in Table 57. The energy minimization using these methods is illustrated in Figure 160 and Figure 161 respectively.

Table 57 Optimization of piroxicam structures using PM3 AM1 and B3LYP/6-31G**methods

Structure	Energy in Kcal		
	PM3	AM1	B3LYP/6-31G**
1	-63.2720	-44.1608	-905332.49
2	-68.9961	-42.4179	-905332.49
3	-64.4348	-41.3737	-905315.71
4	-64.4348	-38.9356	-905315.71
5	-61.8377	-39.8778	-905311.40
6	-64.5569	-41.4641	-905315.71
7	-35.2622	-15.2054	-905316.08
8	-44.8332	-21.7565	-905318.30
9	-48.6455	-28.3046	-905322.54
10	-40.2280	-20.7635	-905316.08
11	-117.3670	-88.8769	-904994.09
12	-113.1880	-84.8689	-904986.61
13	-112.8740	-90.8904	-904986.61
14	-117.3670	-94.3326	-904994.09
15	84.3994	105.0249	-905559.50
16	79.0977	98.6767	-905568.72
17	85.8393	102.5596	-905570.37
18	77.3249	96.8885	-905578.57
19	79.3249	98.8045	-905568.72
20	84.3994	105.0249	-905559.50

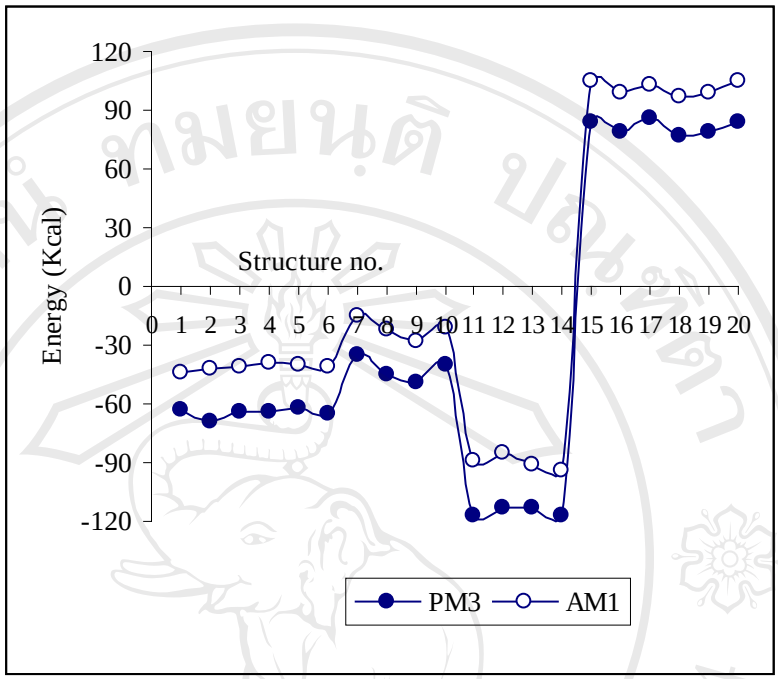

Figure 160 Energy optimization of piroxicam conformations using PM3 and AM1 method

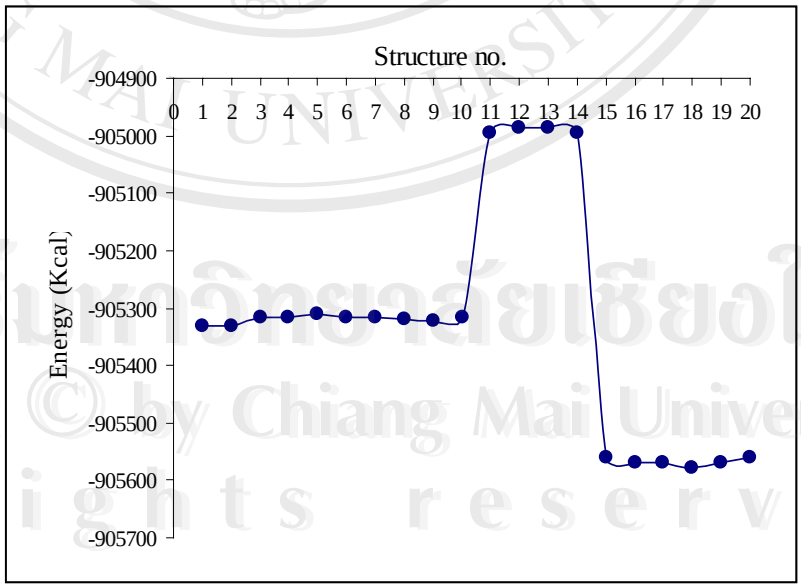

Figure 161 Energy optimization of piroxicam conformations using B3LYP/6-31G**

The energy minimization of piroxicam using different methods of calculations provided consistent information. The conformations of anionic species (11)-(14) show the lowest energies compared to the conformations of the other species. Cationic drug structures [number (15)-(20)] contain the highest energy. This was in agreement with the previously reported that the cationic form of piroxicam could not detected (Luger et al., 1996). The zwitterions show somewhat higher energy level than the neutral drug. Nevertheless, the zwitterionic form commonly exists in aqueous solution. The neutral form might be hypothetical conformation because in solution, the ionization takes place at either or both of the ionizable groups depending on the pH of the medium. Unfortunately, the energies of the anionic and the cationic forms can not be directly compared due to the effect of protonation.

The energy calculation by PM3 and AM1 method provides the comparable results however, the lowering in energy is more evidenced with PM3 method. Therefore, it was used for energy optimization of piroxicam-BCD complexes.

3.6.2.2 Energy optimization of piroxicam-BCD complexes

The conformational study of the piroxicam-BCD complexes was performed using PM3 method. Twenty conformations of piroxicam were introduced into the cavity of BCD in two different orientations. The energy of the complexes of each orientation is shown in Table 58 and in Figure 162.

It was found that energy level of the complexes shown in Figure 162 was entirely superimposed indicating no significant difference in the energy change in different orientation of piroxicam in BCD cavity. In other words, it is possible for piroxicam-BCD complex formed by initially introduce either benzene ring or pyridyl

ring towards the narrow end of BCD. The most stable piroxicam conformations form more stable complexes with BCD.

Table 58 Optimization of piroxicam-BCD complexes by PM3 method

Piroxicam structures	Energy in Kcal	
	bcdpiroxnn	bcdpiroxnna
1	-1527.50	-1530.10
2	-1532.94	-1534.36
3	-1526.40	-1528.30
4	-1527.56	-1527.74
5	-1529.38	-1526.87
6	-1529.78	-1529.42
7	-1509.20	-1503.49
8	-1508.79	-1520.42
9	-1514.12	-1516.83
10	-1506.84	-1508.42
11	-1596.33	-1596.24
12	-1592.29	-1593.63
13	-1592.98	-1593.88
14	-1593.46	-1594.86
15	-1381.93	-1377.21
16	-1387.17	-1386.73
17	-1380.59	-1378.78
18	-1386.81	-1387.45
19	-1387.80	-1385.11
20	-1381.72	-1377.13

bcdpiroxnn means the benzene ring of piroxicam was orientated into the narrow end of BCD cavity

bcdpiroxnna means the pyridyl ring of piroxicam was orientated into the narrow end of BCD cavity

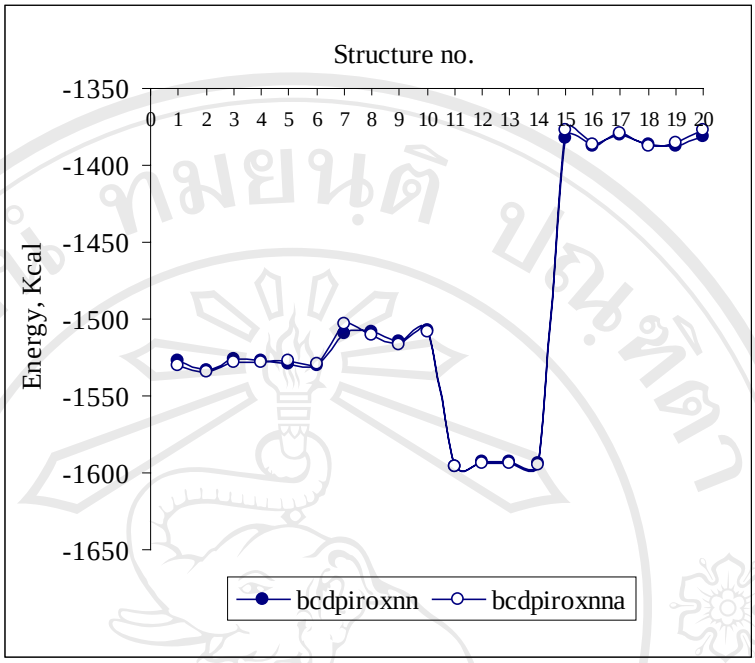

Figure 162 Energy optimization of piroxicam-BCD complex using PM3 method